

**UNIVERSIDADE DE SÃO PAULO  
INSTITUTO DE QUÍMICA**

**Programa de Pós-Graduação em Ciências Biológicas (Bioquímica)**

**RODRIGO LUCAS DE FARIA**

**Efeitos deletérios da oxidação de  
plasmalogênios de fosfatidiletanolamina  
via oxigênio molecular singlete**

Versão corrigida da Tese conforme Resolução CoPGr 5890  
O original se encontra disponível na Secretaria de Pós-Graduação do IQ-USP

São Paulo

Data do Depósito na SPG:  
**28/03/2023**

RODRIGO LUCAS DE FARIA

**Deleterious effects of phosphatidylethanolamine  
plasmalogen oxidation via singlet molecular oxygen**

*Tese apresentada ao Instituto de Química da  
Universidade de São Paulo para obtenção do  
Título de Doutor em Ciências (Bioquímica)*

*Orientador: Prof<sup>a</sup>. Dr<sup>a</sup>. Sayuri Miyamoto*

São Paulo  
2023



Universidade de São Paulo  
**Instituto de Química**

"Efeitos deletérios da oxidação de  
plasmalogênios de fosfatidiletanolamina via  
oxigênio molecular singlete"

**RODRIGO LUCAS DE FARIA**

Tese de Doutorado submetida ao Instituto de Química da Universidade de São Paulo como parte dos requisitos necessários à obtenção do grau de Doutor em Ciências obtido no Programa Ciências Biológicas (Bioquímica) - Área de Concentração: Bioquímica.

---

**Profa. Dra. Sayuri  
Miyamoto(Orientadora e  
Presidente)**

**APROVADO(A) POR:**

---

**Prof. Dr. Etelvino Jose Henriques  
BecharaIQ - USP**

---

**Profa. Dra. Rosangela  
ItriIF - USP**

---

**Profa. Dra. Glaucia Regina Martinez** *(por  
videoconferência)*  
**UFPR**

**SÃO PAULO  
10 de julho de 2023**

Autorizo a reprodução e divulgação total ou parcial deste trabalho, por qualquer meio convencional ou eletrônico, para fins de estudo e pesquisa, desde que citada a fonte.

Ficha Catalográfica elaborada eletronicamente pelo autor, utilizando o programa desenvolvido pela Seção Técnica de Informática do ICMC/USP e adaptado para a Divisão de Biblioteca e Documentação do Conjunto das Químicas da USP

Bibliotecária responsável pela orientação de catalogação da publicação:  
Marlene Aparecida Vieira - CRB - 8/5562

d224e de Faria, Rodrigo Lucas  
Efeitos deletérios da oxidação de plasmalogênios de fosfatidiletanolamina via oxigênio molecular singlete / Rodrigo Lucas de Faria. - São Paulo, 2023.  
185 p. + CD

Tese (doutorado) - Instituto de Química da Universidade de São Paulo. Departamento de Bioquímica.

Orientador: Miyamoto, Sayuri

1. Plasmalogênio. 2. Fotoquímica. 3. Lipidômica. 4. Oxigênio molecular singlete. 5. Espectrometria de massas. I. T. II. Miyamoto, Sayuri, orientador.

***Dedico este trabalho à  
minha família.***

## AGRADECIMENTOS

Agradeço imensamente aos meus pais Helio e Eliana por sempre me apoiarem nos meus sonhos e que ajudaram em muito a definir o meu caráter, e cujas lembranças estarão sempre na minha memória. Aos meus irmãos Ronaldo e Cristiane por sempre estarem ao meu lado.

Agradeço aos meus grandes amigos do Bonde: Carusin (Giovane) Anima (Diogo), Garçom (Lucas), Belo (Henrique), Komura-chan (Marcelo), Marcel, Arcanjo Uriel, Jacob, Raul, Lodo (Leonardo), C&A (Melissa) e Sussumu. Nós estamos completando 10 anos de Bonde neste 2023

Agradeço muito à Professora Dr<sup>a</sup>. Sayuri Miyamoto pela oportunidade de fazer parte do seu grupo de trabalho e pelo incentivo e pelos ensinamentos durante esses anos.

Agradeço imensamente aos Professores Dr. Maurício Batista e Professor Dr. Paolo Di Mascio pela imensa ajuda e conselhos ao longo do doutorado.

Agradeço imensamente (*In memoriam*) ao Professor Dr. Luiz Fernando da Silva Junior por ter sido o meu primeiro orientador e ter me ajudado e me ensinado muito em apenas um ano de iniciação científica.

Agradeço aos meus colegas de laboratório pela ajuda e boas conversas: Alex, Karen, Larissa, Rodrigo Santiago, Adriano, Lucas Dantas, Isabela, Lucas Viviane, Rosangela, Hector e Maria Fernanda, também aos ICs que eu aprendi muito ensinando: Marina, Humberto e Mateus. Agradeço também aos técnicos Adriana Wendel, Sirley Mendes, Izaura Toma, Alessandra, Giovana, Fernando Coelho e Emerson Marques por todo o apoio e colaboração. Agradeço muito à Thais por ter me dado muitos chocolates e um origami modular muito bonito que eu guardo com muito carinho.

Agradeço muito à Dr<sup>a</sup> Helena Couto Junqueira por ter sempre me ajudado e ensinando sobre leds, fotoquímica, lipossomos e utilização de diferentes equipamentos.

Agradeço muito à Dr<sup>a</sup> Fernanda Manso Prado por tudo. Sempre disposta a me ajudar e me ensinar. Pela imensa ajuda e expertise nos experimentos a análise de quimiluminescência, além de ter me ensinado muito sobre HPLC e Massas.

Agradeço ao Instituto de Química e a Universidade de São Paulo que me acolheram e me proporcionaram oportunidades para o meu crescimento profissional.

Agradeço à Fundação de Amparo à Pesquisa do Estado de São Paulo (FAPESP, Processo número 2017/16140-7), à Coordenação de Aperfeiçoamento de Pessoal de Nível Superior (CAPES) e ao Conselho Nacional de Desenvolvimento Científico e Tecnológico (CNPq) pelo apoio financeiro e institucional que viabilizou a execução dessa tese.

Como meu pai sempre dizia:  
“A vida é dura para quem é mole.  
Então, *take it easy...step by step*”



## Resumo

Faria, R.L. **Deleterious effects of phosphatidylethanolamine plasmalogen oxidation via singlet molecular oxygen**. 2023. 151p. Tese - Programa de Pós-Graduação em Ciências Biológicas (Bioquímica). Instituto de Química, Universidade de São Paulo, São Paulo.

Plasmalogênios são fosfolipídeos presentes em todos os tecidos humanos. Representam cerca de 20% de todos os fosfolipídeos. Caracterizam-se pela presença de uma ligação do tipo éter vinílico na cadeia alifática da posição sn-1 do glicerol, enquanto na posição sn-2 do glicerol é esterificado, na grande maioria das vezes, à ácidos graxos poliinsaturados (PUFAs). Embora estudos tenham demonstrados os efeitos protetores de plasmalogênios em modelos celulares submetidos à estresse oxidativo, os mecanismos propostos para seu efeito antioxidante são controversos. Por exemplo, a reação do grupo vinil éter com espécies reativas de oxigênio (ROS) gera produtos reativos como dioxetanos e aldeídos, os quais podem propagar os danos oxidativos. Grupos ricos em elétrons, como o vinil éter de plasmalogênios, formam dioxetano com oxigênio singlete por reação de (2+2) ciclo adição. Dioxetanos são geralmente instáveis e se decompõem rapidamente por termólise, gerando carbonila excitada. Esta espécie excitada pode decair para o estado fundamental emitindo luz visível, mas também pode transferir energia para o oxigênio molecular no estado fundamental ( $O_2(3\Delta_g^-)$ ), desta forma, produzindo oxigênio molecular singlete ( $O_2(1\Delta_g)$ )<sup>11</sup>. Este processo de formação de  $O_2(1\Delta_g)$  é chamado de “fotoquímica no escuro”. Além disso, hidroperóxidos lipídicos na presença de íons oxidantes, como ferro  $2+$ , também podem gerar  $O_2(1\Delta_g)$  por mecanismo de Russel. Portanto, a oxidação de plasmalogênio via  $O_2(1\Delta_g)$  pode propagar reações de oxidação por “fotoquímica no escuro” e mecanismo de Russel. Para testar esta hipótese, o presente estudo tem como metas: a) realizar análise oxi-lipídica qualitativa e quantitativa (lipídica de lipídeos não-oxidados e oxidados) com foco no remodelamento lipídico induzido por oxidação via oxigênio singlete gerado por fotooxidação em queratinócitos HaCat, b) caracterizar os principais produtos oxidados (dioxetanos, aldeídos, lisofosfolipídeos, etc.) derivados da reação do plasmalogênio com oxigênio singlete, c) estudar os mecanismos de oxidação de plasmalogênio e os efeitos da oxidação de plasmalogênios em modelos de membranas e em células, d) Análise de ácidos graxos livres por UPLC-Fluorescência, pois há um grande interesse em conhecer a composição de ácidos graxo em amostras biológicas, pois alterações nesses lipídeos estão associadas a condições patológicas, além de serem precursores de sinalizadores como prostaglandina.

**Palavras-chave:** Espectrometria de massas, oxidação lipídica, plasmalogênios, análise de aldeídos lipídicos, mecanismos de geração de oxigênio molecular singlete.

## ABSTRACT

Faria, R. L. **Deleterious effects of phosphatidylethanolamine plasmalogen oxidation via singlet molecular oxygen**. 2023. 151P. Thesis - Graduate Program in Biological Sciences (Biochemistry). Institute of Chemistry, University of São Paulo, São Paulo.

Plasmalogens are phospholipids present in all human tissues. They represent about 20% of all phospholipids. They are characterized by the presence of a vinyl ether-type bond in the aliphatic chain at the sn-1 position of glycerol, while at the sn-2 position of glycerol it is esterified, in most cases, to polyunsaturated fatty acids (PUFAs). Although studies have demonstrated the protective effects of plasmalogens in cellular models subjected to oxidative stress, the proposed mechanisms for their antioxidant effect are controversial. For example, the reaction of the vinyl ether group with reactive oxygen species (ROS) generates reactive products such as dioxetanes and aldehydes, which can propagate oxidative damage. Electron-rich groups, such as the vinyl ether of plasmalogens, form dioxetane with singlet oxygen by a (2+2) cycloaddition reaction. Dioxetanes are generally unstable and decompose rapidly by thermolysis, generating excited carbonyl. This excited species can decay to the ground state by emitting visible light, but it can also transfer energy to molecular oxygen in the ground state ( $O_2(3\Delta_g)$ ), thus producing singlet molecular oxygen ( $O_2(1\Delta_g)$ )<sup>11</sup>. This process of  $O_2(1\Delta_g)$  formation is called "photochemistry in the dark". Furthermore, lipid hydroperoxides in the presence of oxidizing ions, such as iron 2+, can also generate  $O_2(1\Delta_g)$  by Russell mechanism. Therefore, plasmalogen oxidation via  $O_2(1\Delta_g)$  can propagate oxidation reactions by "photochemistry in the dark" and Russell mechanism. To test this hypothesis, the present study aims to: a) perform a qualitative and quantitative oxylipidomics analysis (lipidomics of non-oxidized and oxidized lipids) focusing on lipid remodeling induced by oxidation via singlet oxygen generated by photooxidation in HaCat keratinocytes, b) characterize the main oxidized products (dioxetanes, aldehydes, lysophospholipids, etc.) derived from the reaction of plasmalogen with singlet oxygen, c) study the mechanisms of plasmalogen oxidation and the effects of plasmalogen oxidation on models of membranes and cells, d) Analysis of free fatty acids by UPLC-Fluorescence, as there is great interest in knowing the composition of fatty acids in biological samples, as changes in these lipids are associated with pathological conditions, in addition to being precursors of signals such as prostaglandin.

**Keywords:** Mass spectrometry, lipid oxidation, plasmalogens, analysis of lipid aldehydes, singlet molecular oxygen generation mechanisms.

# Summary

1. Introduction .....	15
1.1 Reactive Oxygen Species and oxidative stress .....	15
1.2 Singlet Molecular Oxygen Reactions and photosensitization reactions.....	16
1.3 Lipids and fatty acids diversity .....	18
1.4 Lipid peroxidation .....	19
1.5 Structure of plasmalogens .....	20
1.6 Plasmalogen biosynthesis .....	22
1.7 Reaction of plasmalogens with different reactive species .....	24
1.8 Summary of the results obtained in this study.....	26
1.9 References .....	27
2. Objective.....	36
2.1 General objective .....	36
2.1 Specific objectives .....	36
CHAPTER 1 .....	37
Highlights .....	38
Abbreviations .....	39
Abstract .....	40
1. Introduction.....	41
2. Material and Methods .....	42
2.1 Materials.....	42
2.2 Cleaning and preparing the homogenate .....	42
2.3 Preparing the homogenate .....	42
2.4 Lipid extractions and treatment with phospholipase A1 (PLA1).....	43
2.5 Flash column purification .....	44
2.6 TLC analysis.....	44
2.7 HPLC analysis .....	45
2.8 Lipidomics analysis.....	45

2.9 Data processing.....	46
3. Results .....	47
3.1 Cleaning and preparing the homogenate .....	47
3.2 Lipid extractions and treatment with phospholipase A1 (PLA1) .....	48
3.3 Silica gel column purification.....	49
3.4 Lipidomic Analysis .....	52
3.5 Identification plasmalogen of phosphatidylserine methyl ester (PSMe) by MS/MS .....	54
3.6 Alternative qualitative and quantitative analysis of PE plasmalogen by TLC or UHPLC.....	56
4. Discussion .....	57
5. Acknowledgements .....	59
6. References .....	59
7. Supplementary figures.....	64
8. Supplementary tables .....	65
CHAPTER 2 .....	66
Highlights .....	67
Abbreviations .....	68
Abstract .....	70
1. Introduction.....	71
2. Results .....	74
2.1 Characterization of phosphoethanolamine plasmalogen photooxidation products .....	74
2.2 Determination of the ratio between plasmalogen photooxidation routes.....	77
2.3 Characterization of alpha beta unsaturated fatty aldehyde (Ald 18:1 $\Delta^2$ ) produced by the reduction of plasmalogen hydroperoxides.....	79
2.4 Chemiluminescence of plasmalogens dioxetane and triplet carbonyl identification .....	82
2.5 Characterization of radical reaction products of pPE (p18-OOH/18:1) with Ce <sup>+4</sup> and Fe <sup>+2</sup> .....	85
2.6 Characterization of singlet molecular oxygen generated by the reaction of hydroperoxides pPE (p18-OOH/18:1) and Ce <sup>4+</sup> .....	88

3. Discussion .....	89
4. Material and Methods .....	93
2.1 Materials.....	93
2.2 Plasmalogen photooxidation.....	94
2.3 Lipid analysis by ESI-QTOF MS/MS .....	95
2.4 Optimization of aldehyde derivatization conditions with CHH.....	96
2.5 Aldehydes analysis by ESI-QTOF MS/MS .....	97
2.6 Excited triplet species light emission in the visible region.....	97
2.7 Singlet molecular oxygen emission in the near infrared region.....	97
5. Acknowledgements .....	98
6. References .....	98
7. Supplementary figures.....	103
8. Supplementary tables .....	110
CHAPTER 3 .....	111
Highlights .....	112
Abbreviations .....	113
Abstract .....	115
1. Introduction.....	116
2. Material and Methods .....	117
2.1 Materials.....	117
2.2 HaCat cell plating .....	118
2.3 Photosensitizers stock solution.....	118
2.4 Lipid extraction from HaCat cells .....	118
2.5 Time-dependent photooxidation of extracted lipids .....	119
2.6 Lipid analysis by UPLC-MS/MS .....	119
2.7 Data processing .....	120
2.8 Carboxyfluorescein encapsulated liposomes and membrane leak assay ..	120
2.9 Aldehydes analysis by ESI-QTOF MS/MS .....	121
3. Results and Discussion .....	122

3.3 Reactivity of lipids from HaCat Keratinocyte Cells.....	122
3.2 PE plasmalogens facilitate membrane leakage.....	127
4. Conclusions .....	133
5. Acknowledgements .....	133
6. References .....	133
7. Supplementary figures.....	138
CHAPTER 4 .....	144
Highlights .....	145
Abbreviations .....	146
Abstract .....	147
1. Introduction.....	149
2. Material and Methods .....	151
2.1 Materials.....	151
2.2 Animals.....	151
2.3 Lipid extraction and Fatty acids derivatization .....	152
2.4 Free fatty analysis by UHPLC-Fluorescence .....	153
2.5 Lipid analysis by UPLC-MS/MS (HRMS) .....	154
2.6 HRMS data processing .....	154
3. Results .....	155
3.1 Derivatization of fatty acids with CHH. ....	155
3.2 FFA analysis by LC-Fluorescence and LC-high resolution mass spectrometry .....	158
3.3 Lipidomic analysis of feeds used to supplement wild-type and ALS rats ..	160
3.4 FFA analysis by HPLC-Fluorescence of blood plasma from ALS and WT rats supplemented with different diets .....	162
4. Discussion .....	164
5. Acknowledgements .....	166
6. References .....	166
7. Supplementary figures.....	171
8. Supplementary tables .....	174

Final remarks.....	181
CURRICULUM VITAE .....	183

## 1. Introduction

### 1.1- Reactive Oxygen Species and oxidative stress

Reactive Oxygen Species (ROS) are a group of molecules that include free radicals such as superoxide anion ( $O_2^{\cdot-}$ ), hydroxyl radical ( $\cdot OH$ ), and non-radical species such as hydrogen peroxide ( $H_2O_2$ ) and singlet oxygen ( $^1O_2$ )(1). ROS can be generated through several mechanisms, including the electron transport chain in mitochondria, inflammatory responses, cyclooxygenation, lipoxygenation, lipid peroxidation, metabolism of xenobiotics, and ultraviolet radiations(2–4).

ROS are produced in normal cellular metabolism, and they have important roles in various biological processes, (e.g., cell signaling, immune responses). However, excessive production of ROS can cause damage to cellular components such as DNA, proteins, and lipids(5).

On the other hand, cells have antioxidant defense systems that act by preventing/inhibiting oxidation reactions(3). Antioxidants are defined as substances present in low concentrations that effectively prevent or inhibit the formation or reaction of an oxidizing species(6). These species are classified as enzymatic, for example: the enzymes superoxide dismutase (SOD), catalase (CAT), glutathione peroxidase (GPx) and peroxiredoxins (Prdx); and non-enzymatic such as carotenoids, flavonoids, vitamins E and C, in addition to thiol compounds such as GSH.

In the case of membrane poly unsaturated fatty acids (PUFAs), it is known that vitamin E and GPx4 and Prdx6 enzymes play a fundamental role in antioxidant defense mechanisms(6,7). Overall, ROS are important regulators of cellular homeostasis, but their excessive production can lead to cellular damage and disease(8).

Redox homeostasis refers to the balance between the production and elimination of ROS and reactive nitrogen species (RNS) in living organisms(6,9). ROS and RNS are naturally occurring molecules that are involved in various biological processes such as cell signaling, immune response, and gene expression regulation(9).

Oxidative stress is defined as the imbalance between the production of oxidizing



agents (ROS and RNS) and antioxidants (**Figure 1**)(6,9). This imbalance leads to damage to important biomolecules such as DNA, RNA, proteins, lipids, etc. Oxidative stress has been linked to a wide range of diseases, including cancer, cardiovascular disease, neurodegenerative diseases such as Alzheimer's and Parkinson's, diabetes, and autoimmune disorders. It is also thought to contribute to the aging process itself(6,8,10,11).

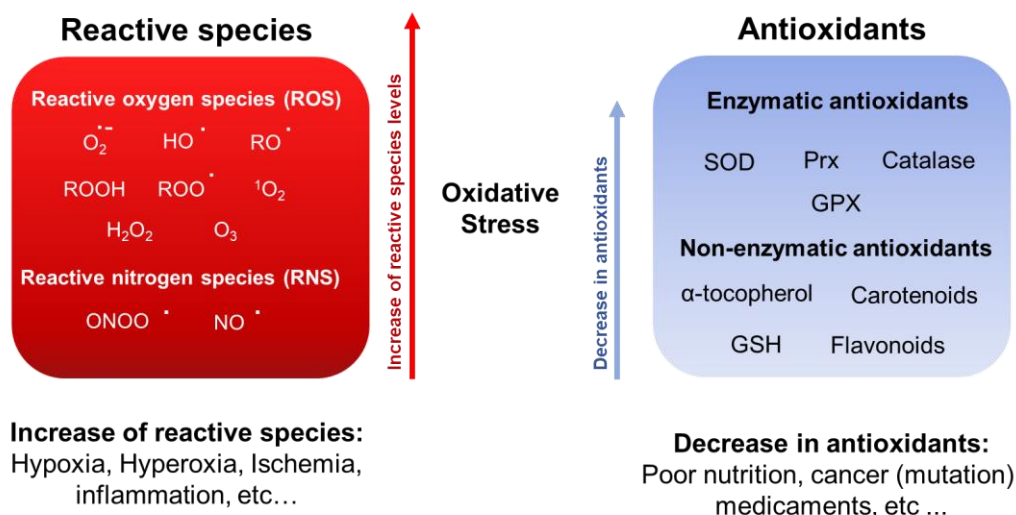


**Figure 1:** Oxidative stress occurs when there is imbalance between cell production of reactive (ROS and RNS) and antioxidant species. Under homeostasis conditions, professional and antioxidant production is in a stable balance. Excessive reactive species production or antioxidant depletion can cause oxidative stress.

### 1.2-Singlet Molecular Oxygen Reactions and photosensitization reactions

Molecular oxygen ( $O_2$ ) is a species with two unpaired electrons in the antibonding  $\pi^*$  orbital ( $O_2(^3\Sigma_g^+)$ ). But when electronically excited it can acquire two singlet states ( $O_2(^1\Sigma_g^-)$  and  $O_2(^1\Delta_g)$ ) but the  $O_2(^1\Sigma_g^-)$  state is more unstable and is quickly converted to  $O_2(^1\Delta_g)$  (table 1)(12).

On the other hand,  $O_2(^1\Delta_g)$  can decay to the ground state or it can interact with other species by oxidation reaction, hence it is a ROS, or it can transfer energy to the species and decay to the ground state. There are several antioxidants that receive

energy from  $O_2(^1\Delta_g)$  without oxidizing such as: carotenoids, bilirubin, tocopherols, phenols and azide(12,13).

**Table 1:** Electronic distribution in the molecular orbitals of molecular oxygen in the ground state ( $O_2(^3\Sigma_g^+)$ ) and singlet excited states ( $O_2(^1\Sigma_g^-)$  and  $O_2(^1\Delta_g)$ ).

Electronic State	Unfilled molecular orbital $\pi^*$	Energy (kcal/mol)	Life time in water ( $\mu$ s)
Excited singlet $^1\Sigma_g^-$	$\uparrow \quad \downarrow$	37.5	0.001
Excited singlet $^1\Delta_g$	$\uparrow\downarrow \quad \text{---}$	22.5	4
Ground state $^3\Sigma_g^+$	$\uparrow \quad \uparrow$		

$O_2(^1\Delta_g)$  is generated in biological systems by different mechanisms, and can be divided into light-dependent (photosensitization) and light-independent (dark reactions)(14,15). Generation of  $O_2(^1\Delta_g)$  by reaction in the dark (chemiexcitation) may have an enzymatic origin such as: peroxidases (myeloperoxidase) or oxygenases (lipoxygenases); and non-enzymatic such as: hydrogen peroxide with hypochlorite or peroxynitrite, the reaction of ozone with biomolecules, thermolysis of dioxetanes or recombination of peroxy radicals derived from biomolecules (such as lipids)(14,16,17).

Singlet excited molecular oxygen ( $^1O_2$ ) is a biologically relevant ROS capable of reacting efficiently with cellular constituents. In biological systems, singlet oxygen can be produced by the immune system's white blood cells to kill invading pathogens. However, if the production of singlet oxygen exceeds the body's ability to neutralize it, it can lead to oxidative damage(14). This excited state can be generated in a variety of ways, such as through skin exposure to ultraviolet light(18) or through chemical reactions with certain substances(14). Singlet oxygen is highly reactive and can participate in a wide range of chemical reactions(19).

Photosensitization reactions are chemical reactions triggered by the absorption of light by a photosensitizer, which can be a molecule that absorbs light and transfers its energy to another molecule or a metal ion that catalyzes a reaction through the transfer of electrons. There are two types of photosensitization reactions (**Figure 2**): Type I photosensitization reactions involve the transfer of an electron from the photosensitizer to a substrate molecule, while Type II photosensitization reactions involve the transfer of energy from the photosensitizer to molecular oxygen, generating singlet oxygen. Both types of photosensitization reactions can have important biological functions, but they can also be detrimental if they lead to the production of reactive species that damage cellular components.(20–22).

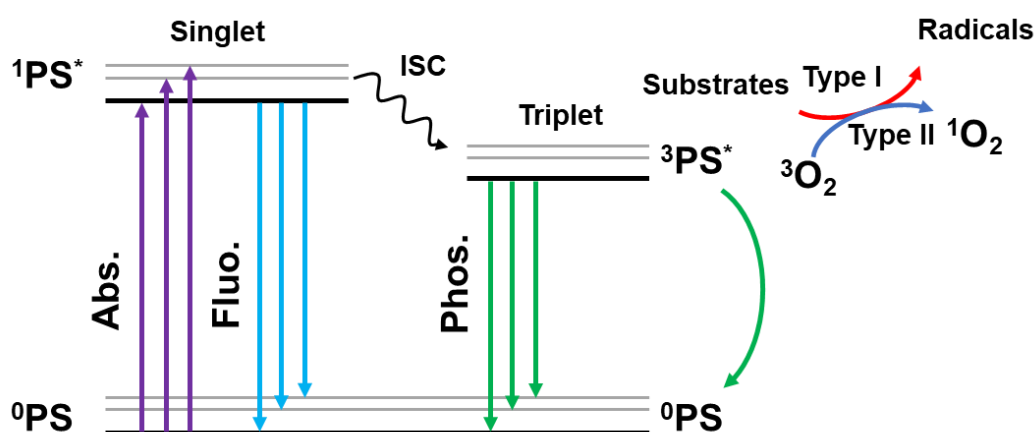


**Figure 2:** The triplet excited state of the photosensitizer ( $^0PS$ ) can be formed by photoexcitation of the singlet ground state ( $^1PS^*$ ) to a singlet excited state.  $^3PS^*$  is produced by intersystem crossing (ISC) from  $^1PS^*$ .  $^3PS^*$  can react directly with substrates and form radical species (type I) or  $^3PS^*$  can transfer energy to molecular oxygen and produce singlet molecular oxygen (type II)(23).

### 1.3- Lipids and fatty acids diversity

Lipids are a broad class of organic molecules that are characterized by their insolubility in water and solubility in nonpolar solvents such as ether, chloroform, and benzene. They include a diverse range of compounds and lipids can be classified into several

categories, such as fatty acyls, glycerophospholipids, glycerolipids, sterol lipids, sphingolipids, prenol lipids and saccharolipids (24).

Lipids play important roles in living organisms, such as serving as a source of energy, forming the structural basis of cell membranes, and participating in signaling pathways. They are also involved in many physiological processes, including cell growth and division, hormone production, and immune function(25,26).

Fatty acids are a type of lipid molecule that consists of a hydrocarbon chain and a carboxyl group at end. They can be classified into different categories based on their length of carbon chain, degree of saturation (presence of double bonds), and position of the double bonds in the chain(27). Some common classes of fatty acids include:

**Saturated fatty acids:** These fatty acids do not contain any double bonds and have a straight carbon chain. Examples include palmitic acid (FA 16:0) and stearic acid (FA 18:0). **Monounsaturated fatty acids (MUFA):** These fatty acids contain one double bond and have a bent carbon chain. Examples include oleic acid (C18:1) and palmitoleic acid (FA 16:1). **Polyunsaturated fatty acids (PUFA):** These fatty acids contain two or more double bonds and also have a bent carbon chain. Examples include linoleic acid (FA 18:2) and arachidonic acid (FA 20:4) (27).

Overall, fatty acids play important roles in the body, including as a source of energy, as building blocks for cell membranes, and as precursors for signaling molecules(27,28).

#### **1.4- Lipid peroxidation**

Lipid peroxidation occurs when oxidizing species react by abstracting electrons (hydrogen) from unsaturated lipids, inducing a cascade of radical reactions (3-step reaction: initiation, propagation, termination) that lead to the formation of lipid hydroperoxides (LOOH) as primary products(29). LOOHs are relatively unstable and may participate in secondary reactions that lead to the formation of peroxy and/or alkoxy radicals. These, in turn, can propagate the oxidation process, through the generation of new lipid radicals (**Figure 3 A**)(29,30). PUFAs are particularly susceptible to lipid

peroxidation due to the presence of bis-allylic hydrogen atoms, which are highly reactive and easily abstracted by radicals(29). Alternatively, these radicals (peroxy/alkoxyl) can undergo intramolecular cyclization reactions or acyl chain breakage producing, respectively, cyclic compounds similar to prostaglandins (eg isoprostanes, neuroprostanes) and an enormous variety of reactive aldehydes (**Figure 3 B**)(29,31). Thus, lipid peroxidation causes changes in the permeability and fluidity of cell membranes, drastically altering cell integrity and function(32).

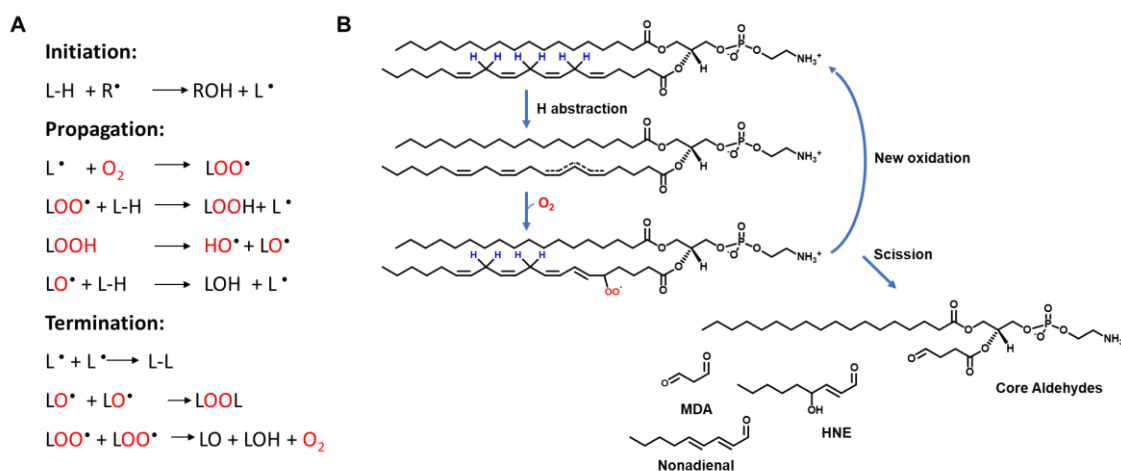


**Figure 3:** The lipid peroxidation reaction. The first step is initiation with generation of lipid radicals. LH represents an unsaturated fatty acid, and  $R^{\bullet}$  a radical, such as a hydroxyl radical ( $HO^{\bullet}$ ). The second step is propagation with creation of new lipid radicals. Carbon-centered radical ( $L^{\bullet}$ ) reacts rapidly with dioxygen producing lipid peroxy radical ( $LOO^{\bullet}$ ). The final step is termination, either by antioxidants or another radical. (B) Mechanism of lipid peroxidation in phospholipid, the bis-allylic hydrogen atoms in blue, over oxidation leads to fatty acids scission and produces aldehydes.

### 1.5- Structure of plasmalogens

Plasmalogens are glycerophospholipids distinguished by the presence of a vinyl ether linkage at the sn-1 position of glycerol (Figure 2), while being enriched with polyunsaturated fatty acids (PUFAs) (33,34). Plasmalogens are

present in all human tissues and make up around 20% of all phospholipids. They are found in high levels in blood cells (such as erythrocytes, neutrophils, and eosinophils), spermatozoa, and are particularly abundant in cardiac and cerebral tissues (33,34). Notably, the brain has the highest concentrations of plasmalogens in the phosphoethanolamine (PE) category, accounting for up to 85% molar of PE or 30% molar of total phospholipids within these membranes (34).

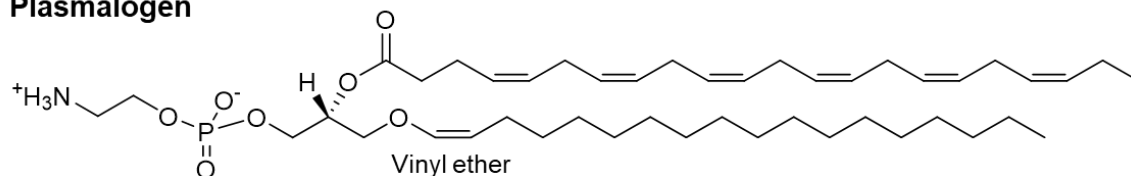
Given their prevalence across diverse membrane systems and tissue types, plasmalogens have been shown to play a crucial role in various biological functions. These include their role as integral constituents of cellular membranes, influencing membrane dynamics (35–38). As plasmalogens conventionally house polyunsaturated fatty acids (PUFA) in the sn-2 position (33,39), they are believed to function as reservoirs for biologically active lipid mediators and potentially act as antioxidants.

Numerous studies substantiate the proposition that plasmalogens may function as antioxidants due to the heightened reactivity of their vinyl ether moieties with reactive oxygen species (ROS)(39–41). In vitro investigations using macrophages (RAW)(39) and human pulmonary arterial endothelial cells (PAEC)(40) deficient in plasmalogen biosynthesis have shown that these cells are more susceptible to cell death induced by oxidative stress, compared to control cells(33). Consequently, it has been hypothesized that the vinyl ether group is sacrificially oxidized, thereby protecting the PUFA at the sn-2 position(41), thus preventing lipid peroxidation.

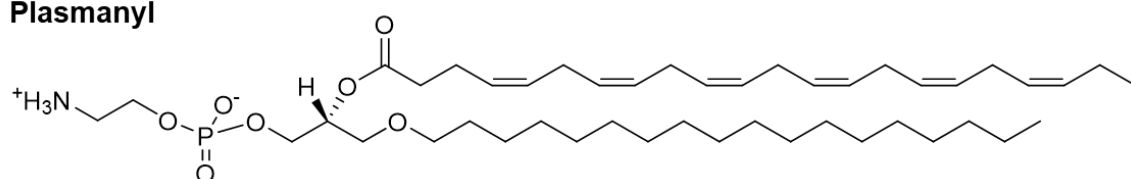
Furthermore, decreased plasmalogen levels have been associated with several

pathological conditions characterized by increased levels of reactive oxygen species (ROS), such as aging and neurological disorders like Alzheimer's, Parkinson's, and Down syndrome (39,42,43). Hence, biological scenarios marked by oxidative stress may lead to a decrease in plasmalogen levels.

### Plasmalogen



### Plasmanylin



### Diacylphospholipid

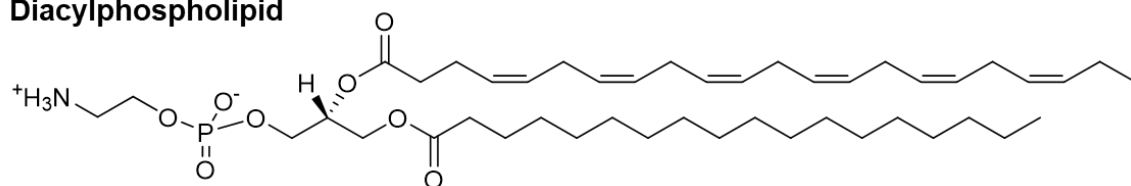


**Figure 3:** Different structures of phosphatidylethanolamine esterified with EPA (FA 20:5): plasmalogen pPE(p18/EPA), plasmanylin oPE(o18/EPA) and diacyl PE (18:0/EPA).

## 1.6- Plasmalogen biosynthesis

The synthesis of plasmalogens involves several enzymatic steps that occur mainly in the endoplasmic reticulum (ER) and peroxisome. The first step is the conversion of dihydroxyacetone phosphate (DHAP) to glycerone phosphate by the enzyme glycerone phosphate acyltransferase (GNPAT) in the peroxisome. Glycerone phosphate is then converted to 1-alkenyl-glycerone phosphate (plasmanylin-glycerone phosphate, 1-O-alkyl-DHAP) by the enzyme alkylglycerone phosphate synthase (AGPS) in the peroxisome(33,34,44). FAR1 (fatty acyl-CoA reductase 1) is an enzyme that has been shown to play a key role in the biosynthesis of plasmalogens by catalyzing the reduction of fatty acyl-CoA to fatty alcohol(45). The last stages of synthesis take place in

the endoplasmic reticulum(33,46). Overall, plasmalogen synthesis is a complex process that involves multiple enzymes and subcellular compartments(46).

Plasmalogens play a vital role in physiological processes, as evidenced by human genetic disorders that result from a scarcity of plasmalogens(33,46,47). This scarcity resulted from reduced peroxisomal GNPAT and AGPS activities(33,48). Patients exhibited severe symptoms such as mental retardation, hypotonia, adrenal dysfunction, cataracts, deafness, facial dysmorphism, chondrodysplasia, and failure to thrive, often leading to death within a year(47–49).

Numerous autosomal recessive disorders have been extensively investigated, characterized by deficient peroxisomes or impaired function(33,46,48,50). These disorders can be categorized into three groups: A, B, and C(33).

Group A disorders involve the widespread loss of peroxisomes, which compromises various functions, such as Zellweger syndrome and neonatal adrenoleukodystrophy.

Group B disorders involve an inability to accurately target specific proteins to peroxisomes, while the overall function remains intact. Rhizomelic chondrodysplasia punctata (RCDP) is a rare genetic disorder characterized by various symptoms, such as short stature, limb anomalies, facial dysmorphism, cataracts, severe mental retardation, and increased mortality(34,46,50). Typically, defects in the PEX7 gene (RCPD type 1)(50), which is responsible for the peroxisome targeting sequence 2 (PTS2), lead to a loss of PTS2-dependent protein targeting(49).

Group C disorders are characterized by the loss of a specific peroxisomal function or enzyme. Instances involve deficiencies in plasmalogen biosynthesis enzymes. Some sources categorize these as Type 2 and Type 3 based on the absence of GNPAT or AGPS, respectively(33).



The significance of plasmalogens for normal development is underscored by disorders in which their biosynthesis is deficient(46). The impact of plasmalogen reduction, as observed in certain diseases, necessitates comprehensive research to understand both the biochemical and cellular processes that affect plasmalogen levels and the mechanisms underlying the pathophysiology of these disorders(33,46,49).

While numerous functions have been attributed to plasmalogens, their exact physiological role remains elusive. Investigating these assigned functions in patients with defective plasmalogen biosynthesis or reduced levels will be crucial for comprehending the consequences of their loss.

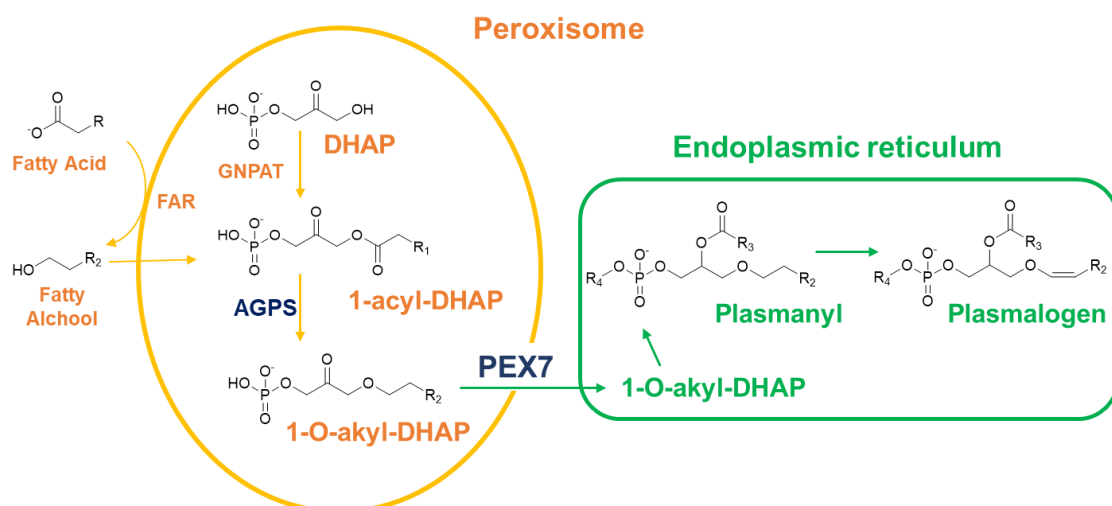


**Figure 4:** Overview over the biosynthetic pathway of plasmalogens. Abbreviations used in this diagram: DHAP (dihydroxyacetone-phosphate), Far1 (fatty acyl CoA reductase 1), glycerone phosphate O-acyltransferase (GNPAT), alkylglycerone phosphate synthase (AGPS), Peroxisomal Biogenesis Factor 7 (PEX7).

### 1.7- Reaction of plasmalogens with different reactive species

Plasmalogens also stand out for their supposed antioxidant role(39). However, the proposed antioxidant mechanisms are controversial in view of the products formed in the plasmalogen reaction. It is known that the oxygen of the vinyl ether group is  $\text{sp}^2$  and

because of this, resonance occurs between the three atoms of this group rich in electrons, thus making plasmalogens targets of reactive species such as: peroxy radicals, singlet oxygen, metals and acid. hypochlorous(39,51–53). The scheme in **Figure 5** summarizes the main plasmalogen reactions with reactive species present in biological systems.

A common product of all reactions are aldehydes, which are capable of modifying other biomolecules such as: DNA, proteins and lipids. In addition to aldehydes, the reaction of the vinyl ether group with singlet oxygen generates a dioxetane intermediate, an unstable species that rapidly decomposes, generating excited carbonyls, long-chain aldehydes and lysophospholipids (**Figure 5**)(54,55). Excited carbonyls can transfer energy to molecular oxygen producing oxygen in the singlet state ( $^1O_2$ ), an excited electrophilic species capable of modifying various biomolecules. In this way the formation of dioxetane could propagate the oxidation reactions.

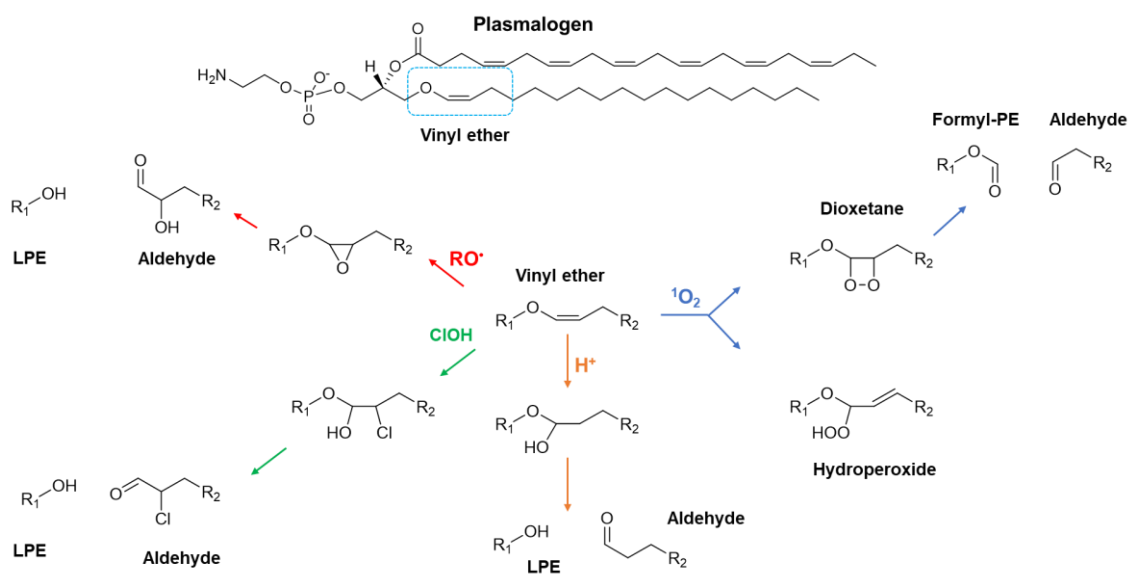


**Figure 5:** Main plasmalogen reactions with reagents present in biological systems, namely: radicals ( $\bullet OH$ ,  $\bullet OOH$ ), acids ( $H^+$ ), singlet oxygen ( $^1O_2$ ) and hypochlorous acid ( $ClOH$ ). Common products: aldehydes and lysophospholipids (LPE).

Plasmalogens stand out as an important factor in the survival of cells under oxidative stress. Although many studies classify it as an antioxidant lipid, the mechanism of action

is not known. Initially, it was proposed that the antioxidant action of plasmalogens would be related to the presence of the vinyl ether group, but more recent studies suggest that the protective action of plasmalogens goes beyond consuming reactive species, and also that the lipid composition of the membrane influences the antioxidant action.

### **1.7- Summary of the results obtained in this study**

Plasmalogens are unique phospholipids that have a vinyl ether group at the sn1 position of glycerol. They are known for their heightened reactivity towards reactive oxygen species (ROS) because of their electron-rich nature. This study focused on understanding the mechanisms involved in plasmalogen reactions when exposed to reactive oxygen species (ROS), including singlet oxygen produced through photooxidation. The initial focus required the development of plasmalogen purification techniques from beef and pig brains (Chapter 1).

The purified plasmalogens that were acquired served as the basis for method development and preliminary experiments prior to using commercial standards. This enabled the development of low-temperature photooxidation techniques (Chapter 2) for the analysis of fatty aldehydes. These methods were essential not only for studying membrane leakage, which required 15 mg of lipids for liposome preparation (chapter 3), but also for overcoming the limitations of commercial standards. Notably, the purification process demonstrated remarkable reproducibility across different brain sources and resulted in the simultaneous extraction of value-added lipids such as cerebroside and sulfatides. Intriguingly, a novel variant of phosphatidylserine methyl ester plasmalogen emerged in the purified fractions, offering potential for uncovering its mysterious role in brain function.

While the reactivity of plasmalogens with singlet oxygen is well-established, there is a lack of research investigating the resulting products. To address this gap, the study analyzed the various products resulting from photooxidation using diverse techniques to uncover distinct reactivity profiles (Chapter 2). The research uncovered evidence of dioxetane production through chemiluminescence, which is a harmful outcome for

cellular health. Moreover, the study demonstrated that plasmalogen dioxetane generation propagates oxidation by producing additional singlet oxygen. Simultaneously, the study characterized hydroperoxide formation, revealing a mechanism distinct from dioxetane production. Remarkably, plasmalogen hydroperoxide readily yields alpha-beta unsaturated fatty aldehydes upon reduction, while metal-induced oxidation produces diacyl phospholipids with alpha-beta unsaturated carbonyls. Validation of these species relied on reacting them with a thiol group-sensitive fluorescent probe, introducing a simple technique for their detection and revealing their reactivity with thiol groups. This finding is significant in the modification of proteins and biomolecules.

Chapter 3 explores the prevalence of phosphoethanolamine plasmalogens in HaCat keratinocyte cells and their increased reactivity in photosensitivity reactions. Leveraging insights from Chapter 2, the study explored how pPE oxidation could disrupt membrane integrity. Intriguingly, membranes rich in plasmalogens ruptured solely upon exposure to singlet oxygen in the presence of reductants, indicating an unexpected vulnerability associated with antioxidant mechanisms.

Expanding upon the expertise gained in analyzing fatty aldehydes resulting from plasmalogen oxidation, the study extended its methodologies to include free fatty acid analysis (FFA, chapter 4). This approach was promptly optimized and used to analyze plasma samples from SOD1 G93A transgenic mice that were exposed to different diets. The study revealed that dietary variations had a greater impact on FFA profiles than ALS disease itself, indicating the wide applicability of this method for future research.

In essence, this research unraveled the intricate behaviors of plasmalogens under oxidative stress, shedding light on their roles in cellular health, oxidation pathways, and potential protein modifications. By expanding methodological horizons, this study not only contributes to a deeper understanding of lipid biochemistry but also provides valuable tools for future scientific inquiries.

## **1.8- References**

1. Darley-USmar V, Halliwell B. Blood radicals: reactive nitrogen species, reactive

- oxygen species, transition metal ions, and the vascular system. *Pharm Res* [Internet]. 1996 May;13(5):649–62. Available from: <http://www.ncbi.nlm.nih.gov/pubmed/8860419>
2. Ray PD, Huang B-W, Tsuji Y. Reactive oxygen species (ROS) homeostasis and redox regulation in cellular signaling. *Cell Signal* [Internet]. 2012 May;24(5):981–90. Available from: <http://www.ncbi.nlm.nih.gov/pubmed/22286106>
  3. Halliwell B. Free radicals and antioxidants – quo vadis? *Trends Pharmacol Sci* [Internet]. 2011 Mar;32(3):125–30. Available from: <http://dx.doi.org/10.1016/j.tips.2010.12.002>
  4. Darley-Usmar V, Halliwell B. Blood radicals: reactive nitrogen species, reactive oxygen species, transition metal ions, and the vascular system. *Pharm Res*. 1996 May;13(5):649–62.
  5. Murphy MP, Holmgren A, Larsson N-G, Halliwell B, Chang CJ, Kalyanaraman B, et al. Unraveling the biological roles of reactive oxygen species. *Cell Metab* [Internet]. 2011 Apr 6;13(4):361–6. Available from: <http://www.ncbi.nlm.nih.gov/pubmed/21459321>
  6. Halliwell B, Gutteridge JMC. *Free Radicals in Biology & Medicine*. Oxford Univ Press. 2015;5:961.
  7. Maiorino M, Conrad M, Ursini F. GPx4, Lipid Peroxidation, and Cell Death: Discoveries, Rediscoveries, and Open Issues. *Antioxid Redox Signal* [Internet]. 2017 May 30;4:ars.2017.7115. Available from: <http://online.liebertpub.com/doi/10.1089/ars.2017.7115>
  8. Murphy MP, Holmgren A, Larsson N-G, Halliwell B, Chang CJ, Kalyanaraman B, et al. Unraveling the biological roles of reactive oxygen species. *Cell Metab*. 2011 Apr;13(4):361–6.

9. Miyata Y, Matsuo T, Sagara Y, Ohba K, Ohyama K, Sakai H. A mini-review of reactive oxygen species in urological cancer: Correlation with NADPH oxidases, angiogenesis, and apoptosis. *Int J Mol Sci*. 2017;18(10).
10. Duracková Z. Some current insights into oxidative stress. *Physiol Res* [Internet]. 2010;59(4):459–69. Available from: <http://www.ncbi.nlm.nih.gov/pubmed/19929132>
11. Dorszewska J, Kowalska M, Prendecki M, Piekut T, Kozłowska J, Kozubski W. Oxidative stress factors in Parkinson's disease. *Neural Regen Res* [Internet]. 2021;16(7):1383. Available from: <https://journals.lww.com/10.4103/1673-5374.300980>
12. Ronsein GE, Miyamoto S, Bechara E, Di Mascio P, Martinez GR. Oxidação de proteínas por oxigênio singleto: mecanismos de dano, estratégias para detecção e implicações biológicas. *Quim Nova* [Internet]. 2006 Jun;29(3):563–8. Available from: [http://www.scielo.br/scielo.php?script=sci\\_arttext&pid=S0100-40422006000300027&lng=pt&nrm=iso&tlng=pt](http://www.scielo.br/scielo.php?script=sci_arttext&pid=S0100-40422006000300027&lng=pt&nrm=iso&tlng=pt)
13. Steinbeck MJ, Khan AU, Karnovsky MJ. Intracellular singlet oxygen generation by phagocytosing neutrophils in response to particles coated with a chemical trap. *J Biol Chem* [Internet]. 1992 Jul 5;267(19):13425–33. Available from: <http://www.ncbi.nlm.nih.gov/pubmed/1320020>
14. Di Mascio P, Martinez GR, Miyamoto S, Ronsein GE, Medeiros MHG, Cadet J. Singlet Molecular Oxygen Reactions with Nucleic Acids, Lipids, and Proteins. *Chem Rev* [Internet]. 2019 Feb 13;119(3):2043–86. Available from: <https://pubs.acs.org/doi/10.1021/acs.chemrev.8b00554>
15. Baader WJ, Stevani C V., Bechara EJH. "Photo"chemistry Without Light? *Rev Virtual Química* [Internet]. 2015;7(1):74–102. Available from: <http://www.gnresearch.org/doi/10.5935/1984-6835.20150005>

16. Miyamoto S, Martinez GR, Medeiros MHG, Di Mascio P. Singlet molecular oxygen generated from lipid hydroperoxides by the Russell Mechanism: Studies using <sup>18</sup>O-labeled linoleic acid hydroperoxide and monomol light emission measurements. *J Am Chem Soc* [Internet]. 2003 May;125(20):6172–9. Available from: <http://pubs.acs.org/doi/abs/10.1021/ja029115o>
17. Adam W, Cilento G. Four-Membered Ring Peroxides as Excited State Equivalents: A New Dimension in Bioorganic Chemistry. *Angew Chemie Int Ed English* [Internet]. 1983 Jul;22(7):529–42. Available from: <http://doi.wiley.com/10.1002/anie.198305291>
18. Baier J, Maisch T, Maier M, Landthaler M, Bäuml W. Direct detection of singlet oxygen generated by UVA irradiation in human cells and skin. *J Invest Dermatol*. 2007;127:1498–506.
19. Frimer AA. The Reaction of Singlet Oxygen with Olefins: The Question of Mechanism. *Chem Rev*. 1979;79(5):359–87.
20. Foote CS. Photosensitized Oxygenations and the Role of Singlet Oxygen. *Acc Chem Res*. 1968;1(4):104–10.
21. Manring LE, Kanner RC, Foote CS. Chemistry of Singlet Oxygen. 43. Quenching by Conjugated Olefins. *J Am Chem Soc*. 1983;105(14):4707–10.
22. Baptista MS, Cadet J, Di Mascio P, Ghogare AA, Greer A, Hamblin MR, et al. Type I and Type II Photosensitized Oxidation Reactions: Guidelines and Mechanistic Pathways. *Photochem Photobiol*. 2017;93(4):912–9.
23. Josefsen LB, Boyle RW. Photodynamic therapy and the development of metal-based photosensitisers. *Met Based Drugs*. 2008;2008.
24. Fahy E, Subramaniam S, Brown HA, Glass CK, Merrill AH, Murphy RC, et al. A comprehensive classification system for lipids. *J Lipid Res* [Internet]. 2005

- May;46(5):839–61. Available from:  
<https://linkinghub.elsevier.com/retrieve/pii/S0022227520339687>
25. Gutteridge JM. Lipid peroxidation and antioxidants as biomarkers of tissue damage. *Clin Chem [Internet]*. 1995 Dec;41(12 Pt 2):1819–28. Available from:  
<http://www.ncbi.nlm.nih.gov/pubmed/7497639>
  26. Barrera G. Oxidative stress and lipid peroxidation products in cancer progression and therapy. *ISRN Oncol [Internet]*. 2012;2012:137289. Available from:  
<http://www.pubmedcentral.nih.gov/articlerender.fcgi?artid=3483701&tool=pmcentrez&rendertype=abstract>
  27. Fahy E, Subramaniam S, Brown HA, Glass CK, Merrill AH, Murphy RC, et al. A comprehensive classification system for lipids. *J Lipid Res*. 2005 May;46(5):839–61.
  28. Dyall SC, Balas L, Bazan NG, Brenna JT, Chiang N, da Costa Souza F, et al. Polyunsaturated fatty acids and fatty acid-derived lipid mediators: Recent advances in the understanding of their biosynthesis, structures, and functions. *Prog Lipid Res [Internet]*. 2022;86(February):101165. Available from:  
<https://doi.org/10.1016/j.plipres.2022.101165>
  29. Niki E, Yoshida Y, Saito Y, Noguchi N. Lipid peroxidation: Mechanisms, inhibition, and biological effects. *Biochem Biophys Res Commun [Internet]*. 2005 Dec;338(1):668–76. Available from:  
<https://linkinghub.elsevier.com/retrieve/pii/S0006291X05017766>
  30. Ayala A, Muñoz MF, Argüelles S. Lipid Peroxidation: Production, Metabolism, and Signaling Mechanisms of Malondialdehyde and 4-Hydroxy-2-Nonenal. *Oxid Med Cell Longev [Internet]*. 2014;2014:1–31. Available from:  
<http://www.hindawi.com/journals/omcl/2014/360438/>



31. Esterbauer H, Schaur RJ, Zollner H. Chemistry and biochemistry of 4-hydroxynonenal, malonaldehyde and related aldehydes. *Free Radic Biol Med*. 1991;11(1):81–128.
32. Bacellar IOL, Oliveira MC, Dantas LS, Costa EB, Junqueira HC, Martins WK, et al. Photosensitized Membrane Permeabilization Requires Contact-Dependent Reactions between Photosensitizer and Lipids. *J Am Chem Soc* [Internet]. 2018 Aug 10;140(30):9606–15. Available from: <http://pubs.acs.org/doi/10.1021/jacs.8b05014>
33. Nagan N, Zoeller RA. Plasmalogens: biosynthesis and functions. *Prog Lipid Res* [Internet]. 2001 May;40(3):199–229. Available from: <https://linkinghub.elsevier.com/retrieve/pii/S0163782701000030>
34. Braverman NE, Moser AB. Functions of plasmalogen lipids in health and disease. *Biochim Biophys Acta* [Internet]. 2012 Sep;1822(9):1442–52. Available from: <https://linkinghub.elsevier.com/retrieve/pii/S0925443912001160>
35. Rog T, Koivuniemi A. The biophysical properties of ethanolamine plasmalogens revealed by atomistic molecular dynamics simulations. *Biochim Biophys Acta - Biomembr*. 2016;1858(1):97–103.
36. Gorgas K, Teigler A, Komljenovic D, Just WW. The ether lipid-deficient mouse: Tracking down plasmalogen functions. *Biochim Biophys Acta - Mol Cell Res* [Internet]. 2006 Dec;1763(12):1511–26. Available from: <https://linkinghub.elsevier.com/retrieve/pii/S0167488906002539>
37. Koivuniemi A. The biophysical properties of plasmalogens originating from their unique molecular architecture. *FEBS Lett*. 2017;591(18):2700–13.
38. Glaser PE, Gross RW. Plasmalogen ethanolamine facilitates rapid membrane fusion: A stopped-flow kinetic investigation correlating the propensity of a

- Major Plasma Membrane Constituent to Adopt an HII Phase with Its Ability to Promote Membrane Fusion. *Biochemistry* [Internet]. 1994 May 17;33(19):5805–12. Available from: <https://pubs.acs.org/doi/abs/10.1021/bi00185a019>
39. Zoeller RA, Lake AC, Nagan N, Gaposchkin DP, Legner MA, Lieberthal W. Plasmalogens as endogenous antioxidants: somatic cell mutants reveal the importance of the vinyl ether. *Biochem J* [Internet]. 1999 Mar 15;338(3):769–76. Available from: <http://www.pubmedcentral.nih.gov/articlerender.fcgi?artid=1220115&tool=pmcentrez&rendertype=abstract>
40. Zoeller RA, Grazia TJ, LaCamera P, Park J, Gaposchkin DP, Farber HW. Increasing plasmalogen levels protects human endothelial cells during hypoxia. *Am J Physiol Circ Physiol* [Internet]. 2002 Aug 1;283(2):H671–9. Available from: <https://www.physiology.org/doi/10.1152/ajpheart.00524.2001>
41. Broniec A, Klosinski R, Pawlak A, Wrona-Krol M, Thompson D, Sarna T. Interactions of plasmalogens and their diacyl analogs with singlet oxygen in selected model systems. *Free Radic Biol Med*. 2011;50(7):892–8.
42. Paul S, Lancaster GI, Meikle PJ. Plasmalogens: A potential therapeutic target for neurodegenerative and cardiometabolic disease. *Prog Lipid Res* [Internet]. 2019 Apr;74(April):186–95. Available from: <https://doi.org/10.1016/j.plipres.2019.04.003>
43. Murphy EJ, Schapiro MB, Rapoport SI, Shetty HU. Phospholipid composition and levels are altered in down syndrome brain. *Brain Res*. 2000;867(1–2):9–18.
44. Wallner S, Schmitz G. Plasmalogens the neglected regulatory and scavenging lipid species. *Chem Phys Lipids*. 2011;164(6):573–89.
45. Honsho M, Asaoku S, Fujiki Y. Posttranslational regulation of fatty acyl-CoA

- reductase 1, Far1, controls ether glycerophospholipid synthesis. *J Biol Chem.* 2010;285(12):8537–42.
46. Brites P, Waterham HR, Wanders RJA. Functions and biosynthesis of plasmalogens in health and disease. *Biochim Biophys Acta - Mol Cell Biol Lipids.* 2004;1636(2–3):219–31.
47. Steinberg SJ, Dodt G, Raymond G V., Braverman NE, Moser AB, Moser HW. Peroxisome biogenesis disorders. *Biochim Biophys Acta - Mol Cell Res.* 2006;1763(12):1733–48.
48. Braverman NE, Raymond G V., Rizzo WB, Moser AB, Wilkinson ME, Stone EM, et al. Peroxisome biogenesis disorders in the Zellweger spectrum: An overview of current diagnosis, clinical manifestations, and treatment guidelines. *Mol Genet Metab [Internet].* 2015;117(3):313–21. Available from: <http://dx.doi.org/10.1016/j.ymgme.2015.12.009>
49. Motley AM, Hetteema EH, Hogenhout EM, Brites P, ten Asbroek ALMA, Wijburg FA, et al. Rhizomelic chondrodysplasia punctata is a peroxisomal protein targeting disease caused by a non-functional PTS2 receptor. *Nat Genet [Internet].* 1997 Apr;15(4):377–80. Available from: <http://www.nature.com/doi/10.1038/nm0798-822>
50. Braverman NE, Steinberg SJ, Fallatah W, Duker A, Bober MB. Rhizomelic Chondrodysplasia Punctata Type 1 [Internet]. *GeneReviews®.* 1993. 1–24 p. Available from: <https://www.ncbi.nlm.nih.gov/books/NBK1270/>
51. Ford DA, Rosenbloom KB, Gross RW. The primary determinant of rabbit myocardial ethanolamine phosphotransferase substrate selectivity is the covalent nature of the sn-1 aliphatic group of diradyl glycerol acceptors. *J Biol Chem.* 1992;267(16):11222–8.

52. Stadelmann-Ingrand S, Favreliere S, Fauconneau B, Mauco G, Tallineau C. Plasmalogen degradation by oxidative stress: production and disappearance of specific fatty aldehydes and fatty  $\alpha$ -hydroxyaldehydes. *Free Radic Biol Med* [Internet]. 2001 Nov;31(10):1263–71. Available from: <http://linkinghub.elsevier.com/retrieve/pii/S0891584901007201>
53. Thompson DH, Inerowicz HD, Grove J, Sarna T. Structural Characterization of Plasmenylcholine Photooxidation Products. *Photochem Photobiol* [Internet]. 2003;78(4):323. Available from: [http://doi.wiley.com/10.1562/0031-8655\(2003\)078%3C0323:SCOPPP%3E2.0.CO;2](http://doi.wiley.com/10.1562/0031-8655(2003)078%3C0323:SCOPPP%3E2.0.CO;2)
54. Jenkins CM, Yang K, Liu G, Moon SH, Dilthey BG, Gross RW. Cytochrome c is an oxidative stress–activated plasmalogenase that cleaves plasmenylcholine and plasmenylethanolamine at the sn-1 vinyl ether linkage. *J Biol Chem*. 2018;293(22):8693–709.
55. Farquhar JW. Identification and gas-liquid chromatographic behavior of plasmalogen aldehydes and their acetal, alcohol, and acetylated alcohol derivatives. *J Lipid Res*. 1962;3(1):21–30.

## **Objective**

### **General objective**

Investigate deleterious and pro-oxidant effects of plasmalogen, focusing on the characterization of oxidation products and the impacts on membrane stability. Characterize different plasmalogen oxidation products by derivatization methods with fluorescent probes.

### **Specific objectives**

**Chapter 1:** To develop a purification method for plasmalogen phosphoethanolamine (pPE) and to obtain material for the next stages of the study.

**Chapter 2:** To study the pro-oxidant action of photo-oxidized plasmalogens through the formation of singlet molecular oxygen via photochemistry in the dark and the Russel mechanism.

**Chapter 3:** To study the reactivity of lipids extracted from photooxidized HaCat keratinocytes and to compare the reactivity of plasmalogens with other classes of membrane lipids. Compare the stability of photooxidation products and determine if plasmalogen hydroperoxides are less stable compared to other classes. Finally, a mimetic model of membranes will be used to analyze how plasmalogens alter the stabilized phototoxicity of membranes.

**Chapter 4:** To develop a sensitive method for the analysis of free fatty acids and apply it to blood plasma of amyotrophic lateral sclerosis (ALS) model rats supplemented with different diets.

## CHAPTER 1

### **A rapid and simple method to purify PE plasmalogens, cerebrosides and sulfatides from bovine or porcine brains**

Rodrigo Lucas de Faria<sup>1</sup> and Sayuri Miyamoto<sup>1\*</sup>

Department of Biochemistry, Institute of Chemistry, University of Sao Paulo,  
Sao Paulo, Brazil.

\* Corresponding Author: Sayuri Miyamoto. E-mail address:  
miyamoto@iq.usp.br

Institutional address: Departamento de Bioquímica, Instituto de Química,  
Av. Prof. Lineu Prestes 1524, CP 26077, CEP 05313-970, Butantã, São  
Paulo, SP. Brazil. Phone: + 55 1130911413

## Highlights

- Phosphatidylethanolamine plasmalogen purification with high purity.
- Using simple and quick methods.
- Simultaneously, cerebroside and sulfatide are obtained in high purity.
- Characterization of products by lipidomic analysis by high resolution mass spectrometry.
- Simpler alternative methods of plasmalogen analysis (TLC and HPLC).
- Identification of phosphatidylserine methyl ester plasmalogen.

**Abbreviations:**

**ARA**, arachidonic acid

**BHT**, Butylated hydroxytoluene

**DNPH**, dinitrophenylhydrazine

**HRMS**, high resolution mass spectrometry

**LPE**, Lyso phosphatidylethanolamine

**GPC**, Glycerophosphocholine

**GPE**, Glycerophosphatidylethanolamine

**NALD**, Neonatal adrenoleukodystrophy

**oPE**, Phosphatidylethanolamine plasmalogen

**PA**, Phosphatidic acid

**PE**, Phosphatidylethanolamine

**PI**, Phosphatidylinositol

**PLA1**, phospholipase A1

**pPE**, Phosphatidylethanolamine plasmalogen

**pPSMe**, Phosphatidylserine methyl ester plasmalogen

**PS**, Phosphatidylserine

**PUFAs**, Polyunsaturated fatty acids

**Q10**, Coenzyme Q or ubiquinone-10

**RCDP**, Rhizomelic punctate chondrodysplasia

**ROS**, Reactive oxygen species

**UHPLC**, ultra-high-performance liquid chromatography

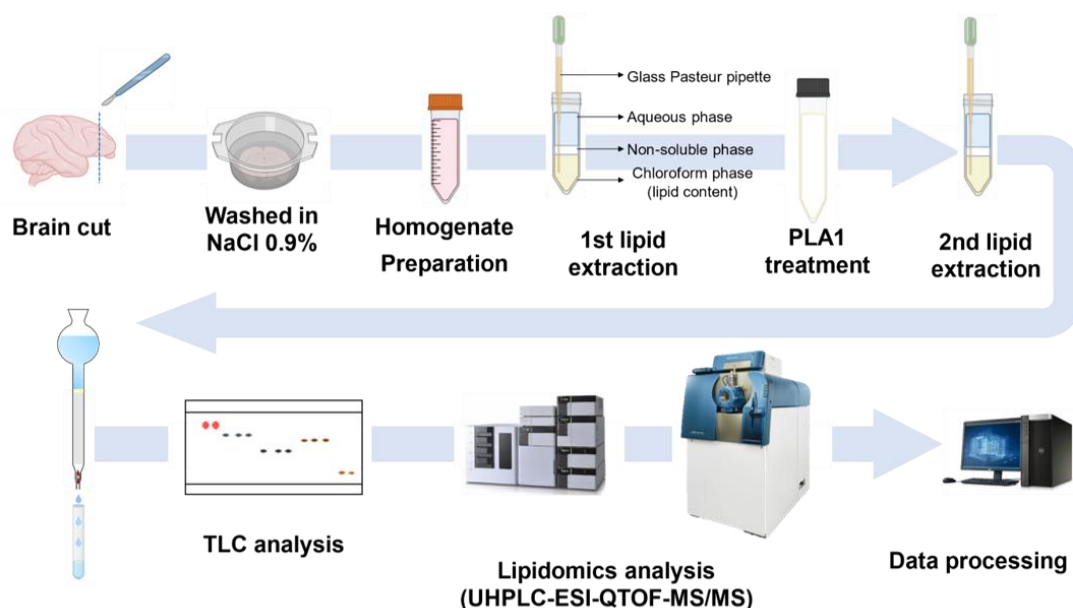
**TLC**, thin layer chromatography



## Abstract

Plasmalogens are phospholipids characterized by having a vinyl ether-type bond in the sn1 chain of glycerol. Plasmalogens are present in all human tissues and represent around 20% of all phospholipids. Many papers report that plasmalogens have antioxidant effects. However, it is still controversial, as many studies show that the oxidation of plasmalogens produces reactive aldehyde species that can have deleterious effects. Thus, further studies are needed, mainly *in vivo*, to confirm the antioxidant action of plasmalogens. However, plasmalogen are value-added lipids that make many studies expensive to perform. In this work, we describe a simple method of purifying plasmalogen from phosphoethanolamine (pPE) with approximately 80% purity from bovine or porcine brain using phospholipase A1 treatment and flash column-chromatography. Purified products were characterized by TLC and lipidomic analysis via high resolution mass spectrometry (HRMS). Besides the purification of pPE the method also allowed to obtain cerebrosides and sulfatides. Overall, this method provides an efficient and cost-effective approach to purifying lipids with added value that can enable studies that require good amounts of PE plasmalogen.

## Graphical abstract



## Introduction

Plasmalogens are present in all human tissues and represent approximately 20% of the total mass of phospholipids (1). The brain is the tissue with the highest amounts of phosphoethanolamine (PE) plasmalogens, representing up to 85 mol% of PE, or, 30 mol% of total phospholipids of these membranes (2).

Mutations on plasmalogen biosynthesis or low levels of plasmalogen have been associated with several genetic neurological and metabolic disorders (eg, rhizomelic punctate chondrodysplasia (RCDP), Zellweger syndrome, and neonatal adrenoleukodystrophy (NALD))(3). Furthermore, lower levels of plasmalogens have been implicated in a variety of disease states, including aging, Alzheimer's disease, Parkinson's disease, Down syndrome, and heart disease and/or myocardial infarction(4). However, some *in vitro* studies in cell models have shown that supplementation recovers plasmalogen levels and improves the response to oxidative stress or recovery of cellular activity(5).

Plasmalogens are characterized by the presence of a vinyl ether bond in the aliphatic chain at the sn-1 position of glycerol, while at the sn-2 position of glycerol it is esterified, in most cases, to polyunsaturated fatty acids (PUFAs)(4). Although the vinyl-ether bond at the sn-1 position is relatively resistant to enzymatic degradation, it is quite susceptible to oxidation induced by a variety of oxidizing reagents(6). Then, plasmalogens are generally considered as endogenous antioxidants and there are several studies highlighting the antioxidant action of plasmalogen in cell cultures and in experimental animals(4). However, the proposed mechanisms for its antioxidant effect are controversial. For example, plasmalogen reaction with reactive oxygen species (ROS) generates reactive products such as aldehydes(7,8). Additionally, recent studies have pointed out that plasmalogen confer sensitivity to ferroptosis by increasing cell susceptibility to lipid peroxidation(9,10). Therefore, plasmalogens antioxidant activity is still a matter of debate and more studies, especially *in vivo*, are needed to better understand the cellular consequences of plasmalogen oxidation before it can truly be

described as an endogenous antioxidant(11). Furthermore, Nishimukai et al(12) showed that rats fed a diet containing purified bovine brain phospholipids had a large increase in plasmalogen levels in blood plasma and liver.

Despite the great interest, commercial plasmalogens are costly and the purification methods are not productive and require robust equipment such as HPLC. Here, we report a rapid and easy purification of approximately 50 mg of purified pPE from 8 g tissue (bovine or porcine brain) in 2 days of work using common laboratory glassware and simple techniques. Furthermore, approximately 10 mg of sulfatides and 80 mg of cerebrosides can be obtained simultaneously during the purification. These sphingolipids are important for the integrity, formation and maintenance of myelin(13).

## **Materials and methods**

### **Materials**

The bovine (380 g) and porcine (92 g) brains was obtained from a local supplier and transported quickly, in ice-cold medium, to the laboratory and stored in -20°C. Phospholipase A1 from *Thermomyces lanuginosus*, sodium chloride, sodium phosphate monobasic, sodium phosphate dibasic, deferoxamine mesylate salt, 2,4-Dinitrophenylhydrazine (DNPH) from Sigma-Aldrich, USA. 18(Plasm)-18:1 PE Avanti Polar Lipids, USA.

### **Cleaning and preparing the homogenate**

The brain was placed in a beaker of adequate size and washed 3 times with saline solution (NaCl 9%). Plasmalogens are very reactive and oxidize easily, especially in the presence of metals such as iron present blood. The brain was cutter with a scalpel into pieces of approximately 1 cm<sup>3</sup>. The pieces were rinsed 3 times with saline solution. The pieces not used was store at -80°C, to prevent the pPE from degrading.

### **Preparing the homogenate**

In a 50 ml Falcon tube was add 8 g of wet tissue and PBS 10 mM pH 7.4 with desferrioxamine mesylate 0.1 mM until reaching the 40 ml. Caution, do not add the 40

ml PBS as the tissue is voluminous and may exceed the maximum volume of the Falcon tube.

Then, the Falcon tube content was passed to a 40 mL dounce tissue grinder. Better use more soft tissue grinder to not destroy the cells too much so that metals present in the interior start to oxidize the plasmalogen and degrade them.

### **Lipid extractions and treatment with phospholipase A1 (PLA1)**

In a heavy duty round bottom centrifuge tubes 35 mL was add 5 mL of 200mg/mL homogenate (1 g tissue) and 5 mL of methanol with ice-cold 10 mM BHT, then vortexed for 1 min. We recommend making 8 tubes simultaneously, to use all the homogenate prepared in the previous step. Then, was add 15 mL of chloroform: ethyl acetate (4:1, v/v) and vortexed for 30 s per tube and centrifuged (10000g, 5 min, 4°C). The lower phase was collected using a glass Pasteur pipette to a 500 mL conical flask.

The aqueous phase was re-extracted with additional 15 mL of chloroform: ethyl acetate (4:1, v/v) and pass to the conical flask. Avoid collecting the non-soluble phase, as it is mainly composed of protein and will make it difficult for the next steps. However, it is possible to remove it with a glass Pasteur pipette and the conical flask facilitates the removal of this unwanted phase.

The organic phase was passed to a 500 mL flask round and gently evaporate the solvent using a rotavapor instrument by slowly decreasing the pressure but keeping the bath temperature at 20°C. Avoid heating the bath to dry the solvent, prefer Rotavapor which has low temperature condensers such as -78°C (ethanol or acetone with dry ice).

To PLA1 treatment, was add 5 mL of chloroform: ethyl acetate (4:1, v/v) to transfer the lipids solution to a heavy duty round bottom centrifuge tube with screw caps of 15 mL, then rinsed with more 5 mL of chloroform: ethyl acetate solution. The lipid solution was dried with nitrogen gas stream while slowly rotating the tube at an inclined angle to produce a uniform lipid film. Then was add 15 ml of 20% PLA1 enzyme solution in 100 mM PBS pH 4.5. The tube was vortexed for 30 s and incubated in an ultrasonic bath at 50°C for 4 h. After the first 30 min it should form a white emulsion. After the PLA1

treatment, the tube was placed in an ice bath for 10 min to lower the temperature for a second extraction. Then the extraction was repeated and the dried lipid was stored overnight at -80 °C for flash column purification. In the first extraction was used 8 tubes and second is used 3 tubes.

### **Flash column purification**

The column (dimensions, O.D.x 2 cm x 30 cm) was packed with 10 g of silica gel by slurry method, in which silica gel is mixed with chloroform. The silica was dried in a hot air oven at 100°C for 1 hour. Then, was applied pressure to the column to compress the silica. The advantage of slurry methods is that they eliminate the formation of air bubbles in the column as it is compacted.

To remove de died lipid from round flask, was add 5 mL of chloroform and vortexed for 30 s. Then slowly applied to the silica column with the glass Pasteur pipette and rinsed the sample flask with more 2 mL of chloroform. We used for chromatography the eluents in table 1 and was collected the 10 mL fractions each. Do not use pressure to collect the first and second fractions as the column may crack. The fractions were monitored by TLC analysis, eluting with a solvent composed of chloroform / methanol / water (25/10/1; v / v / v) and applied 10 µL of each fraction for better visualization. The TLC plate was visualized by charring with H<sub>2</sub>SO<sub>4</sub> 50% in water, PE plasmalogen PE has 0.55, cerebrosides 0.58 and sulfatides 0.39. The fractions were combined and died by rotavapor instrument. After removing the solvent there will be a gelatinous solid to the PE plasmalogen and a white powder for sulfatides and cerebrosides.

### **TLC analysis**

In a 2 mL glass vial was add 100 uL of 1 mg/ml purified PE plasmalogen in CHCL<sub>3</sub> and 200 uL of chloroform/methanol (1:1, v/v) containing 0.1 M HCl. The solution was incubated at 37°C for 40 min and 400 rpm to cleave the vinyl binding from the plasmalogen(14). After treatment with HCl, all the pPE must be consumed and produce LPE. The plasmalogen consumption was monitored by TLC. For qualitative analyses, the TLC plate was stained with a solution of DNPH (4 g DNPH, 15 mL H<sub>2</sub>SO<sub>4</sub>, 20 mL

H<sub>2</sub>O, 50 mL ethanol). Spots containing plasmalogens appear yellow. For a better view, scan the plate and change the color to grayscale. It is not necessary to warm up to visualize with aldehyde staining. For quantification was followed as described by Reich et al. (15), the TLC plate was visualized by charring with H<sub>2</sub>SO<sub>4</sub> 50% in water and the plate was scanned and analyzed by Image J software (<http://rsbweb.nih.gov/ij/>).

### **HPLC analysis**

HPLC with PDA detection was performed using a Shimadzu HPLC system (Shimadzu, Japan) with two pump solvent delivery system (Model LC-20AD, Prominence Liquid Chromatograph, Shimadzu, Japan), automatic injector (Model SIL-20AC).

The analysis was performed under isocratic conditions in normal phase with a Hilic column (2.6 µm 100 Å, 100x2.1 mm), with a flow of 0.3 mL.min<sup>-1</sup> and temperature 40°C in isocratic mode of 37% Hexane: Isopropanol: H<sub>2</sub>O (360: 480: 89; v / v / v) and 63% Hexane: Isopropanol (360: 480; v / v), with absorbance monitored at 205 nm.

### **Lipidomics analysis**

Mass spectrometry was carried out using an TripleTOF 6600 (Sciex, Framingham, MA) mass spectrometer operating in information-dependent analysis (IDA). The ionization was by electrospray. The separation was performed using ultra-high performance liquid chromatography (UHPLC Nexera, Shimadzu, Kyoto, Japan) with two pump solvent delivery system (Model LC-30AD), automatic injector (Model SIL-30AC).

The liquid chromatography was performed in reverse-phase (CORTECS® C18 column, 1.6 µm, 2.1 mm i.d. × 100 mm, Waters®) with gradient elution of mobile phase A [water/acetonitrile (60:40)] and mobile phase B [isopropanol/acetonitrile/water (88:10:2)] both phases containing ammonium acetate or ammonium formate (final concentration of 10 mM) for experiments performed in negative or positive ionization mode, respectively. The gradient conditions used were 40% B to 100% B in 10 min and held for 2 min, then decreased from 100% to 40% B over 1 min and held at 40% B for 7 min. The injection volume was 2 µL, the flow rate was 0.200 mL/min, and column temperature was 35°C.

Before MS analysis, it is essential that the instrument is tuned according to the

manufacturers' protocols. When analyzing concentrated samples, it is important to make serial dilutions and start with the lowest concentration, otherwise contamination of the lines/ source can occur.

Source conditions: temperature 450°C; curtain gas, 25 psi; nebulizer and heater gases at 45 psi; The MS was operated in both positive and negative ionization modes, and the scan range set at a mass-to-charge ratio of 200–2000 Da. Data acquisition using Analyst® 1.7.1. Data for lipid molecular species identification and quantification was obtained by Information Dependent Acquisition (IDA®). The cycle time period of 1.05 s with 100 ms acquisition time for MS1 scan and 25 ms acquisition time to obtain the top 36 precursor ions. The ion spray voltage of –4.5 kV and 5.5 kV (for negative and positive modes, respectively) and the cone voltage at +/-80 V were set to analysis. The collision energies are set +/-50 V, typically required for MS/MS phospholipids.

### Data processing

Detected lipids were manually identified by MS/MS spectrum using PeakView®. Areas of identified lipids were obtained using MultiQuant® (version 3.0.2). For semi-quantification, the R-3.5.0 software was used. Briefly, the area of each identified lipid was divided by the area of its respective internal standard (**Table 1**), multiplied by the amount of internal standard added at the beginning of lipid extraction and, finally, corrected by the correction factor obtained from calibration curves. Data processing the MS/MS data was analyzed with PeakView®, and lipid molecular species were identified by an in-house manufactured

**Table 1:** Lipid classes normalized by the respective internal standards.

Lipid Class	PC	PE	PS	PG	PI	CL	AEG	Cer
Internal Standard	PC (17:0/17:0)	PE (17:0/17:0)	PC (17:0/17:0)	PG (17:0/17:0)	PC (17:0/17:0)	CL (4x14:0)	PC (17:0/17:0)	Cer (d18:1/17:0)
Lipid Class	SM	CE	Cholesterol	Q10	DAG	TAG	DAE	

<b>Internal</b>	SM	TAG	TAG	TAG	TAG	TAG	TAG
<b>Standard</b>	(d18:1/17:0)	(3x17:0)	(3x17:0)	(3x17:0)	(3x17:0)	(3x17:0)	(3x17:0)

## Results

### Cleaning and preparing the homogenate

The main objective of this study was to develop an efficient and easy purification protocol to obtain Plasmalogen PE in high purity (80%) using equipment commonly found in research laboratories. The protocol has been optimized to work with 8 g of tissue at a time and have approximately of 50 mg of pPE but also 10 mg of sulfatides and 80 mg of cerebroside are obtained (**Figure 1**. Diagram of the summarized procedure for purifying PE plasmalogens, sulfatides and cerebroside.).

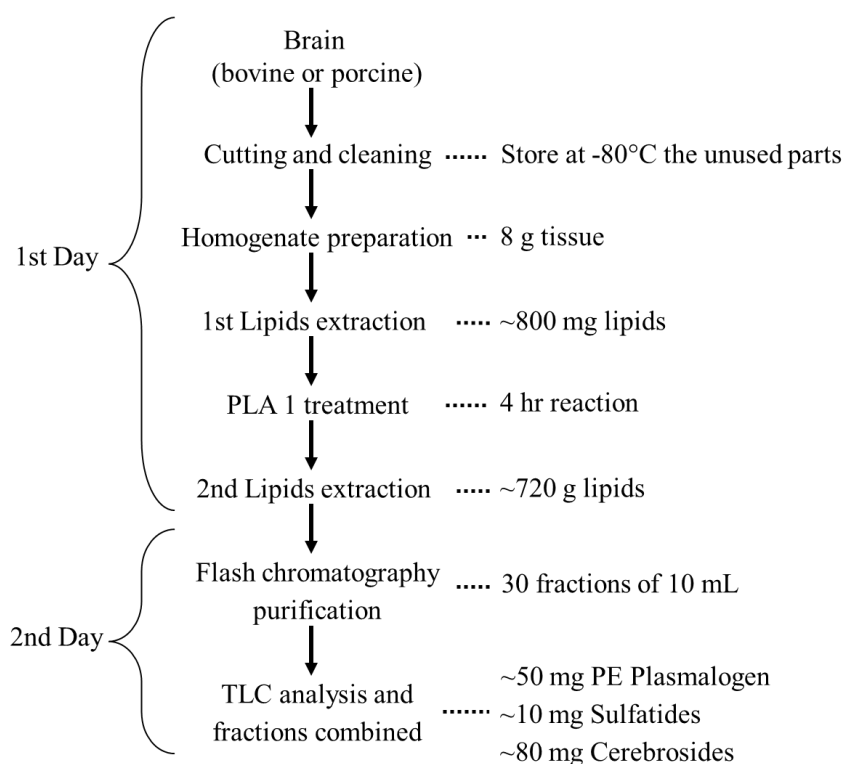


**Figure 1.** Diagram of the summarized procedure for purifying PE plasmalogens, sulfatides and cerebroside.

To expand the scope of possible animal brains, in this study, we performed purification of lipids of interest in bovine and porcine brains (**Figure 2**). The brain is the most enriched tissue in plasmalogen. We used porcine and bovine brain with



approximately 180 g 400 g, respectively.

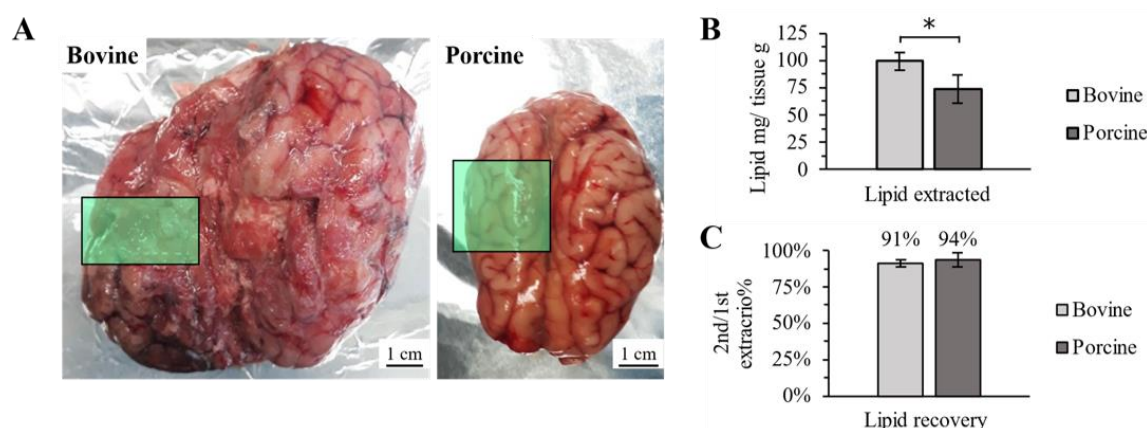


**Figure 2.** (A) Bovine and porcine brains, tissue used for purification indicated in green area ;(B) Lipid mass extracted by mass of wet tissue from bovine and porcine brain, (\* p-value <0.05); (C) Lipid recovery from 2nd extraction.

First, we washed the brain with ice-cold saline to remove residual blood, to prevent the iron present from oxidizing the plasmalogen(16). Then the brain was cut into smaller pieces using a scalpel or a very sharp knife, as the brain is a soft organ and unsharpened knives can mash it. Next, we prepared brain homogenate using a gentle tissue grinder such as Dounce or Potter-Elvehjem. Gentle tissue disruption is indicated to minimize cell disruption(17) and avoid the release of oxidants such as iron and enzymes that generate ROS (18). Brain pieces were homogenized with PBS, pH 7.4, containing deferoxamine, a highly selective iron chelating agent that completely silences the iron redox activity(19).

Tissue parts that are not used immediately can be stored in a -40°C or -80°C freezer for at least 90 days. However, avoid unnecessary thawing as plasmalogen can easily degrade.(20)

### **Lipid extractions and treatment with phospholipase A1 (PLA1)**

For lipid extraction, first we mixed the homogenate with methanol containing the antioxidant butylated hydroxytoluene (BHT) to the homogenate to prevent lipid peroxidation that can degrade plasmalogen. Then, we added chloroform/ethyl acetate

(4:1; v/v)(21) and collected the organic phase. Solvents were evaporated by rotary evaporator and the total amount of extracted lipids were quantified by weight. The bovine brain showed to be richer in lipids, with lipids corresponding to approximately 10% of the wet mass, while the porcine brain contained approximately 7.5%. (**Figure 2.B**).

Next, total lipid extracts were resuspended in PBS pH 5.5 and treated with phospholipase A1 (PLA1), which hydrolyzes the ester linkage in the sn1 chain of the glycerolipids. By this treatment, only the diacyl PE is hydrolyzed to lyso PE (LPE), while plasmalogens are kept intact. This procedure facilitates the separation of diacyl PE from plasmalogen by chromatography (22), because diacyl PE and plasmalogen, while LPE is much more polar (14). After PLA1 treatment, lipids were re-extracted with minimal loss (<10%) of total lipids (**Figure 2.C**).

We optimized the lipid extraction steps by reducing the waste of organic solvents in both extraction steps. The brain is the second the human organ that has highest amount of lipids, representing approximately 50% of its dry weight (23). Then, it was possible to use more tissue mass for less organic solvent, while tissue with a high protein content there is difficult the separation between the three phases (aqueous, insoluble and organic). In the 2nd extraction, only 1/3 of the volume of the 1st extraction is used, but always with clear phase separation (**Figure S1**).

### **Silica gel column purification**

After the second lipid extraction we have obtained approximately 720 mg of total lipid. This pool was purified by silica column (eluent gradient, Table 1) and 30 fractions of 10 mL were collected. Then we performed TLC analysis with a reference plasmalogen PE standard (pPE (p18/18:1)) to identify the fractions with PE plasmalogen. Five main bands were observed on TLC and identified by lipidomic analysis (next section) to be fractions enriched in cholesterol (2 to 5), cerebroside (7 to 9), sulfatides (11 to 14), PE plasmalogen(18 to 22) and lyso PE (24-26) (**Figure 3.A**).

These fractions were combined and evaporated by rotary evaporator to give relatively

pure cerebroside (approximately 80 mg of a white powder); sulfatide (approximately 10 mg of a white powder) and plasmalogen PE (50 mg of a colorless gelatinous solid) (**Figure 3.B**). The fraction containing cholesterol (160 mg), showed impurities of more non-polar species such as Q10 and other unidentified ones (**Figure 3.B**). The fraction enriched in LPE (5 mg) also presented impurities of more polar substances (data not shown). Overall, the purification method proved to be reproducible and there were no significant differences of lipid mass between bovine and porcine brains, however there is a tendency to obtain more cerebroside in bovine brain (**Figure 3.C**). The intermediate polarity of the lipid classes of interest (Plasmalogen PE, Cerebroside and Sulfatide) allows the use of simpler chromatographic methods and without the use of large amounts of eluent or collection of fractions with small volumes (less than 1 mL).

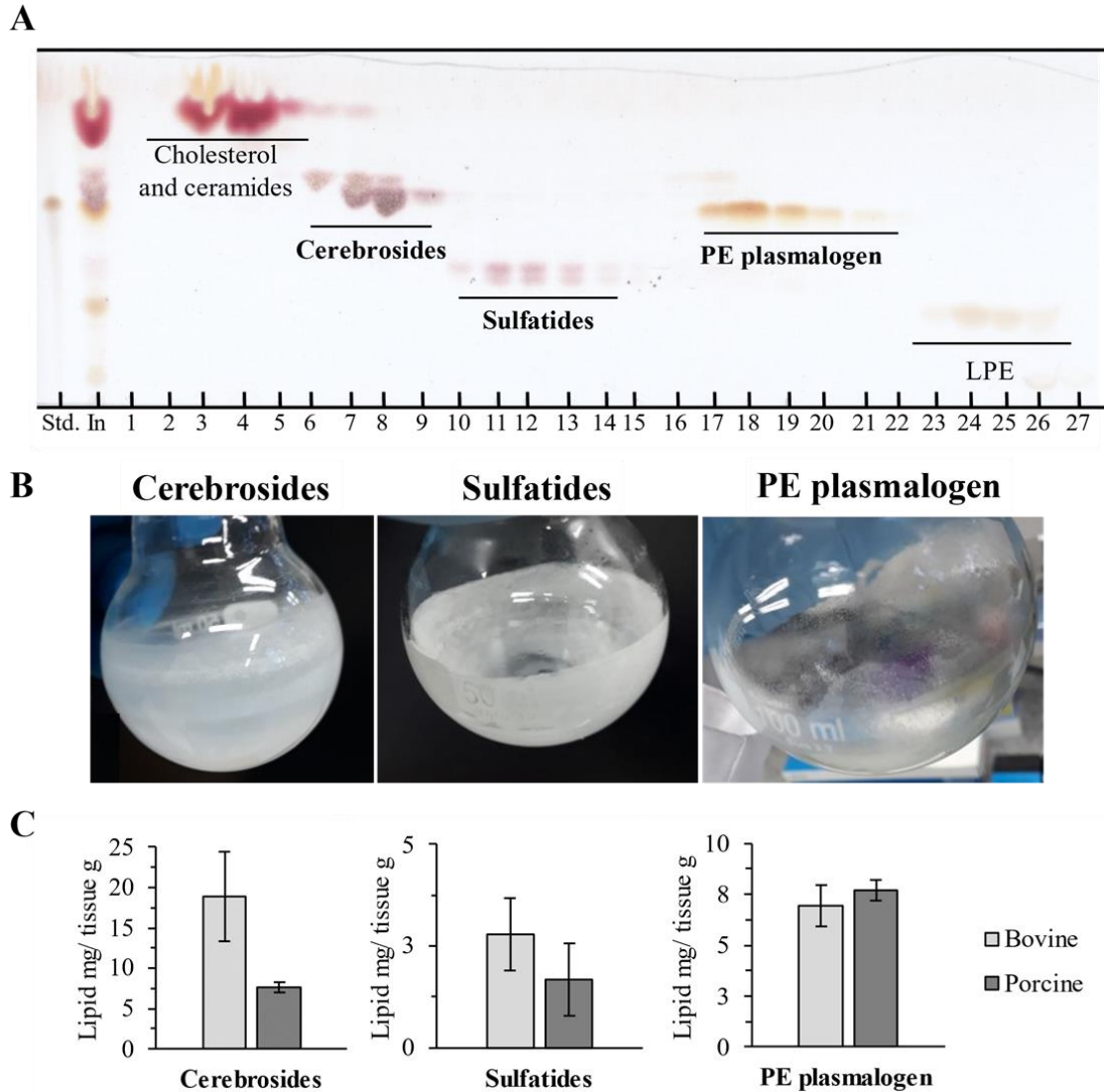


**Figure 3.** (A) TLC analysis of fractions collected from silica column. (In) lipid pool after treatment with initial PLA1; (Std.) pPE(p18/18:1) standard; (1 to 27) number of fractions collected from purification; (B) Physical appearance of purified lipids: cerebrosides and sulfatides are white powder and PE plasmalogen is colorless gelatinous solid; (C) Lipid mass ratio of purified lipids to the initial mass of wet tissue.

We optimized the protocol to work with the highest amount of starting tissue and found that 8 g of tissue is the most practical. Above this mass, we had problems purifying on a silica column.

## Lipidomic Analysis

To evaluate the efficacy of PLA1 treatment, we performed lipidomic analysis by UPLC-ESI-QTOF-MS/MS of the lipid pool before (1st extraction) and after PLA1 treatment (2nd extraction). We identified 194 different lipids (**complementary table S1**). As expected, the PLA1 treatment converted diacyl PE into LPE, without loss of PE plasmalogen (**Figure 4**).

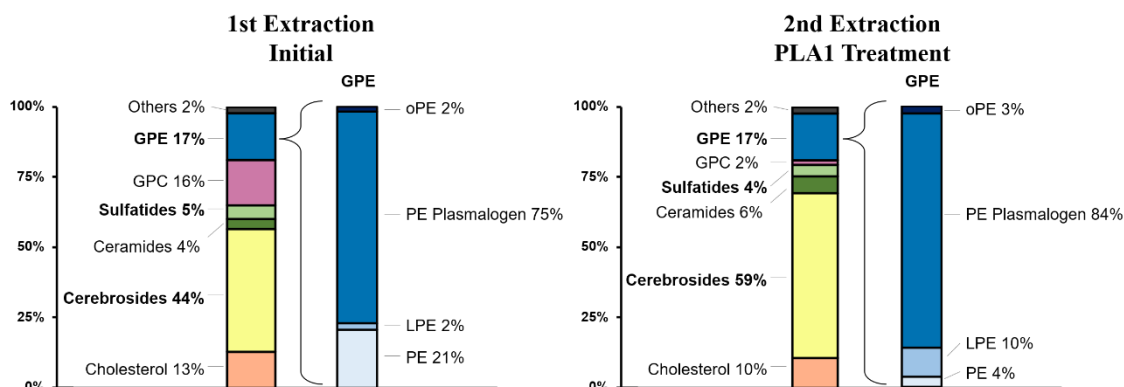


**Figure 4.** Bovine brain extract lipid composition before (1st extraction) and after PLA1 treatment (2nd extraction). Abbreviations: GPE (glycerophosphoethanolamines), PE (diacyl phosphoethanolamines), oPE (plasmanyl PE), LPE (lyso PE), PC (diacylphosphatidylcholine)

The fractions purified from PLA1-treated lipids by silica gel column chromatography were verified by TLC. Five main bands were observed (**Figure 3.A**) and submitted to lipidomic analysis to characterize the lipid composition of each band. The first band (fractions 2 to 5) is composed of more nonpolar lipids, mainly cholesterol (**Figure S2.B**). The second band (fractions 7 to 9) is composed mainly by cerebrosides and was obtained with purity of  $86 \pm 3\%$  and  $94 \pm 3\%$  from bovine and porcine brain, respectively. Even though there are many cerebrosides with a significant difference between bovine and porcine brains, the composition of the most abundant cerebrosides still similar. (**Figure 5.A**). The third band (fractions 10 to 14) is composed mainly by sulfatides and was obtained with a purity of  $83 \pm 3\%$  and  $81 \pm 4\%$  from bovine and porcine brain, respectively. The composition of sulfatides is similar for both brains

(Figure 5.B). The fourth band (fractions 18-22) is mainly composed of PE plasmalogens and was obtained with a purity of  $83 \pm 3\%$  and  $70 \pm 10\%$  from bovine and porcine brains respectively. The composition of plasmalogen PE is similar for both brains. The last group (fractions 23-26) and is mainly composed of LPE product of diacyl hydrolysis by the action of PLA1 (data not shown).

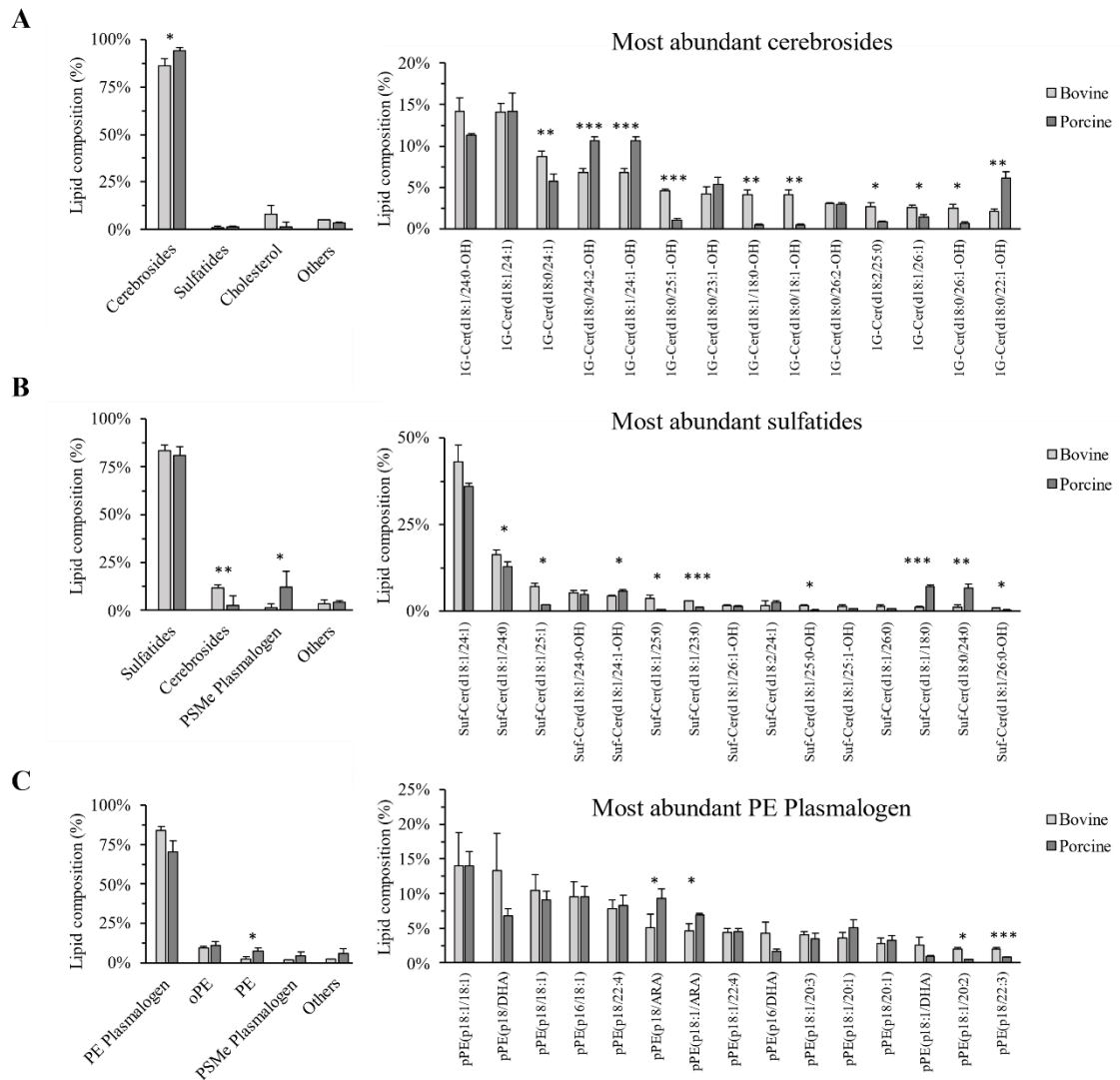


**Figure 5.** Lipid composition of purified lipids from bovine and porcine brains analyzed by UHPLC-ESI-QTOF-MS/MS. Purified lipids represented by lipid class (left) and the 15 most abundant species (right) of (A) Cerebrosides, (B) Sulfatides; (C) PE Plasmalogen. (\* p-value <0.05, \*\* p-value <0.01, \*\*\* p-value <0.001).

The purified plasmalogen fraction also contained minor amounts of plasmanil PE (oPE), an ether phospholipid analogue of plasmalogen that is distinguished by the absence of a double bond on the carbon adjacent to the ether bond (24), diacyl PE and plasmalogen of phosphatidylserine methyl ester (PSMe) (**Figure 5.C**).

### **Identification of plasmalogen of phosphatidylserine methyl ester (PSMe) by MS/MS**

We found 14 lipids in purified samples of plasmalogen PE that showed the same fragmentation pattern (MS/MS spectrum) of plasmalogens and plasmanil, with 1 peak from fatty acid of the sn-2 chain and the lipid peak without the fatty acid (**Figure 6**). This unknown lipid has 3 characteristic peaks: 152.9958, 198.0173 and 165.9911.

The 152.9958 has been suggested a phospholipid-specific negative ion (25). However, it is more present in MS/MS spectra of phosphatidylinositol (PI), phosphatidic acid (PA) and phosphatidylserine (PS). The peaks 198.0173 and 165.9911 may belong to the polar head group and indicate that there is a neutral loss of 32.0273 which corresponds to MeOH. Then, these phospholipids could be PS methyl ester (PSMe).

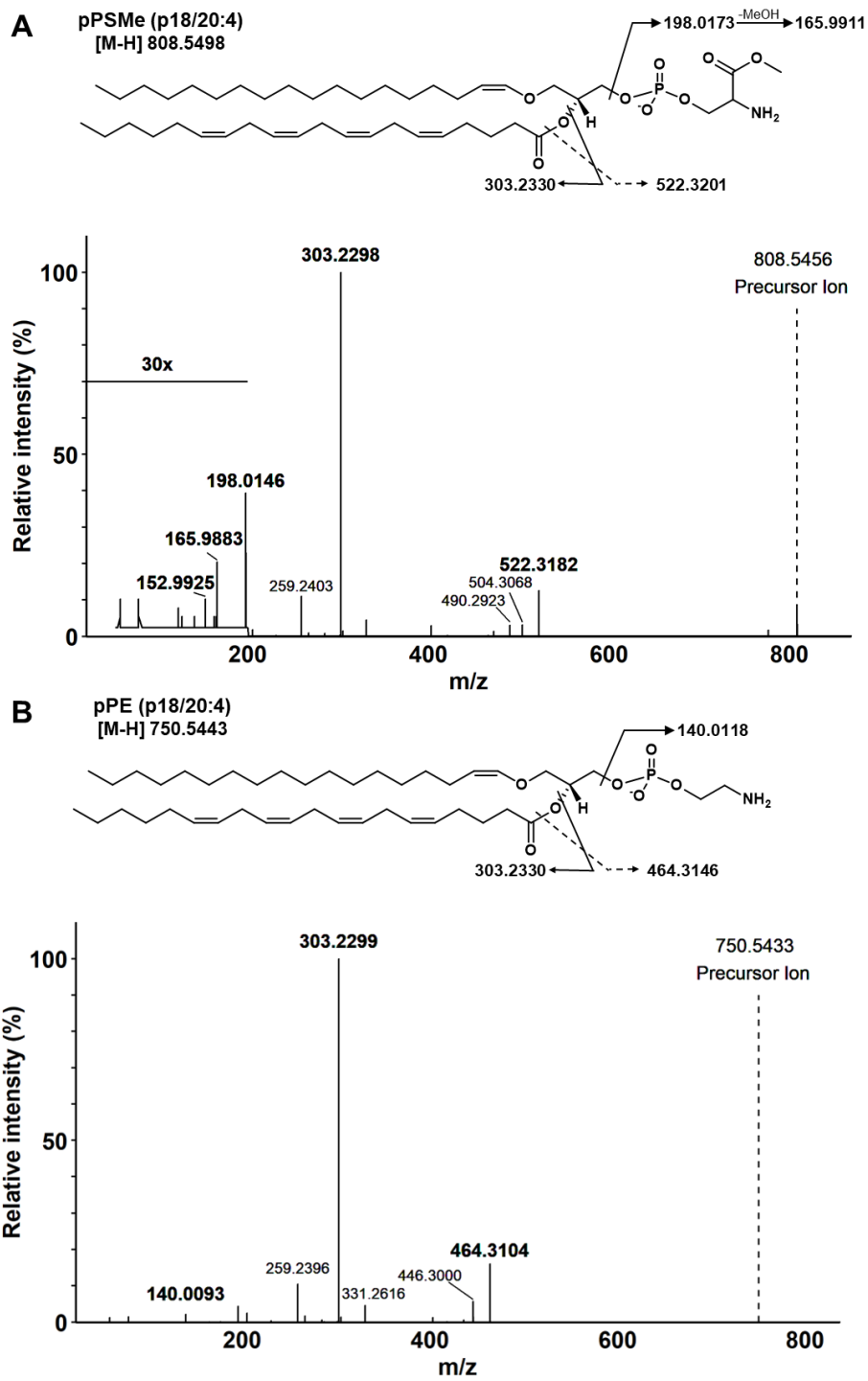


**Figure 6.** MS/MS spectrum (A) PSMe Plasmalogen (p18/ARA); (B) PE Plasmalogen pPE (p18/ARA).



## **Alternative qualitative and quantitative analysis of PE plasmalogen by TLC or UHPLC**

Mass spectrometry is used in this work to obtain accurate composition of purified products. However, lipidomic analysis is an expensive method. Alternatively, TLC analysis can be used as a rapid and low-cost test to characterize the purified plasmalogen. Plasmalogens are degraded into LPE and fatty aldehydes under acidic conditions (14). Thus, pPE are easily detected by charring TLC plates with DNPH in acidic medium. Using this staining slightly yellowish spots appears when plasmalogens are present. For better visualization of the colored bands, it is recommended to desaturate the image (**Figure 7A**).

The TLC can be charring with acid and the purity of pPE can be estimated by samples treated with acid, see in methods, in (**Figure 7B**) the plasmalogen purity is proximally 80%, close as in mass spectrometry. Acid-treated samples can also be analyzed by UHPLC at 205 nm (**Figure 7C**) and resulting in a purity of proximally 76%, slightly lower than mass spectrometry.

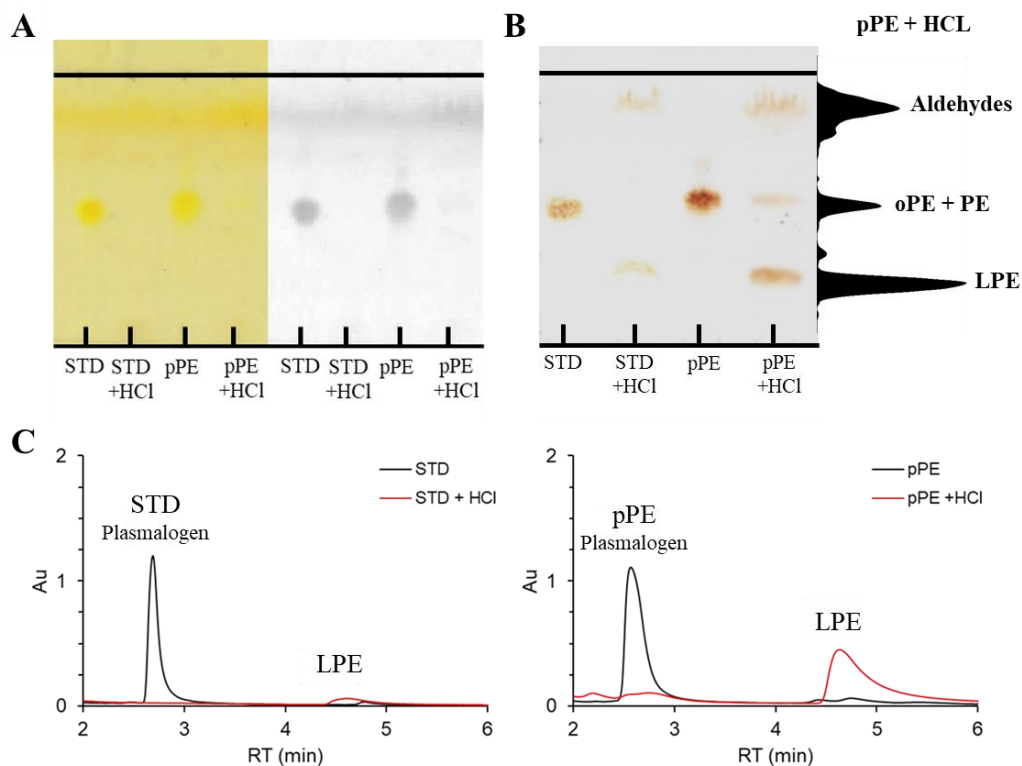


**Figure 7:** TLC analysis of PE plasmalogen standard [PE (p18/18:1)] (STD) and purified PE plasmalogen (pPE) before and after hydrolysis with 0.05 M HCl at 37 °C for 40 min. (A) TLC plate revealed with acidic DNPH solution showing plasmalogen as yellow spots; (B) TLC showing brown lipid bands formed by the carbonization of the original TLC plate, right: graphical representations of the purified plasmalogen sample after hydrolyzing with HCl; (C) Typical HPLC chromatogram at 205 nm of PE (p18/18:1) standard and purified plasmalogen before and after HCl treatment.

## Discussion

We describe here in detail a simple, robust and reproducible protocol for a bovine and porcine brain plasmalogen purification protocol. The protocol was optimized to obtain 50 mg of pPE in just 2 working days, in addition to being able to simultaneously purify 80 mg of cerebrosides and 10 mg of sulfatides. Cerebrosides and sulfatides are costly glycosphingolipids and are important lipids for the development, integrity and maintenance of myelin(13).The methods described in the literature for plasmalogen PE

purification are less efficient, as they are not very productive and use large amounts of solvent and robust equipment such as HPLC(22,26). In this work we verified the efficacy of PLA1 treatment to hydrolyze diacyl PE while keeping PE plasmalogens intact by lipidomic analysis (**Figure 5.**). PLA1 treatment converted diacyl PE species to LPE which facilitates the purification of plasmalogen species (**Figure 3.A**). Finally, we analyzed the purified products and quantified the purity of the purified product by high resolution mass spectrometry (**Figure 5**).

This purification protocol has few steps and requires less than 1L of organic solvent from 8 g of wet tissue. In addition to reduce the amount of organic solvent in the extraction steps, we also opted for silica column purification, this method purifies more products using less time and eluent (organic solvent) than HPLC. During the 1960s and 1970s, silica column purification techniques were widely used to separate lipid mixtures into their component parts in order to obtain milligram lipid classes for characterization studies (27). However, with more sensitive characterization methods that require fewer samples, this type of purification method has become less used. Due to the difficulty of replicating this type of chromatography, as changes in column dimensions, type of silica and even packaging method can change reproducibility(27). To reduce these difficulties, we describe in detail the entire silica column purification method, which resulted in very reproducible purifications.

Reducing the amount of solvent may have lost efficiency in lipid extraction, mainly for PC, SM and PS. However, the levels of PE and Cerebrosides and Sulfatides are proportional to those expected for human brains(28).

We identified a type of phosphatidylserine plasmalogen whose serine carboxyl group is methylated (PSMe) (**Figure 6.**) in the purified PE plasmalogen fractions. There are few studies on this type of phospholipid, but it is known that methylated PS does not induce apoptosis(29). This might be relevant in a neuron context. However, analysis with standards stills needed to truly ensure the structure and pattern of fragmentation.

Lipidomic analyzes are expensive, time-consuming and difficult. For this reason,

we describe here other simpler methods by TLC and HPLC analysis that facilitate the quantification and identification of plasmalogens in the purified fractions. Therefore, this protocol can be widely used by different types of laboratories.

### **Acknowledgments:**

This work was supported by FAPESP [CEPID-Redoxoma 2013/07937-8, FAPESP DD 2017/16140-7 to Faria, R.L.], CNPq [Miyamoto, S. 424094/2016-9, Di Mascio, P. 302120/2018-1], Capes and Pró-Reitoria de Pesquisa da USP.

### **References**

1. Braverman NE, Moser AB. Functions of plasmalogen lipids in health and disease. *Biochim Biophys Acta - Mol Basis Dis* [Internet]. 2012 Sep;1822(9):1442–52. Available from: <https://linkinghub.elsevier.com/retrieve/pii/S0925443912001160>
2. Han X, Holtzman DM, McKeel DW. Plasmalogen deficiency in early Alzheimer's disease subjects and in animal models: molecular characterization using electrospray ionization mass spectrometry. *J Neurochem*. 2001;77:1168–80.
3. Steinberg SJ, Dodt G, Raymond G V., Braverman NE, Moser AB, Moser HW. Peroxisome biogenesis disorders. *Biochim Biophys Acta - Mol Cell Res*. 2006;1763(12):1733–48.
4. Nagan N, Zoeller RA. Plasmalogens: biosynthesis and functions. *Prog Lipid Res* [Internet]. 2001 May;40(3):199–229. Available from: <https://linkinghub.elsevier.com/retrieve/pii/S0163782701000030>
5. Paul S, Lancaster GI, Meikle PJ. Plasmalogens: A potential therapeutic target for neurodegenerative and cardiometabolic disease. *Prog Lipid Res* [Internet]. 2019 Apr;74(April):186–95. Available from: <https://doi.org/10.1016/j.plipres.2019.04.003>

6. Broniec A, Klosinski R, Pawlak A, Wrona-Krol M, Thompson D, Sarna T. Interactions of plasmalogens and their diacyl analogs with singlet oxygen in selected model systems. *Free Radic Biol Med*. 2011;50(7):892–8.
7. Stadelmann-Ingrand S, Favreliere S, Fauconneau B, Mauco G, Tallineau C. Plasmalogen degradation by oxidative stress: production and disappearance of specific fatty aldehydes and fatty  $\alpha$ -hydroxyaldehydes. *Free Radic Biol Med* [Internet]. 2001 Nov;31(10):1263–71. Available from: <http://linkinghub.elsevier.com/retrieve/pii/S0891584901007201>
8. Felde R, Spiteller G. Plasmalogen Oxidation in Human Serum-Lipoproteins. *Chem Phys Lipids*. 1995;76(2):259–67.
9. Zou Y, Henry WS, Ricq EL, Graham ET, Phadnis V V., Maretich P, et al. Plasticity of ether lipids promotes ferroptosis susceptibility and evasion. *Nature* [Internet]. 2020;585(7826):603–8. Available from: <http://dx.doi.org/10.1038/s41586-020-2732-8>
10. Cui W, Liu D, Gu W, Chu B. Peroxisome-driven ether-linked phospholipids biosynthesis is essential for ferroptosis. *Cell Death Differ* [Internet]. 2021;28(8):2536–51. Available from: <http://dx.doi.org/10.1038/s41418-021-00769-0>
11. Broniec A, Źądło A, Pawlak A, Fuchs B, Kłosiński R, Thompson D, et al. Interaction of plasmalogen with free radicals in selected model systems. *Free Radic Biol Med* [Internet]. 2017;106(February):368–78. Available from: <http://linkinghub.elsevier.com/retrieve/pii/S0891584917300904>
12. Nishimukai M, Wakisaka T, Hara H. Ingestion of plasmalogen markedly increased plasmalogen levels of blood plasma in rats. *Lipids* [Internet]. 2003 Dec;38(12):1227–35. Available from: <http://doi.wiley.com/10.1007/s11745-003-1183-9>
13. Coetzee T, Fujita N, Dupree J, Shi R, Blight A, Suzuki K, et al. Myelination in the Absence of Galactocerebroside and Sulfatide: Normal Structure with Abnormal

- Function and Regional Instability. *Cell* [Internet]. 1996 Jul;86(2):209–19.  
Available from: <https://linkinghub.elsevier.com/retrieve/pii/S0092867400800938>
14. Saitoh M, Itoh M, Takashima S, Mizuguchi M, Iwamori M. Phosphatidyl ethanolamine with increased polyunsaturated fatty acids in compensation for plasmalogen defect in the Zellweger syndrome brain. *Neurosci Lett*. 2009;449(3):164–7.
  15. Reich A, Schwudke D, Meurer M, Lehmann B, Shevchenko A. Lipidome of narrow-band ultraviolet B irradiated keratinocytes shows apoptotic hallmarks. *Exp Dermatol*. 2010;19(8):103–10.
  16. Willmore LJ, Triggs WJ. Iron-induced lipid peroxidation and brain injury responses. *Int J Dev Neurosci* [Internet]. 1991;9(2):175–80. Available from: <http://doi.wiley.com/10.1016/0736-5748%2891%2990009-B>
  17. Matsumoto A. Isolated and electron microscopic observations of intracytoplasmic inclusions containing *Chlamydia psittaci*. *J Bacteriol*. 1981;145(1):605–12.
  18. Alves de Almeida E, Celso Dias Bainy A, Paula de Melo Loureiro A, Regina Martinez G, Miyamoto S, Onuki J, et al. Oxidative stress in *Perna perna* and other bivalves as indicators of environmental stress in the Brazilian marine environment: Antioxidants, lipid peroxidation and DNA damage. *Comp Biochem Physiol Part A Mol Integr Physiol* [Internet]. 2007 Apr;146(4):588–600. Available from: <https://linkinghub.elsevier.com/retrieve/pii/S1095643306001644>
  19. Chen J, Marks E, Lai B, Zhang Z, Duce JA, Lam LQ, et al. Iron Accumulates in Huntington's Disease Neurons: Protection by Deferoxamine. Skoulakis EMC, editor. *PLoS One* [Internet]. 2013 Oct 11;8(10):e77023. Available from: <https://dx.plos.org/10.1371/journal.pone.0077023>
  20. Chen Z, Jia J, Wu Y, Chiba H, Hui S-P. LC/MS Analysis of Storage-Induced Plasmalogen Loss in Ready-to-Eat Fish. *Food Chem* [Internet]. 2022 Feb;132320. Available from: <https://doi.org/10.1016/j.foodchem.2022.132320>

21. Yoshida Y, Kodai S, Takemura S, Minamiyama Y, Niki E. Simultaneous measurement of F2-isoprostane, hydroxyoctadecadienoic acid, hydroxyeicosatetraenoic acid, and hydroxycholesterols from physiological samples. *Anal Biochem* [Internet]. 2008 Aug;379(1):105–15. Available from: <https://linkinghub.elsevier.com/retrieve/pii/S0003269708002509>
22. Hirashima Y, Farooqui AA, Murphy EJ, Horrocks LA. Purification of plasmalogens using *Rhizopus delemar* lipase and *Naja naja naja* phospholipase A2. *Lipids* [Internet]. 1990 Jun;25(6):344–8. Available from: <http://doi.wiley.com/10.1007/BF02544345>
23. Hamilton JA, Hillard CJ, Spector AA, Watkins PA. Brain Uptake and Utilization of Fatty Acids, Lipids and Lipoproteins: Application to Neurological Disorders. *J Mol Neurosci* [Internet]. 2007 Sep 10;33(1):2–11. Available from: <http://link.springer.com/10.1007/s12031-007-0060-1>
24. Zoeller RA, Lake AC, Nagan N, Gaposchkin DP, Legner MA, Lieberthal W. Plasmalogens as endogenous antioxidants: somatic cell mutants reveal the importance of the vinyl ether. *Biochem J* [Internet]. 1999 Mar 15;338(3):769–76. Available from: <http://www.pubmedcentral.nih.gov/articlerender.fcgi?artid=1220115&tool=pmcentrez&rendertype=abstract>
25. Pulfer M, Murphy RC. Electrospray mass spectrometry of phospholipids. *Mass Spectrom Rev* [Internet]. 2003 Sep;22(5):332–64. Available from: <https://onlinelibrary.wiley.com/doi/10.1002/mas.10061>
26. MAWATARI S, YUNOKI K, SUGIYAMA M, FUJINO T. Simultaneous Preparation of Purified Plasmalogens and Sphingomyelin in Human Erythrocytes with Phospholipase A 1 from *Aspergillus oryzae*. *Biosci Biotechnol Biochem* [Internet]. 2009 Dec 23;73(12):2621–5. Available from: <https://academic.oup.com/bbb/article/73/12/2621-2625/5947937>
27. Hanahan DJ. *A Guide to Phospholipid Chemistry* [Internet]. Oxford University

Press; 1997. Available from:

<https://oxford.universitypressscholarship.com/view/10.1093/oso/9780195079814.001.0001/isbn-9780195079814>

28. Krafft C, Neudert L, Simat T, Salzer R. Near infrared Raman spectra of human brain lipids. *Spectrochim Acta Part A Mol Biomol Spectrosc* [Internet]. 2005 May;61(7):1529–35. Available from:  
<https://linkinghub.elsevier.com/retrieve/pii/S1386142504005852>
29. Uchida K, Emoto K, Daleke DL, Inoue K, Umeda M. Induction of Apoptosis by Phosphatidylserine. *J Biochem* [Internet]. 1998 Jun 1;123(6):1073–8. Available from: <https://academic.oup.com/jb/article-lookup/doi/10.1093/oxfordjournals.jbchem.a022045>



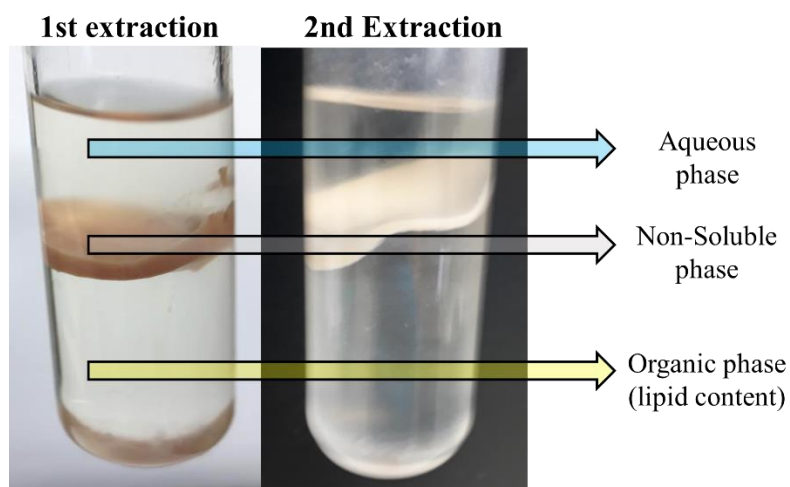


**Figure S1.** Extraction tube after centrifugation during the 1st and 2nd lipid extraction, the arrows indicate the three phases formed: aqueous, insoluble and organic (lipid content).

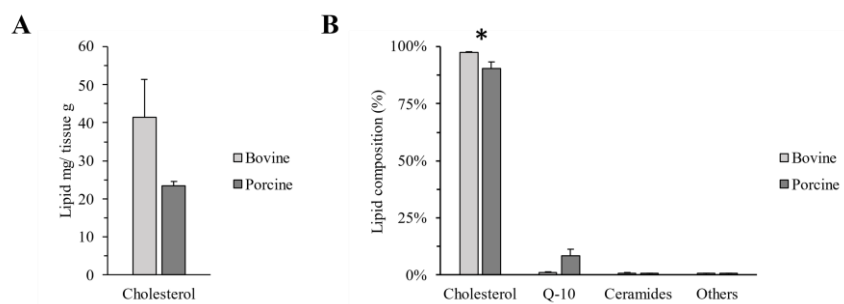


**Figure S2.** (A) Ratio of the lipid mass of purified lipids to the initial mass of wet tissue; (B) Lipid composition of fraction 2 to 5 analyzed by UHPLC-ESI-QTOF-MS/MS (\* p-value <0.05).

## Supplementary Table:

**Table S1:** Lipid composition of 1st and 2nd extraction from bovine brain.

Lipideos	1st Extraction	2ndExtraction	Lipideos	1st Extraction	2ndExtraction	Lipideos	1st Extraction	2ndExtraction
1G-AEG (o16/16:0)	4.202	103.316	Sulf cer (d18:1/26:1-OH)	0.032	0.383	PE (18:1/DHA)	55.6	3,119.7
1G-AEG (o16/18:0)	0.005	0.084	Sulf cer (d18:1/27:1-OH)	0.005	0.046	pPE (p16/18:1)	38,806.9	50,921.4
1G-AEG (o16/20:1)	0.014	0.231	Sulf cer (d18:2/24:1)	0.046	0.084	pPE (p16/20:1)	43,721.4	58,652.8
1G-AEG (o18/20:1)	0.106	1.119	Sulf cer (d18:2/25:1)	0.003	0.497	pPE (p16/20:2)	41,339.0	74,195.3
1G-cer (d18:0/18:1-OH)	1.005	8.631	Sulf cer (d18:2/26:1)	0.005	0.062	pPE (p16/20:3)	9,474.9	6,110.4
1G-cer (d18:0/20:1-OH)	0.023	0.128	Sulf cer (d18:2/26:1-OH)	0.006	0.064	pPE (p16/22:1)	1,555.8	1,182.6
1G-cer (d18:0/22:1-OH)	0.528	3.380	cer (d18:0/18:0)	0.171	0.404	pPE (p16/22:3)	5,528.0	1,141.2
1G-cer (d18:0/23:1-OH)	1.141	8.314	cer (d18:0/24:1)	0.346	1.102	pPE (p16/22:4)	24,291.2	25,024.7
1G-cer (d18:0/24:1-OH)	4.483	34.812	cer (d18:1/16:0)	2.618	56.814	pPE (p16/ARA)	9,912.3	6,187.2
1G-cer (d18:0/24:2-OH)	2.015	13.386	cer (d18:1/18:0)	5.408	15.442	pPE (p16/DHA)	49,037.9	12,089.0
1G-cer (d18:0/25:1-OH)	1.505	10.479	cer (d18:1/20:0)	1.293	2.349	pPE (p17/18:1)	35.2	348.9
1G-cer (d18:0/26:1-OH)	0.694	4.416	cer (d18:1/22:0)	0.069	0.280	pPE (p17/20:1)	60,317.0	66,571.2
1G-cer (d18:0/26:2-OH)	0.729	4.773	cer (d18:1/23:0)	0.102	0.404	pPE (p17/22:4)	2,211.3	3,061.0
1G-cer (d18:1/18:0)	0.317	3.135	cer (d18:1/23:1)	0.126	0.681	pPE (p17/DHA)	2,947.8	1,745.4
1G-cer (d18:1/22:0)	0.235	1.972	cer (d18:1/24:0)	0.346	1.102	pPE (p18/16:0)	1,889.2	2,236.5
1G-cer (d18:1/23:0)	0.526	4.251	cer (d18:1/24:1)	1.439	5.624	pPE (p18/18:1)	1,826.2	2,988.6
1G-cer (d18:1/24:0)	2.636	21.077	cer (d18:1/25:0)	0.071	0.160	pPE (p18/20:1)	667.0	578.0
1G-cer (d18:1/24:0-OH)	4.483	34.812	cer (d18:1/25:1)	0.153	0.501	pPE (p18/20:1)	667.0	578.0
1G-cer (d18:1/24:1)	0.660	5.399	cer (d18:1/26:0)	0.020	0.032	pPE (p18/22:1)	1,085.8	496.8
1G-cer (d18:1/24:1)	4.793	42.226	cer (d18:1/26:1)	0.107	0.294	pPE (p18/22:3)	2,264.0	408.1
1G-cer (d18:1/24:1-OH)	2.015	13.386	cer (d18:2/18:0)	0.830	1.249	pPE (p18/22:4)	43,203.6	35,927.4
1G-cer (d18:1/25:0)	0.763	5.455	cer (d18:2/22:0)	0.065	0.274	pPE (p18/24:3)	488.9	844.9
1G-cer (d18:1/25:1)	0.814	6.117	cer (d18:2/24:1)	0.081	0.256	pPE (p18/ARA)	33,724.9	14,985.1
1G-cer (d18:1/26:0)	0.267	1.644	cer (d18:2/25:0)	0.153	0.501	pPE (p18/DHA)	153,986.7	63,801.6
1G-cer (d18:1/26:1)	0.684	5.202	LPE (18:0)	0.004	0.010	pPE (p18/DPA)	43,855.3	33,115.4
1G-cer (d18:2/24:0-OH)	2.015	13.386	LPE (18:1)	0.945	6.748	pPE (p18:1/18:1)	41,339.0	74,195.3
1G-cer (d18:2/25:0)	0.814	6.117	LPE (20:1)	0.193	1.511	pPE (p18:1/19:1)	749.6	1,547.5
1G-OA-cer (d18:0+18:0/24:0-OH)	0.030	0.016	LPE (20:3)	0.056	0.040	pPE (p18:1/20:1)	12,345.2	20,087.2
1G-OA-cer (d18:1+16:0/24:0)	0.029	0.030	LPE (22:1)	0.004	0.013	pPE (p18:1/20:2)	9,789.9	8,419.0
1G-OA-cer (d18:1+16:0/24:0-OH)	0.066	0.001	LPE (22:2)	0.002	0.027	pPE (p18:1/20:3)	33,724.9	14,985.1
1G-OA-cer (d18:1+16:0/24:1)	0.066	0.018	LPE (22:3)	0.012	0.040	pPE (p18:1/21:1)	379.3	1,027.6
1G-OA-cer (d18:1+16:0/24:1-OH)	0.038	0.017	LPE (22:4)	0.601	2.504	pPE (p18:1/22:1)	1,542.7	918.2
1G-OA-cer (d18:1+18:0/24:0)	0.028	0.005	LPE (ARA)	0.584	0.203	pPE (p18:1/22:3)	43,203.6	35,927.4
1G-OA-cer (d18:1+18:0/24:1)	0.102	0.015	LPE (DHA)	3.367	2.815	pPE (p18:1/22:4)	43,855.3	33,115.4
1G-OA-cer (d18:1+18:1/24:0-OH)	0.084	0.027	LPE (DPA)	0.032	0.029	pPE (p18:1/24:1)	2,601.4	859.8
1G-OA-cer (d18:1+18:1/24:1)	0.062	0.010	LPE (16:0)	0.021	0.038	pPE (p18:1/24:3)	6,879.4	6,544.2
Acyl-1G-cer (d18:1/24:1+18:1)	0.022	0.009	LPE (16:1)	0.000	0.002	pPE (p18:1/24:4)	2,786.3	1,579.7
SM (d18:1/16:0)	0.560	13.097	LPE (18:1)	0.002	0.022	pPE (p18:1/ARA)	29,516.5	20,283.9
SM (d18:1/18:0)	14.741	48.368	LPE (22:3)	0.126	0.511	pPE (p18:1/DHA)	33,174.5	6,702.3
SM (d18:1/20:0)	3.213	5.523	LpPE (p16)	0.004	0.153	PC (16:0/16:0)	0.8	66.6
SM (d18:1/24:0)	5.238	24.174	LpPE (p18:1)	0.003	0.229	PC (16:0/16:1)	0.5	44.5
SM (d18:1/24:1)	3.890	39.236	oPE (o16/20:1)	4,356.478	1,558.654	PC (16:0/18:1)	2.3	341.9
SM (d18:1/25:1)	1.682	9.044	oPE (o16/22:3)	12,751.048	20,750.767	PC (16:0/DHA)	0.1	6.1
SM (d18:1/26:1)	0.842	5.424	oPE (o16/22:4)	5,527.971	1,141.242	PC (16:1/18:0)	2.3	341.9
Sulf cer (d18:0/22:0)	0.020	0.326	oPE (o16/DHA)	29,516.456	20,283.942	PC (18:0/18:1)	0.0	0.1
Sulf cer (d18:0/23:0-OH)	0.010	0.147	oPE (o18/20:1)	1,243.490	1,990.790	PC (18:0/ARA)	0.4	4.9
Sulf cer (d18:1/22:0)	0.038	0.417	oPE (o18/22:3)	1,542.696	918.184	PC (18:1/18:1)	0.1	9.1
Sulf cer (d18:1/22:0-OH)	0.013	0.093	oPE (o18/22:4)	7,018.028	9,407.962	PI (18:0/ARA)	289.0	5,150.1
Sulf cer (d18:1/22:1)	0.048	0.488	oPE (o18/DPA)	43,203.571	35,927.436	pPC (p18/16:0)	0.4	8.3
Sulf cer (d18:1/22:1-OH)	0.001	0.297	oPE (o18:0/DHA)	43,855.339	33,115.420	pPSM (p16/18:1)	0.0	0.2
Sulf cer (d18:1/23:0)	0.073	0.736	oPE(o18/22:1)	311.188	57.812	pPSM (p16/22:4)	0.4	9.5
Sulf cer (d18:1/23:0-OH)	0.015	0.355	PE (16:0/18:1)	1,441.765	15,082.921	pPSM (p16/DHA)	0.1	0.7
Sulf cer (d18:1/23:1)	0.014	0.149	PE (16:0/DHA)	0.064	1.536	pPSM (p18/18:1)	0.3	4.6
Sulf cer (d18:1/24:0)	0.494	6.013	PE (16:1/18:1)	337.493	1,205.628	pPSM (p18/20:1)	0.1	2.8
Sulf cer (d18:1/24:0-OH)	0.182	2.289	PE (18:0/18:1)	712.766	2,595.283	pPSM (p18/22:4)	0.2	2.3
Sulf cer (d18:1/24:1)	0.901	9.345	PE (18:0/20:1)	104.294	194.726	pPSM (p18/ARA)	0.4	9.5
Sulf cer (d18:1/24:1-OH)	0.065	0.797	PE (18:0/22:4)	945.311	6,137.493	pPSM (p18:1/18:1)	0.0	0.1
Sulf cer (d18:1/24:2-OH)	0.565	11.013	PE (18:0/ARA)	4,355.895	34,029.123	pPSM (p18:1/ARA)	0.1	2.1
Sulf cer (d18:1/25:0)	0.028	0.138	PE (18:0/DHA)	5,391.437	88,440.505	pPSM(p16/20:1)	0.3	4.6
Sulf cer (d18:1/25:0-OH)	0.021	0.211	PE (18:0/DPA)	260.881	3,317.597	pPSM(p18/18:1)	0.3	4.6
Sulf cer (d18:1/25:1)	0.119	1.260	PE (18:1/18:1)	1,606.752	19,719.419	pPSM(p18/DHA)	0.8	18.2
Sulf cer (d18:1/25:1-OH)	0.012	0.156	PE (18:1/18:2)	141.070	404.259	pPSM(p18:1/20:1)	0.3	4.4
Sulf cer (d18:1/26:0)	0.026	0.277	PE (18:1/20:1)	5.130	22.615	pPSM(p18:1/DHA)	0.3	2.4
Sulf cer (d18:1/26:0-OH)	0.021	0.181	PE (18:1/22:1)	551.610	1,138.019	pPSM(p20/18:1)	0.3	4.4
Sulf cer (d18:1/26:1)	0.133	1.740	PE (18:1/ARA)	223.896	3,359.369			

## CHAPTER 2

### **Plasmalogens pro-oxidant action by generation of singlet molecular O<sub>2</sub>(<sup>1</sup>Δg) and characterization of oxidation products by tandem mass spectrometry**

Rodrigo Lucas de Faria<sup>1</sup>, Fernanda Manso Prado<sup>1</sup>, Helena Couto Junqueira<sup>1</sup>, Karen Campos Fabiano<sup>1</sup>, Mauricio da Silva Baptista<sup>1</sup>, Paolo Di Mascio<sup>1</sup>, Sayuri Miyamoto<sup>1</sup>

1 Departamento de Bioquímica, Instituto de Química,  
Universidade de São Paulo, São Paulo, SP,

\* Corresponding Author: Sayuri Miyamoto. E-mail address:  
miyamoto@iq.usp.br

Institutional address: Departamento de Bioquímica, Instituto de Química, Av.  
Prof. Lineu Prestes 1524, CP 26077, CEP 05313-970, Butantã, São Paulo, SP.  
Brazil. Phone: + 55 1130911413

## Highlights

- Plasmalogens react efficiently with  $O_2(^1\Delta g)$  and produce two main products, dioxetanes and hydroperoxides.
- Dioxetanes produce  $O_2(^1\Delta g)$  and other excited species by chemiluminescence.
- Plasmalogen hydroperoxides are more reactive compared to other lipid hydroperoxides due to the adjacent ether and produce  $O_2(^1\Delta g)$ .
- Plasmalogen hydroperoxides when oxidized produce a new diacyl phospholipid that contains a fatty acid esterified with an alpha beta unsaturated carbonyl.

Plasmalogen hydroperoxides when reduced produce fatty aldehydes with alpha beta unsaturated carbonyl.

- Plasmalogen has a pro-oxidant action producing  $O_2(^1\Delta g)$  by two distinct and relevant mechanisms in the cellular environment.

**Abbreviations:**

**Ald 17:0**, Heptadecanal

**Ald 18:1  $\Delta$ 2**, Octadecenal

**Ald 16:0**, Hexadecanal

**Ald 16:1  $\Delta$ 2**, Hexedecanal

**ALDOPC**, 1-palmitoyl-2-(9'-oxo-nonanoyl)-sn-glycero-3-phosphocholine

**ARA**, Arachidonic acid

**CHH**, 7-(Diethylamino)coumarin-3-carbohydrazide

**Ce4+**, Ammonium cerium(IV) nitrate

**CHCl<sub>3</sub>**, Chloroform

**CSH**, Mercapto-4-methylcoumarin

**D<sub>2</sub>O**, Deuterium oxide

**DBA**, 9,10-Diphenylanthracene

**DMN**, 1,4-Dimethylnaphthalene

**DMNO<sub>2</sub>**, 1,4-Dimethylnaphthalene endoperoxides

**DPA**, 9,10-diphenylanthracene

**DPAO<sub>2</sub>**, 9,10-diphenylanthracene endoperoxides

**Fe<sup>2+</sup>**, Iron(II) sulfate hydrate

**GPx<sub>4</sub>**, Glutathione peroxidase 4

**HHE**, 4-hydroxy Hexenal

**HNE**, 4-hydroxy Nonenal

**HRMS**, high resolution mass spectrometry

**LPE**, Lyso phosphatidylethanolamine

**MB**, Methylene blue

**NIR**, Near-infrared

**PE**, phosphatidylethanolamine

**pPE**, PE plasmalogen

**pPE-OOH**, PE plasmalogen hydroperoxides

**Prdx6**, Peroxiredoxin-6

**PUFAs**, Polyunsaturated fatty acids

**ROS**, Reactive oxygen species

**RT**, Retention time

**UHPLC**, Ultra-high-performance liquid chromatography

**UVA**, Ultraviolet A

**TPP**, Triphenyl phosphine

## Abstract

Plasmalogens are glycerophospholipids with a vinyl-ether linkage at the sn-1 position of the glycerol backbone. Even though they are found in all human tissues, being especially abundant in the brain and heart, the biological role of plasmalogens remains unclear. It has been suggested that plasmalogens are antioxidants because of the high reactivity of their vinyl ether groups with reactive oxygen species (ROS). However, it has been suggested that when plasmalogens react with singlet oxygen ( $O_2(1\Delta_g)$ ), they produce two primary oxidation products: a hydroperoxyl and an unstable dioxetane intermediate. Dioxetanes can produce  $O_2(1\Delta_g)$  by transferring energy to molecular oxygen ( $O_2(3\Sigma_g^-)$ ). Herein, we describe evidence of the generation of  $O_2(1\Delta_g)$  from dioxetanes by chemical trapping and light emission at 1,270 nm. This is a strong indication of the monomolecular decay of  $O_2(1\Delta_g)$ . Furthermore, we also describe another route of  $O_2(1\Delta_g)$  production by the oxidation of plasmalogen hydroperoxides by cerium ( $Ce^{4+}$ ) and iron ( $Fe^{2+}$ ) ions, a process known as the Russell mechanism. The oxidation products were characterized by high-resolution tandem mass spectrometry (ESI-MS/MS) and it was determined that 98% of them form hydroperoxides. However, the degradation of hydroperoxides generates fatty diacyl phospholipids and aldehydes with alpha-beta unsaturated carbonyls that can bind to thiol groups by Michael addition. Although plasmalogens are considered antioxidants, this study shows that they can act as a pro-oxidant and generate other products with deleterious action.

**Keywords:** Plasmalogen, Singlet molecular oxygen, Plasmalogen Hydroperoxides, Plasmalogen oxidation mechanism.

## Introduction

Plasmalogens are glycerophospholipids with a vinyl-ether bond at the sn-1 position of the glycerol backbone and a sn-2 acyl chain enriched in polyunsaturated fatty acids [1], [2]. Plasmalogens are phospholipids found in all human tissues, including the membranes of neutrophils, eosinophils, and sperm. It is especially abundant in the brain and heart [1], [2]. Several pathologies are associated with defects in plasmalogen biosynthesis. Some examples are neurodegenerative diseases, Zellweger syndrome, and rhizomelic chondrodysplasia punctata [3]. *In vitro* studies in macrophages (RAW) and human pulmonary arterial endothelial cells (PAEC) deficient in plasmalogen biosynthesis have shown that they are more rapidly killed by oxidative stress than controls [4], [5].

Oxidative stress is defined as an imbalance between the generation of reactive species, such as free radicals and reactive oxygen species (ROS), and antioxidants that protect biomolecules against oxidative damage [6]. ROS damage can cause disturbances in cell metabolism, including DNA strand breakage and lipid peroxidation [7].

Several studies support the hypothesis that plasmalogens act as antioxidants due to the high reactivity of their vinyl ether groups with ROS [1], [4], [8]. Supposedly, the vinyl ether group is sacrificed to protect the PUFA in the sn-2 position [9], thus preventing lipid peroxidation.

It has been suggested that when plasmalogens react with  $O_2$  ( $^1\Delta g$ ), they produce two primary oxidation products: a hydroperoxyl and an unstable dioxetane intermediate [9]. Singlet oxygen ( $O_2$  ( $^1\Delta g$ )) exhibits substantial reactivity towards electron-rich organic molecules, including the plasmalogen



vinyl ether group. However, a robust characterization of the formation of dioxetanes is still lacking, and the relationship between the formation of hydroperoxides and dioxetanes is still unknown [9]–[11].

Unstable dioxetanes decompose rapidly by thermolysis, generating excited carbonyl. This excited species can decay to the ground state by emitting visible light, but they can also transfer energy to molecular oxygen ( $O_2(3\Sigma_g^-)$ ) producing  $O_2(1\Delta_g)$  [12], [13]. Therefore, it is not yet clear whether plasmalogens act as antioxidants, have an oxidative action, or both.

The energy transfer reaction from an electronically excited species to  $O_2(3\Sigma_g^-)$  producing  $O_2(1\Delta_g)$  without a photoexcited species is called "photochemistry in the dark." Here, we hypothesized that the oxidation of plasmalogen via  $O_2(1\Delta_g)$  can propagate oxidation reactions through "photochemistry in the dark," resulting in the production of a new molecule of  $O_2(1\Delta_g)$  (**figure 1, rote A**).

On the other hand, it is also proposed that plasmalogens oxidized via  $O_2(1\Delta_g)$  can produce hydroperoxides, which are also very harmful species. Lipid hydroperoxides can react in a biological system with free metal ions, heme proteins, or other oxidants and thereby generate highly reactive lipid radicals, including alkoxy and peroxy radicals [11]. Lipid peroxy radicals also produce  $O_2(1\Delta_g)$  by the Russell mechanism [10] (**figure 1 rote B**). Thus, the oxidation of plasmalogens via  $O_2(1\Delta_g)$  can propagate the oxidation by two different mechanisms.

We describe evidence of pro-oxidant actions of plasmalogens through the production of excited carbonyls and  $O_2(1\Delta_g)$  generated by energy transfer and the Russell mechanism. We have also characterized the plasmalogen oxidation

products via  $O_2 (1\Delta g)$ , formyl phospholipid, and plasmalogen hydroperoxide by tandem mass spectrometry. In addition, a method for measuring aldehydes was developed, which made it possible to demonstrate the quantitative ratio between dioxetane and hydroperoxide products of plasmalogens that were oxidized via  $O_2 (1\Delta g)$ . We also describe some of the degradation products of lipid hydroperoxides: alpha-beta unsaturated diacyl phospholipid and a long-chain aldehyde. Our findings may help elucidate the actual role plasmalogens play in cellular oxidative stress.

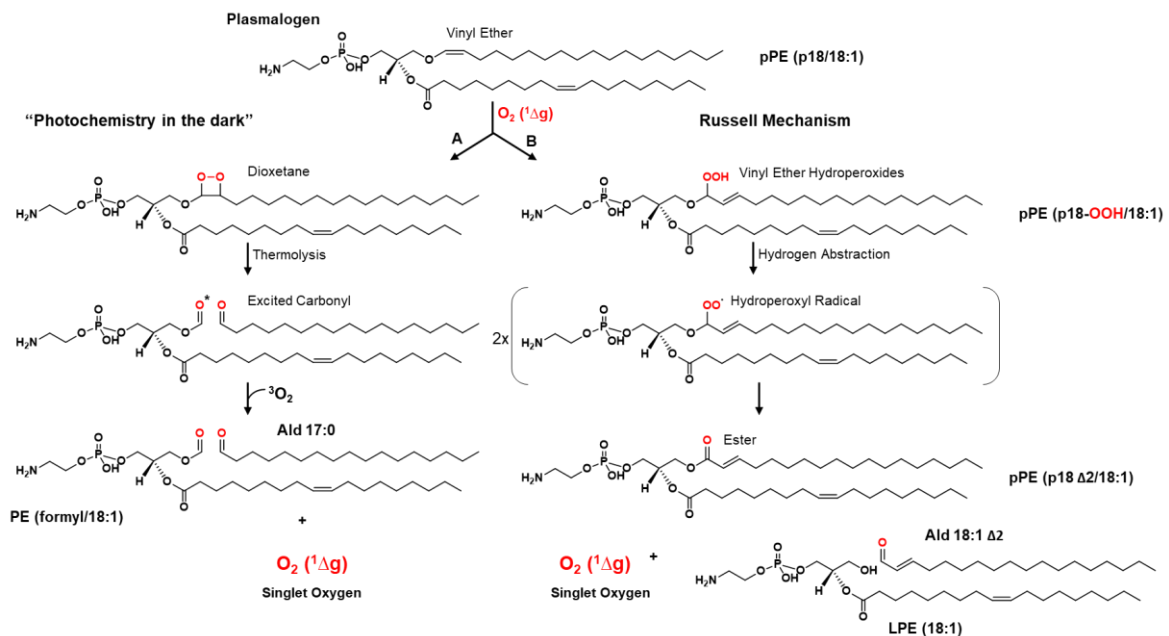


**Figure 1:** Plasmalogen oxidation mechanism via singlet oxygen ( $O_2 (1\Delta g)$ ), and there are two possible routes leading to the production of a new  $O_2 (1\Delta g)$ . **Route A** involves "photochemistry in the dark," which produces a dioxetane intermediate that can propagate the oxidation reaction and produce a new  $O_2 (1\Delta g)$  from  $O_2 (3\Delta g)$ . **Route B** is the Russell mechanism, in which oxidation of hydroperoxides produces peroxy radicals. Two radicals then react with each other, producing a hydroxyl and carbonyl.

## Results

### Characterization of phosphoethanolamine plasmalogen photooxidation products:

To characterize the PE plasmalogen photooxidation products, the pPE plasmalogen solution (p18:1/18:1) was photooxidized in the presence of MB at a low temperature (-40°C). The low temperature was used to prevent the decomposition of unstable intermediates, such as dioxetanes. Aliquots of the samples at different times were collected, and the oxidation products were analyzed by a high-resolution LC-Q-TOF-MS/MS system. Photooxidation promoted a rapid consumption of the pPE (p18/18:1) peak at 10.3 min, which was almost completely consumed after 30 min. Additionally, a major product with similar polarity at 9.6 min was formed, along with some minor polar products at earlier retention times (e.g., 4.3 min) (**Figure 2A**).

Structural characterization of the oxidation products was done by analyzing the exact mass of the precursor ions (MS1) and their fragmentation products (MS/MS or MS2) in the negative ionization mode. The pPE (p18/18:1) used as a starting material showed characteristic MS1 (**Figure 2B**) and MS2 mass spectra (**Figure 2C**) with a precursor ion at  $m/z$  728.5601 and fragment ions at  $m/z$  140.0118 referring to the phosphoethanolamine group, the ion at  $m/z$  281.2486 corresponding to the 18:1 acyl chain, and the ions at  $m/z$  446.3023 and 464.3146 arising from the loss of the 18:1 acyl chain as an acid and a ketene, respectively (**Figure 2C**).

The MS1 mass spectra of pPE oxidation product detected at 9.6 min showed a  $m/z$  value consistent with the addition of two oxygen atoms ( $m/z$

760.5483). We assigned this product to contain plasmalogen with an alkyl ether hydroperoxide group at the sn1 position. The fragmentation profile of pPE(p18-OOH/18:1) showed a prominent fragment ion at  $m/z$  281.2486, which arises from both the dissociation of the sn2-18:1 fatty acyl chain and the dissociation and dehydration of the sn1 ether hydroperoxide alkyl chain (**Figure 2F**). To confirm the formation of an ether hydroperoxide group at the pPE sn1 position, we reduced the hydroperoxide with triphenylphosphine (TPP). This reduction generates a hemiacetal that can quickly cleave to generate LPE (18:1) and a fatty aldehyde (Ald 18:1  $\Delta 2$ ) (**Figure 2G**). Reduction with TPP increased the LPE levels (**Figure 2H**), confirming the addition of hydroperoxide in the vinyl ether position in the plasmalogen. If the position of the hydroperoxide were different from the vinyl ether position, we would have detected a pPE hydroxide, which was not the case (**Figure S3**).

In addition to plasmalogen hydroperoxide, we also detected two minor polar products that eluted at around 4.3 min one corresponding to the lysophosphatidylethanolamine (LPE (18:1)) and the other corresponding to a PE (formyl/18:1) (**Figure 2B**). PE (Formyl/18:1) and LPE (18:1) share a similar fragmentation pattern that shows ions corresponding to the 18:1 fatty acyl chain in the sn2 position and the phosphoethanolamine group in the sn3 position. These two species differ in the  $m/z$  value of the precursor ion, since the formyl PE has a mass shift of +27.99 Da due to the formyl group in the sn1 position (**Figure 2D and E**). Formyl PE is a product of dioxetane thermal decomposition. However, it can be easily hydrolyzed to Lyso PE [14].

The formation of pPE containing the alkyl ether hydroperoxide group at the sn1 position was also studied using pPE purified from bovine brain (**Figure S1**), which contains a mixture of different types of PE plasmalogens (**Table S1**). This pPE mixture was photooxidized under the same conditions and analyzed by LC-MS. The same characteristic fragmentation profile, showing prominent ions arising from the dissociation of the fatty acyl chain from the sn2 position and the dissociation of the sn1 alkyl ether hydroperoxide chain with a mass shift of -18 due to the dehydration of the hydroperoxide group, was observed (**Figure S2**). Thus, together, these results confirm the formation of plasmalogens containing an alkyl ether hydroperoxide group at the sn1 position in the photooxidation of bovine brain pPE.

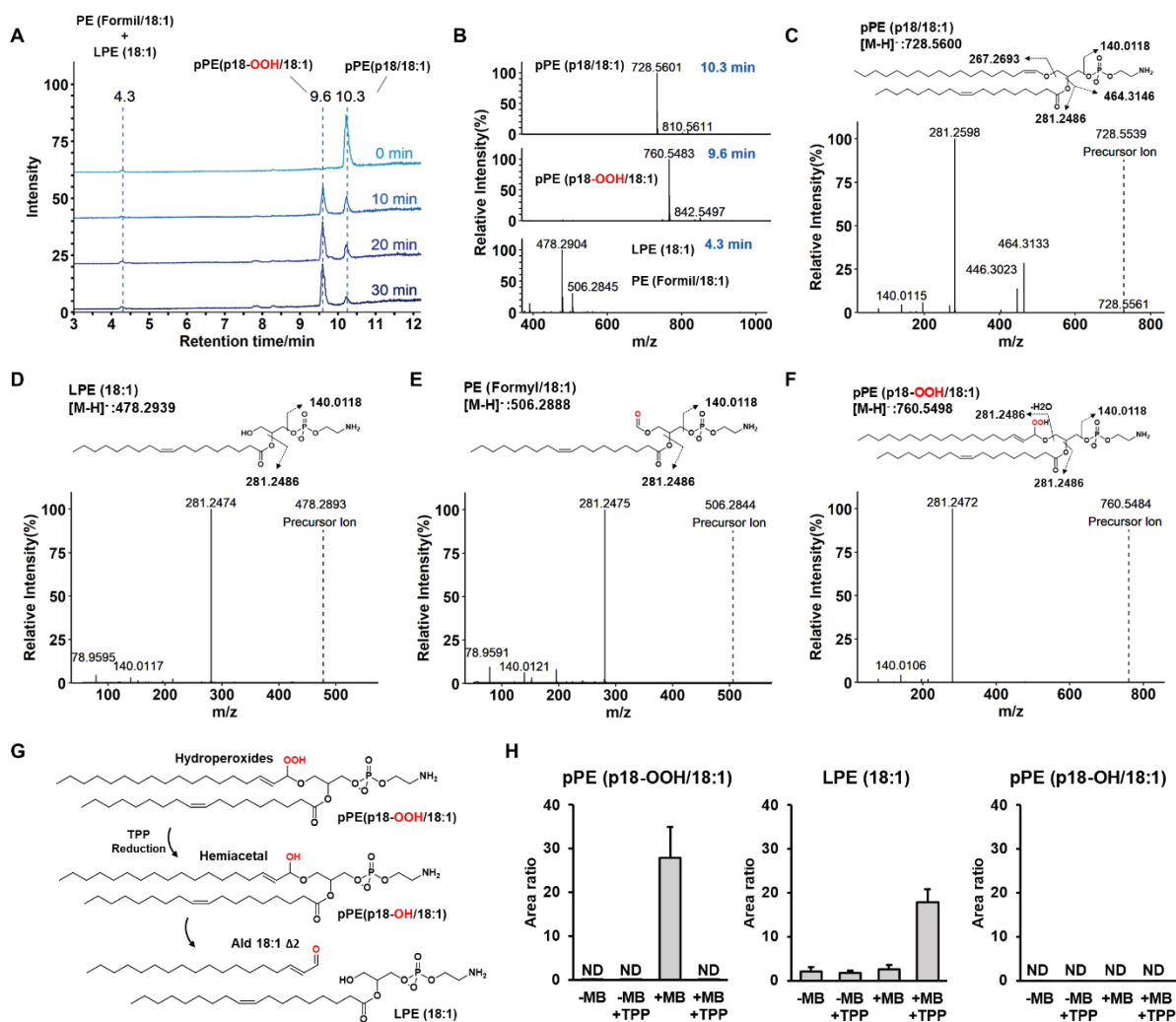


**Figure 2:** Characterization of photooxidation products of pPE(p18/18:1): (A) Total ion chromatography (TIC) of photooxidation with peaks corresponding to pPE (p18/18:1) at 10.3 min and the products formed in pPE (p18-OOH/18:1) at 9.6 min and PE(formyl/18:1) at 4.3 min; (B) MS1 of the peaks shown in A; MS2 of the ions corresponding to: (C) LPE(18:1), (D) PE (formyl/18:1), (E) pPE(p18-OOH;18:1), and (F) pPE(p18/18:1); (G) Mechanism of reduction of vinyl ether hydroperoxide from pPE(p18-OOH/18:1); (H) Quantification of photooxidation products with reduction using triphenylphosphine (TPP).

### Determination of the ratio between plasmalogen photooxidation routes:

Singlet oxygen ( $O_2 ({}^1\Delta_g)$ ) is a ROS, and as such, it reacts efficiently with plasmalogen, more than a hundred times faster than it does with diacyl glycerol analog[9]. Several authors have suggested two oxidation products from the

reaction between O<sub>2</sub> (1Δg) and plasmalogen: (**Figure 1, route A**) dioxetanes that are thermally degraded into formyl phospholipid and fatty aldehyde, and (**Figure 1, route B**) allyl hydroperoxide at sn-1 position[8], [9], [14].

However, the proportion of the products is still unknown. Our first approach was to use the peak area obtained from pPE (p18-OOH/18:1) and PE (formyl/18:1), normalized by the saturated internal standard (PE (14:0/14:0)). The pPE (p18/18:1) oxidation products showed the same pattern of formation, with pPE (p18-OOH/18:1) as the main product representing about 98%, and PE (formyl/18:1) representing only about 2% (**Figure 3B**). However, formyl PE can be hydrolyzed, which explains its decrease after 20 min.

We determined the proportion of aldehydes as another approach to estimate the relative proportion between the dioxetane and hydroperoxide products. Since dioxetane undergoes thermolysis, it produces a fatty aldehyde with 17 carbons (Ald 17:0), while pPE hydroperoxide, when reduced, produces a fatty aldehyde with 18 carbons (Ald 18:1 Δ<sub>2</sub>) (**Figure 3A**).

In samples irradiated without a photosensitizer, the aldehydes were not detected. However, when irradiated in the presence of MB, both aldehydes were observed, with Ald 17:0 being the major product. When irradiated in the presence of MB and then mixed with TPP, we observed a great increase in Ald 18:1 Δ<sub>2</sub>, with a proportion of 97%, and only 3% of Ald 17:0 (**Figure 3D**).

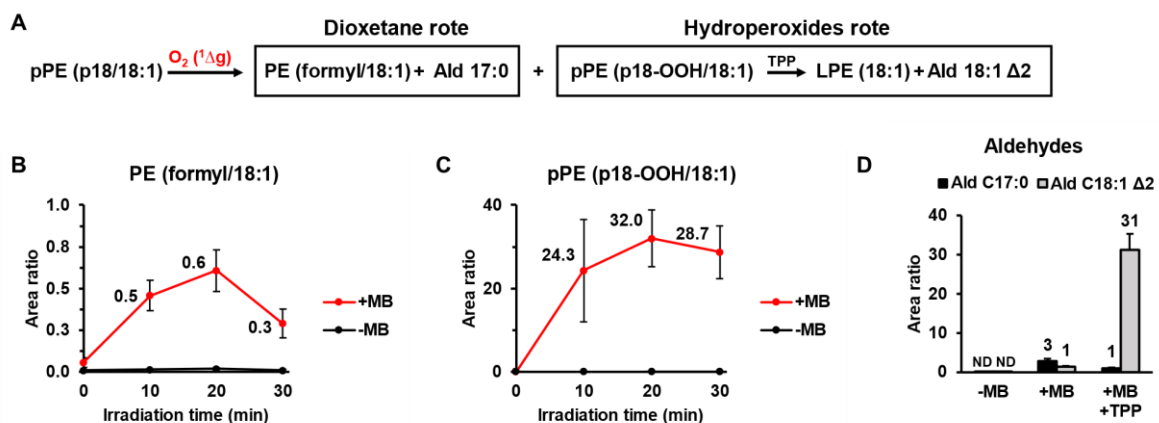


**Figure 3:** (A) Possible routes of oxidation of pPE (p18/18:1) via  $\text{O}_2 (^1\Delta g)$ : production of a dioxetane intermediate that degrades into PE (formyl/18:1) and Ald 17:0; concurrent route with production of a hydroperoxide pPE (p18-OOH/18:1) which can be reduced by TPP, thus producing LPE (18:1) and Ald 18:1  $\Delta 2$ . (B) Kinetics of formation of PE (formyl/18:1) (dioxetane product, left) and pPE (p18-OOH/18:1) (hydroperoxide, right); (C) Determination of CHH-derivatized aldehydes from samples of pPE (p18/18:1) irradiated for 30 min, under the conditions: (-MB) without methylene blue; (+MB) with methylene blue, (+MB + TPP) with MB and with TPP.

### Characterization of alpha beta unsaturated fatty aldehyde (Ald 18:1 $\Delta 2$ ) produced by the reduction of plasmalogen hydroperoxides

Aldehydes are not ionizable groups. For the analysis of this species, it is necessary to carry out a derivatization reaction. In this study, we used the 7-(Diethylamino) coumarin-3-carbohydrazide (CHH) as a probe to react with aldehyde groups. The MS/MS spectrum of the derivatized aldehydes has a characteristic ion of CHH probe with  $m/z$  244.0968 and may generate another characteristic ion of the aldehyde, but with much lower intensity [15].

The fatty aldehyde Ald 17:0, produced by thermolysis of dioxetane pPE (18:1/18:1), showed the same fragmentation pattern as the commercial Ald 17:0,



with a precursor ion at  $m/z$  512.3847 and fragment ions at  $m/z$  252.2702 referring to the fatty aldehyde (**Figure 4A and B**).

For Ald 18:1  $\Delta$  2, precursor ions were observed at  $m/z$  512.3847, and fragment ions were observed at  $m/z$  279.2830, referring to the fatty aldehyde. (**Figure 4C**). However, this data only indicates that the aldehyde has a chain of 18 carbons and 1 unsaturation. However, it is not possible to guarantee that it is an alpha-beta unsaturated aldehyde.

In order to confirm production of an alpha-beta unsaturated aldehyde (Ald 18  $\Delta$ 2) by reduction of plasmalogen hydroperoxides. We developed a novel analysis method using the fluorescent probe 7-Mercapto-4-methylcoumarin (CSH). Aldehydes such as 4-hydroxynonenal (HNE) [16] and hexadecenal (Ald 16:1  $\Delta$ 2) [17] are highly susceptible to Michael addition on the beta-carbon of the alpha-beta unsaturated group with nucleophiles such as thiol of CSH probe. Nevertheless, the addition of CSH on the beta-carbon does not eliminate the aldehyde group[17]. Thus, it is possible to derivatize the aldehyde group with the CHH probe (**Figure 4D**).

Initially, we performed tests using Ald 16:1  $\Delta$ 2, a commercially available aldehyde containing the alpha-beta unsaturated group, and Ald 16:0 as a control. As CSH does not react with aldehyde groups, we performed a second derivatization reaction using CHH for the aldehyde group (Figure S4 A and B). As expected, the analysis by UHPLC-fluorescence showed that only Ald 16:1  $\Delta$ 2 was derivatized with both probes, while Ald 16:0 was only derivatized with CHH (**Figure S4C**).

Using CSH and CHH as probes, we performed the characterization of the aldehydes formed in pPE photooxidation by mass spectrometry. It is possible to identify the doubly derivatized aldehyde, resulting in an MS/MS spectrum with peaks characteristic of the neutral loss of each probe in Ald 16:1  $\Delta$ 2 commercial standard (**Figure 4D**). The same pattern was observed in Ald 18:1  $\Delta$ 2 produced by pPE (p18-OOH/18:1) (**Figure 4E**). In this way, we were able to characterize the fatty aldehydes produced by plasmalogen photooxidation through derivatization of aldehyde and carbonyl groups.

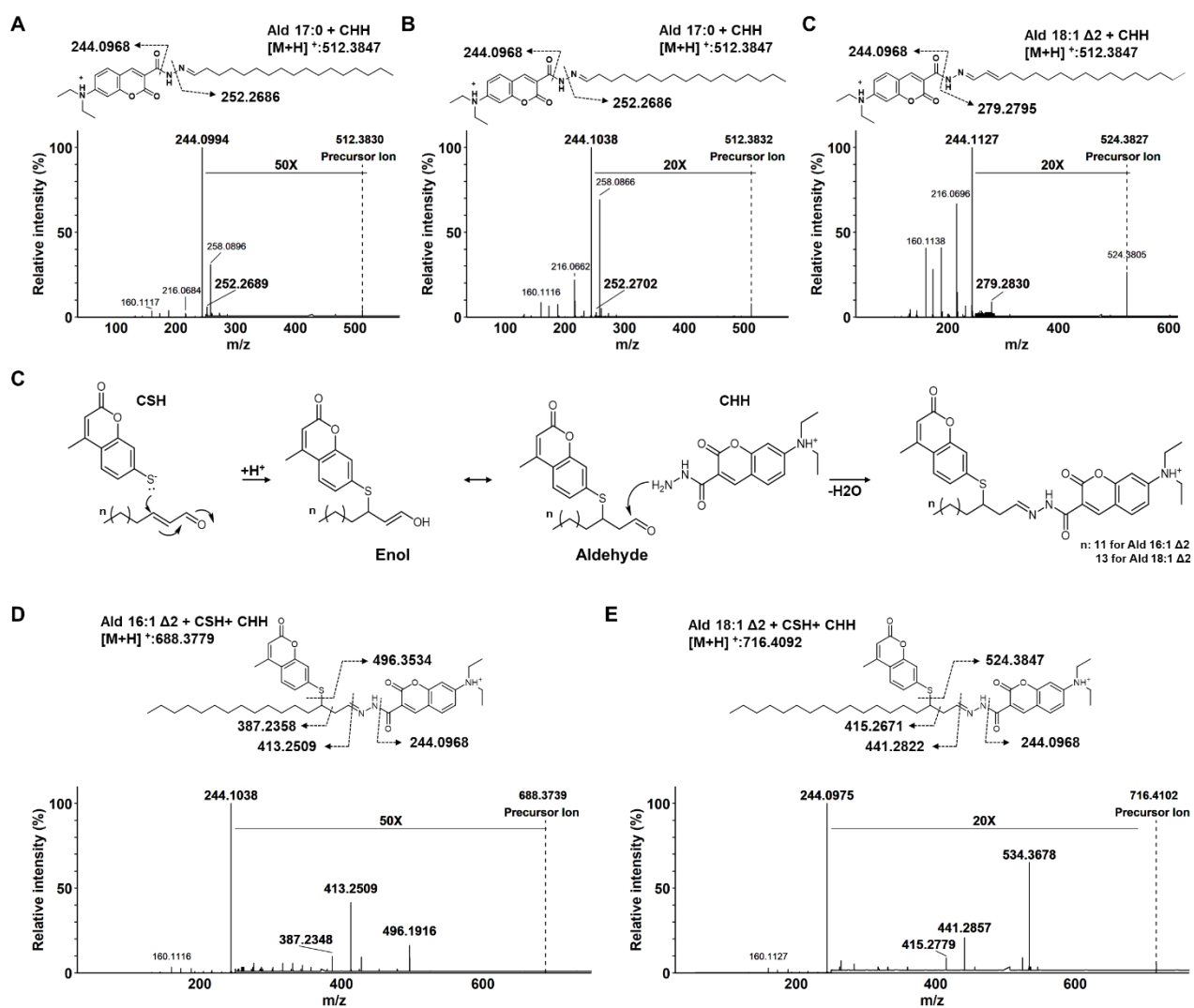


**Figure 4:** Fragmentation pattern of CHH-derivatized long chain aldehydes (A) commercial standard of Heptadecanal (Ald 17:0); (B) Ald 17:0 produced in photooxidation of pPE (p18/18:1), dioxetane product and (C) Ald 18:1  $\Delta$ 2, product

of pPE (p18-OOH/18:1), reduction; (D) Reaction mechanism of derivatization of aldehydes with alpha beta unsaturated carbonyl, is initially performed with CSH probe that reacts with alpha beta unsaturated carbonyl by Michael addition, followed by derivatization with CHH that reacts with aldehyde group; Fragmentation pattern of CSH-CHH-derivatized fatty aldehydes with alpha beta unsaturated carbonyl (E) Ald 16:1  $\Delta^2$  commercial (F) Ald 18:1  $\Delta^2$  product of pPE (p18-OOH/18:1) reduction.

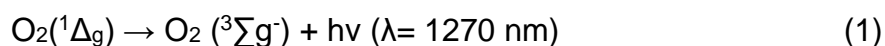
## **Chemiluminescence of plasmalogens dioxetane and triplet carbonyl identification:**

The identification of PE (formyl/18:1) and Ald 17:0 in plasmalogen photooxidation suggests the formation of a dioxetane intermediate. Dioxetane thermolysis produces electronically excited carbonyls [18], [19]. Excited carbonyls can undergo "dark photochemistry," which can result in typical photochemical reactions without the presence of photoexcited species [20]. During this process, the excited carbonyl species transfers energy to another ground-state species, such as molecular oxygen ( $O_2$  ( $3\Sigma_g^-$ )), resulting in the production of singlet molecular oxygen ( $O_2$  ( $1\Delta_g$ )).

The excited carbonyl may also decay to the ground state and emit visible light (**Figure 5A**). We photooxidized 1 mM pPE (p18/18:1) at  $-40^\circ\text{C}$  to preserve the dioxetanes and detect the light emitted by excited carbonyls. The sample was then allowed to naturally heat up to RT.  $O_2$  ( $1\Delta_g$ ) reacts with vinyl ether to produce dioxetane via cyclization [14]. Diacyl PE (18:1/18:1) was used as a negative control for photooxidation because it lacks a vinyl ether bond. Visible light emission in the photooxidized pPE (p18/18:1) sample (**Figure 5B**) suggests the formation of excited carbonyl species.

Dioxetanes thermolysis produces singlet and triplet excited carbonyls. However, it is only the triplet carbonyls that can transfer energy to O<sub>2</sub> (3Σ<sub>g</sub><sup>-</sup>) and result in the production of O<sub>2</sub> (1Δ<sub>g</sub>) [21]. A strategy to determine if triplet carbonyls are produced is by adding the enhancer dibromo anthracene (DBA). DBA is efficiently excited by triplet carbonyls, and when it decays to the ground state, it emits visible light [18]. This increases the visible light emitted during the decomposition of dioxetanes, which produce triplet excited carbonyls. We added DBA after photooxidation at low temperature and measured the emitted light again. We observed a significant increase in the emitted light in the presence of DBA (**Figure 5C**).

O<sub>2</sub> (1Δ<sub>g</sub>) reacts with electron-rich groups, such as olefins, dienes, and polycyclic aromatic compounds [11]. Additionally, O<sub>2</sub> (1Δ<sub>g</sub>) can decay to the ground state of O<sub>2</sub> (3Σ<sub>g</sub><sup>-</sup>) while emitting near-infrared (NIR) light at 1270 nm (equation 1) [11].



To confirm O<sub>2</sub> (1Δ<sub>g</sub>) production, we repeated the photo-oxidation of pPE (p18/18:1) at a low temperature and measured the emitted light at 1270 nm. PE (18:1/18:1) was used as a negative control. We observed weak emission for several minutes at 1270 nm only in the photooxidized pPE (p18/18:1) (**Figure 5D**). The emission at 1270 nm has a similar kinetics to the reaction when DBA was added (**Figure 5C**). O<sub>2</sub> (3Σ<sub>g</sub><sup>-</sup>) and DBA receive energy from excited triplet carbonyls by the same mechanism, may for this reason for the similar kinetic behavior. Near-infrared (NIR) emission with peak light at 1270 nm is characteristic of the monomolecular decay of O<sub>2</sub> (1Δ<sub>g</sub>). Although we observed

emitted light at 1270 nm, it was not possible to obtain a resolved NIR emission spectrum to confirm the production of O<sub>2</sub> (1Δg) by NIR emission alone due to a low signal-to-noise ratio.

For this reason, we utilized an alternative method to detect the generation of O<sub>2</sub> (1Δg) through chemical trapping with 9,10-diphenylanthracene (DPA). This species reacts efficiently with O<sub>2</sub> (1Δg) to produce a stable endoperoxide (DPAO<sub>2</sub>) (**Figure 5A**) [10], [21]. We added DPA after photooxidation at low temperature and incubated the solution was at RT for 1 hour in the dark. HPLC analysis revealed the formation of DPAO<sub>2</sub> (**Figure 5E and Figure S5**), this way suggesting the production of O<sub>2</sub> (1Δg) via “photochemistry in dark” from plasmalogen photooxidized (**Figure 1, route A**).

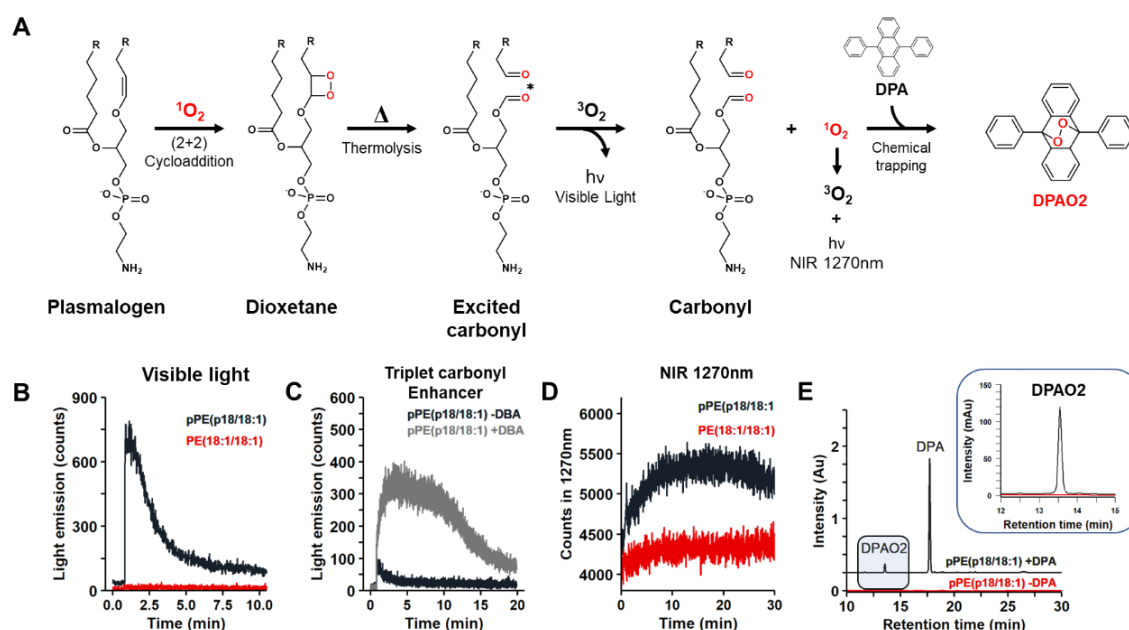


**Figure 5:** (A) The oxidation mechanism of plasmalogen with O<sub>2</sub> (1Δg) produces a dioxetane intermediate that can propagate the oxidation reaction by producing a new molecule of O<sub>2</sub> (1Δg). Additionally, there is a chemical trapping mechanism of O<sub>2</sub> (1Δg) with 9,10-Diphenylanthracene (DPA) that produces the corresponding endoperoxide (DPAO<sub>2</sub>); (B) Time course of total visible light emission of 1 mM pPE(p18/18:1) and PE(18:1/18:1) photooxidized at -40°C and naturally heated to RT; (C) Time course of total visible light emission of 1 mM

pPE(p18/18:1) photooxidized at -40°C and naturally heated to RT with the addition of 10 mM DBA, a triplet carbonyl enhancer; (D) Time course of NIR emission at 1270 nm from O<sub>2</sub> (1Δg) monomolecular light emission of 1 mM pPE(p18/18:1) or PE (18:1/18:1) photooxidized at -40°C and then heated to 37°C; (E) Chromatogram from chemical trapping of O<sub>2</sub> (1Δg) with DPA to produce DPAO<sub>2</sub> from pPE photooxidized by HPLC at 210 nm.

### **Characterization of radical reaction products of pPE (p18-OOH/18:1) with Ce<sup>+4</sup> and Fe<sup>+2</sup>**

Plasmalogen hydroperoxide (pPE (p18-OOH/18:1)) accounted for 98% of the product formed during photooxidation of pPE (p18/18:1). Lipid hydroperoxides react with metals like Fe<sup>2+</sup> and Ce<sup>4+</sup> to produce peroxy radicals and O<sub>2</sub> (1Δg) via the Russell mechanism [25].

The Russell mechanism involves peroxy radicals reacting to form a linear tetra oxide intermediate that decomposes into ketone, hydroxyl, and molecular oxygen singlet[22]. Fatty acid hydroperoxides produce alcohol and ketone as oxidized lipid products [10]. Plasmalogen hydroperoxide has an ether group. This reaction may produce a hemiacetal and an ester. The ester leads to a diacyl PE (18:1 Δ<sub>2</sub>/18:1), while the hemiacetal decomposes to produce LPE (18:1) and Ald 18:1 Δ<sub>2</sub> (**Figure 2G**). To confirm the expected product formation via the Russell mechanism, we incubated 5 μM pPE (p18-OOH/18:1) with 50 μM Ce<sup>4+</sup> and Fe<sup>2+</sup> in a solution of CHCl<sub>3</sub>: methanol:water (90:9:1 v/v/v) for 1 hour. We used photooxidized PE (18:1/18:1) as a positive control and incubated it under the same conditions (**Figure 6B**).

pPE (p18-OOH/18:1) was consumed and producing expected products of the Russell mechanism for plasmalogen hydroperoxides the diacyl PE (18:1

$\Delta 2/18:1$ ) and LPE ( $18:1$ ). Additionally, we observed the expected products of positive hydroperoxide control (PE ( $18:1/18:1$ )-OOH): the alcohol [PE ( $18:1/18:1$ )-OH] and ketone [PE ( $18:1/18:1$ )=O] (Figure 6C).

Furthermore, pPE (p18-OOH/ $18:1$ ) was fully consumed by both  $Ce^{4+}$  and  $Fe^{2+}$  while PE ( $18:1/18:1$ )-OOH was more consumed in the presence of  $Ce^{4+}$  ion due to its higher oxidation potential of  $Ce^{4+}$ . These data indicate that pPE (p18-OOH/ $18:1$ ) is more reactive with metal ions than the diacyl analogue (PE ( $18:1/18:1$ )-OOH).

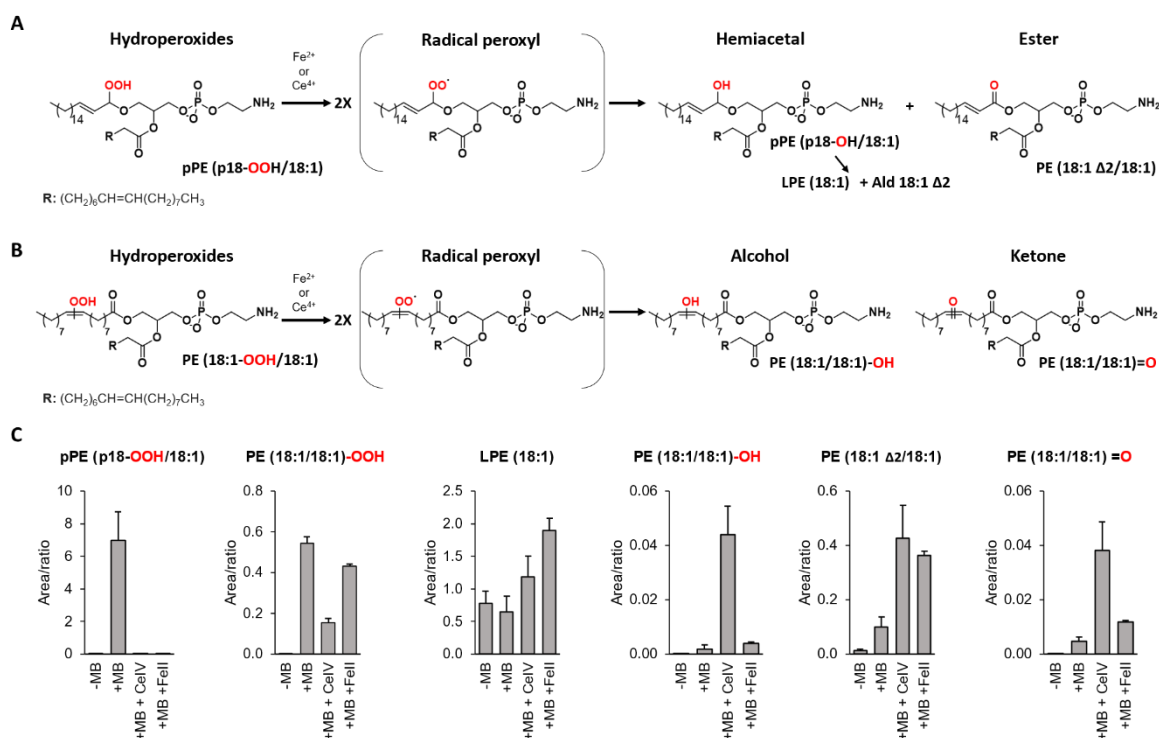


**Figure 6:** (A) Reaction mechanism of plasmalogen hydroperoxide pPE (p18-OOH/ $18:1$ ) and (B) diacyl hydroperoxide PE ( $18:1/18:1$ )-OOH with  $Fe^{2+}$  and  $Ce^{4+}$ , producing a peroxy radical intermediate and resulting in carbonyl and hydroxyl products; (C) Consumption of pPE-OOH incubated with  $Fe^{2+}$  and  $Ce^{4+}$  resulted in the production of LPE ( $18:1$ ) and PE ( $18:1 \Delta 2/18:1$ ) compared to the positive control. Incubation of PE ( $18:1 /18:1$ )-OOH with  $Fe^{2+}$  and  $Ce^{4+}$  resulted in the production of alcohol PE ( $18:1 /18:1$ )-OH and ketone PE ( $18:1 /18:1$ )=O.

The oxidation of pPE (p18-OOH/18:1) to PE (18:1 $\Delta$ 2/18:1) is an isomer of PE (18:1/18:1), but with an alpha-beta unsaturated fatty acid in the sn1 position. The UHPL-ESI-QTOF-MS/MS analysis reveals that both products have the same MS/MS spectrum (Figure S6), but with different retention times (Figure 7A).

To confirm the alpha-beta unsaturated carbonyl in diacyl PE (18:1 $\Delta$ 2/18:1), we incubated the pPE(p18-OOH/18:1) oxidated by Ce<sup>4+</sup> in presence of CSH. We identified by mass spectrometry analysis an adduct of PE (18:1 $\Delta$ 2/18:1) with the CSH probe, and the MS/MS spectrum confirmed a probe fragment at m/z 191.0172 (Figure 7B). Taken together, we were able to identify the two lipid products of Russell's mechanism for plasmalogen hydroperoxides (Figure 1, route B).

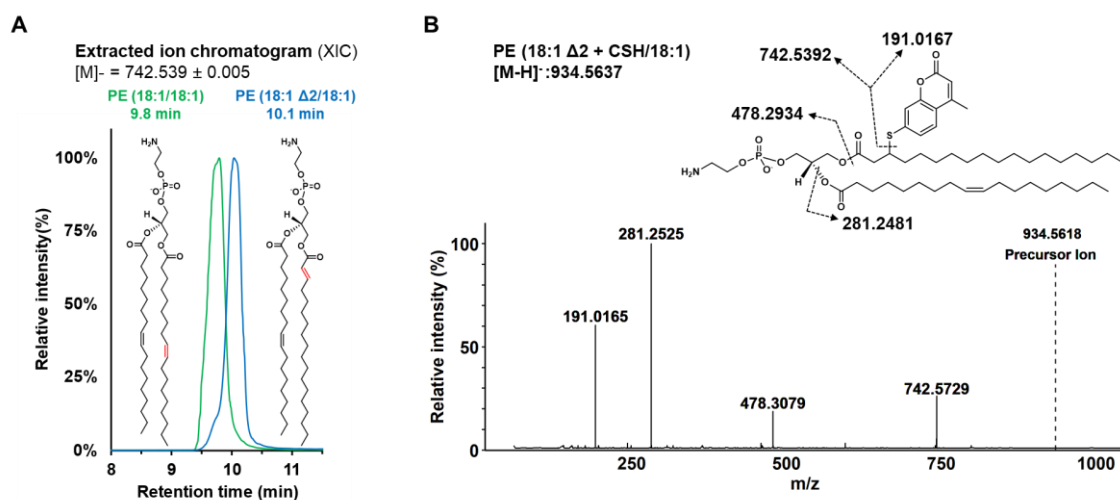


**Figure 7:** (A) Extracted ion chromatogram (XIC) of [M]<sup>-</sup> = 742.539 from a sample of photooxidized pPE(p18/18:1) treated with Ce<sup>4+</sup> (blue) and a commercial standard PE (18:1/18:1) (green);(B) MS/MS spectrum of PE(18:1 $\Delta$ 2/18:1) derivatized with CSH.



## Characterization of singlet molecular oxygen generated by the reaction of hydroperoxides pPE (p18-OOH/18:1) and Ce<sup>4+</sup>

The lipid products identified in the reaction of pPE (p18-OOH/18:1) with Ce<sup>4+</sup> or Fe<sup>2+</sup> are consistent with a mechanism that involves the reaction of two peroxy radicals, as described by the Russell mechanism. To demonstrate O<sub>2</sub> (1Δg) production via the Russell mechanism (**Figure 1, route B**), we monitored 1270 nm light emission during the reaction of 5 μM pPE (p18-OOH/18:1) with 75 μM Ce<sup>4+</sup>, and we observed an intense emission signal (**Figure 8A**). We conducted the same measurements using linoleic acid hydroperoxide (LAOOH) as a positive control for O<sub>2</sub> (1Δg) production via the Russell's mechanism (**Figure 8B**)[10]. Both lipid hydroperoxides produced light emission at 1270 nm with very similar intensity and kinetics, thus supporting that plasmalogen hydroperoxide can produce O<sub>2</sub> (1Δg) via the Russell mechanism.

As the signal obtained at 1270 nm was very intense, it was possible to obtain the infrared emission spectrum that unequivocally confirms the production of O<sub>2</sub> (1Δg) (**Figure 8C**). DMNO<sub>2</sub> is a classical chemical generator of O<sub>2</sub> (1Δg) when thermally decomposed. For comparison, the spectrum obtained from the decomposition of DMNO<sub>2</sub> was also acquired (**Figure 8D**). These results clearly demonstrate that 1O<sub>2</sub> is produced by the reaction of pPE (p18-OOH/18:1) in the presence of Ce<sup>4+</sup>. Knowing the decomposition kinetics of DMNO<sub>2</sub> (Figure S6), it is possible to quantify the amount of 1O<sub>2</sub> produced. The amount of pPE (p18-OOH/18:1) produced in the presence of Ce<sup>4+</sup> was 3.2%, consistent with Russell's mechanism[10].

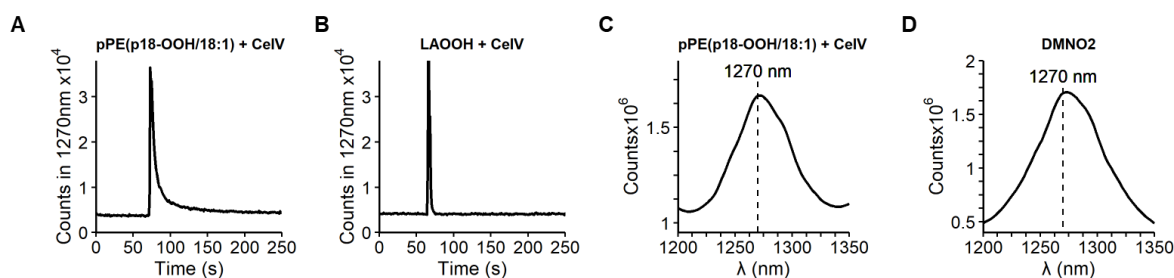


**Figure 8:** Analysis of O<sub>2</sub> (1 $\Delta$ g) produced by Russell by light emission in near-infrared (NIR): (A) Kinetics of emission at 1270 nm were measured by a cut-off filter for plasmalogen hydroperoxides pPE (p18-OOH/18:1) and (B) LAOOH (positive control), both at 5  $\mu$ M, with the addition of 75  $\mu$ M Ce<sup>4+</sup> in a single-phase reaction (CDCl<sub>3</sub>:MeOD(D5):D<sub>2</sub>O; 308;91.4;0.6; v/v/v); (C) NIR emission spectrum of pPE (p18-OOH/18:1) at 100  $\mu$ M with a single 75  $\mu$ M Ce<sup>4+</sup> and a positive control of O<sub>2</sub> (1 $\Delta$ g) produced by thermal decomposition of 1mM DMNO<sub>2</sub>.

## Discussion

In this study, we show that plasmalogen photooxidation can propagate pro-oxidant reactions by generating singlet oxygen (O<sub>2</sub> (1 $\Delta$ g)) through two routes: (route A) the [2 + 2] cycloaddition of O<sub>2</sub> (1 $\Delta$ g) in the plasmalogen vinyl ether group, producing a dioxetane intermediate. The production of a new O<sub>2</sub> (1 $\Delta$ g) occurs by transferring energy from the excited triplet carbonyl produced by dioxetane thermolysis at room temperature (RT) to the molecular oxygen (O<sub>2</sub> (3 $\Sigma$ g<sup>-</sup>)); (route B) Additionally, the reaction of O<sub>2</sub> (1 $\Delta$ g) with electron-rich groups, such as vinyl ether from plasmalogens [11], [23], produces an allylic hydroperoxide acetal (**Figure 1**). These hydroperoxides can react with metal ions, producing a new O<sub>2</sub> (1 $\Delta$ g) by the Russell mechanism.

To demonstrate the formation of dioxetanes, we first established the oxidation reaction at a low temperature (-40°C) to avoid dioxetane thermolysis. The plasmalogen was still consumed quickly at low temperatures, and radical reactions occurred significantly less often than at room temperature. Thus,

virtually all pPE was reacting with O<sub>2</sub> (1Δg). Electrospray ionization tandem mass spectrometry analysis (ESI-MS/MS) was used to characterize the oxidized products. Two types of products were identified from the photooxidation of plasmalogen pPE(p18/18:1): PE (formyl/18:1) and plasmalogen hydroperoxide (pPE(p18-OOH/18:1), **Figure 2**).

O<sub>2</sub> (1Δg) is added to the first carbon in the sn-1 chain of plasmalogen, which can produce an allylic hydroperoxide acetal. The incorporation of the hydroperoxide at the sn-1 position was confirmed by reducing pPE(p18-OOH/18:1) with TPP (**Figure 3G**), which reduces acetal hydroperoxide to hemiacetal. This then decomposes into lysophospholipid (LPE (18:1), **Figure 3H**) and fatty acid aldehyde (Ald 18:1 Δ2). Other studies have already identified LPE and formyl PE using mass spectrometry [8], [9], [24]. However, here we also characterize plasmalogen hydroperoxide.

TPP efficiently reduces pPE hydroperoxides and produces LPE and fatty aldehydes. Then, it would be interesting to investigate which antioxidant enzymes can reduce the acetal hydroperoxide of pPE, as GPx4 and Prdx6 are currently only known to reduce fatty acid hydroperoxides in phospholipids[11], [25]. In addition, the accumulation of phospholipid hydroperoxides activates mechanisms of ferroptosis, which is a type of programmed cell death [25], [26].

Long-chain fatty aldehydes can be produced by plasmalogen dioxetane thermolysis and also by the reduction of plasmalogen hydroperoxide. However, aldehydes are not readily ionizable groups [15]. Therefore, we developed a method to detect aldehydes based on their reaction with a probe (CHH) that enhances their ionization in positive ionization mode and analysis by ESI-MS/MS

[15], [27]. An aldehyde with 17 carbons (Ald 17:0) was detected and used as a specific product derived from pPE (p18/18:1) dioxetane thermolysis. On the other hand, an aldehyde with 18 carbons containing an alpha-beta unsaturated ketone (Ald 18:1  $\Delta$ 2) was also detected after reduction with TPP, which was used as a marker for the formation of plasmalogen hydroperoxides (pPE (p18-OOH/18:1)). Thus, plasmalogen photooxidation primarily produces hydroperoxide, not dioxetane, as demonstrated by relative quantification of the two aldehydes. Aldehyde quantification revealed that almost all (98%) were hydroperoxides (**Figure 3D**), consistent with the ratio of plasmalogen hydroperoxide to formyl phospholipid (97%) (**Figure 3A and B**).

Thermolysis of dioxetanes produces an electronically excited carbonyl that emits visible light when it decays to the ground state [18]. **Figure 5A** shows the light emission of photooxidized pPE (p18:1/18:1) at -40°C and then left at RT. It has a long kinetic and a peak of light emission at 6 minutes. The identification of formyl PE and Ald 17:0 has already been observed in other studies, and it is suggested that the formation of a dioxetane intermediate occurs due to these products [8], [14]. However, our study is the first to show the formation of dioxetane through light emission.

We found that dioxetane produces triplet carbonyl that can transfer energy to O<sub>2</sub> ( $3\Sigma g^-$ ) to produce O<sub>2</sub> ( $1\Delta g$ ) [28]. However, triplet carbonyl can also cause damage in biological environments by transferring energy to other biomolecules in cells and propagating damage, including DNA modification [29]. Thus, triplet carbonyl is a product of plasmalogen photooxidation with deleterious action.

The reactivity of plasmalogen hydroperoxide is not well studied. In this work, we show that the reduction of hydroperoxide, instead of producing alcohol, produces an unstable hemiacetal that degrades into fatty aldehyde (Ald 18:1  $\Delta$ 2) and lysophospholipid (LPE 18:1). We also studied the reactivity in the presence of oxidizing metal ions ( $\text{Fe}^{2+}$  and  $\text{Ce}^{4+}$ ), and again, we observed that the products are different from those of other phospholipid hydroperoxides (**Figure 6**). Instead of producing alcohol and ketone, plasmalogen hydroperoxides produce hemiacetal and an unsaturated alpha-beta diacyl PE. Both alpha-beta unsaturated products (Ald 18:1  $\Delta$ 2 and PE (18:1  $\Delta$ 2/18:1)) from pPE(p18-OOH/18:1) were identified through a reaction with a probe containing thiol. It has recently been shown that alpha-beta unsaturated long-chain aldehydes modify Bax/Bak proteins and cause oligomerization of these proteins, which activates the process of apoptosis [17]. Therefore, these products are deleterious because they can modify the types of peptides or metabolites.

The emission at 1270 nm is characteristic of monomolecular emission of  $\text{O}_2$  (1 $\Delta$ g). Through this phenomenon, we show evidence of  $\text{O}_2$  (1 $\Delta$ g) production by the Russell mechanism from hydroperoxide, as well as by "photochemistry in the dark" due to dioxetane thermolysis. Another evidence supporting the formation of  $\text{O}_2$  (1 $\Delta$ g) by "photochemistry in the dark" is the addition of a chemical trap (DPA).  $\text{O}_2$  (1 $\Delta$ g) reacts rapidly and specifically with DPA ( $k = 1.3 \times 10^6 \text{ M}^{-1}\text{s}^{-1}$ ) to produce a stable endoperoxide product, DPAO<sub>2</sub>. **Figure 5E** shows the formation of DPAO<sub>2</sub>.

Plasmalogens are phospholipids present in cell membranes. Therefore, it would be more appropriate to perform the tests with liposomes in phosphate-

buffered saline. However, the light emission tests were performed in chloroform medium because this solvent has a low boiling point (-63°C). Thus, we were able to perform photooxidation at -40°C. Furthermore, another advantage of working with chloroform is that the O<sub>2</sub> (1Δg) lifetime is approximately 28 times longer in chloroform than in water [30], which increases the intensity of the emitted light.

Taken together, the results discussed herein provide strong evidence of the generation of O<sub>2</sub> (1Δg) by photooxidized plasmalogen and the production of other deleterious products, such as triplet carbonyls, fatty aldehydes, alpha-beta-fatty aldehydes, and alpha-beta-phospholipids.

Although plasmalogens are considered antioxidants, this study shows that they can act as a pro-oxidant. Thus, we can assume that antioxidant action may depend on the severity of oxidative stress. Because in more intense stresses, plasmalogens can intensify oxidative stress instead of attenuating it.

## **MATERIALS AND METHODS**

### **MATERIALS**

Chloroform-d (Cod: 151823, Lot: # MKBF3607V), Methylene blue (MB, Cod: 151823, Lot: # MKBF3607V), 7-(Diethylamino)coumarin-3-carbohydrazide (CHH, cod: 36798, Lot: # BCCF3603), trans,trans-2,4-Nonadienal (cod: 61410, Lot: # BCBR3933V), trans,trans-2,4-Decadienal (cod: 90628, Lot: # BCBW7178), Tridecanal (cod: 269239, Lot: # MKCB9020), Hexenal(cod: 76717, Lot: #BCBW3602), 9,10-Dibromoanthracene (cod: D38855, Lot: # 02503EH), 9,10-Diphenylanthracene (cod: D205001), Methanol-d<sub>4</sub> (MeOD,cod: 441384, Lot: 01006TH), Ammonium cerium(IV) nitrate (Ce<sup>4+</sup>, cod: 215473), Iron(II) sulfate hydrate (Fe<sup>2+</sup>, cod: 307718, Lot:STBJ9273) Deuterium oxide (D<sub>2</sub>O, cod: 151882,

Lot: MKBP9326V), 7-Mercapto-4-methylcoumarin (CSH, cod: 63759, Lot: BCCD3153),

were acquired from Sigma Aldrich (Saint Louis, MO, USA). 1-palmitoyl-2-(9'-oxo-nonanoyl)-sn-glycero-3-phosphocholine (ALDOPC, cod: 870605P, Lot: 870605P-1MG-F-014), 1-(1Z-octadecenyl)-2-oleoyl-sn-glycero-3-phosphoethanolamine (pPE(p18/18:1), cod: 852758P, Lot: 852758P -10MG-A-024), 1,2-dimyristoyl-sn-glycero-3-phosphoethanolamine (PE(14:0/14:0), cod: 850745P, Lot: 5738P-NA-070), 16:1 aldehyde (Ald 16:1  $\Delta$ 2, cod: 857459P, Lot: 857459P -1MG-D-010) were acquired from Avanti Polar Lipids (Alabaster, AL, USA). 4-hydroxy Hexenal (HHE, Cod: 32060, Lot: 0411894-9), 4-hydroxy Nonenal (HNE, Cod: 32100, Lot: 0411894-9), Hexadecanal (Ald 16:0, cod: 9001996, Lot: 050947-4) were acquired from Cayman Chemicals (Ann Arbor, MI), Heptadecanal (Ald (17:0), cod: H1295, Lot: MBUJA-MQ), pentadecanal (Ald (15:0), cod: P1869, Lot: KODWM-IE) were acquired from Tokyo Chemical Industry (Nihonbashi-honcho, Chuo-ku, Tokyo, Japan). 1,4-Dimethylnaphthalene (DMN) endoperoxide (DMNO<sub>2</sub>) was also prepared by UVA irradiation of DMN/methylene blue and then quantified spectrophotometrically[31].

#### **Plasmalogen photooxidation.**

Purified pPE 5 mM (750 g/mol) and MB 300  $\mu$ M in CHCl<sub>3</sub> or CDCl<sub>3</sub> was irradiated with LED with maximum emission of 632 nm and  $41 \pm 1$  Wm<sup>-2</sup> for 30 min in a bath at -40°C (dry ice and ACN), aliquots were collected throughout the reaction and analyzed by ESI-QTOF MS/MS or used luminescence emission. pPE(p18/18:1) was also used in 1mM and 50  $\mu$ M MB, under the same oxidation conditions and analyzed by MS. The LED with maximum emission and power was determined by a Fieldmate power meter (Coherent - Portland, OR) coupled to an OP2-Vis

detector.

### **Lipid analysis by ESI-QTOF MS/MS**

Lipids were analyzed by ESI-QTOF (Triple TOF® 6600, Sciex, Concord, US) interfaced with an ultra-high performance liquid chromatography (UHPLC Nexera, Shimadzu, Kyoto, Japan). The samples were loaded into a CORTECS® (UPLC® C18 column, 1.6 µm, 2.1 mm i.d. × 100 mm) with a flow rate of 0.2 mL min<sup>-1</sup> and the oven temperature maintained at 35 °C. For reverse-phase LC, mobile phase A consisted of water/acetonitrile (60:40), while mobile phase B composed of isopropanol/acetonitrile/water (88:10:2). Mobile phases A and B contained ammonium acetate at a final concentration of 10 mM for experiments performed in negative or positive ionization mode, respectively. Lipids were separated by a 20 min linear gradient as follows: from 40 to 100% B over the first 10 min., hold at 100% B from 10–12 min., decreased from 100 to 40% B during 12–13 min., and hold at 40% B from 13–20 min. The MS was operated in both positive and negative ionization modes, and the scan range set at a mass-to-charge ratio of 200–2000 Da. Data for lipid molecular species identification and quantification was obtained by Information Dependent Acquisition (IDA®). Data acquisition using Analyst® 1.7.1 was performed with a cycle time period of 1.05 s with 100 ms acquisition time for MS1 scan and 25 ms acquisition time to obtain the top 36 precursor ions. An ion spray voltage of -4.5 and the cone voltage at -80 V were set to analysis. Additional parameters included curtain gas set at 25 psi, nebulizer and heater gases at 45 psi and interface heater of 450 °C. The LC-MS/MS data were analyzed with PeakView®. Lipid molecular species were manually identified based on their exact masses, specific fragments and/or neutral losses. Also, a maximum error of 5 mDa was defined for the attribution of



the precursor ion. After identification, the area of lipid species was obtained by MS data using MultiQuant®. Each peak integration was carefully inspected for correct peak detection and accurate area determination.

### **Optimization of aldehyde derivatization conditions with CHH**

The aldehyde analysis method was based from Mansano et al.[32]. Initially it was found that the best concentration of formic acid to catalyze the derivatization reaction was 0.1% v/v (**figure 8S A**), the optimal CHH excess was 20x in aldehydes (**figure 8S B**) with a reaction time of 120 min (**figure 8S C**). The samples were analyzed by ultra-high performance liquid chromatography (UHPLC Nexera, Shimadzu, Kyoto, Japan), 5µ microliter of the sample was injected into a reversed-phase column water cortex C8 (100 × 4.6 mm, 1.7 µm particle size) with a flow rate of 0.2 mL min<sup>-1</sup> and the oven temperature maintained at 35 °C and RF-10Axl fluorescence detector. The HPLC mobile phase consisted of water with 0.1% formic acid (A) and methanol with 0.1% formic acid (B), and the flow rate was 0.3 mL/min. The separation of the fluorescent adducts was done using the following condition: 60% B for 2 min, 60-100% in 9 min, 92% B for 3 min, and 100-60% B in 1 min and 60% for 3min. The excitation and emission wavelengths were fixed at 450 and 468 nm. The chromatography method was optimized so that aldehydes formed by lipid peroxidation method (HHE, HNE, Hexenal, Nodienal and Decadienal) were analyzed together with fatty aldehydes (Ald (13:0), Ald (15:0), Ald17:0)), however, separating the unreacted CHH(**figure 8S D**).

For alpha beta unsaturated samples. Before incubation with CHH, 100 uM of photooxidized pPE with or without Fe<sup>2+</sup>/Ce<sup>4+</sup> was incubated with 5 mM CSH in ACN with 0.1% TEA for 2 hr at RT.

### **Aldehydes analysis by ESI-QTOF MS/MS**

The aldehydes derivatized with CHH were analyzed by ESI-QTOF (Triple TOF® 6600, Sciex, Concord, US) interfaced with an ultra-high performance liquid chromatography (UHPLC Nexera, Shimadzu, Kyoto, Japan). The chromatographic conditions were the same as for the fluorescence analysis. Excess CHH can damage the mass spectrometer, for this reason the first 5 min are discarded (**figure 8S E**), but all aldehydes are identified (**figure 8S F**), the conditions of the mass spectrometer were the same as for lipid analysis in positive mode. The final derivation conditions were: 50  $\mu$ M aldehydes or 50  $\mu$ M pPE, 1 mM CH in IPA with 0.1% formic acid.

### **Excited triplet species light emission in the visible region.**

All reactions were carried out in a quartz tube under constant stirring at room temperature (final volume = 600  $\mu$ L). The light emission in the visible region was immediately recorded by a FLSP 920 photon counter (Edinburgh Instruments, Edinburgh, UK) with a PMT Hamamatsu detector R9110, maintained at  $-20$  °C by a PMT cooler CO1 (Edinburgh Instruments). 5 mM of purified Plasmalogen photo-oxidized at  $-40$ °C in  $\text{CHCl}_3$  or  $\text{CDCl}_3$  was added to a cuvette and naturally warmed to room temperature. For carbonyl enhancer experiments, DBA or DPA were added prior to reading with a final concentration of 10 mM.

### **Singlet molecular oxygen emission in the near infrared region**

The monomol light emission of  $\text{O}_2$  ( $^1\Delta_g$ ) was measured with a special photocounting apparatus developed in our laboratory, equipped with a monochromator capable of selecting emissions in the near-infrared (IR) region (950-1400 nm). The spectra were recorded by a FLSP 920 photon counter (Edinburgh Instruments, Edinburgh, UK) consisting of a PMT detector coupled to

the device, a PMT Hamamatsu H10330A-45 apparatus maintained at -60 °C by a thermoelectric cooler to reduce the dark current (Hamamatsu city, Japan). The power was provided by a high voltage DC power supply, and the applied potential was set to -0.8 kV. The light emitted from the sample was processed through a monochromator (TMS/DTMS300, Edinburgh Analytical Instruments, UK) equipped with a diffraction grating capable of selecting wavelengths in the infrared region. The phototube output was connected to the computer, and the signal was acquired. The monochromator was controlled and the data was acquired using the F-900 version 6.22 software program (Edinburgh Analytical Instruments, Livingston, UK).

Light emissions at specified wavelength (1270 nm) intervals were obtained with cut-off filters (Melles Griot Inc., Carlsbad, CA) placed between the cuvette and the photomultiplier. All sample components were mixed and poured into a mirrored walls glass cuvette (35 × 7 × 55 mm) maintained at 25 °C.

#### **Acknowledgments:**

This work was supported by FAPESP [CEPID-Redoxoma 2013/07937-8, FAPESP DD 2017/16140-7 to Faria, R.L.], CNPq [Miyamoto, S. 424094/2016-9, Di Mascio, P. 302120/2018-1], Capes and Pró-Reitoria de Pesquisa da USP.

#### **References:**

- [1] N. Nagan and R. A. Zoeller, "Plasmalogens: biosynthesis and functions," *Prog. Lipid Res.*, vol. 40, no. 3, pp. 199–229, May 2001.
- [2] N. E. Braverman and A. B. Moser, "Functions of plasmalogen lipids in health and disease.," *Biochim. Biophys. Acta*, vol. 1822, no. 9, pp. 1442–

- 52, Sep. 2012.
- [3] X. Q. Su, J. Wang, and A. J. Sinclair, "Plasmalogens and Alzheimer's disease: a review," *Lipids Health Dis.*, vol. 18, no. 1, p. 100, Dec. 2019.
- [4] R. A. Zoeller, A. C. Lake, N. Nagan, D. P. Gaposchkin, M. A. Legner, and W. Lieberthal, "Plasmalogens as endogenous antioxidants: somatic cell mutants reveal the importance of the vinyl ether," *Biochem. J.*, vol. 338, no. 3, pp. 769–776, Mar. 1999.
- [5] R. A. Zoeller, T. J. Grazia, P. LaCamera, J. Park, D. P. Gaposchkin, and H. W. Farber, "Increasing plasmalogen levels protects human endothelial cells during hypoxia," *Am. J. Physiol. Circ. Physiol.*, vol. 283, no. 2, pp. H671–H679, Aug. 2002.
- [6] S. Reuter, S. C. Gupta, M. M. Chaturvedi, and B. B. Aggarwal, "Oxidative stress, inflammation, and cancer: How are they linked?," *Free Radic. Biol. Med.*, vol. 49, no. 11, pp. 1603–1616, 2010.
- [7] B. Halliwell and S. Chirico, "Lipid peroxidation: its mechanism, measurement, and significance," *Am. J. Clin. Nutr.*, vol. 57, no. 5, pp. 715S-725S, May 1993.
- [8] D. H. Thompson, H. D. Inerowicz, J. Grove, and T. Sarna, "Structural Characterization of Plasmalogen Photooxidation Products," *Photochem. Photobiol.*, vol. 78, no. 4, p. 323, 2003.
- [9] A. Broniec, R. Klosinski, A. Pawlak, M. Wrona-Krol, D. Thompson, and T. Sarna, "Interactions of plasmalogens and their diacyl analogs with singlet oxygen in selected model systems," *Free Radic. Biol. Med.*, vol. 50, no. 7, pp. 892–898, 2011.
- [10] S. Miyamoto, G. R. Martinez, M. H. G. Medeiros, and P. Di Mascio,

- “Singlet molecular oxygen generated from lipid hydroperoxides by the Russell Mechanism: Studies using  $^{18}\text{O}$ -labeled linoleic acid hydroperoxide and monomol light emission measurements,” *J. Am. Chem. Soc.*, vol. 125, no. 20, pp. 6172–6179, May 2003.
- [11] P. Di Mascio, G. R. Martinez, S. Miyamoto, G. E. Ronsein, M. H. G. Medeiros, and J. Cadet, “Singlet Molecular Oxygen Reactions with Nucleic Acids, Lipids, and Proteins,” *Chem. Rev.*, vol. 119, no. 3, pp. 2043–2086, Feb. 2019.
- [12] G. Cilento and W. Adam, “PHOTOCHEMISTRY and PHOTOBIOLOGY WITHOUT LIGHT,” *Photochem. Photobiol.*, vol. 48, no. 3, pp. 361–368, Sep. 1988.
- [13] G. R. Martinez, J.-L. Ravanat, J. Cadet, S. Miyamoto, M. H. G. Medeiros, and P. Di Mascio, “Energy Transfer between Singlet ( $^1\Delta_g$ ) and Triplet ( $^3\Sigma_g^-$ ) Molecular Oxygen in Aqueous Solution,” *J. Am. Chem. Soc.*, vol. 126, no. 10, pp. 3056–3057, Mar. 2004.
- [14] O. H. Morand, R. A. Zoeller, and C. R. H. Raetz, “Disappearance of plasmalogens from membranes of animal cells subjected to photosensitized oxidation,” *J. Biol. Chem.*, vol. 263, no. 23, pp. 11597–11606, 1988.
- [15] I. Milic, R. Hoffmann, and M. Fedorova, “Simultaneous detection of low and high molecular weight carbonylated compounds derived from lipid peroxidation by electrospray ionization-tandem mass spectrometry,” *Anal. Chem.*, vol. 85, no. 1, pp. 156–162, 2013.
- [16] P. J. M. Boon, H. S. Marinho, R. Oosting, and G. J. Mulder, “Glutathione conjugation of 4-hydroxy-trans-2,3-nonenal in the rat in vivo, the isolated

- perfused liver and erythrocytes," *Toxicol. Appl. Pharmacol.*, vol. 159, no. 3, pp. 214–223, 1999.
- [17] D. T. Cohen, T. E. Wales, M. W. McHenry, J. R. Engen, and L. D. Walensky, "Site-Dependent Cysteine Lipidation Potentiates the Activation of Proapoptotic BAX," *Cell Rep.*, vol. 30, no. 10, pp. 3229-3239.e6, Mar. 2020.
- [18] W. Adam and G. Cilento, "Four-Membered Ring Peroxides as Excited State Equivalents: A New Dimension in Bioorganic Chemistry," *Angew. Chemie Int. Ed. English*, vol. 22, no. 7, pp. 529–542, Jul. 1983.
- [19] P. Di Mascio, L. H. Catalani, and E. J. H. Bechara, "Are dioxetanes chemiluminescent intermediates in lipoperoxidation?," *Free Radic. Biol. Med.*, vol. 12, no. 6, pp. 471–478, Jan. 1992.
- [20] W. J. Baader, C. V. Stevani, and E. J. H. Bechara, "Photo'chemistry Without Light?," *Rev. Virtual Química*, vol. 7, no. 1, pp. 74–102, 2015.
- [21] M. J. Steinbeck, A. U. Khan, and M. J. Karnovsky, "Intracellular singlet oxygen generation by phagocytosing neutrophils in response to particles coated with a chemical trap.," *J. Biol. Chem.*, vol. 267, no. 19, pp. 13425–33, Jul. 1992.
- [22] G. A. Russell, "Deuterium-isotope Effects in the Autoxidation of Aalkyl Hydrocarbons. Mechanism of the Interaction of PEroxy Radicals 1," *J. Am. Chem. Soc.*, vol. 79, no. 14, pp. 3871–3877, Jul. 1957.
- [23] A. A. Frimer, "The Reaction of Singlet Oxygen with Olefins: The Question of Mechanism," *Chem. Rev.*, vol. 79, no. 5, pp. 359–387, 1979.
- [24] A. Broniec *et al.*, "Interaction of plasmenylcholine with free radicals in selected model systems," *Free Radic. Biol. Med.*, vol. 106, no. February,

- pp. 368–378, 2017.
- [25] M. Maiorino, M. Conrad, and F. Ursini, “GPx4, Lipid Peroxidation, and Cell Death: Discoveries, Rediscoveries, and Open Issues,” *Antioxid. Redox Signal.*, vol. 4, p. ars.2017.7115, May 2017.
- [26] S. Doll and M. Conrad, “Iron and ferroptosis: A still ill-defined liaison,” *IUBMB Life*, vol. 69, no. 6, pp. 423–434, Jun. 2017.
- [27] S. Tomono, N. Miyoshi, and H. Ohshima, “Comprehensive analysis of the lipophilic reactive carbonyls present in biological specimens by LC/ESI-MS/MS,” *J. Chromatogr. B*, vol. 988, pp. 149–156, Apr. 2015.
- [28] M. Vacher *et al.*, “Chemi- and Bioluminescence of Cyclic Peroxides,” *Chem. Rev.*, vol. 118, no. 15, pp. 6927–6974, Aug. 2018.
- [29] S. Premi *et al.*, “Chemiexcitation of melanin derivatives induces DNA photoproducts long after UV exposure,” *Science (80-. )*, vol. 347, no. 6224, pp. 842–847, Feb. 2015.
- [30] J. M. Aubry, B. Mandard-Cazin, M. Rougee, and R. V. Bensasson, “Kinetic Studies of Singlet Oxygen [4 + 2]-Cycloadditions with Cyclic 1,3-Dienes in 28 Solvents,” *J. Am. Chem. Soc.*, vol. 117, no. 36, pp. 9159–9164, 1995.
- [31] C. M. Mano *et al.*, “Excited singlet molecular O<sub>2</sub> ((1)Δ<sub>g</sub>) is generated enzymatically from excited carbonyls in the dark.,” *Sci. Rep.*, vol. 4, p. 5938, 2014.
- [32] F. V. Mansano *et al.*, “Highly Sensitive Fluorescent Method for the Detection of Cholesterol Aldehydes Formed by Ozone and Singlet Molecular Oxygen,” *Anal. Chem.*, vol. 82, no. 16, pp. 6775–6781, Aug. 2010.

Supplementary Figures:

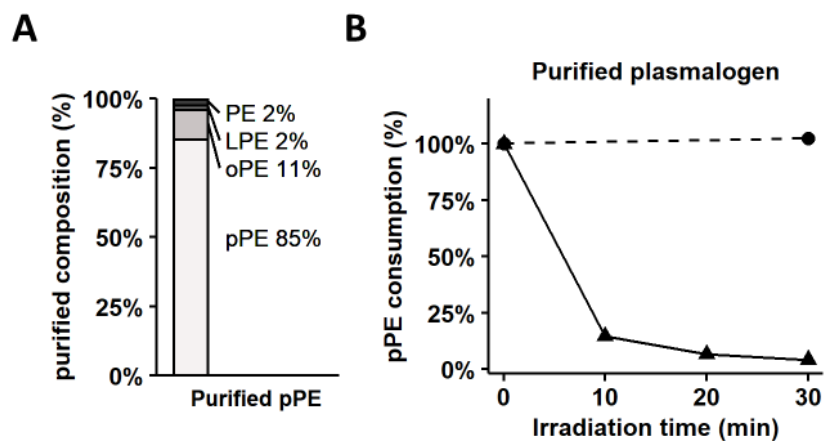


**Figure S1:** (A) Composition of purified PE plasmalogen; (B) Consumption of pPE purified by photooxidation in the presence of methylene blue (—▲—) and control without methylene blue (---).



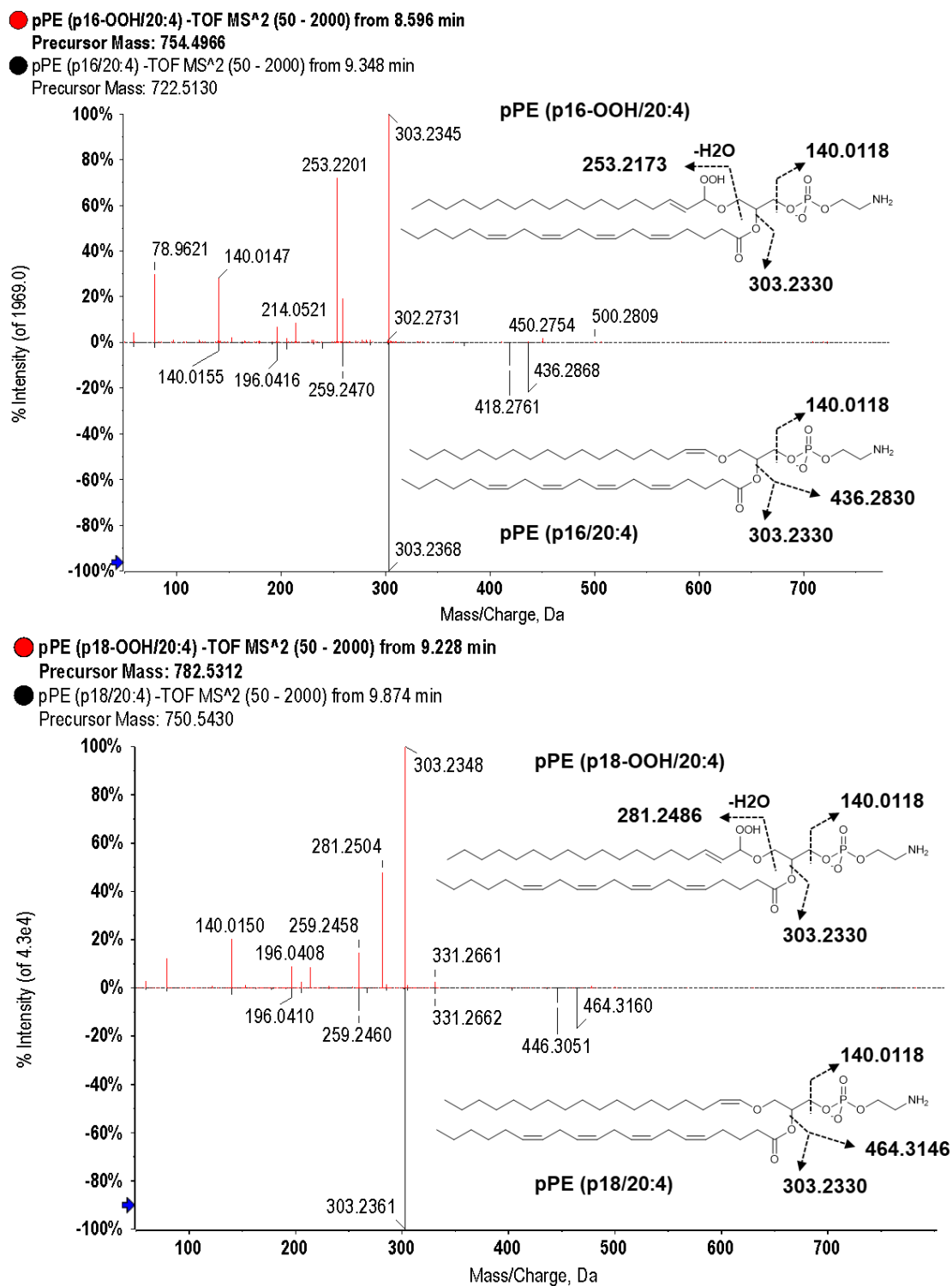


**Figure S2:** Tandem mass spectrometry (MS/MS) comparison of plasmalogen and hydroperoxides from purified plasmalogen photooxidized: (Top) pPE(p16-OOH/20:4) and pPE(p16/20:4); (lower) pPE(p18-OOH/20:4) and pPE(p18/20:4).

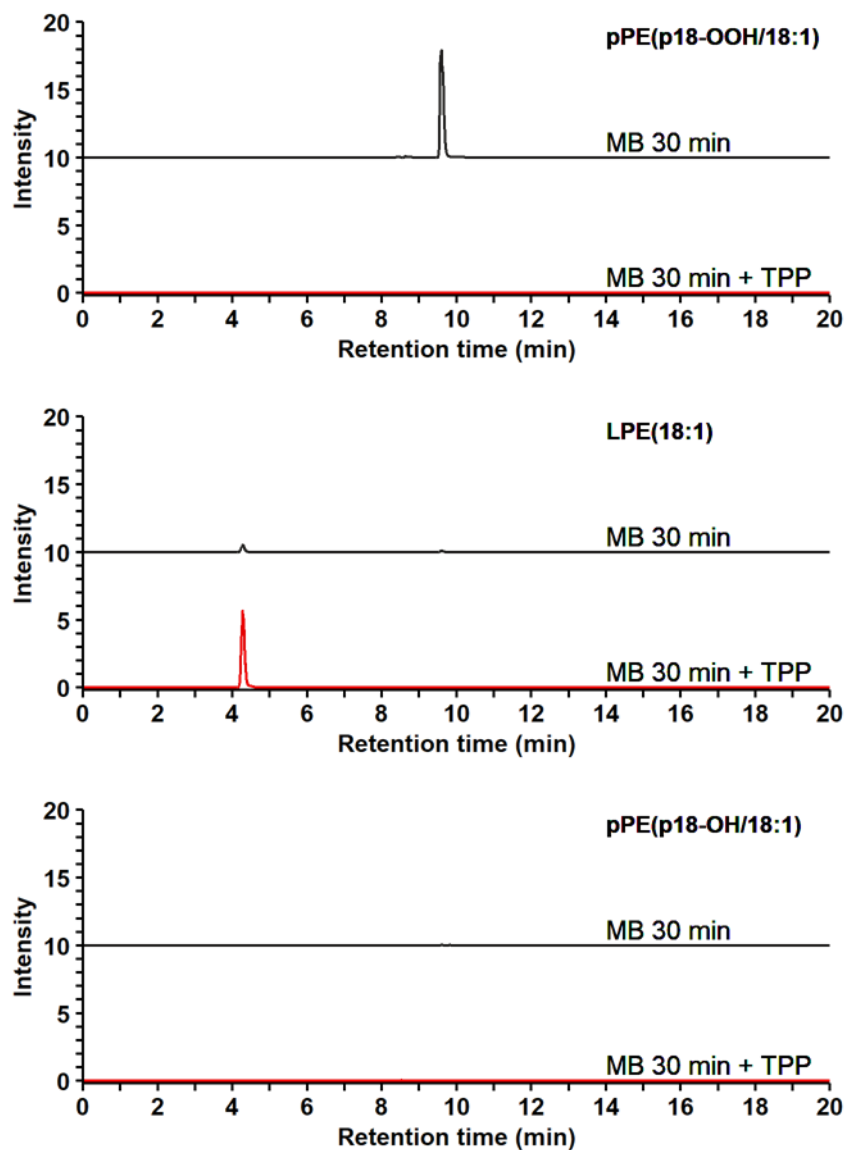


**Figure S3:** Extracted ion chromatogram (XIC) from pPE(p18/18:1) standard photooxidated in presense of MB for 30 minutes with (red line) or without (black line) TPP: (Top) XIC m/z:760.55-760.56 from pPE (p18-OOH/18:1); (Middle) XIC m/z:478.29-478.230 from LPE (18:1); (Bottom) XIC m/z: 744.55-744.56 from pPE (p18-OH/18:1).

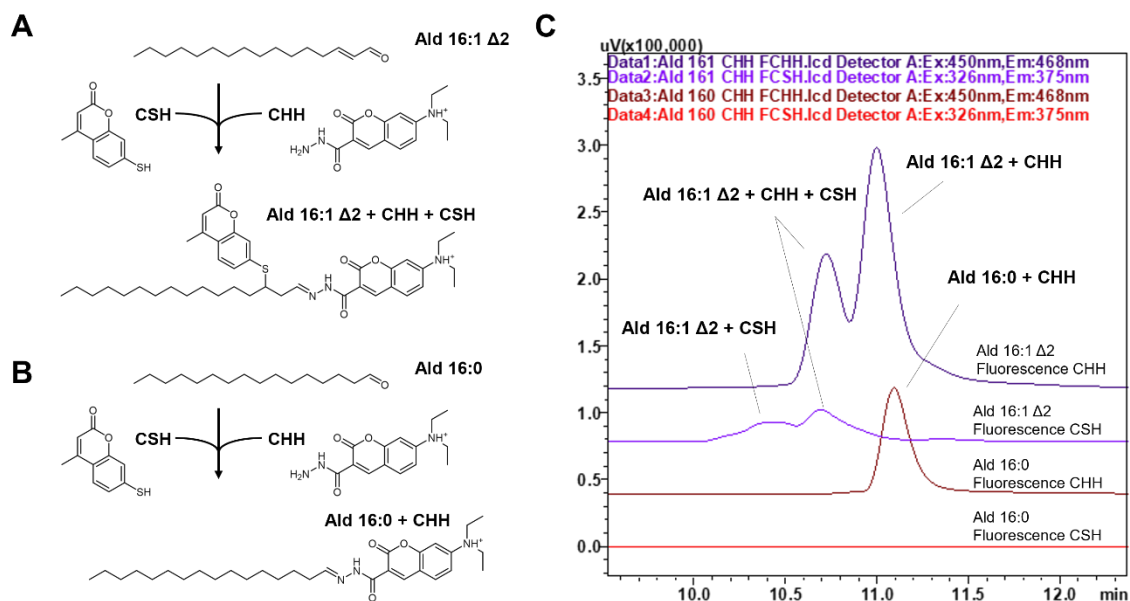


**Figure S4:** (A) Ald 16:1  $\Delta 2$  derivatization mechanism with CSH and CHH probes; (B) Ald 16:0 derivatization mechanism with CSH and CHH probes; (C) chromatograms of Ald 16:1  $\Delta 2$  and Ald 16:0 reactions with CSH and CHH probes and analyzed by fluorescence of CSH (excitation: 326 nm and emission: 375 nm) and CHH (excitation: 450 nm and emission: 468 nm).

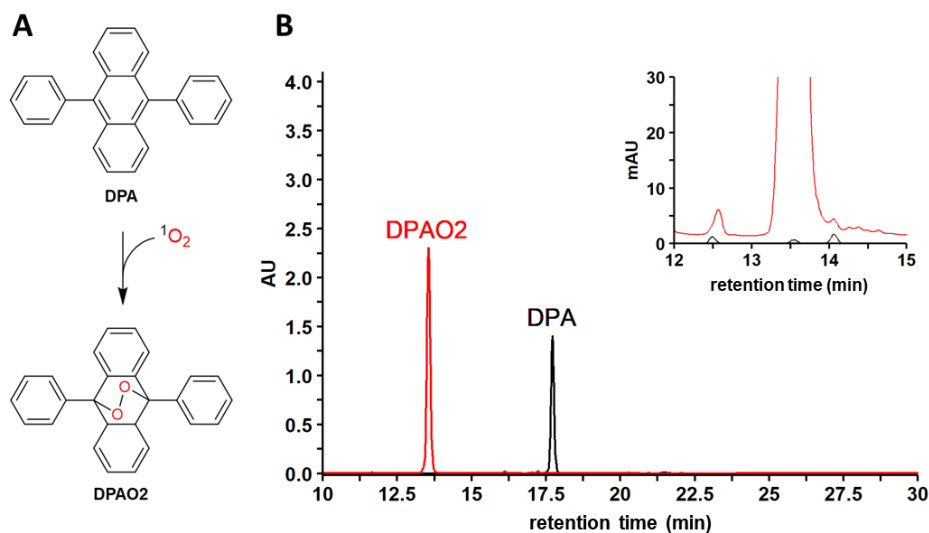


**Figure S5:** (A) Chemical trapping mechanism of  $O_2$  ( $^1\Delta g$ ) with 9,10-Diphenylanthracene (DPA) producing the corresponding endoperoxide (DPAO2) (B) Chromatogram of controls DPA and DPAO2.

● Spectrum from 2022.11.09\_RodrigoS\_RodrigoF\_15\_NEG\_Lipidomics\_pPEOOH\_CeIV\_2.wiff (...NEG\_Lipidomics\_pPEOOH\_CeIV\_2, Experiment 2, -TOF MS<sup>2</sup> (50 - 2000) from 9.679 min  
 Precursor: 742.5 Da  
 ● Spectrum from 2022.11.10\_RodrigoS\_RodrigoF\_03\_NEG\_Lipidomics\_DOPE\_Ct\_1.wiff (sample 1...rigoF\_03\_NEG\_Lipidomics\_DOPE\_Ct\_1, Experiment 2, -TOF MS<sup>2</sup> (50 - 2000) from 9.408 min  
 Precursor: 742.5 Da

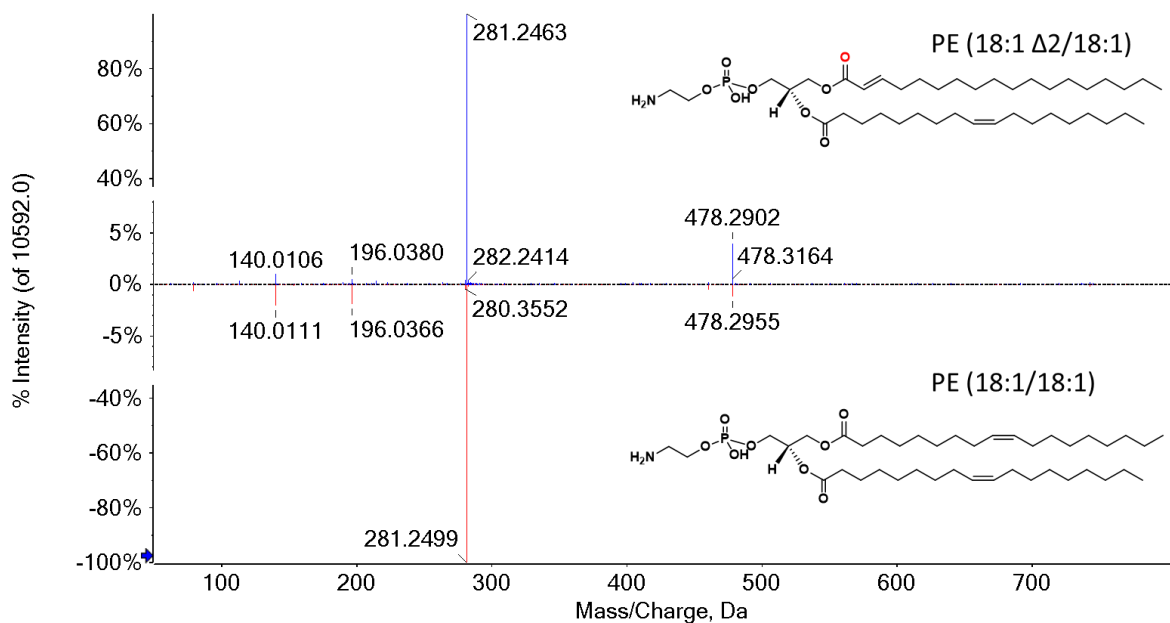


**Figure S6:** MS/MS spectra of commercial standard PE (18:1/18:1) and PE (18:1Δ2/18:1) produced by oxidation of pPE (p18/18:1).

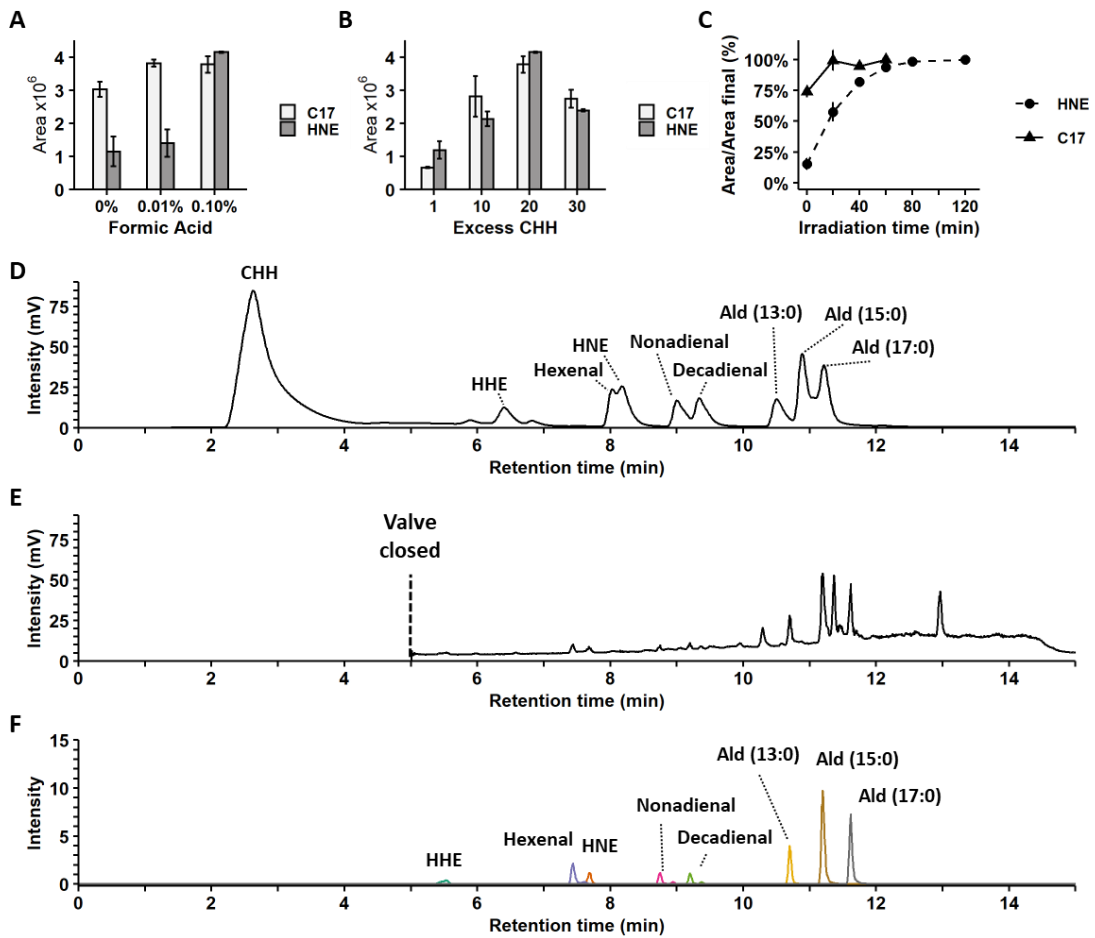


**Figure S7:** Determination of aldehydes derivatized with CHH: (A) Concentration of formic acid in v/v with Ald(17:0) and HNE aldehydes.,(B) CHH concentration in relation to Ald(17:0) aldehydes or HNE in 0.1% formic acid. (C) Derivatization kinetics of Ald(17:0) or HNE with 20x CHH and 0.1% formic acid. (D) Mix chromatogram of derivatized aldehydes with 20x CHH and 0.1% formic acid. (E) Total ion chromatogram form derivatized aldehydes (F) XICs of aldehydes derivatized with CHH.

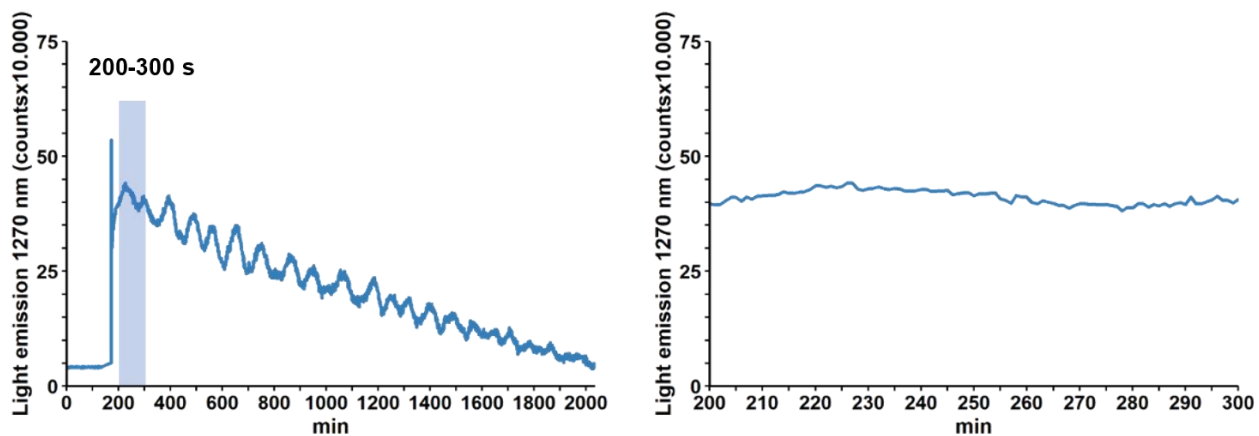


**Figure S8:** Emission at 1270 nm filter cutoff of 116  $\mu\text{M}$  DMNO<sub>2</sub> in 400  $\mu\text{L}$  CDCL<sub>3</sub>:MeOD(d<sub>5</sub>):D<sub>2</sub>O solution 308: 91.4:0.6 v/v/v (A) Kinetics of decomposition until reaching baseline (B) profile from 200 to 300 s.

## Supplementary tables.

**Table S1:** Composition of purified and photooxidized pPE at different times and with the addition of reducing hydroperoxide (TPP). The composition was normalized by the total lipid area in the initial condition (0 min).

Component Name	0 min	10 min	20 min	30 min	30 min + TPP
pPE(p16/18:1)	8.9%	1.8%	1.0%	0.1%	0.0%
pPE(p16/20:1)	11.1%	2.1%	1.1%	0.1%	0.0%
pPE(p16/20:3)	0.4%	0.0%	0.0%	0.0%	0.0%
pPE(p16/22:3)	2.6%	0.3%	0.1%	0.0%	0.0%
pPE(p16/22:4)	4.2%	0.6%	0.3%	0.0%	0.0%
pPE(p16/ARA)	1.7%	0.2%	0.1%	0.0%	0.0%
pPE(p16/DHA)	3.7%	0.3%	0.1%	0.0%	0.0%
pPE(p17/18:1)	1.4%	0.2%	0.1%	0.0%	0.0%
pPE(p17/20:1)	0.7%	0.1%	0.0%	0.0%	0.0%
pPE(p17/22:4)	0.6%	0.1%	0.0%	0.0%	0.0%
pPE(p17/DHA)	0.5%	0.1%	0.0%	1.7%	0.0%
pPE(p18/16:0)	0.1%	0.0%	0.0%	0.0%	0.0%
pPE(p18/18:1)	1.1%	0.5%	0.5%	0.3%	0.2%
pPE(p18/20:1)	4.4%	0.6%	0.3%	0.0%	0.0%
pPE(p18/22:1)	0.2%	0.2%	0.3%	0.1%	0.0%
pPE(p18/22:3)	1.0%	1.1%	1.5%	0.7%	0.6%
pPE(p18/22:4)	7.5%	1.1%	0.6%	0.0%	0.0%
pPE(p18/24:3)	0.2%	0.0%	0.0%	0.0%	0.0%
pPE(p18/ARA)	3.3%	0.5%	0.2%	0.0%	0.0%
pPE(p18/DHA)	9.5%	1.4%	0.6%	0.0%	0.0%
pPE(p18/DPA)	0.4%	0.0%	0.0%	0.0%	0.0%
pPE(p18:1/18:1)	14.0%	2.6%	1.4%	0.1%	0.1%
pPE(p18:1/19:1)	0.5%	0.0%	0.0%	0.0%	0.0%
pPE(p18:1/20:1)	4.8%	0.9%	0.4%	0.1%	0.0%
pPE(p18:1/20:2)	0.9%	0.2%	0.2%	0.1%	0.1%
pPE(p18:1/20:3)	0.3%	0.0%	0.3%	0.0%	0.0%
pPE(p18:1/21:1)	0.4%	0.0%	0.0%	0.0%	0.0%
pPE(p18:1/22:1)	1.0%	0.4%	0.4%	0.2%	0.1%
pPE(p18:1/22:3)	1.7%	0.2%	0.1%	0.0%	0.0%
pPE(p18:1/24:1)	0.1%	0.0%	0.0%	0.0%	0.0%
pPE(p18:1/24:3)	0.4%	0.1%	0.0%	0.0%	0.0%
pPE(p18:1/24:4)	0.2%	0.0%	0.0%	0.0%	0.0%
pPE(p18:1/DHA)	2.2%	0.1%	0.1%	0.0%	0.0%
pPE(p18:1-OOH/18:1)	1.6%	7.7%	9.7%	9.3%	0.0%
pPE(p16-OOH/18:1)	1.2%	4.9%	6.2%	6.4%	0.0%
pPE(p16-OOH/20:1)	1.0%	5.7%	7.4%	7.7%	0.0%
pPE(p16-OOH/22:3)	0.1%	1.0%	1.3%	1.4%	0.0%
pPE(p16-OOH/22:4)	0.5%	2.2%	2.8%	2.7%	0.0%
pPE(p16-OOH/DHA)	0.3%	1.8%	2.2%	2.0%	0.0%
pPE(p17-OOH/18:1)	0.5%	0.1%	0.1%	0.1%	0.0%
pPE(p18:1-OOH/18:1-OOH)	0.0%	0.4%	0.9%	1.8%	0.0%
pPE(p18:1-OOH/20:1)	0.3%	2.3%	3.0%	2.9%	0.0%
pPE(p18:1-OOH/20:2)	0.0%	0.3%	0.4%	0.4%	0.0%
pPE(p18:1-OOH/21:1)	0.0%	0.1%	0.2%	0.2%	0.0%
pPE(p18:1-OOH/22:1)	0.0%	0.4%	0.5%	0.5%	0.0%
pPE(p18:1-OOH/22:2)	0.0%	0.2%	0.3%	0.2%	0.0%
pPE(p18:1-OOH/22:3)	0.1%	0.6%	0.8%	0.8%	0.0%
pPE(p18:1-OOH/22:4-OOH)	0.0%	0.0%	0.1%	0.2%	0.0%
pPE(p18:1-OOH/ARA)	0.2%	2.0%	2.8%	2.3%	0.0%
pPE(p18:1-OOH/DHA)	1.2%	4.1%	5.3%	5.0%	0.0%
pPE(p18-OOH/18:1)	1.0%	5.7%	7.4%	7.7%	0.0%
pPE(p18-OOH/20:1)	0.1%	2.0%	2.6%	2.9%	0.0%
pPE(p18-OOH/22:1)	0.0%	0.1%	0.1%	0.2%	0.0%
pPE(p18-OOH/22:3)	0.1%	0.8%	1.1%	1.2%	0.0%
pPE(p18-OOH/22:4)	0.6%	3.4%	4.3%	3.9%	0.0%
pPE(p18-OOH/22:4-OOH)	0.0%	0.0%	0.1%	0.3%	0.0%
pPE(p18-OOH/ARA)	0.3%	1.6%	2.1%	2.1%	0.0%
pPE(p18-OOH/DHA)	1.2%	4.1%	5.3%	5.0%	0.0%
pPE(p18-OOH/DPA)	0.0%	0.1%	0.2%	0.2%	0.0%

## CHAPTER 3

### **Deleterious effects of plasmalogen phosphatidylethanolamine on membrane leakage induced by photooxidation reaction**

Rodrigo Lucas de Faria, Fernanda Manso Prado<sup>1</sup>, Helena Couto Junqueira<sup>1</sup>, Karen Campos Fabiano<sup>1</sup>, Mauricio da Silva Baptista<sup>1</sup>, Paolo Di Mascio<sup>1</sup>, Sayuri Miyamoto<sup>1</sup>

1 Departamento de Bioquímica, Instituto de Química,  
Universidade de São Paulo, São Paulo, SP,

\* Corresponding Author: Sayuri Miyamoto. E-mail address:  
miyamoto@iq.usp.br

Institutional address: Departamento de Bioquímica, Instituto de Química, Av.  
Prof. Lineu Prestes 1524, CP 26077, CEP 05313-970, Butantã, São Paulo, SP.  
Brazil. Phone: + 55 1130911413



## Highlights

- 21% of HaCat keratinocyte membrane lipids are PE plasmalogen.
- PE plasmalogen were the most reactive lipids by photosensitization.
- Plasmalogen hydroperoxides are much more reactive compared to diacyl phospholipid hydroperoxides.
- Plasmalogen hydroperoxides when reduced produces lyso phospholipids that leads to membrane leakage.
- Glutathione is able to reduce plasmalogen hydroperoxides.

**Abbreviations:**

**ARA**, Arachidonic acid

**CF**, Carboxyfluorescein

**DMMB**, Dimethylene blue

**DHA**, Docosahexaenoic acid

**DHPN**, N,N'-di(2,3-dihydroxypropyl)-3,3'-(1,4-naphthydylene)dipropanamide

**DHPO<sub>2</sub>**, DHPN endoperoxides

**EPA**, Eicosapentaenoic acid

**GPC**, Glycerophosphocholine

**GPE**, Glycerophosphatidylethanolamine

**GSH**, Glutathione

**LPC**, Lysophosphatidylcholine

**LPE**, Lysophosphatidylethanolamine

**MB**, Methylene blue

**MUFAs**, Monounsaturated fatty acids

**oPE**, Plasmanyl phosphatidylethanolamine

**oPC**, Plasmanylyl phosphatidylcholine

**PC**, Phosphatidylcholine

**PDT**, Photodynamic therapy

**PE**, Phosphatidylethanolamine

**PG**, Phosphatidylglycerol

**PI**, Phosphatidylinositol

**POPC**, 1-palmitoyl-2-oleoyl-sn-glycero-3-phosphocholine

**pPC**, Phosphatidylcholine plasmalogens

**pPE**, Phosphatidylethanolamine plasmalogens

**pPI**, Phosphatidylinositol plasmalogens

**PS**, Phosphatidylserine

**PS\***, Excited photosensitizer

**PUFAs**, Polyunsaturated fatty acids

**ROS**, Reactive oxygen species

**SAPC**, 1-stearoyl-2-arachidonoyl-sn-glycero-3-phosphocholine

**SP**, Sphingolipids

**SM**, sphingomyelin

**UHPLC**, ultra-high-performance liquid chromatography

**TPP**, triphenyl phosphine

## **Abstract**

Plasmalogens are a type of phospholipids that are found in cell membranes, particularly in the brain, heart, and nervous system. They are unique because they have a vinyl ether bond at the sn-1 position of the glycerol backbone. Photodynamic therapy (PDT) is a medical treatment that uses a photosensitizing agent, a specific wavelength of light, and oxygen to destroy abnormal cells or tissue. Singlet oxygen plays a crucial role in this therapy. The photosensitizer is then activated by exposure to a specific wavelength of light, which causes the production of reactive oxygen species (ROS) including singlet oxygen. Singlet oxygen is highly reactive to vinyl ether bond at the sn-1 position of the glycerol backbone from plasmalogens. The reaction of singlet oxygen with plasmalogen produces vinyl ether hydroperoxides and dioxetanes. Dioxetanes are unstable and degrade to formyl phospholipids and fatty aldehydes, however vinyl ether hydroperoxides appear to be more reactive and when degraded or reduced, produce lysophospholipids and fatty aldehydes. Then, both plasmalogen photooxidation pathways produce species that make the membrane more unstable that generate membrane leakage. Thus, membrane disruption can be facilitated by the presence of plasmalogen. In this work we show that plasmalogens are more reactive lipids by photooxidation reaction and produce hydroperoxide that degrade faster. We also studied how the presence of plasmalogen can facilitate membrane leakage using liposomes encapsulated with carboxyfluorescein.

## Introduction

Photodynamic therapy (PDT) involves administration photosensitizer followed irradiation with visible light, this process eliminates unwanted cells and has been successfully used for the treatment of various diseases, including cancer, bacterial and fungal infections, and age-related macular degeneration [1]–[3].

PDT is a process that involves the activation of a photosensitizer through exposure to light of a specific wavelength, which subsequently triggers either a type I or type II photochemical reaction[4]. In type I reactions, the photosensitizer accepts an electron from a nearby molecule, resulting in the formation of a radical cation. This radical cation can then react with molecular oxygen to produce superoxide and other reactive oxygen species (ROS)[1], [4]. On the other hand, in type II reactions, the photosensitizer transfers energy to molecular oxygen, leading to the formation of singlet molecular oxygen ( $^1\text{O}_2$ )[4], [5]. This highly reactive molecule can cause oxidative damage to nearby biomolecules[5], [6].

Damage caused by ROS to the lipid membrane can trigger lipid peroxidation[7], which can be initiated by both type I and type II reactions, leading to the development of lipid hydroperoxides (LOOH) [8]. The process of lipid peroxidation occurs when oxidizing species react by abstracting protons (hydrogen) from unsaturated lipids, inducing a series of radical reactions that culminate in the formation of LOOH as primary products. LOOHs are relatively unstable and may participate in secondary reactions that result in the formation of peroxy and/or alkoxy radicals[9], [10]. These radicals (peroxy/alkoxy) can either propagate the oxidation process by generating new lipid radicals or undergo intramolecular cyclization reactions or acyl chain breakage, producing cyclic compounds similar to prostaglandins (e.g., isoprostanes, neuroprostanes) and a vast array of reactive aldehydes[11], [12]. Consequently, lipid peroxidation induces alterations in the permeability and fluidity of cell membranes, significantly affecting cell integrity and function [2], [8].

Polyunsaturated fatty acids (PUFAs) are highly susceptible to reactive oxygen species (ROS) due to the presence of bis-allylic hydrogen, which facilitates proton abstraction by radicals[10]. PUFAs are primarily esterified into phosphatidylcholine (PC) and phosphatidylethanolamine (PE), the two most prevalent classes of phospholipids in biological membranes. In skin fibroblasts, PUFAs constitute approximately 50% of PE and 85% of plasmalogens containing PE [13]. The enrichment of PUFAs in plasmalogens was confirmed through lipidomic analysis conducted in this study using HaCat keratinocyte cells. Plasmalogens contain a vinyl ether bond at the sn-1 position, which is vulnerable to attack by ROS and other oxidants[14]–[16]. Plasmalogens react with  $^1\text{O}_2$  to produce two primary oxidation products: a hydroperoxyl and an unstable dioxetane. Plasmalogen hydroperoxides are highly reactive and can produce LPE, which has been shown to destabilize the membrane and cause leakage. Both oxidation products of pPE can cause membrane leakage[17].

This work, we investigate how pPE can facilitate membrane leakage by photooxidizing lipids extracted from HaCat keratinocytes, which are known for their high susceptibility to oxidation. The pPE hydroperoxide was found to be more unstable compared to other lipid hydroperoxides. Liposome models containing pPE were also examined, and it was discovered that pPE can induce leakage with only  $^1\text{O}_2$ , but this only occurs in the presence of reductants.

## **MATERIALS AND METHODS**

### **MATERIALS**

Trypan blue, monobasic sodium phosphate, dibasic sodium phosphate, ammonium acetate and ammonium formate, sodium chloride (NaCl), were purchased from Sigma Aldrich (St. Louis, MO). 1,2-diheptadecanoyl-sn-glycero-3-phosphoethanolamine (PE 17:0/17:0), 1,2-diheptadecanoyl-sn-glycero-3-phosphocholine (PC 17:0/17:0), 1,2-diheptadecanoyl-sn-glycero-3-phospho-L-serine (PS 17:0/17:0), 1,2-diheptadecanoyl-sn-glycero-3-phospho-(1'-rac-glycerol) (PG 17:0/17:0), 1-heptadecanoyl-2-hydroxy-sn-

glycero-3-phosphocholine (LPC 17:0/17:0), 1',3'-bis[1,2-dimyristoyl-sn-glycerol-3-phospho]-sn-glycerol (CL 14:0/14:0/14:0/14:0), N-heptadecanoyl-D-erythro-sphingosylphosphorylcholine (SM d18:1/17:0) e N-decanoyl-D-erythro-sphingosine (Cer d18:1/10:0) were acquired from Avanti Polar Lipids (Alabaster, AL). Acetonitrile, isopropanol, chloroform, ethyl acetate and methanol were purchased from J.T.Baker (Center Valley, PA). All aqueous solutions were prepared with ultrapure water purified through the Direct-Q3 System treated with Chelex 100 resin and filtered with 0.22 µm filters (Merck Milipore, Germany). Dulbecco MEM cell culture media (DMEM), fetal bovine serum (FBS), trypsin solution, antibiotic and antimycotic solution containing penicillin (10 I.U./mL), streptomycin (10 mg/mL) and amphotericin B (1 µg/mL) were purchased from Vitrocell.

#### **HaCat cell plating**

Cells were resuspended using trypsin and subsequently counted using a Neubauer chamber and an optical microscope with the aid of Trypan blue dye. After counting,  $7 \times 10^4$  cells were distributed in cell culture plates of 21 mm<sup>2</sup> and  $2.8 \times 10^5$  cells in cell culture bottles of 75cm<sup>2</sup> and were kept in an incubator at 37°C and 5% CO<sub>2</sub> for one week until 80% of confluency, the supplemented DMEM medium with FBS at 10% (v/v) was changed every 2 days.

#### **Photosensitizers stock solution**

The methylene blue (MB) stock solution was prepared in HPLC-grade ethanol and had the concentration determined from the Lambert-Beer Law using molar absorptivity coefficient  $2(\epsilon_{\max})$ ,  $9.6 \times 10^4$  L.mol<sup>-1</sup>.cm. From the MB stock solution, DMEM media containing MB with concentrations of 10 µmol.L<sup>-1</sup>, 5 µmol.L<sup>-1</sup> and 2 µmol.L<sup>-1</sup> were prepared.

#### **Lipid extraction from HaCat cells**

Lipids were extracted according to Yoshida et. al. Briefly, a 100 µL aliquot of the homogenate (20 mg of tissue) was added to 400 µL of 10 mM PBS (pH 7.4) with 0.1 mM deferoxamine, 400 µL of methanol and 100 µL of internal standard in methanol. The

mixture was homogenized for 30 s on a vortex, and after the addition of 2 mL of chloroform: ethyl acetate (4:1, v/v) it was again homogenized for 30 s on a vortex. The mixture was centrifuged at 1500xg for 3 min at 4°C, the lower organic phase was collected and transferred to a vial and dried under N<sub>2</sub> flow. The dry lipid extract was reconstituted with 100 µL of isopropanol.

### **Time-dependent photooxidation of extracted lipids**

Photooxidation was performed following the method by Miyamoto et. al adapted. Briefly, the lipids extracted from 2x10<sup>6</sup> cells were solubilized in 2 mL of CHCl<sub>3</sub> and 1 µL of MB 50 mmol.L<sup>-1</sup> in methanol was added. The reaction was conducted in a 4 mL transparent vial irradiated by a 500 W tungsten lamp at 10 cm distance at different reaction times. After the reaction, the solvent was removed by N<sub>2</sub> flow and resuspended in 100 µL of isopropanol for UPLC-MS/MS analysis.

Photooxidation was also performed with light emitting diodes (LEDs), at a maximum emission wavelength of 657 nm and 20 mW/cm<sup>2</sup> of irradiance for 5 and 10 minutes. After the reaction, the solvent was removed by N<sub>2</sub> flow and resuspended in 100 µL of isopropanol. Half of the resuspended product was reduced with triphenylphosphine (TPP), initially the solvent was removed by N<sub>2</sub> flow and then 50 µL of TPP 10 mg.L<sup>-1</sup> was added. Then, UPLC-MS/MS analysis of the oxidized and reduced products was performed.

### **Lipid analysis by UPLC-MS/MS**

Extracted or photooxidized lipids were analyzed by UPLC (Nexera, Shimadzu, Kyoto, Japan) coupled to a TripleTOF 6600 mass spectrometer (Sciex, Framingham, MA). The lipids were separated on a UPLC Cortecs® C18 column (2.1 x 100 mm; 1.6 µm particle size; Waters) maintained at 35°C with a flow of 0.2 mL/min in positive mode (ESI<sup>+</sup>) and negative (ESI<sup>-</sup>). The mobile phase used was (A) water:acetonitrile (60:40%) and (B) isopropanol:acetonitrile:water (88:10:2) containing 10 mM ammonium acetate (ESI<sup>-</sup>) or ammonium formate (ESI<sup>+</sup>).



The gradient during the run was: 40-100% B at 10 min, 100%B at 10-12 min, 100-40%B at 12-13 min, and 40% B at 13-20 min. The applied spray voltage was 4500 (ESI-) and 5500 (ESI+). The applied cone voltage was (+/-) 80 V. Information-dependent acquisition (IDA) was used for MS/MS analysis with collision energy of 10 eV. CUR was set to 25 psi, GS1 and GS2 to 45 psi, and the temperature to 450°C.

### Data processing

Detected lipids were manually identified by MS/MS spectrum using PeakView®. Areas of identified lipids were obtained using MultiQuant® (version 3.0.2). For semi-quantification, the R-3.5.0 software was used. Briefly, the area of each identified lipid was divided by the area of its respective internal standard (**Table 1**), multiplied by the amount of internal standard added at the beginning of lipid extraction and, finally, corrected by the correction factor obtained from calibration curves. Data processing the MS/MS data was analyzed with PeakView®, and lipid molecular species were identified by an in-house manufactured

**Table 1:** Lipid classes normalized by the respective internal standards.

<b>Lipid Class</b>	<b>PC</b>	<b>PE</b>	<b>PS</b>	<b>PG</b>	<b>PI</b>	<b>CL</b>	<b>AEG</b>	<b>Cer</b>
<b>Internal Standard</b>	PC (17:0/17:0)	PE (17:0/17:0)	PC (17:0/17:0)	PG (17:0/17:0)	PC (17:0/17:0)	CL (4x14:0)	PC (17:0/17:0)	Cer (d18:1/17:0)
<b>Lipid Class</b>	<b>SM</b>	<b>CE</b>	<b>Cholesterol</b>	<b>Q10</b>	<b>DAG</b>	<b>TAG</b>	<b>DAE</b>	
<b>Internal Standard</b>	SM (d18:1/17:0)	TAG (3x17:0)	TAG (3x17:0)	TAG (3x17:0)	TAG (3x17:0)	TAG (3x17:0)	TAG (3x17:0)	

### Carboxyfluorescein (CF) encapsulated liposomes and membrane leak assay

Liposomes containing different mass percentages of POPC and pPE or SAPE were prepared as described in Bacellar et al[2]. Briefly, lipid films were prepared in glass tubes

containing lipid solution in CHCL<sub>3</sub>, the solvent was removed by N<sub>2</sub> flow, thus leaving a 15 mg lipid film on the tube wall. The films were hydrated with 0.5 mL of CF 50 mM in Tris buffer 10 mM (pH = 8), for complete removal of lipids, the tube was sonicated in an ultrasonic bath (Branson 1200 ultrasonic) and vortexed. The resulting suspension was extruded through a polycarbonate membrane (pore diameter 100 nm, Whatman-Maidstone, England) using an Avanti Polar Lipids mini-extruder. The extruded suspension was eluted through a Sephadex G-50 exclusion column equilibrated with a solution of 300 mM sodium chloride in 10 mM Tris buffer (pH = 8) to remove unencapsulated Carboxyfluorescein (CF). At this pH, CF is anionic and does not cross the membrane; consequently, the resulting liposome suspension contains only CF in the internal compartment of the liposomes.

Samples were prepared in 96-well plates, with each well containing 15  $\mu$ L of liposome suspension, 15  $\mu$ M of photosensitizer (MB or DMMB, except for controls without photosensitizer) and sufficient amount of sodium chloride solution 300 mmol.L<sup>-1</sup> in 10 mM Tris buffer (pH = 8) to reach a final volume of 300  $\mu$ L. The plate was irradiated with an array of LEDs with maximum emission at 631 nm and irradiance was  $72 \pm 1$  W m<sup>-2</sup> at a distance of 20 cm from the light source, the irradiance was  $72 \pm 1$  W m<sup>-2</sup>. CF fluorescence was monitored using a Synergy H1 microplate reader (BioTek Instruments, Winooski, VT), exciting at 480 nm and detecting at 517 nm. The same equipment was used to measure the absorbance of PS (657 nm) and CF (480nm) under the same conditions. At the end point, 10  $\mu$ L of 100x Triton (10% in water) was added to disrupt the remaining liposomes. CF increase values were calculated by dividing the fluorescence intensity at any time by the final and initial difference fluorescence intensity of the same sample, or most intense point, as described in Bacellar et.al[18].

#### **Aldehydes analysis by ESI-QTOF MS/MS**

Photooxidized 1 mM pPE (p18/18:1) liposome was made and then incubated with 1 mM TPP or 1 mM GSH in 10 mM PBS pH 7.4 for 1 hr at RT, 10  $\mu$ L of liposome solution was used for aldehyde analysis. The aldehydes derivatized with CHH were analyzed by ESI-

QTOF (Triple TOF® 6600, Sciex, Concord, US) interfaced with an ultra-high performance liquid chromatography (UHPLC Nexera, Shimadzu, Kyoto, Japan). The chromatographic conditions were the same as for the fluorescence analysis. Excess CHH can damage the mass spectrometer, for this reason the first 5 min are discarded, but all aldehydes are identified, the conditions of the mass spectrometer were the same as for lipid analysis in positive mode. The final derivatization conditions were: 50  $\mu$ M aldehydes or 50  $\mu$ M pPE, 1 mM CH in IPA with 0.1% formic acid.

## **Results and discussion**

### **Reactivity of lipids from HaCat Keratinocyte Cells**

Keratinocytes make up about 95% of epidermal cells[19] and immortalized human keratinocytes known as HaCat cells are commonly studied in skin biology and pathophysiology [20]. Lipids are essential constituents of the cellular membrane and play diverse roles in cellular processes[21]. HaCat cells exhibit a lipid profile that is comparable to that of typical human fibroblasts[22], [23]. We analyzed the lipid composition of HaCat cells and found that glycerophospholipids, especially phosphoethanolamine and phosphatidylcholine, were the most abundant (63%). Sphingolipids, mainly sphingomyelin, accounted for 37% of the lipids, and plasmalogens were the most abundant lipid ethers. Plasmalogens represented slightly over half of the total GPE and less than half of all GPC (**Figure 1A**).

Among the glycerolipids, GPE are made up of more PUFA while GPC are more saturated (**Figure 1B**). Plasmalogens are more enriched in PUFAs and in HaCat more than half of pPE is esterified with PUFA, being responsible for retaining more than 60% of all PUFAs found in HaCat (**Figure 1C**).

Plasmalogens are a type of phospholipids that contain a vinyl ether bond at the sn-1 position of the glycerol backbone instead of a fatty acid residue. Plasmalogens are enriched in polyunsaturated fatty acids (PUFAs) at sn-2 position, which are highly susceptible to lipid peroxidation (**Figure 1D**).

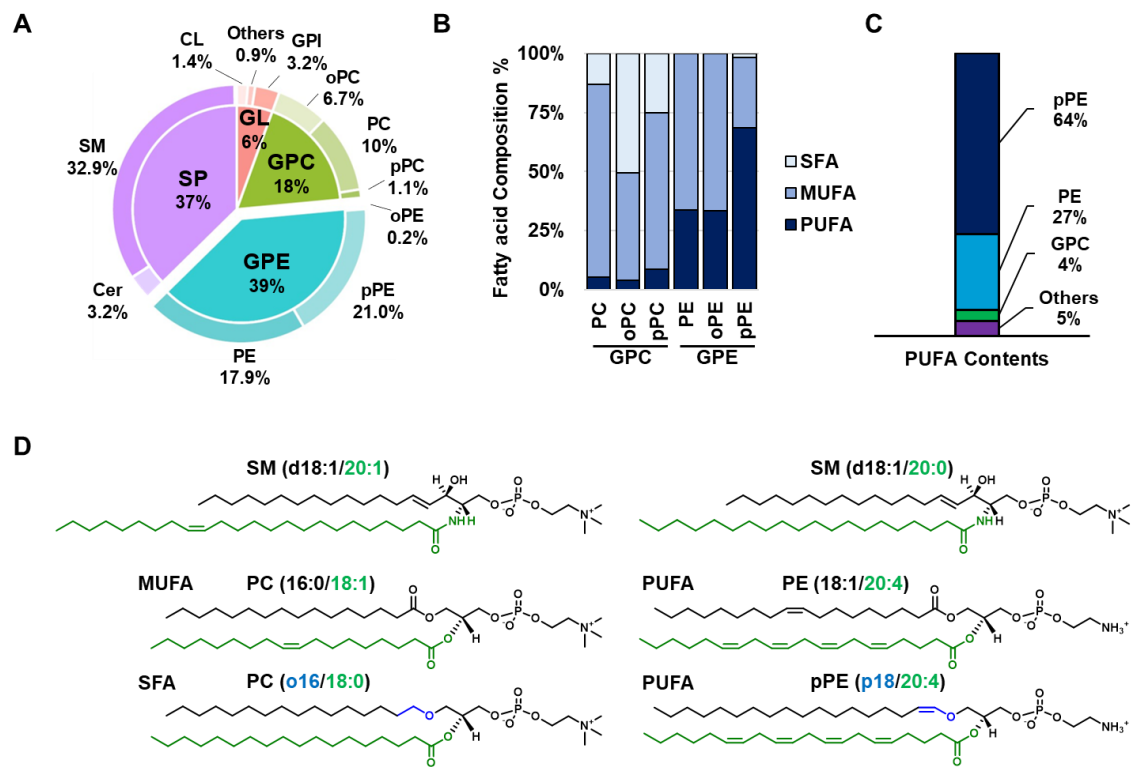


**Figure 1:** (A) Lipid composition of HaCat cells; (B) composition in relation to saturated fatty acids (SFA), monounsaturated (MUFA) and polyunsaturated (PUFA) of the GPC and GPE classes; (C) Availability of polyunsaturated acids (PUFA) in HaCat lipids; (D) Structures of the most abundant classes and subclasses in HaCat cells: Sphingomyelin saturated with chain of unsaturated (SM (d18:1/20:1)) and saturated (SM (d18:1/20:0)) fatty acids; Structures of glycerophospholipids containing only saturated chains (SFA), with at least one monounsaturated chain (MUFA) and with at least one polyunsaturated chain (PUFA) and Comparison between the structures of the subclasses of glycerophosphatidylethanolamine GPE, diacyl PE (PE) and PE plasmalogen (pPE); and subclasses of glycerophosphatidylcholine (GPC), diacyl (PC) and PC plasmanyl (oPC).

Lipids are responsible for maintaining the integrity of cellular membranes. Extensive lipid peroxidation can alter the assembly, composition, structure, and dynamics of membranes[24], [25]. To determine which lipids are more susceptible to oxidation, we subjected lipids extracted from HaCat to photooxidation in the presence of MB and monitored the reaction for 4 hours (**Figure 2A**). Among the main classes, GPE

was the most consumed, and there was rapid consumption within the first 30 minutes of the reaction, likely due to the presence of pPE (**Figure 2B**). Although pPE is more enriched in PUFA than diacylphosphatidylethanolamine (PE), there is no difference in the consumption of pPE bound to PUFA and MUFA. However, PUFA-bound PE is consumed more rapidly (**Figure 2C**). In this way, plasmalogens (pPEs) are the most commonly consumed lipids due to the presence of a vinyl ether bond.

Therefore, it is important to know which lipids are more susceptible to oxidation and to understand the stability of the resulting oxidized product. During lipidomics analysis, we identified 219 non-oxidized lipids manually by analyzing their fragmentation patterns. Next, we explored the various potential oxidation products, such as hydroperoxides, ketones, hydroxides, and chain break products [2]. However, we only detected hydroperoxides and identified 84 oxidized lipids across all lipid classes (as shown in the fragmentation pattern, **Figure S1-S6**). Among the most abundant lipids, GPC and GPE exhibit the greatest variety, including both oxidized forms (Oxylipids) and non-oxidized (lipids) (**Figure 2D**). Nevertheless, the identified Oxylipid precursors accounted for 61% of all non-oxidized initial lipids, with GPE constituting 93% (**Figure 2E**). By employing this approach, we achieved a comprehensive coverage of the oxidized products, which facilitated a more precise kinetic analysis of the production of oxidized lipids.

The kinetics of Oxylipid production were examined for the most abundant classes, and it was observed that GPC and GPE exhibited similar production rates during the initial 60 minutes. However, the production of GPE hydroperoxides decreased as the reaction continued (**Figure 2F**). This phenomenon can be attributed to the rapid production of hydroperoxides of pPE (pPE-OOH), which subsequently decreased (**Figure 2G**). The rapid decrease in pPE-OOH levels could be associated with a Type I reaction that involves a photosensitizer (methylene blue, MB), which generates an alkoxyl radical (pPE-O<sup>•</sup>). This radical then abstracts a proton and produces a hemiacetal.

As demonstrated in Chapter 2, hemiacetals are unstable and decompose into fatty aldehydes and LPE (Figure 2H). This decomposition leads to a significant increase in LPE levels, while LPC levels remain constant (Figure 2I).

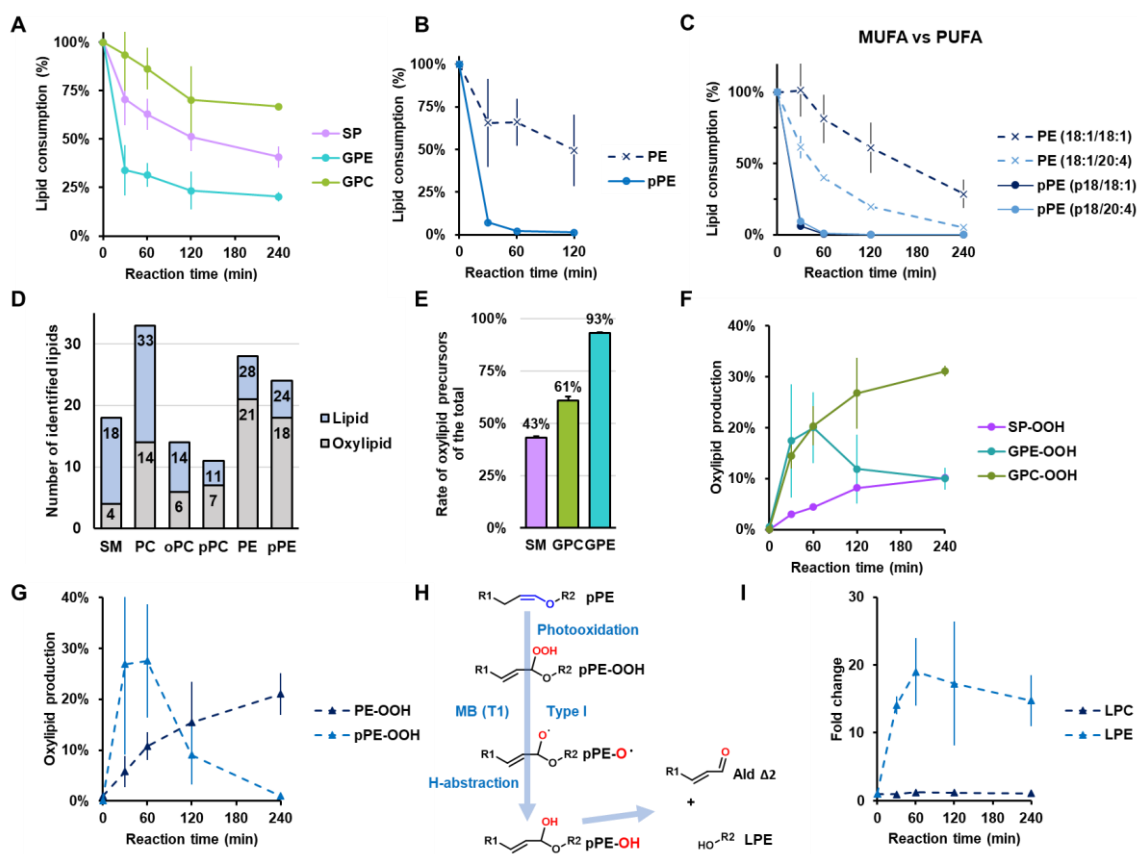


**Figure 2:** (A) Consumption of the main lipid classes present in HaCat cells by the photooxidation reaction over 240 min, normalizing the initial amount as 100%; (B) Consumption of the main GPE subclasses by the photooxidation reaction over 240 min, normalizing the initial amount as 100%; (C) Comparison between plasmalogen consumption of PE and diacyl PE analogue, esterified to MUFA (18:1) and PUFA (20:4); (D) Number of the identified non-lipid and oxydased lipids molecular species per lipid subclasses; (E) Proportion between the initial non-oxidized equivalent by the initial total of the main classes, with 100% the total per class; (F) Kinetics of formation of oxidized lipids by class, having as 100% the sum of the initial non-oxidized equivalents; (G); Kinetics of formation of oxidized lipids by subclass, of GPE having as 100% the sum of initial non-oxidized equivalents; (K) Oxidation mechanism of PE plasmalogens (pPE),

producing pPE hydroperoxide (pPE-OOH), which, when reacting with a Type I photosensitizer, produces an alkoxyl radical (pPE-O●) and, when abstracting a proton, produces a hemiacetal (pPE-OH) which then degrades to lyso PE (LPE); (I) Kinetics of formation of lyso phospholipids from PE (LPE) and PC (LPC), by fold change.

**Abbreviation:** SP, sphingomyelin; GPE, glycerophosphatidylethanolamine; diacylphosphatylethanolamine, PE; PE plasmalogen, pPE; GPC, glycerophosphatidylcholine; diacylphosphatylcholine, PC; plasmalogen PC, pPC, pasmany PC, oPC; SP hydroperoxide, SP-OOH, GPE hydroperoxide, GPE-OOH; GPC hydroperoxide, GPC-OOH; monounsaturated fatty acid (MUFA); polyunsaturated fatty acid (PUFA).

Taken together, we observed that GPE exhibits a higher level of reactivity compared to GPC (**Figure 3**), which can be attributed to the greater prevalence and number of plasmalogens. While other lipids may also possess reactive properties (**Figure S7**), they cannot match the ability of plasmalogens to generate unstable hydroperoxides. As such, PPEs are abundant lipids present in HaCat keratinocyte cells. Upon undergoing photooxidation, pPE rapidly produces pPE-OOH, which has been identified as the most unstable hydroperoxide. The degradation product of LPE was also observed. Therefore, pPE may play a crucial role in maintaining membrane stability.

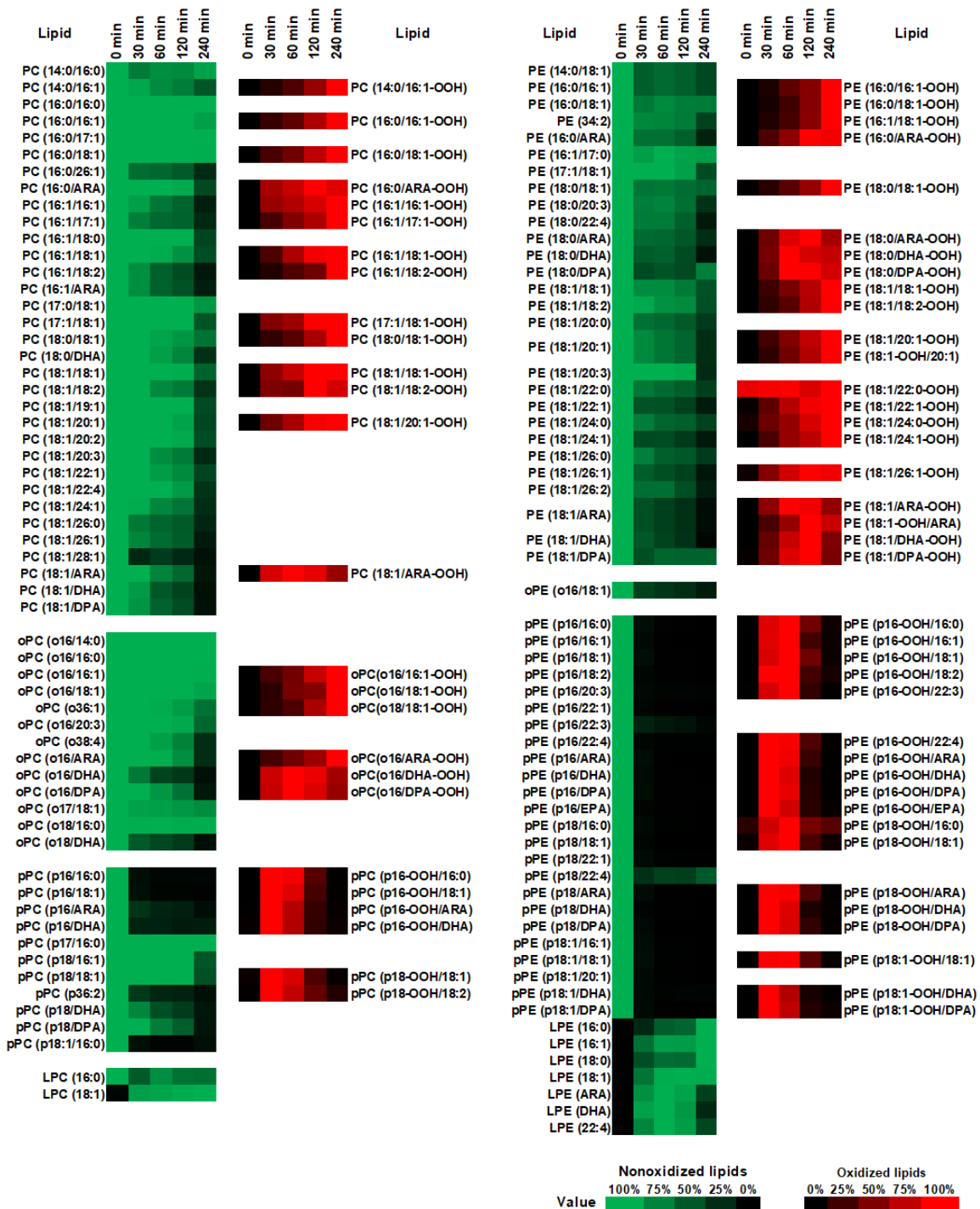


**Figure 3:** Heatmap representing PC lipid changes of lipids extracted from HaCat cells and photooxidized over 240 min (4hr), consumption of lipids not in shades of green, considering 100% the initial value, and formation of oxidized lipids in shades of red, considering the highest value as 100%.



## PE plasmalogens facilitate membrane leakage

The mechanism proposed by Bacellar et al. [2] for membrane leakage describes how lipid hydroperoxides react with excited photosensitizer ( $PS^*$ ) to form truncated species, such as aldehydes, that destabilize the membrane. These hydroperoxides are present in the fatty acid chain that is esterified to a phospholipid.

Plasmalogens, when oxidized by singlet oxygen ( $^1O_2$ ), produce dioxetanes that decompose into aldehydes and formyl PE, which is a truncated species. However, as described earlier, only 2% of plasmalogens follow this pathway. The primary pathway for the oxidation of plasmalogens involves the formation of hydroperoxides, which are highly reactive and break down into aldehydes and LPE (as explained in the chapter 2). Both pathways produce species that can cause membrane leakage as a result. (PE formyl and LPE [17], as shown in **Figure 4**).

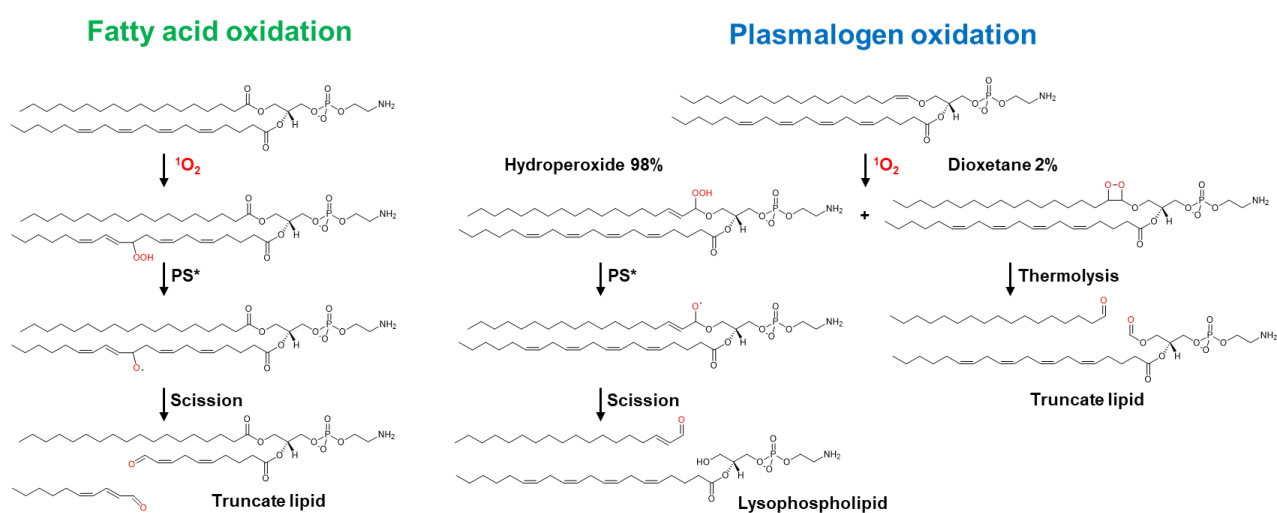


**Figure 4:** Mechanisms of phospholipid oxidation that generate truncated species and smooth phospholipids.

Plasmalogen stand out due to the high reactivity and degradation of hydroperoxides, in addition, they act on the membrane in order to change the fluidity and thickness [13]. However, it still unknown how the oxidation of plasmalogens could act on

the stability of the membrane.

In order to study how plasmalogen transmission influences membrane leakage, a study was carried out on liposomes encapsulated with carboxyfluorescein and photooxidized in the presence of two types of photosensitizers: MB (methylene blue) and DMMB. (dimethyl methylene blue, **Figure 5 A**). DMMB, because it is more lipophilic, causes more damage via radical pathway because it reacts more easily with lipid hydroperoxides [2], [18].

Initially, three types of liposomes were used: the first composed entirely of POPC (PC (16:0/18:1)); second composed of 50% by mass of purified ox brain pPE and 50% POPC; third 50% by mass of SAPE (PE (18:0/20:4)) and 50% POPC. The plasmalogen used was purified from beef brain and therefore has polyunsaturated fatty acids (PUFAs) in the sn2 chain of glycerol. PUFAs can influence membrane leakage, as these fatty acids are more susceptible to oxidation, mainly via radicals.[10]. To study the influence of PUFAs on membrane leakage, leakage assays were performed with liposomes containing SAPE, which has a fatty acid with 4 unsaturation, and compared with liposomes containing purified pPE.

In presence of MB, the SAPE-containing liposome ruptured faster (**Figure 5 B**), indicating an antioxidant action of pPE that reduces lipid peroxidation [26]. However, with DMMB, the liposome containing pPE ruptured faster, indicating that DMMB may be reacting with the pPE-OOH hydroperoxide and causing effective disruption. (**Figure 5 C**). In conditions without PS, there is no leakage (**Figure 5 D**). When analyzing the consumption of PS throughout the reaction, only the POPC liposome with DMMB had a lower consumption (**Figure 5 E e F**).

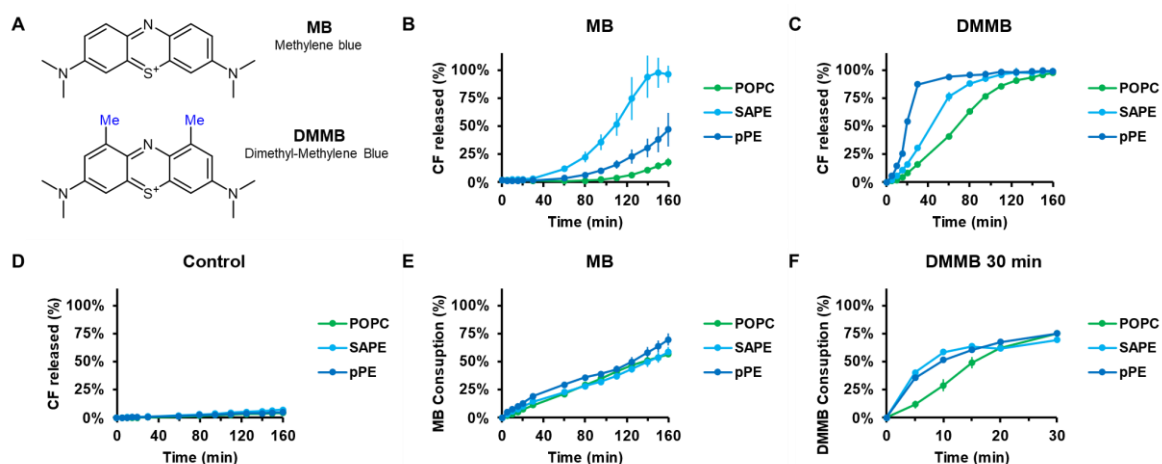


**Figure 5:** (A) Structures of the photosensitizers used; Membrane leakage comparing liposomes with pPE (POPC 50% and purified pPE 50%, mass/mass) and SAPE (POPC 50% and SAPE 50%, mass/mass) and photooxidized with (B) methylene blue (MB), (C) dimethyl methylene blue (DMMB), (C) no PS; PS consumption throughout the reaction (E) with MB and (F) with DMMB.

Under the oxidative conditions that cause membrane leakage of pPE-containing liposomes, photosensitizers appear to act as reductants. Knowing that in a biological environment there would be reduction of hydroperoxide to hydroxide by the action of antioxidants[27], [28]. But with the reduction of hydroperoxides to hydroxides in plasmalogen, it can influence the leakage of the membrane, as a hemiacetal group is formed that hydrolyses forming lysophospholipids that cause leakage [29] (**Figure 6 A**).

Aiming to study the influence of reductants on liposomes photooxidized with MB, a membrane leakage test was performed with a triphenyl phosphine (TPP) reductant, as it is a lipophilic reductant and has already proved to be efficient before. So it was observed that the addition of TPP increases leakage and without MB there is no leakage (**Figure 6 B**). Although MB is less lipophilic, there is still a Type I reaction that can cause membrane leakage.

However, the DHPNO2 endoperoxide generates  $^1O_2$  when heated to  $37^\circ\text{C}$  and without causing radical reactions (**Figure 6 C**). When the membrane leak assay was

performed using liposomes containing purified pPE and SAPE, only DHPNO<sub>2</sub> did not cause leakage (**Figure 6 D**), but in the presence of TPP, only liposomes containing pPE leaked (**Figure 6 E**). Thus, we describe a means of only <sup>1</sup>O<sub>2</sub> causing membrane leakage.

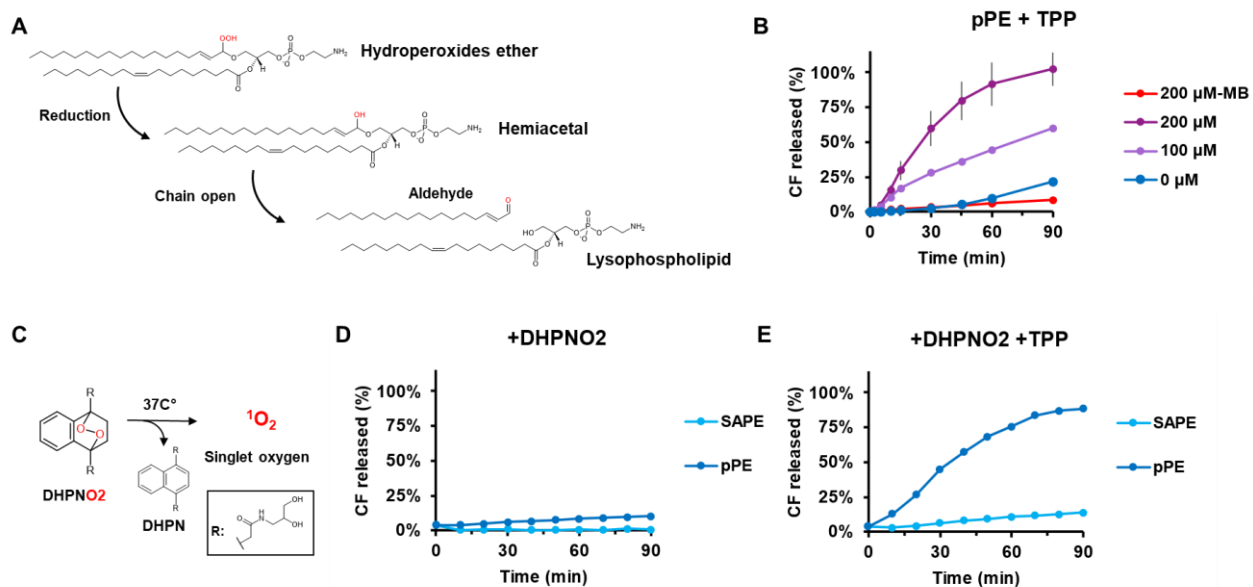


**Figure 6:** (A) Mechanism of reduction of plasmalogen hydroperoxides to hemiacetal, which is degraded into lysophospholipid and aldehyde; (B) Leakage of liposome membrane containing purified pPE and POPC with reducing triphenylphosphine (TPP) with MB or with TPP and without MB (200µM -MB); (C) singlet oxygen (<sup>1</sup>O<sub>2</sub>) formation mechanism by DHPNO<sub>2</sub> degradation; (D) Membrane leak of liposomes containing SAPE or 50% purified pPE and POPC mass with 8 mM DHPNO<sub>2</sub> and heated to 37°C without TPP reductant, (E) with 200 µM TPP.)

Despite the good results with DHPNO<sub>2</sub>, the plasmalogen used was purified and because it is a lipid mixture, there are many types of pPE and among them there are many with PUFAs that add unwanted effects, such as lipid peroxidation.

Then, two new liposomes were used: the first composed of 50% by mass of pPE (p18/18:1) and 50% POPC; according to 50% by mass PE (18:1/18:1) and 50% POPC. Then subjected to the same tests as before. The same results were obtained, but less expressive (**Figure 7**), this may be due to the lower fluidity of the membrane, which makes it less susceptible to leakage [30].

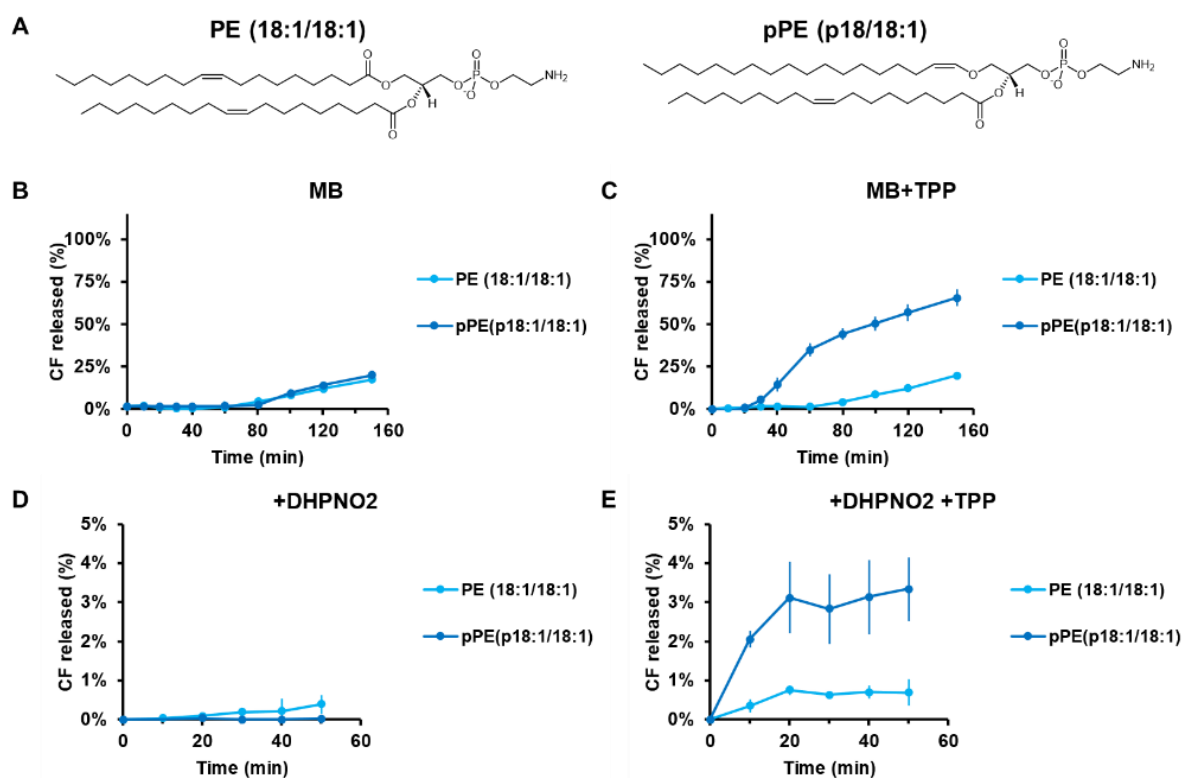


**Figure 7:** pPE (p18:1/18:1) and PE (18:1/18:1) structures used in liposomes; (A) Membrane leakage comparing liposomes with pPE (50% POPC and 50% purified pPE, mass/mass) and PE (POPC 50% and PE 50%, mass/mass) and photooxidized with MB, (B) with 200  $\mu$ M TPP, (C) Pouring with 8 mM DHPNO<sub>2</sub> and heated to 37°C without TPP reducer (E) with 200 $\mu$ M TPP.

Even though TPP is very efficient in reducing plasmalogen hydroperoxides, it is not an endogenous reductant. In order to find an endogenous reductant, phosphoxidized pPE liposomes were made and then reduced with 1 mM reduced glutathione (GSH) and compared with TPP. There was a reduction of hydroperoxides with GSH, but much smaller compared to TPP (**Figure 8**).

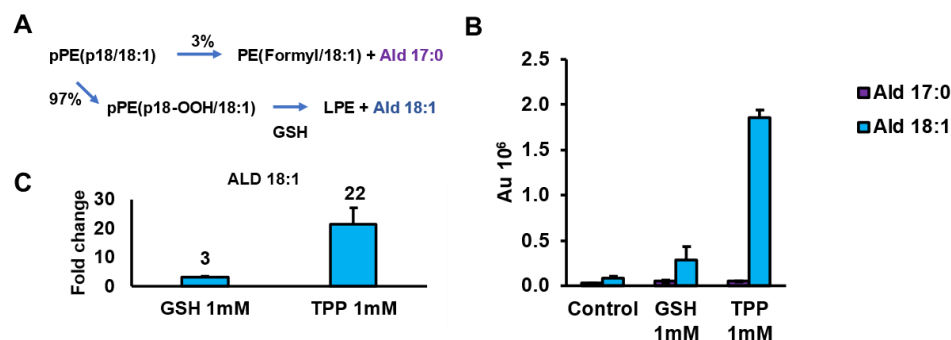


**Figure 8:** (A) Scheme of formation of aldehydes by oxidation followed by reduction of pPE (p18/18:1); (B) UHPLC fluorescence analysis of aldehydes from liposomes containing 100% photooxidized pPE; (C) Aldaldehyde 18:1 increase after GSH and TPP reduction.

## Conclusion

Although plasmalogens are considered antioxidants due to their high reactivity with ROS, it is not known how plasmalogen oxidation can interfere with membrane stability. In this study, we showed that plasmalogens are very abundant in Hacat keratinocytes and are the lipids that are consumed more quickly and produce hydroperoxides that are degraded more quickly. We also showed that the degradation of hydroperoxides makes the membrane more susceptible to leakage. Either by reaction with photosensitizer or reducing agent.

## Acknowledgments

This work was supported by FAPESP [CEPID-Redoxoma 2013/07937-8, FAPESP DD 2017/16140-7 to Faria, R.L.], CNPq [Miyamoto, S. 424094/2016-9, Di Mascio, P. 302120/2018-1], Capes and Pró-Reitoria de Pesquisa da USP.

## References

- [1] L. B. Josefsen and R. W. Boyle, "Photodynamic therapy and the development of metal-based photosensitisers," *Met. Based. Drugs*, vol. 2008, 2008, doi: 10.1155/2008/276109.

- [2] I. O. L. Bacellar *et al.*, "Photosensitized Membrane Permeabilization Requires Contact-Dependent Reactions between Photosensitizer and Lipids," *J. Am. Chem. Soc.*, vol. 140, no. 30, pp. 9606–9615, Aug. 2018, doi: 10.1021/jacs.8b05014.
- [3] T. J. Dougherty *et al.*, "Photodynamic Therapy," *JNCI J. Natl. Cancer Inst.*, vol. 90, no. 12, pp. 889–905, Jun. 1998, doi: 10.1093/jnci/90.12.889.
- [4] M. S. Baptista *et al.*, "Type I and Type II Photosensitized Oxidation Reactions: Guidelines and Mechanistic Pathways," *Photochem. Photobiol.*, vol. 93, no. 4, pp. 912–919, 2017, doi: 10.1111/php.12716.
- [5] P. Di Mascio, G. R. Martinez, S. Miyamoto, G. E. Ronsein, M. H. G. Medeiros, and J. Cadet, "Singlet Molecular Oxygen Reactions with Nucleic Acids, Lipids, and Proteins," *Chem. Rev.*, vol. 119, no. 3, pp. 2043–2086, Feb. 2019, doi: 10.1021/acs.chemrev.8b00554.
- [6] V. Darley-USmar and B. Halliwell, "Blood radicals: reactive nitrogen species, reactive oxygen species, transition metal ions, and the vascular system.," *Pharm. Res.*, vol. 13, no. 5, pp. 649–62, May 1996, doi: 10.1023/a:1016079012214.
- [7] B. Halliwell and S. Chirico, "Lipid peroxidation: its mechanism, measurement, and significance," *Am. J. Clin. Nutr.*, vol. 57, no. 5, pp. 715S-725S, May 1993, doi: 10.1093/ajcn/57.5.715S.
- [8] W. Caetano *et al.*, "Photo-induced destruction of giant vesicles in methylene blue solutions," *Langmuir*, vol. 23, no. 3, pp. 1307–1314, 2007, doi: 10.1021/la061510v.
- [9] J. M. Gutteridge, "Lipid peroxidation and antioxidants as biomarkers of tissue damage.," *Clin. Chem.*, vol. 41, no. 12 Pt 2, pp. 1819–28, Dec. 1995, [Online]. Available: <http://www.ncbi.nlm.nih.gov/pubmed/7497639>.
- [10] E. Niki, Y. Yoshida, Y. Saito, and N. Noguchi, "Lipid peroxidation: Mechanisms, inhibition, and biological effects," *Biochem. Biophys. Res. Commun.*, vol. 338,

- no. 1, pp. 668–676, Dec. 2005, doi: 10.1016/j.bbrc.2005.08.072.
- [11] Y. Yoshida, S. Kodai, S. Takemura, Y. Minamiyama, and E. Niki, “Simultaneous measurement of F2-isoprostane, hydroxyoctadecadienoic acid, hydroxyeicosatetraenoic acid, and hydroxycholesterols from physiological samples,” *Anal. Biochem.*, vol. 379, no. 1, pp. 105–115, Aug. 2008, doi: 10.1016/j.ab.2008.04.028.
- [12] I. Milic, R. Hoffmann, and M. Fedorova, “Simultaneous detection of low and high molecular weight carbonylated compounds derived from lipid peroxidation by electrospray ionization-tandem mass spectrometry,” *Anal. Chem.*, vol. 85, no. 1, pp. 156–162, 2013, doi: 10.1021/ac302356z.
- [13] F. Dorninger *et al.*, “Homeostasis of phospholipids — The level of phosphatidylethanolamine tightly adapts to changes in ethanolamine plasmalogens,” *Biochim. Biophys. Acta - Mol. Cell Biol. Lipids*, vol. 1851, no. 2, pp. 117–128, Feb. 2015, doi: 10.1016/j.bbalip.2014.11.005.
- [14] R. A. Zoeller, A. C. Lake, N. Nagan, D. P. Gaposchkin, M. A. Legner, and W. Lieberthal, “Plasmalogens as endogenous antioxidants: somatic cell mutants reveal the importance of the vinyl ether,” *Biochem. J.*, vol. 338, no. 3, pp. 769–776, Mar. 1999, doi: 10.1042/bj3380769.
- [15] N. Nagan and R. A. Zoeller, “Plasmalogens: biosynthesis and functions,” *Prog. Lipid Res.*, vol. 40, no. 3, pp. 199–229, May 2001, doi: 10.1016/S0163-7827(01)00003-0.
- [16] D. H. Thompson, H. D. Inerowicz, J. Grove, and T. Sarna, “Structural Characterization of Plasmenylcholine Photooxidation Products,” *Photochem. Photobiol.*, vol. 78, no. 4, p. 323, 2003, doi: 10.1562/0031-8655(2003)078<0323:SCOPPP>2.0.CO;2.
- [17] N. J. Zuidam, H. K. M. E. Gouw, Y. Barenholz, and D. J. A. Crommelin, “Physical (in) stability of liposomes upon chemical hydrolysis: the role of lysophospholipids and fatty acids,” *BBA - Biomembr.*, vol. 1240, no. 1, pp. 101–110, 1995, doi:



10.1016/0005-2736(95)00180-5.

- [18] I. O. L. Bacellar, C. Pavani, E. M. Sales, R. Itri, M. Wainwright, and M. S. Baptista, "Membrane Damage Efficiency of Phenothiazinium Photosensitizers," *Photochem. Photobiol.*, p. n/a-n/a, Mar. 2014, doi: 10.1111/php.12264.
- [19] I. Colombo *et al.*, "HaCaT Cells as a Reliable in Vitro Differentiation Model to Dissect the Inflammatory/Repair Response of Human Keratinocytes," *Mediators Inflamm.*, vol. 2017, 2017, doi: 10.1155/2017/7435621.
- [20] E. Boelsma, M. C. H. Verhoeven, and M. Ponc, "Reconstruction of a Human Skin Equivalent Using a Spontaneously Transformed Keratinocyte Cell Line (HaCaT)," *J. Invest. Dermatol.*, vol. 112, no. 4, pp. 489–498, Apr. 1999, doi: 10.1046/j.1523-1747.1999.00545.x.
- [21] T. Kimura, W. Jennings, and R. M. Epand, "Roles of specific lipid species in the cell and their molecular mechanism," *Prog. Lipid Res.*, vol. 62, pp. 75–92, 2016, doi: 10.1016/j.plipres.2016.02.001.
- [22] A. Reich, D. Schwudke, M. Meurer, B. Lehmann, and A. Shevchenko, "Lipidome of narrow-band ultraviolet B irradiated keratinocytes shows apoptotic hallmarks," *Exp. Dermatol.*, vol. 19, no. 8, pp. 103–110, 2010, doi: 10.1111/j.1600-0625.2009.01000.x.
- [23] N. Schürer, A. Köhne, V. Schliep, K. Barlag, and G. Goerz, "Lipid composition and synthesis of HaCaT cells, an immortalized human keratinocyte line, in comparison with normal human adult keratinocytes," *Exp. Dermatol.*, vol. 2, no. 4, pp. 179–185, 1993, doi: 10.1111/j.1600-0625.1993.tb00030.x.
- [24] G. Weber *et al.*, "Lipid oxidation induces structural changes in biomimetic membranes," *Soft Matter*, vol. 10, no. 24, p. 4241, 2014, doi: 10.1039/c3sm52740a.
- [25] J. Van der Paal, E. C. Neyts, C. C. W. Verlackt, and A. Bogaerts, "Effect of lipid peroxidation on membrane permeability of cancer and normal cells subjected to oxidative stress," *Chem. Sci.*, vol. 7, no. 1, pp. 489–498, 2016, doi:

10.1039/C5SC02311D.

- [26] R. C. Murphy, "Plasmalogen Phospholipids : Antioxidant Mechanism and Precursor Pathway for Bioactive Eicosanoids," *Rev. Lit. Arts Am.*, vol. 14, no. 5, pp. 463–472, May 2001, doi: 10.1021/tx000250t.
- [27] B. Halliwell, "Free radicals and antioxidants – quo vadis?," *Trends Pharmacol. Sci.*, vol. 32, no. 3, pp. 125–130, Mar. 2011, doi: 10.1016/j.tips.2010.12.002.
- [28] M. Maiorino, M. Conrad, and F. Ursini, "GPx4, Lipid Peroxidation, and Cell Death: Discoveries, Rediscoveries, and Open Issues," *Antioxid. Redox Signal.*, vol. 4, p. ars.2017.7115, May 2017, doi: 10.1089/ars.2017.7115.
- [29] M. Grit and D. J. A. Crommelin, "The effect of aging on the physical stability of liposome dispersions," *Chem. Phys. Lipids*, vol. 62, no. 2, pp. 113–122, 1992, doi: 10.1016/0009-3084(92)90089-8.
- [30] M. Grit and D. J. A. Crommelin, "Chemical stability of liposomes: implications for their physical stability," *Chem. Phys. Lipids*, 1993, doi: 10.1016/0009-3084(93)90053-6.

## Supplementary Figures:

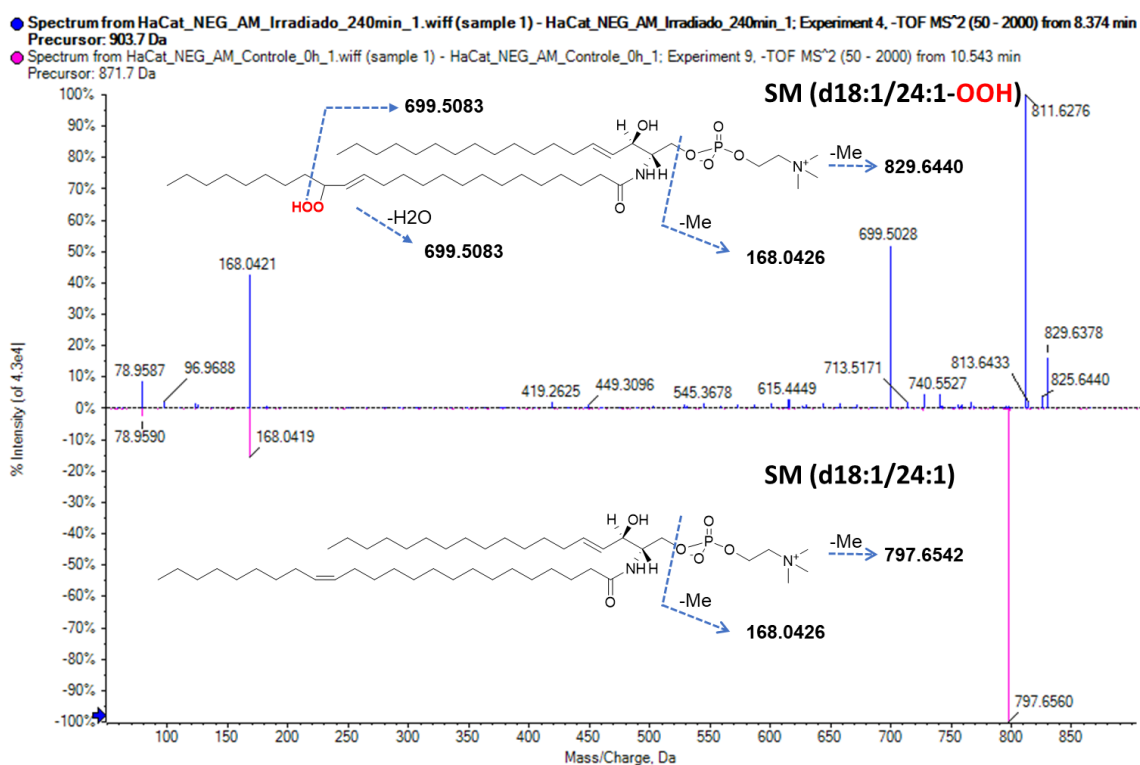


**Figure S1:** Fragmentation spectrum of sphingomyelin (SM(d18:1/24:1)) and comparing with hydroperoxide analogue (SM(d18:1/24:1-OOH)).

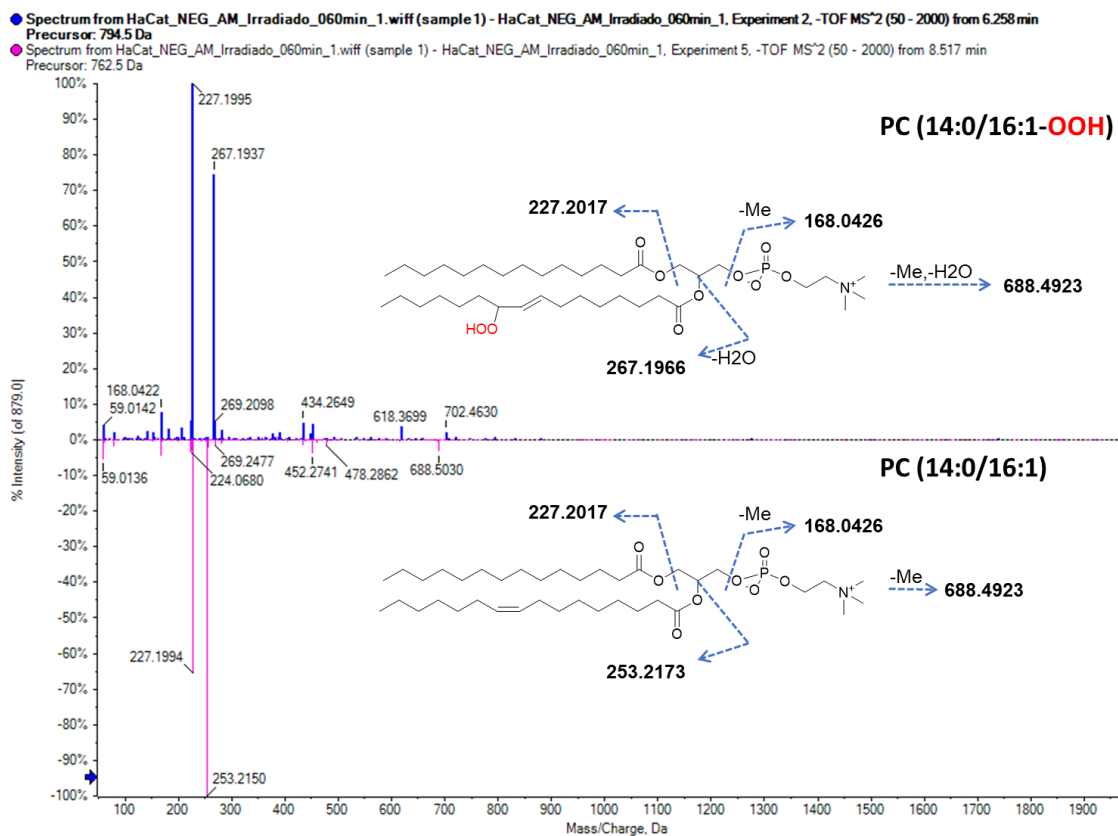


**Figure S2:** Fragmentation spectrum of phosphatidylcholine (PC(14:0/16:1)) and comparing with hydroperoxide analogue (PC(14:0/16:1-OOH)).

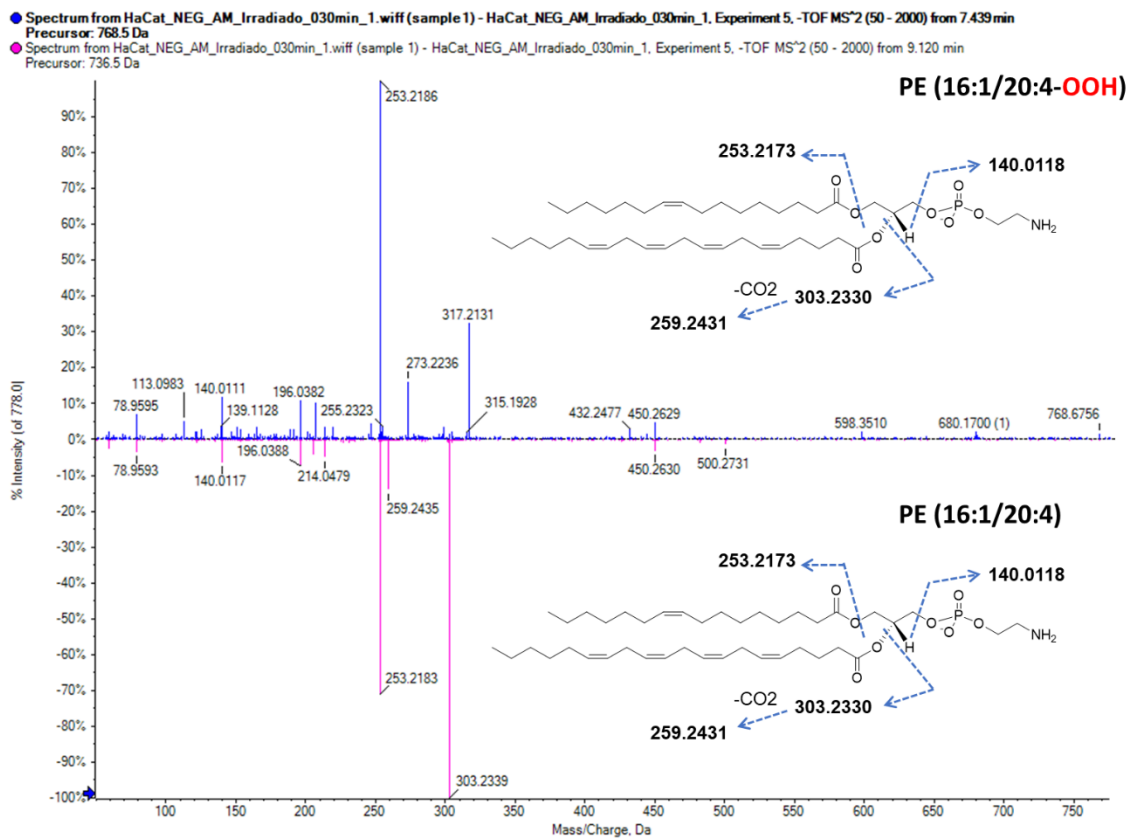


**Figure S3:** Fragmentation spectrum of phosphatidylethanolamine (PE(16:1/20:4)) and comparing with hydroperoxide analogue (PE(16:1/20:4-OOH)).





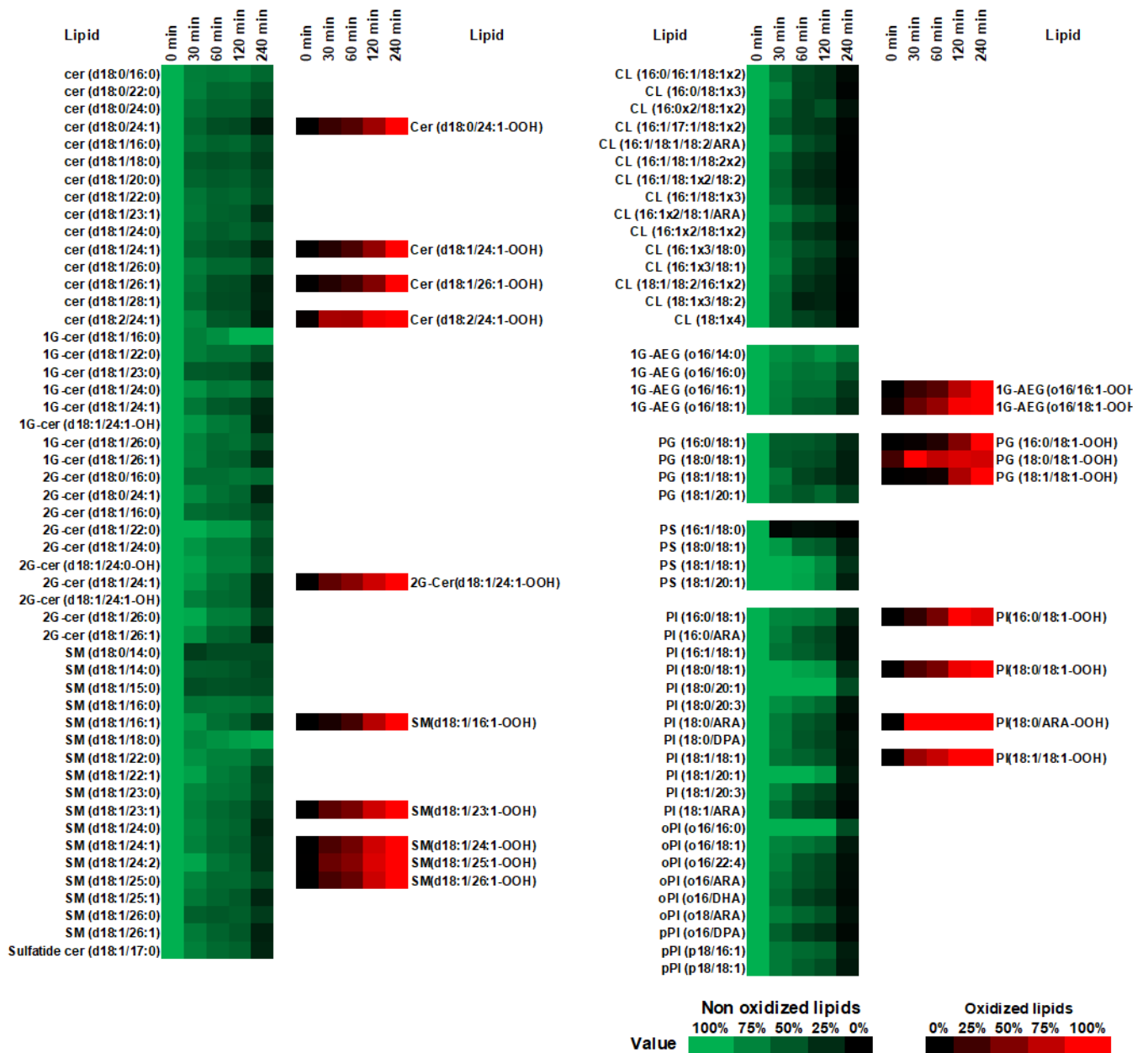


**Figure S6:** Heatmap representing lipid changes of lipids extracted from HaCat cells and photooxidized over 240 min (4hr), consumption of lipids not in shades of green, considering 100% the initial value, and formation of oxidized lipids in shades of red, considering the highest value as 100%.



## CHAPTER 4

### **Determination of changes in plasma free fatty acids in a high-fat diet in amyotrophic lateral sclerosis by UHPLC-Florescence**

Rodrigo Lucas de Faria<sup>1</sup>, Larissa Regina Diniz<sup>1</sup>, Isabela Fernanda Pinto<sup>1</sup>, Adriano Brito<sup>1</sup>, Lucas Danas<sup>1</sup>, Sayuri Miyamoto<sup>1\*</sup>

1 Departamento de Bioquímica, Instituto de Química,  
Universidade de São Paulo, São Paulo, SP,

\* Corresponding Author: Sayuri Miyamoto. E-mail address:  
miyamoto@iq.usp.br

Institutional address: Departamento de Bioquímica, Instituto de Química, Av.  
Prof. Lineu Prestes 1524, CP 26077, CEP 05313-970, Butantã, São Paulo, SP.  
Brazil. Phone: + 55 1130911413

## Highlights

- A sensitive method for analysis of free fatty acids
- Derivatization method uses reducers that participate in the derivatization and prevent lipid peroxidation
- The method uses the same derivatization probe for aldehyde analysis
- Analysis of blood plasma from mouse models of ALS shows a very similar profile between analysis by UHPLC-Florescence and UHPL-ESI-QTOF-MS/MS
- Rats supplemented with a diet rich in fish oil had a reduction in arachidonic acid and an increase in w3 fatty acids (DHA and EPA)

**Abbreviations:**

**ACN**, acetonitrile

**ALS**, amyotrophic lateral sclerosis

**ARA**, arachidonic acid

**Cer**, ceramide

**CHH**, 7-(Diethylamino)coumarin-3-carbohydrazide

**DAG**, diacylglycerols

**DAGE**, 1-O-alkyl diacylglycerol ethers

**DHA**, docosahexaenoic acid

**DPDS**, 2,2'-Dipyridyldisulfide

**EPA**, eicosapentaenoic acid

**FFA**, Free fatty acid

**PC**, phosphatidylcholine

**PE**, phosphatidylethanolamine

**PG**, phosphatidylglycerol

**PI**, phosphatidylinositol

**PS**, phosphatidylserine

**Q10**, ubiquinone-10

**SM**, sphingomyelin

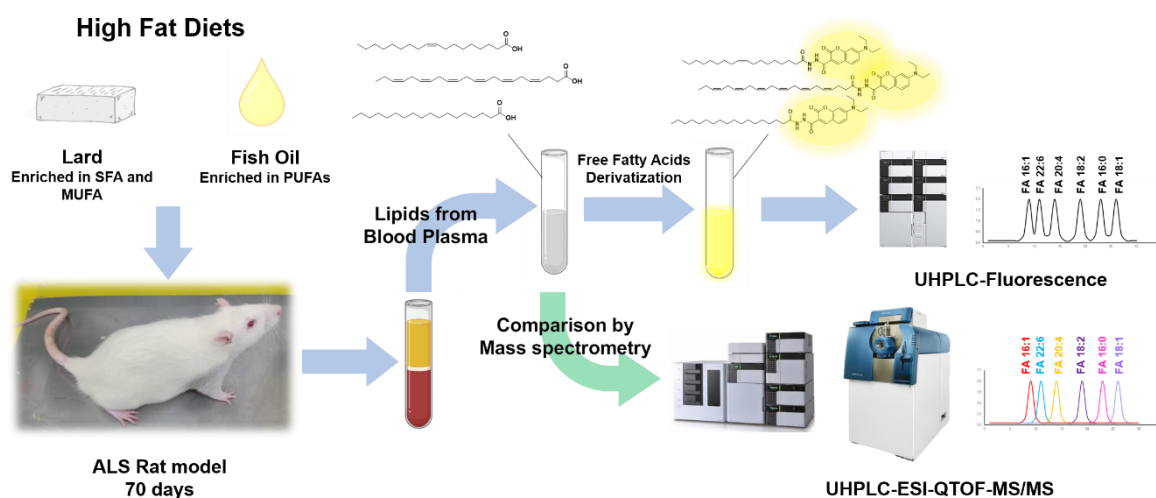
**SOD1**, superoxide dismutase type 1

**TAG**, triacylglycerols

**TPP**, triphenyl phosphine

**UHPLC**, ultra-high-performance liquid chromatography

## Graphical abstract



## Abstract

Fatty acids are structural components of membrane phospholipids and also act as precursors for lipid mediators and an energy source. Lipid mediators from omega-6 arachidonic acid (FA 20:4; ARA) have pro-inflammatory actions. On the other hand, mediators from omega-3 Eicosapentaenoic acid (FA 20:5; EPA) and Docosahexaenoic acid (FA 22:6; DHA) have anti-inflammatory action. Dietary intake rich in omega-3 fatty acids has a variety of anti-inflammatory and immune-modulating effects that may reduce neuroinflammation in neurodegenerative diseases, such as amyotrophic lateral sclerosis (ALS). In order to verify how an omega-3 diet can increase the availability of DHA and EPA in animal models of ALS. We analyzed FFA from the blood plasma of human SOD1 (G93A) transgenic ALS rats and wild types supplemented with three types of diets: rich in fish oil, lard, and standard rodent diet. We observed a significant increase in EPA and DHA, followed by a significant decrease in ARA, in ALS and WT rats supplemented with a diet rich in fish oil. Thus, the disease does not interfere with the absorption of omega-3 fatty acids. For FFA analysis, we developed a novel reverse-phase ultra-high-performance liquid chromatography (UHPLC) coupled with a fluorescence detector. In this work, we used

FFAs derivatized with 7-(Diethylamino)coumarin-3-carbohydrazide (CHH). This reaction does not involve transesterification, thus enabling the quantification of FFAs in the presence of glycerolipids with limits of FFA detection in the range of 0.2–100 pmol. For comparison, we analyze the samples without derivatization using UHPLC coupled with a tandem ESI-QTOF high-resolution mass spectrometric detector (HRMS) for the full characterization and quantitation of the different FFA.

**Keywords:** Free fatty acids analysis, amyotrophic lateral sclerosis (ALS), carboxyl derivatization, UHPLC, fluorescence detector, high-resolution mass spectrometric

## Introduction

Inflammation is the immune system's response to harmful stimuli, such as pathogens or damaged cells, and acts as a vital defense mechanism for health [1]. Although inflammation is a normal response, when it occurs in an uncontrolled or inappropriate manner due to the persistence of an inflammatory stimulus or a failure of normal resolution mechanisms, it can cause excessive damage to host tissues and disease [2], [3]. Chronic inflammation is associated with many neurodegenerative diseases, including Alzheimer's disease, Parkinson's disease, multiple sclerosis, and amyotrophic lateral sclerosis (ALS) [4]–[6].

ALS is an aggressive and rapidly progressing disease that causes death within 5 years of diagnosis, and only 10% of cases have a family history [4]. ALS tissue is characterized by neuroinflammatory changes, and these changes are seen in both sporadic and familial ALS, as well as in transgenic SOD1 mouse/rat models of ALS [7]. Inflammation is not causative, although it can greatly influence pathogenesis. In such cases, there may be potential for anti-inflammatory therapy [5].

The omega-6 arachidonic fatty acid (ARA; FA 20:4) gives rise to lipid mediators that act in inflammatory processes. The metabolism of ARA is a well-recognized target in anti-inflammatory therapies, since many of the ARA derivatives are pro-inflammatory [8]. On the other hand, the omega-3 eicosapentaenoic acid (EPA, FA 20:5) and docosahexaenoic acid (DHA, FA 22:6) derived lipid mediators called resolvins have anti-inflammatory properties. Studies show that a diet high in fish oil can cause an increase in DHA and EPA and a decrease in ARA [8], [9]. Then, a diet rich in fish oil can be beneficial for the survival of patients with ALS, as this disease causes neuroinflammation in pathologically affected tissue.

In this work, we analyzed free fatty acids (FFA) from the plasma of SOD1 G93A and wild-type transgenic rats supplemented with three types of diets: fish oil, lard, and a standard rodent laboratory diet. The FFA profile of animals supplemented with a fish oil diet was very different from animals supplemented with lard and standard rodent diets. However, we did not observe major differences in the FFA profile between ALS and WT animals, regardless of diet. Animals supplemented with a fish oil diet showed a significant increase in DHA and EPA and a significant decrease in ARA, both for WT and ALS animals. Thus, a diet richer in omega-3 from fish oil may be beneficial in reducing the effects of neuroinflammation.

FFAs are detected by HPLC through UV absorbance at 205 nm[10]. However, the molar absorbance of FA changes depending on the number of unsaturations, and saturated FFAs are barely detected[11]. Hence, different HPLC-based FFA analysis methods derivatize the carboxylic acid group of the FFA with fluorescent probes to measure all FFAs according to molar concentration, regardless of FFA unsaturation[10].

For FFA analysis, we developed a novel reverse-phase ultra-high-performance liquid chromatography (UHPLC) coupled with a fluorescence detector, within a relatively short chromatographic run (40 min). In this work, we optimized the derivatization reaction for free fatty acids with a fluorescence probe, 7-(Diethylamino)coumarin-3-carbohydrazide (CHH), through a thioester intermediate produced in the presence of 2,2'-Dipyridyldisulfide (DPDS) and the antioxidant triphenylphosphine (TPP) in a one-pot reaction. This is a low-cost approach that avoids lipid oxidation. This reaction does not involve transesterification, thus enabling the FFAs to be successfully quantified in the presence of glycerolipids, with limits of FFA detection in the linear range of 0.2–100 pmol (signal-to-noise ratio above 20 [12]). For comparison we analyze the samples without derivatization using UHPLC coupled with an electrospray source and a tandem quadrupole-time-of-flight (ESI-QTOF) high-resolution mass spectrometric detector (HRMS) for the full characterization and quantitation of the different classes of fatty acids.

Both methods (fluorescence and HRMS) appreciate the FFA in a similar order of magnitude and proportions.

## **MATERIALS AND METHODS**

### **Reagents**

2,2'-Dipyridyldisulfide (DPDS), triphenyl phosphine (TPP), 7-(Diethylamino)coumarin-3-carbohydrazide (CHH), 1,2-diheptadecanoyl-sn-glycero-3-phosphoethanolamine (PE 17:0/17:0), 1,2-diheptadecanoyl-sn-glycero-3-phosphocholine (PC 17:0/17:0), 1,2-diheptadecanoyl-sn-glycero-3-phospho-L-serine (PS 17:0/17:0), 1,2-diheptadecanoyl-sn-glycero-3-phospho-(1'-rac-glycerol) (PG 17:0/17:0), 1-heptadecanoyl-2-hydroxy-sn-glycero-3-phosphocholine (LPC 17:0/17:0), 1',3'-bis[1,2-dimyristoyl-sn-glycerol-3-phospho]-sn-glycerol (CL 14:0/14:0/14:0/14:0), N-heptadecanoyl-D-erythro-sphingosylphosphorylcholine (SM d18:1/17:0) e N-decanoyl-D-erythro-sphingosine (Cer d18:1/10:0) were acquired from Avanti Polar Lipids (Alabaster, AL).. Methyl tert-butyl ether (MTBE), ammonium formate and ammonium acetate were purchased from Sigma-Aldrich (St Louis, MO, USA). All HPLC grade organic solvents were obtained from Sigma-Aldrich (St Louis, MO, USA). Ultra-pure water was supplied by a Millipore system (Millipore, Billerica, MA, USA).

### **Animals**

Male Sprague Dawley rats overexpressing mutant human SOD1G93A (hSODG93A), obtained from Taconics, were maintained in our animal facility at room temperature with a 12-hour light/dark cycle. Genotyping was performed to detect the exogenous hSOD1G93A transgene by amplifying ear DNA at 20 days of age [13]. At 52 days of age, animals were placed on either a lard or fish oil diet (caloric composition: fat 60%, carbohydrate 20%, protein 20%) or a standard rodent laboratory diet (fat 10%, carbohydrate 70%, protein 20%). At 73±4 days



of age, rats were without any signs of motor impairment. At 122±6 days of age (referred to as the symptomatic group), rats showed partial paralysis in at least one limb, and, importantly, experienced a loss of body weight. Age- and litter-matched wild-type (WT) males served as controls, referred to as WT at 70 days of age. Rats were fasted for 4 hours and anesthetized with isoflurane inhalation at a dose of 4% for induction and 2% for maintenance. All groups had n=5. Blood was collected by cardiac puncture into a tube containing heparin (BD, Franklin Lakes, NJ, USA). Plasma was obtained after centrifugation at 2,000 x g for 10 minutes at 4°C and stored at -80°C until further processing. All procedures were performed in accordance with the National Institute of Health Guidelines for the Humane Treatment of Animals and approved by the local Animal Care and Use Committee of Sao Paulo University (CEUA number 41/2016).

#### **Lipid extraction and Fatty acids derivatization**

Lipids were extracted from plasma using the MTBE method[14]. Briefly, 80 µL of plasma was mixed with 80 µL of MeOH containing FA 13:0 at 4 µM as an internal standard, and 220 µL of ice-cold MeOH. After thoroughly vortexing for 10 seconds, 1 mL of MTBE was added to the mixture, which was stirred for 1 hour at 20°C. Next, 300 µl of water was added to the mixture, followed by vortexing for 10 seconds and resting in an ice bath for 10 minutes. After centrifugation at 10,000 x g for 10 minutes at 4°C, the supernatant containing the lipid extract was transferred to a vial and dried under N<sub>2</sub> gas. The extracted lipids were re-dissolved in 80 µl of isopropanol for the UHLC-Q-TOF-MS/MS analysis or re-dissolved in 80 µl of ANC with 120 µM of TPP, DPDS, and CHH for UHPLC-Fluorescence analysis, and incubated at 20°C overnight. The data were

processed with Post-run Analysis software (Labsolutions version 5.98, Shimadzu). For lipidomics analysis of each diet, the lipids were extracted from the rations of each diet. Using 200 mg/mL homogenate was prepared in PBS pH 7.4 containing 10 mM of deferoxamine mesylate. Then, the same extraction method was used with MTBE on 80  $\mu$ L of homogenate.

For the analysis with the objective of verifying if there is transesterification by the derivatization reaction, we performed the derivatization of PC (16:0/18:1) at a concentration of 10  $\mu$ g/mL in ANC and we derivatized it with 120  $\mu$ M of TPP, DPDS, and CHH and incubated it at 20°C overnight. For the positive control, we hydrolyzed 1 mL of a solution containing 1  $\mu$ g/mL of PC (16:0/18:1) in MeOH. We then added 1 mL of 0.4 M NaOH, which had been previously bubbled with nitrogen. This mixture was subjected to vortexing (15 s) and incubated at 37°C for 30 min in the dark. After this step, the samples were cooled in an ice bath for 10 minutes and then neutralized with 1.2 mL of 2 M HCl. After that, the samples were subjected to a new extraction, this time with 2 mL of hexane. The samples were vortexed for 1 minute and centrifuged at 1500g for 2 minutes at 4°C. The upper organic phase was collected, and the extraction process was repeated with the addition of another 2 mL of hexane. Finally, the organic phases were combined, evaporated under nitrogen flow, and then resuspended in 100  $\mu$ L of ANC with 120  $\mu$ M of TPP, DPDS, and CHH. The mixture was incubated at 20°C overnight.

### **Free fatty analysis by UHPLC-Fluorescence**

The analysis was performed using UHPLC-fluorescence (Nexera, Shimadzu, Kyoto, Japan) on a reversed-phase BEH® C18 column (2.1 x 100 mm; 1.6  $\mu$ m particle size;

Waters) maintained at 40°C with a flow rate of 0.3 mL/min, in a gradient of (A) water with 0.1% formic acid and (B) ACN with 0.1% formic acid. The gradient during the run was: 70-100% B at 30 min, 100% B at 30-35 min, 100-70% B at 35-36 min, and 70% B at 36-40 min.

### **Lipid analysis by UPLC-MS/MS (HRMS)**

The underivatized extracted lipids were analyzed by UPLC (Nexera, Shimadzu, Kyoto, Japan) coupled to a TripleTOF 6600 mass spectrometer (Sciex, Framingham, MA). The lipids were separated on a UPLC Cortecs® C18 column (2.1 x 100 mm; 1.6 µm particle size; Waters) maintained at 35°C with a flow rate of 0.2 mL/min, in positive mode (ESI+) and negative mode (ESI-). The mobile phase used was (A) water:acetonitrile (60:40%) and (B) isopropanol:acetonitrile:water (88:10:2) containing 10 mM ammonium acetate (ESI-) or ammonium formate (ESI+).

The gradient during the run was: 40-100% B at 10 min, 100% B at 10-12 min, 100-40% B at 12-13 min, and 40% B at 13-20 min. The applied spray voltage was 4500 (ESI-) and 5500 (ESI+). The applied cone voltage was (+/-) 80 V. Information-dependent acquisition (IDA) was used for MS/MS analysis with a collision energy of 10 eV. CUR was set to 25 psi, GS1 and GS2 were set to 45 psi, and the temperature was set to 450°C.

### **HRMS data processing**

Lipidomic analysis was performed using the MS-MDIAL (version 5.1) [15] software set to default conditions for identification. Each identified lipid was checked manually, following the fragmentation patterns[16], [17]. Areas of identified lipids were obtained using MultiQuant® (Version 3.0.2). The area of each identified lipid was divided by the area of its respective internal standard, multiplied by the amount of internal standard added at the beginning of lipid

extraction, and finally corrected by the correction factor obtained from calibration curves.

## Results

### Derivatization of fatty acids with CHH

Various fluorescent derivatization reagents have been utilized to quantify carboxylic acids, including fatty acids and prostaglandins, through high-performance liquid chromatography (HPLC) [10]. Alkyl halide compounds have been extensively studied [10], [18]. However, the derivatization reaction only occurs at elevated temperatures in the presence of basic catalysts [10]. This can result in lipid peroxidation and de-esterification of fatty acids. Other diazo probes, such as PDAM and ADAM, can derivatize FFA under mild conditions at room temperature without the need for an activating reagent [10], [18]. However, these probes are unstable and must be synthesized before use, which means they may contain impurities and decomposition products [10].

To prevent these complications, in this work, we used an unusual approach to derivatize FFA. We conducted a two-step reaction, but in a one-pot reaction. The first derivatization step is to produce an intermediate thiolester by reacting FFA in the presence of 2,2'-Dipyridyldisulfide (DPDS) and triphenylphosphine (TPP) [19]. Then, the thiolester reacts with the hydrazide group of the fluorescent probe 7-(Diethylamino)coumarin-3-carbohydrazide (CHH) through an addition-elimination reaction(**Figure 1**).

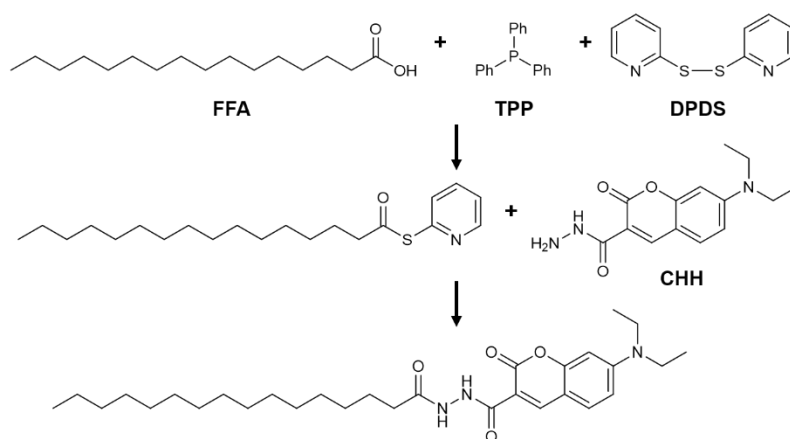


**Figure 1:** Derivatization of carboxyl from free fatty acids mechanism in two stages: 1st formation of thioester by reaction of fatty acid with DPDS and TPP; 2nd Addition followed by elimination by the primary amine of the hydrazide group of CHH.

This derivatization method does not require catalysis that involves altering the pH of the medium, either through acidification or alkalization. Consequently, the hydrolysis of glycerolipids and transesterification do not occur. In order to verify if the derivatization of FFA does not involve transesterification or fatty acid hydrolysis, we conducted an analysis of POPC (PC (16:0/18:1)). For a positive control, we hydrolyzed POPC under basic conditions. The concentration of phospholipid at the end of the experiment was 20  $\mu\text{g/mL}$ . The fluorescence signal was observed only in the hydrolyzed sample (**Figure 2A**). The optimization of the chromatography method aimed to enable the simultaneous analysis of up to 12 fatty acids, utilizing two potential internal standards (FA 13:0 and FA 17:0) and 10 fatty acids that are frequently present in humans. These include the polyunsaturated fatty acids (PUFA) of interest in this study, arachidonic acid (FA 20:4, ARA), eicosapentaenoic acid (FA 20:5, EPA), and docosahexaenoic acid (FA 22:6, DHA) **Figure 2B**.

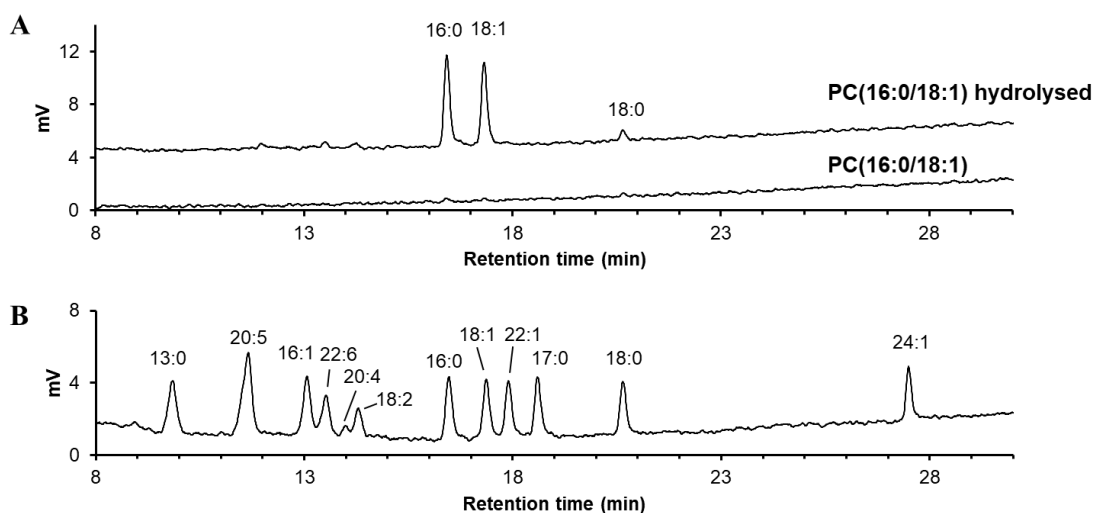


**Figure 2:** Chromatographic separation of free fatty acids that have been derivatized with CHH using UHPLC-Fluorescence: (A) A comparison between the commercial phospholipid PC(16:0/18:1) and PC(16:0/18:1) hydrolyzed with 400 mM NaOH at 37°C for 30 minutes. Only in hydrolyzed sample contain FFA, mainly FA 16:0 and FA 18:1. (B) A mixture of 12 commercially available standard fatty acids, each at a concentration of approximately 10 µg/mL.

The optimization of the FFA derivatization method involved minimizing the excess of reagents, controlling the temperature, and regulating the reaction time, as illustrated in **Figure S1 A**.

In order to verify the occurrence of lipid peroxidation, an analysis was conducted using docosahexaenoic acid (DHA), which contains 6 unsaturations. Initially, DHA and FA 13:0 were derivatized under identical conditions for a duration of 48 hours, resulting in an identical profile (**Figure S2 A**). The FA 13:0 molecule is saturated and, therefore, does not undergo lipid peroxidation. This suggests that DHA did not undergo oxidation. We conducted a comparison between the addition of BHT antioxidant as a positive control, and the results showed no significant difference. The data presented in this study suggest a lack of lipid peroxidation in the derived samples, which may be attributed to an excess of TPP (**Figure S2B**).

To verify the sensitivity of the method, we analyzed FA 13:0 within a range of 0.2 pmol to 100 pmol. We observed a linear increase in all data points with a signal-to-noise ratio greater than 20 [12] (**Figure S3 A**). Next, we constructed a dose-response curve by utilizing a fixed quantity of 13:0 at 20 pmol as an internal standard and increasing amounts of DHA from 5 to 80 pmol. This resulted in a straight line with an angular coefficient close to 1. The same procedure was performed for other fatty acids, including oleic acid (FA 18:1), linoleic acid (FA 18:2), and ARA. The results showed excellent linearity (**Figure S3 B to E**). The method has been proven to be sensitive and produces stable products within a relatively short chromatography time of 40 minutes. The response curves indicate that FA 13:0 can serve as an internal standard due to its good linearity within the analyzed concentration range.

#### **FFA analysis by LC-Fluorescence and LC-high resolution mass spectrometry**

Many cases of familial ALS are associated with mutations in the Superoxide Dismutase 1 (SOD1) gene. We used the SOD1-G93A transgenic rat model for ALS [20]. This animal model has a mutation in SOD1 that increases the production of harmful reactive oxygen species (ROS). The rat model demonstrates a loss of motor neurons, accompanied by gliosis, and the presence of numerous ubiquitinated Lewy-like bodies and axonal swelling. The pathology observed in the spinal cord of these mice more closely resembles that of human ALS [21].

We analyzed the blood plasma of five ALS rats and five wild types (WT) rats using UHPLC-fluorescence and compared the results with those obtained using UHPLC-High Resolution Mass Spectrometry (HRMS). We used asymptomatic rats (70 days old) for this analysis to prevent other factors, such as aging[22] and atrophy[23], from interfering with the physical activity profile in mice with ALS. The disease was the main factor that altered blood plasma FFA (**Figure S4**).

The analysis of FFA in plasma samples from WT and ALS rats using both UHPLC-Fluorescence and UHPLC-high-resolution mass spectrometry (HRMS) techniques was highly comparable. For all FFA, the exhibit comparable magnitudes and distributions in both techniques, and the FFA levels are coherent as described in the literature (**Figure 3**) [19], [24].

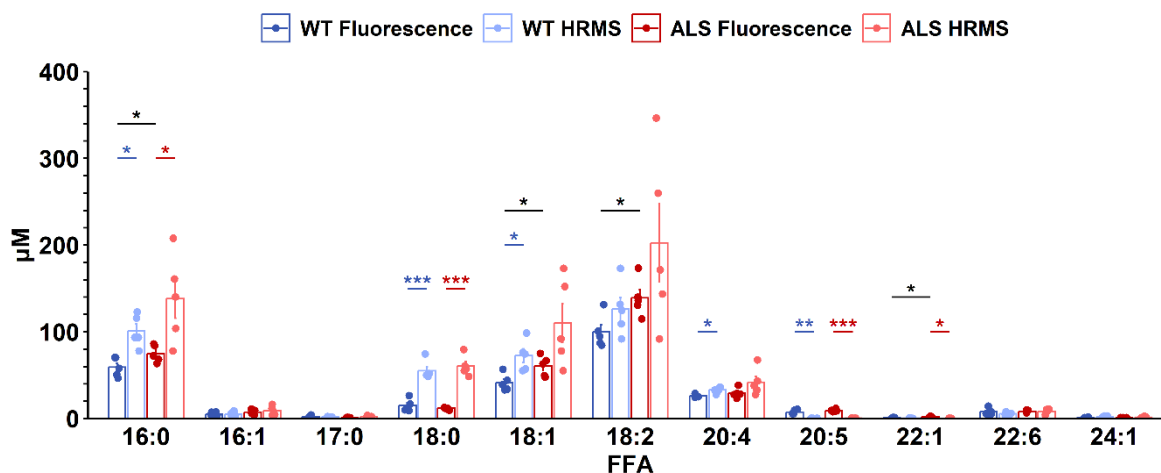


**Figure 3:** Concentration of free fatty acids (FFA) in the plasma of asymptomatic wild-type and ALS rats (70 days old) was analyzed using UHPLC-Fluorescence and UHPLC-HRMS. Error bars show mean  $\pm$  SD. Differences between means are color-coded: blue for WT-Fluorescence vs. WT-HRMS, red for WT-Fluorescence vs. ALS-Fluorescence, and black for WT-Fluorescence vs. ALS-Fluorescence. (\* $p < 0.05$ , \*\* $p < 0.01$ , and \*\*\* $p < 0.001$ ; two-tailed paired t-tests)

We observed an increase in palmitic acid (FA 16:0), oleic acid (FA 18:1), and linoleic acid (FA 18:2) levels using both techniques. ALS induces hyperlipidemia, and it can result in an increase in blood FFA levels [25]. However, only the fluorescence technique provides a significant difference with a  $p$ -value  $< 0.05$ . This could be attributed to the coefficient of variation (CV%) being lower for nearly all of the analyzed FFAs in fluorescence analysis (**Table 1**).



**Table 1:** The coefficient of variation expressed as a percentage (CV%) for the FFA analysis in Figure 3.

CV%	16:0	16:1	17:0	18:0	18:1	18:2	20:4	20:5	22:1	22:6	24:1
<b>WT Fluorescence</b>	18%	40%	59%	48%	23%	19%	6%	33%	85%	50%	30%
<b>WT HRMS</b>	18%	41%	16%	20%	24%	24%	10%	68%	53%	27%	53%
<b>ALS Fluorescence</b>	13%	37%	10%	10%	19%	15%	19%	15%	27%	16%	28%
<b>ALS HRMS</b>	37%	57%	29%	19%	46%	50%	37%	57%	27%	33%	49%

Some FFA quantity variation may be due to unsuitable internal standard, FA 13:0, for HRMS. The detection efficiency can be affected by FFA's unsaturation number and chain length [26]. Isotopic standards are the gold standard for HRMS, providing more precise quantification. However, it is necessary to use one internal standard for each FA, which makes the analysis more costly [27].

The utilization of UHPLC-HRMS offers the benefit of accurately identifying FFAs through the determination of their precise mass and retention time. Nonetheless, this method is associated with high costs and generates data outcomes that necessitate the use of isotopic standards to achieve more precise quantification. The HPLC-Fluorescence analysis demonstrated superior cost-effectiveness and efficacy in identifying the predominant FFA in plasma.

### **Lipidomic analysis of feeds used to supplement wild-type and ALS rats**

Neuroinflammation has many cellular and biochemical characteristics and is one of the symptoms of ALS. [5], [6]. The composition of cell membranes determines the type of inflammatory mediators that will be produced during the inflammatory response[8], [28]. Diets rich in fish oil increase the availability of EPA and DHA, which may reduce neuroinflammation through the action of lipid mediators[8], [28].

To analyze the diet changes in plasma, we supplemented WT and ALS animals with diets low in lipids (control), rich in saturated lipids (lard), or rich in unsaturated lipids (fish oil, **Table 2**).

**Table 2:** Composition of feed used to supplement ALS and wild-type (WT) rats.

	Diet (kcal %)		
	Control	Fish Oil	Lard
Fat	10	60	60
Protein	20	20	20
Carbohydrates	70	20	20

Lipidomics analysis was conducted on three diets (fish oil, lard, and control) to determine their lipid composition (supplementary worksheet). The lipid composition of diets with fish oil and lard is mostly triacylglycerols (supplementary worksheet). The esterified fatty acid profile differed significantly in PUFA content between fish oil and lard. Fish oil had higher levels of EPA (20:5) and DHA (22:6) compared to lard (**Figure 4**).

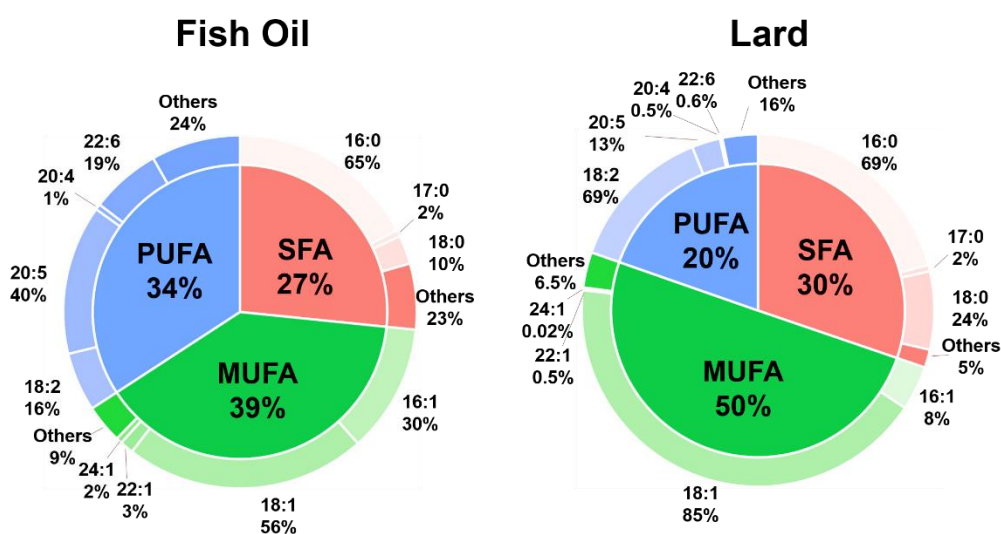


**Figure 4:** The fatty acid composition of triglycerides in diets rich in fish oil and lard was analyzed through lipidomic analysis to supplement ALS and WT rats.

## **FFA analysis by HPLC-Fluorescence of blood plasma from ALS and WT rats supplemented with different diets**

We measured FFAs in the blood plasma of WT and ALS rats to examine the effect of a diet rich in fish oil on the FFA profile in a rat model of ALS. The rats were supplemented with three different diets: one rich in fish oil, one rich in lard, and a low-lipid content diet (control). To evaluate the effects of various diets, we analyzed 120-day-old rats and supplemented them with different diets for 70 days. Each group consisted of 5 rats.

The analysis of the cluster heatmap reveals a cluster of rats supplemented with a diet rich in fish oil. These rats showed an increase in DHA and EPA, a reduction in ARA, and no distinction between ALS and WT. While the profiles of the lard and control diets were more similar, there was a tendency to separate ALS. There were no significant differences in profile or weight between WT and ALS (**Figure 5 A**).

We conducted a PCA analysis to compare the effects of different diets on both WT and ALS mouse models. The results reveal a clear separation between animals that were supplemented with fish oil, without any distinction between WT and ALS animals (**Figure 5 B**). The loading plot indicates that DHA, EPA, and palmitoleic acid (FA 16:1) are distinct from the other diet groups (**Figure 5 C**).

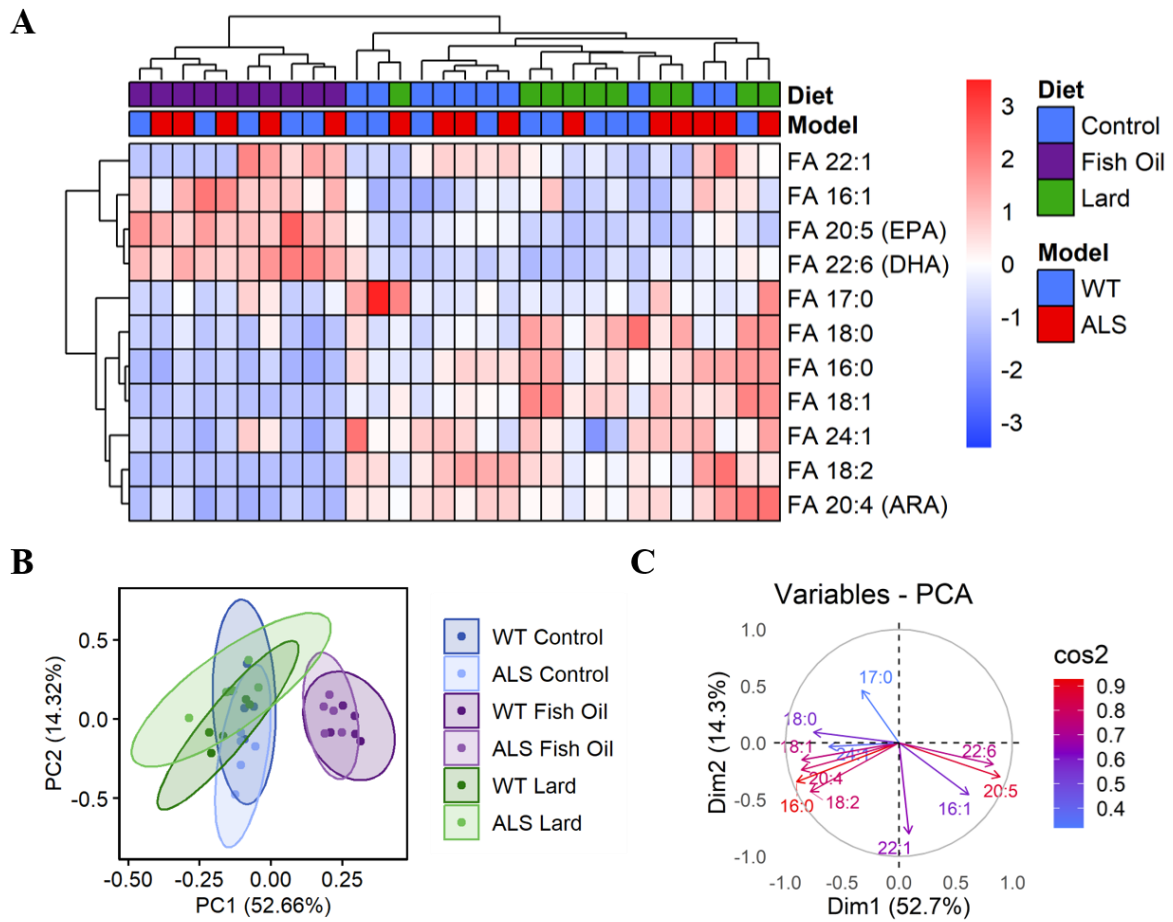


**Figure 5:** (A) Hierarchical clustering heatmap analysis was performed on FFA levels in plasma samples from WT and ALS rats supplemented with three different diets: fish oil, lard, and control. (B) A PCA score plot was generated for PC1 vs PC2. A 95% confidence limit was defined for each sample group by an ellipse with the same color as the corresponding sample group cluster. (C) Loading plot corresponding to PCA analysis.

The concentration of FFA from different diets shows similar patterns as before, with a slight increase in ALS rats for oleic acid (FA 18:1), linoleic acid (FA 18:2), and palmitic acid (FA 16:0) in animals supplemented with the control diet. Animals that were given fish oil had lower levels of these fatty acids, and there was no difference observed between WT and ALS. Animals on a diet rich in lard exhibited similar patterns to the control group, but with an increase in oleic acid and a decrease in linoleic acid. Fish oil supplementation increases levels of EPA, DHA, and ARA compared to a control diet,

regardless of WT or ALS status (**Figure 6**). Other FFAs did not have expressive level changes. (**Figure S5**).

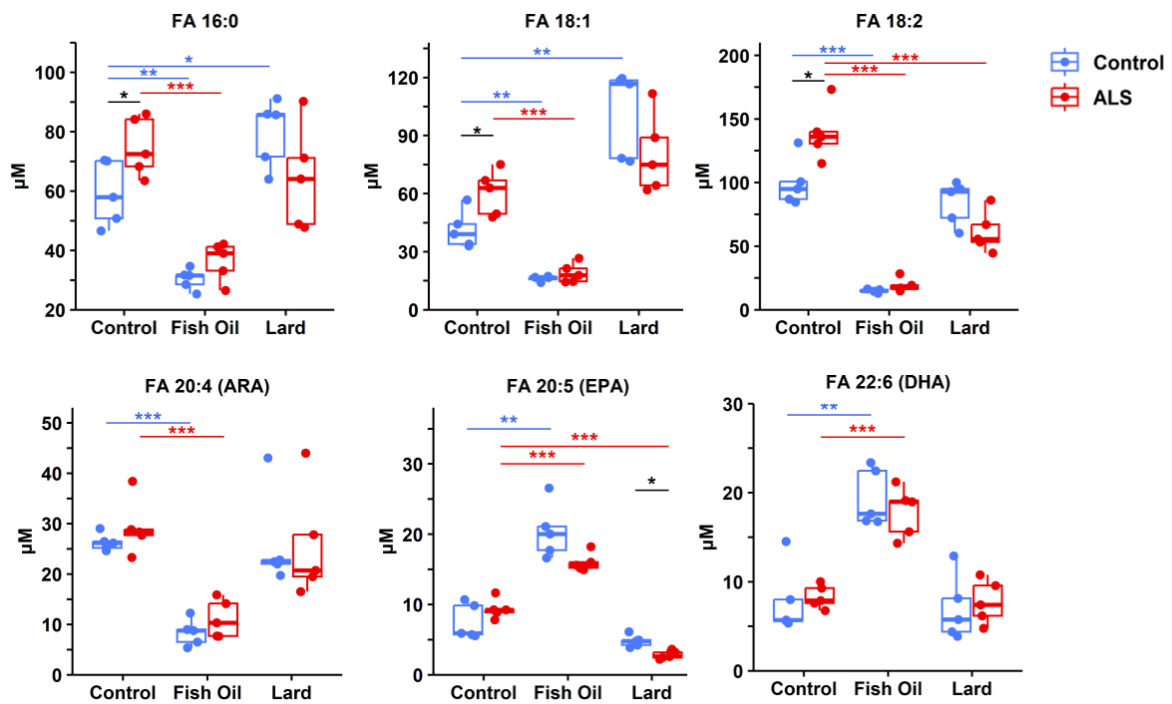


**Figure 6:** Blood plasma from ALS rat models and wild type rats on varied diets were analyzed using box plots. Significant differences were observed in black between the WT and ALS groups that received the same diet, including control, fish oil. Blue color coding indicates significant differences between the fish oil or lard diets and the control diet in WT animals. Red color coding indicates significant differences between the fish oil or lard diets and the control diet in ALS animals (\*  $p < 0.05$ , \*\*  $p < 0.01$ , \*\*\*  $p < 0.001$ ; two-tailed paired t-tests).

### Discussion:

Changes in FFA levels in blood plasma are associated to several pathological conditions like obesity[29], diabetes[30], inflammation[9], and neuroinflammation[28]. The omega-3 fatty acids DHA and EPA produces lipid mediators with anti-inflammatory

actions[8], and another hand, the omega-6 fatty acid ARA produces lipid mediators with pro-inflammatory actions[8].

The literature provides a clear description of the effects of fish oil supplementation, which include an increase in DHA and EPA levels and a reduction in ARA[8], [9], [28]. The present study provides evidence that amyotrophic lateral sclerosis (ALS) does not significantly affect the FFA bloody plasma levels of ALS rat model supplemented with a diet rich in fish oil. Even though, we also observed significant FFA changes in asymptomatic rats. Hence, the administration of fish oil supplements could potentially confer benefits in mitigating the neuroinflammatory effects associated with ALS.

FFAs are present in the bloodstream and are bound to albumin[31]. Therefore, the initial stage of FFA analysis involves extracting lipids to separate FFAs from albumin. In this study, we used MTBE solvent for lipid extraction, which has comparable efficiency to traditional methods[14] and avoid phosphoric acid to precipitate proteins[32] and minimizing acid hydrolysis of esterified fatty acids can reduce inaccurate positive results in FFA analysis.

We developed a novel FFA analysis technique using UHPLC-Fluorescence and validated through HRMS. We used an unusual carboxylic group derivatization method that allows for the inclusion of antioxidants like TPP[19]. The reduced DPDS acts as an antioxidant through its thiol group[33]. An important benefit of this approach is the easy substitution of the fluorescent probe. This method only needs a probe with a primary amine or hydrazine/hydrazide group to create a stable derivatized compound.

We conducted experiments using alternative probes, namely 1-pyrenobutanoic acid hydrazide (PBH) and dansyl hydrazine (Dz), to derivatize fatty acids (Data not shown). Even though these probes have derivatized FFA, the separation of PBH via

chromatography proved to be challenging, which is a similar issue encountered when using 1-Pyrenyldiazomethane (PDAM) due to their closely related structures[10]. While, Dz exhibits weak fluorescence.

On the other hand, the probe 7-(diethylamino)-coumarin-3-carbohydrazide (CHH) proved to be highly efficient in chromatographically separating 12 types of FFAs derivatized and with a relatively short analysis time (40 minutes) and strong fluorescence, making it an excellent choice for FFA analysis. Furthermore, CHH is widely used for the analysis of lipid aldehydes through mass spectrometry and microscopy. Therefore, this method not only proves to be efficient for FFA analysis but also extends the scope of applications to a set of probes typically employed for aldehyde analysis.

### **Acknowledgments:**

This work was supported by FAPESP [CEPID-Redoxoma 2013/07937-8, FAPESP DD 2017/16140-7 to Faria, R.L.], CNPq [Miyamoto, S. 424094/2016-9, Capes and Pró-Reitoria de Pesquisa da USP.

### **References:**

- [1] L. Chen *et al.*, "Inflammatory responses and inflammation-associated diseases in organs," *Oncotarget*, vol. 9, no. 6, pp. 7204–7218, Jan. 2018.
- [2] H. N. Jabbour, K. J. Sales, R. D. Catalano, and J. E. Norman, "Inflammatory pathways in female reproductive health and disease," *REPRODUCTION*, vol. 138, no. 6, pp. 903–919, Dec. 2009.
- [3] C. Nathan and A. Ding, "Nonresolving Inflammation," *Cell*, vol. 140, no. 6, pp. 871–882, Mar. 2010.

- [4] M. T. Carri, A. Ferri, M. Cozzolino, L. Calabrese, and G. Rotilio, "Neurodegeneration in amyotrophic lateral sclerosis: The role of oxidative stress and altered homeostasis of metals," *Brain Res. Bull.*, vol. 61, no. 4, pp. 365–374, 2003.
- [5] P. L. McGeer and E. G. McGeer, "Inflammatory processes in amyotrophic lateral sclerosis," *Muscle Nerve*, vol. 26, no. 4, pp. 459–470, Oct. 2002.
- [6] C. K. Glass, K. Saijo, B. Winner, M. C. Marchetto, and F. H. Gage, "Mechanisms Underlying Inflammation in Neurodegeneration," *Cell*, vol. 140, no. 6, pp. 918–934, Mar. 2010.
- [7] B. J. Turner, "Impaired Extracellular Secretion of Mutant Superoxide Dismutase 1 Associates with Neurotoxicity in Familial Amyotrophic Lateral Sclerosis," *J. Neurosci.*, vol. 25, no. 1, pp. 108–117, Jan. 2005.
- [8] P. C. Calder, "Polyunsaturated fatty acids and inflammatory processes: New twists in an old tale," *Biochimie*, vol. 91, no. 6, pp. 791–795, Jun. 2009.
- [9] P. . Calder, "N-3 polyunsaturated fatty acids, inflammation and immunity: pouring oil on troubled waters or another fishy tale?," *Nutr. Res.*, vol. 21, no. 1–2, pp. 309–341, Jan. 2001.
- [10] T. Toyo'oka, "Fluorescent tagging of physiologically important carboxylic acids, including fatty acids, for their detection in liquid chromatography," *Anal. Chim. Acta*, vol. 465, no. 1–2, pp. 111–130, Aug. 2002.
- [11] M. S. Carvalho, M. A. Mendonça, D. M. M. Pinho, I. S. Resck, and P. A. Z. Suarez, "Chromatographic analyses of fatty acid methyl esters by HPLC-UV and GC-FID," *J. Braz. Chem. Soc.*, vol. 23, no. 4, pp. 763–769, Apr. 2012.
- [12] A. Felinger and G. Guiochon, "Validation of a chromatography data analysis software," *J. Chromatogr. A*, vol. 913, no. 1–2, pp. 221–231, Apr. 2001.
- [13] E. Kasarskis, S. Berryman, J. Vanderleest, A. Schneider, and C. McClain, "Nutritional status of patients with amyotrophic lateral sclerosis: relation to the proximity of death," *Am. J. Clin. Nutr.*, vol. 63, no. 1, pp. 130–137, Jan. 1996.



- [14] V. Matyash, G. Liebisch, T. V. Kurzchalia, A. Shevchenko, and D. Schwudke, "Lipid extraction by methyl-terf-butyl ether for high-throughput lipidomics," *J. Lipid Res.*, vol. 49, no. 5, pp. 1137–1146, 2008.
- [15] H. Tsugawa *et al.*, "A lipidome atlas in MS-DIAL 4," *Nat. Biotechnol.*, vol. 38, no. 10, pp. 1159–1163, Oct. 2020.
- [16] P. T. Ivanova, S. B. Milne, M. O. Byrne, Y. Xiang, and H. A. Brown, "Glycerophospholipid Identification and Quantitation by Electrospray Ionization Mass Spectrometry," in *Methods in Enzymology*, vol. 432, no. 07, 2007, pp. 21–57.
- [17] M. Pulfer and R. C. Murphy, "Electrospray mass spectrometry of phospholipids," *Mass Spectrom. Rev.*, vol. 22, no. 5, pp. 332–364, Sep. 2003.
- [18] P. S. Mukherjee and H. T. Karnes, "Ultraviolet and Fluorescence Derivatization Reagents for Carboxylic Acids Suitable for High Performance Liquid Chromatography: A Review," *Biomed. Chromatogr.*, vol. 10, no. 5, pp. 193–204, Sep. 1996.
- [19] M. Nishikiori, H. Iizuka, H. Ichiba, K. Sadamoto, and T. Fukushima, "Determination of Free Fatty Acids in Human Serum by HPLC with Fluorescence Detection," *J. Chromatogr. Sci.*, vol. 53, no. 4, pp. 537–541, Apr. 2015.
- [20] A. B. Chaves-Filho *et al.*, "Alterations in lipid metabolism of spinal cord linked to amyotrophic lateral sclerosis," *Sci. Rep.*, vol. 9, no. 1, p. 11642, Dec. 2019.
- [21] M. E. Gurney, "The use of transgenic mouse models of amyotrophic lateral sclerosis in preclinical drug studies," *J. Neurol. Sci.*, vol. 152, no. SUPPL. 1, pp. s67–s73, Oct. 1997.
- [22] W. F. DeNino *et al.*, "Contribution of Abdominal Adiposity to Age-Related Differences in Insulin Sensitivity and Plasma Lipids in Healthy Nonobese Women," *Diabetes Care*, vol. 24, no. 5, pp. 925–932, May 2001.
- [23] M. Deguise *et al.*, "Abnormal fatty acid metabolism is a core component of spinal muscular atrophy," *Ann. Clin. Transl. Neurol.*, vol. 6, no. 8, pp. 1519–1532, Aug.

- 2019.
- [24] L. Ghibaudi, J. Cook, C. Farley, M. Van Heek, and J. J. Hwa, "Fat intake affects adiposity, comorbidity factors, and energy metabolism of Sprague-Dawley rats," *Obes. Res.*, vol. 10, no. 9, pp. 956–963, 2002.
- [25] L. Dupuis, P.-F. Pradat, A. C. Ludolph, and J.-P. Loeffler, "Energy metabolism in amyotrophic lateral sclerosis," *Lancet Neurol.*, vol. 10, no. 1, pp. 75–82, Jan. 2011.
- [26] U. Sommer, H. Herscovitz, F. K. Welty, and C. E. Costello, "LC-MS-based method for the qualitative and quantitative analysis of complex lipid mixtures.," *J. Lipid Res.*, vol. 47, no. 4, pp. 804–14, 2006.
- [27] O. Quehenberger, A. M. Armando, and E. A. Dennis, "High sensitivity quantitative lipidomics analysis of fatty acids in biological samples by gas chromatography-mass spectrometry," *Biochimica et Biophysica Acta - Molecular and Cell Biology of Lipids*, vol. 1811, no. 11. Elsevier B.V., pp. 648–656, 2011.
- [28] S. Layé, "Polyunsaturated fatty acids, neuroinflammation and well being," *Prostaglandins, Leukot. Essent. Fat. Acids*, vol. 82, no. 4–6, pp. 295–303, Apr. 2010.
- [29] G. Boden, "Obesity and Free Fatty Acids," *Endocrinol. Metab. Clin. North Am.*, vol. 37, no. 3, pp. 635–646, Sep. 2008.
- [30] A. I. S. Sobczak, C. A. Blindauer, and A. J. Stewart, "Changes in Plasma Free Fatty Acids Associated with Type-2 Diabetes," *Nutrients*, vol. 11, no. 9, p. 2022, Aug. 2019.
- [31] P. D. Berk and D. D. Stump, "Mechanisms of cellular uptake of long chain free fatty acids," in *Lipid Binding Proteins within Molecular and Cellular Biochemistry*, vol. 192, no. 1–2, Boston, MA: Springer US, 1999, pp. 17–31.
- [32] S. Tiziani *et al.*, "Optimized metabolite extraction from blood serum for 1H nuclear magnetic resonance spectroscopy," *Anal. Biochem.*, vol. 377, no. 1, pp. 16–23, Jun. 2008.

- [33] P. Di Mascio, M. Murphy, and H. Sies, "Antioxidant defense systems: the role of carotenoids, tocopherols, and thiols," *Am. J. Clin. Nutr.*, vol. 53, no. 1, pp. 194S-200S, Jan. 1991.

## Supplementary figures

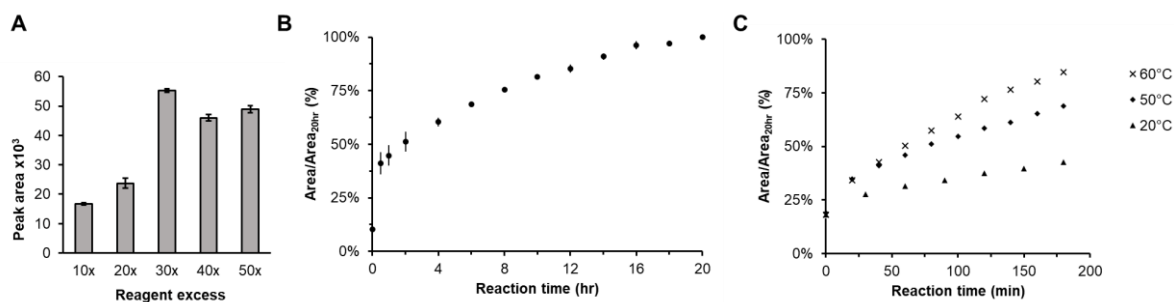


**Figure S1:** Optimization of conditions for free fatty acid derivatization: (A) Reaction of 10  $\mu$ M FA 13:0 with 10-, 20-, 30-, 40-, and 50-fold excess of DPDS, TPP, CHH resulted in the CHH, maximum when a with 30-fold excess of reagents was used; (B) The kinetics of the derivatization process of 10  $\mu$ M FA 13:0 with a 30-fold excess (or 300  $\mu$ M) of DPDS, TPP, and CHH, each at 20°C; (C) Kinetics of the derivatization of 10  $\mu$ M FA 13:0 with a 30-fold excess (or 300  $\mu$ M) of DPDS, TPP, and CHH at various temperatures.

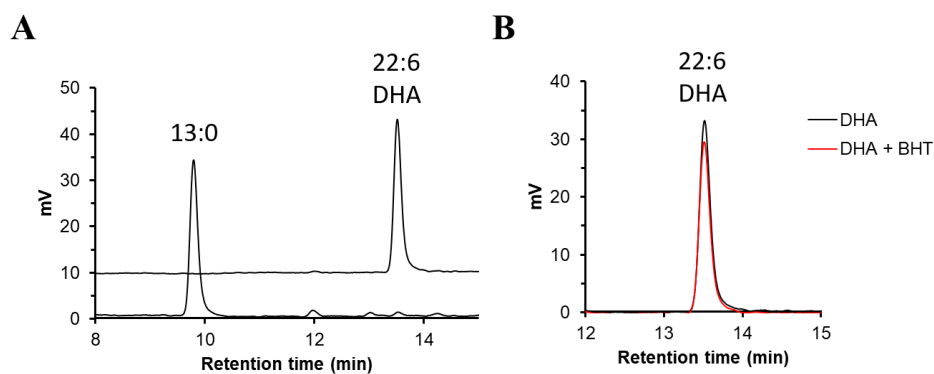


**Figure S2:** Analysis of the Stability of Polyunsaturated Fatty Acids: (A) Comparison of 20 pmol of FA 13 and 20 pmol of FA 22:6 (DHA) after 48 hours of derivatization reaction at room temperature; (B) Comparison of 20 pmol of FA 22:6 (DHA) with and without 1 mM of the antioxidant BHT after 48 hours of the derivatization reaction at room temperature.

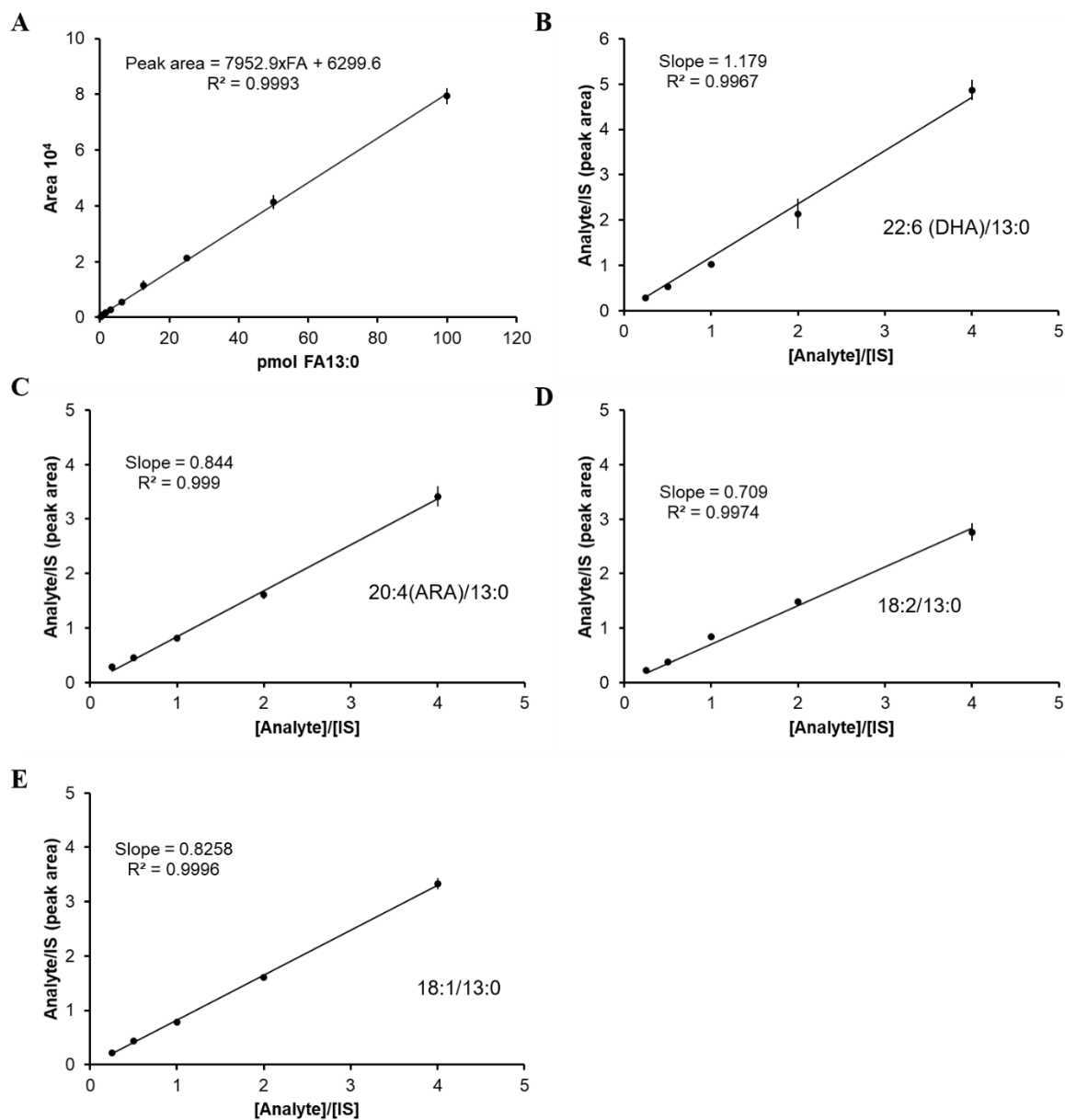


**Figure S3:** Linearity test of FFA analysis using CHH derivatization: (A) Signal intensities of FA 13:0 at 100 pmol (100  $\mu\text{M}$ ) were measured with serial dilution down to 0.2 pmol (200 nM) with  $n=3$ ; Calibration curve with internal standard FA 13:0 maintained at 20 pmol (4  $\mu\text{M}$ ) responses, ranging from 80 pmol to 5 pmol of: (B) FA 22:6 (DHA), (C) FA 20:4 (ARA), (D) FA 18:2 and (E) FA 18:1.

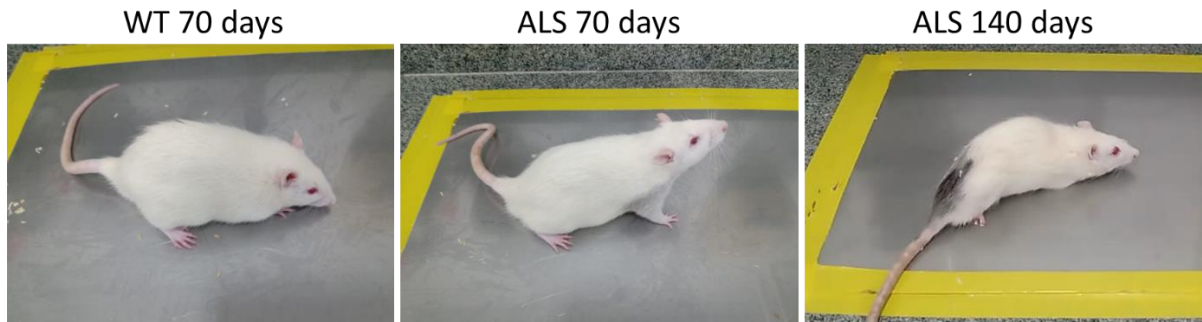


**Figure S4:** Male Sprague Dawley rats, including both wild type (WT) and transgenic rats overexpressing mutant human SOD1G93A (ALS), were used in this study. The rats were either asymptomatic at 70 days old and asymptomatic, or 140 days old and symptomatic.

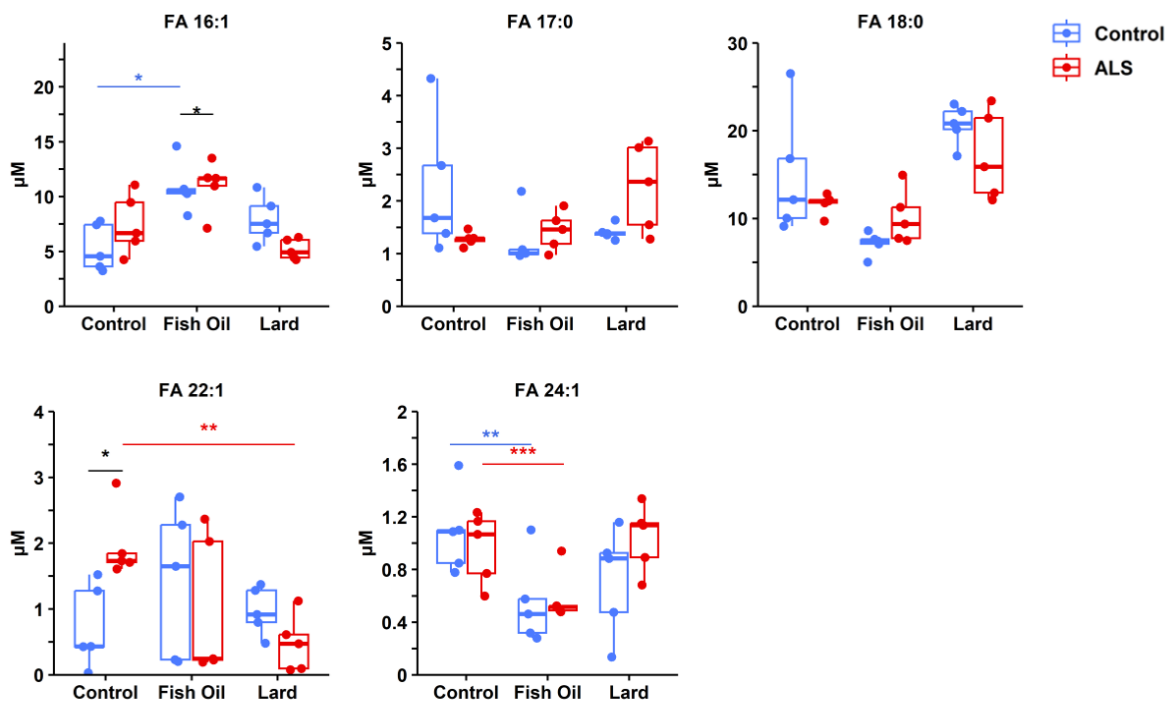


**Figure S5:** Blood plasma from ALS rat models and wild type rats on varied diets were analyzed using box plots. Significant differences were observed in black between the WT and ALS groups that received the same diet, including control, fish oil. Blue color coding indicates significant differences between the fish oil or lard diets and the control diet in WT animals. Red color coding indicates significant differences between the fish oil or lard diets and the control diet in ALS animals (\*  $p < 0.05$ , \*\*  $p < 0.01$ , \*\*\*  $p < 0.001$ ; two-tailed paired t-tests).

## Supplementary tables

Supplementary table 1: Composition of rations in duplicates:

Lipid	FishOil 1	FishOil 2	Lard 1	Lard 2	Control 1	Control 2
CE 22:6	0.7	0.8	0.0	0.0	0.0	0.0
DG 14:0/16:0	1.1	1.1	0.1	0.1	0.6	9.1
DG 16:0/16:0	1.1	1.1	0.4	0.4	42.8	731.3
DG 16:0/18:1	8.3	8.1	4.6	5.4	703.0	12153.1
DG 16:0/18:2	5.1	5.1	3.9	4.6	2281.1	36740.4
DG 17:1/18:1	0.3	0.3	0.1	0.1	11.9	184.8
DG 18:0/18:1	1.7	1.6	1.3	1.5	129.3	2247.9
DG 18:0/22:6	2.8	2.8	0.0	0.0	0.1	1.3
DG 18:1/18:1	3.5	3.4	3.9	4.5	1774.4	32046.4
DG 18:1/18:2	2.3	2.3	3.8	4.6	4520.6	75027.2
DG 18:2/18:2	3.6	3.5	2.8	3.5	5498.1	105920.3
DG 18:2/20:2	0.2	0.2	0.1	0.1	6.0	123.0
DG 20:1/18:2	0.2	0.2	0.1	0.2	35.5	643.5
DG 22:0/18:1	0.1	0.1	0.0	0.0	6.9	118.8
DG 24:0/18:2	0.1	0.1	0.0	0.0	9.7	154.5
DG O-17:1/13:1	0.2	0.2	0.0	0.0	0.0	0.4
DG O-19:1/15:1	0.4	0.3	0.0	0.0	4.1	56.4
DG O-19:2/15:1	0.3	0.3	0.0	0.0	17.5	265.8
DG O-19:2/17:2	0.0	0.1	0.0	0.0	32.7	544.8
DG O-19:2/17:3	0.1	0.0	0.0	0.0	75.2	1218.1
DG O-21:1/15:1	0.1	0.1	0.0	0.0	0.9	12.6
DGDG 16:0/18:2	0.0	0.0	0.0	0.0	50.7	680.4
DGDG 18:1/18:1	0.0	0.0	0.0	0.0	6.6	94.4
DGDG 18:1/18:2	0.0	0.0	0.0	0.0	16.0	220.5
DGDG 18:2/18:2	0.0	0.0	0.0	0.0	95.8	1286.2
DGDG 18:2/18:3	0.0	0.0	0.0	0.0	14.8	220.8
DGDG 18:3/18:3	0.0	0.0	0.0	0.0	6.1	88.9
LPC 16:0	0.4	0.4	0.4	0.4	0.8	0.5
LPC 18:0	0.0	0.0	0.0	0.0	0.0	0.0
LPC 18:1	0.0	0.0	0.0	0.0	0.0	0.0
LPC 18:2	0.0	0.0	0.0	0.0	2.8	1.8
LPC 18:3	0.0	0.0	0.0	0.0	0.1	0.0
MGDG 16:0/18:2	0.0	0.0	0.0	0.0	7.7	112.2
MGDG 18:2/18:2	0.0	0.0	0.0	0.0	22.8	295.2
PC 16:0/18:1	0.0	0.0	0.0	0.0	1.0	1.1
PC 16:0/18:2	0.0	0.0	0.0	0.0	3.0	3.0
PC 16:0/18:3	0.0	0.0	0.0	0.0	0.2	0.1
PC 18:1/18:1	0.0	0.0	0.0	0.0	1.1	1.1
PC 18:1/18:2	0.0	0.0	0.0	0.0	2.1	2.2
PC 18:2/18:2	0.0	0.0	0.0	0.0	3.8	3.7
PC 18:2/18:3	0.0	0.0	0.0	0.0	0.6	0.5
PE 16:0/18:1	0.3	0.2	0.0	0.1	0.4	0.6
PE 16:0/18:2	0.2	0.1	0.0	0.0	1.5	2.2
PE 17:2/19:2	0.0	0.0	0.0	0.0	1.1	1.6
PE 18:1/18:2	0.1	0.0	0.0	0.0	0.4	0.7
PG 16:0/18:2	0.0	0.0	0.0	0.0	1.0	0.9
PG 18:2/18:2	0.0	0.0	0.0	0.0	0.3	0.3
SE 28:1/18:2	0.0	0.0	0.0	0.0	43.1	665.2
SE 29:1/18:2	0.1	0.1	0.1	0.1	302.2	4672.1
TG 10:0/16:0/18:1	0.1	0.1	5.6	0.4	0.2	8.6
TG 10:0/16:0/18:2	1.3	1.2	5.5	6.6	2.4	41.0
TG 10:0/16:1/18:1	0.1	0.1	5.5	0.1	0.4	3.9
TG 10:0/16:1/18:2	0.2	0.2	2.0	2.4	2.1	30.4
TG 10:0/17:1/18:1	0.5	0.5	0.3	0.4	2.2	32.5
TG 10:0/18:1/18:2	7.1	6.8	10.8	0.3	0.4	4.2
TG 10:0/18:1/18:3	0.6	0.6	3.2	3.9	1.2	20.7

TG 10:0/18:2/18:3	9.9	0.1	0.4	0.5	0.8	13.3
TG 12:0/16:0/18:0	0.0	0.0	0.0	0.0	0.0	0.4
TG 12:0/16:0/18:1	20.1	21.3	6.1	1.8	1.4	14.7
TG 12:0/18:2/18:3	55.6	53.4	0.4	0.4	1.5	21.6
TG 14:0/14:0/16:1	5.2	5.5	5.6	7.0	1.4	20.1
TG 14:0/14:0/18:1	20.1	21.3	6.1	6.8	1.4	14.7
TG 14:0/15:0/18:1	5.1	5.3	0.3	0.5	0.2	3.8
TG 14:0/15:0/20:5	7.0	6.5	0.2	0.1	0.5	1.3
TG 14:0/16:0/16:0	0.6	0.6	0.8	0.8	0.4	9.0
TG 14:0/16:0/16:4	13.3	12.6	0.0	3.9	0.1	20.7
TG 14:0/16:0/18:0	0.4	0.4	2.1	2.0	6.1	94.9
TG 14:0/16:0/18:1	46.8	49.9	15.6	17.8	3.3	50.5
TG 14:0/16:0/18:2	39.1	41.5	25.5	28.7	4.4	76.0
TG 14:0/16:0/20:4	48.3	50.0	0.2	48.6	24.6	385.6
TG 14:0/16:0/20:5	108.7	115.8	0.9	1.9	0.2	170.5
TG 14:0/16:1/16:1	11.8	12.5	16.7	20.4	1.7	33.6
TG 14:0/16:1/16:2	7.1	6.8	10.8	12.8	1.3	18.4
TG 14:0/16:1/16:4	9.9	9.8	0.4	0.5	0.8	1.0
TG 14:0/16:1/17:2	1.1	1.2	0.0	0.2	0.1	1.3
TG 14:0/16:1/18:3	32.5	32.2	4.0	4.9	2.2	37.3
TG 14:0/18:2/18:3	6.6	6.0	4.6	5.2	11.5	7.2
TG 15:0/15:0/17:1	5.1	5.3	0.3	0.5	0.2	3.8
TG 15:0/16:0/18:1	10.9	11.0	1.7	2.2	2.2	27.2
TG 15:0/16:0/18:2	8.4	9.0	2.2	3.0	4.1	66.9
TG 15:0/16:0/20:5	15.1	15.7	1.5	1.6	18.6	274.2
TG 15:0/16:1/16:1	2.6	2.8	0.4	0.5	0.2	4.4
TG 15:0/16:1/18:2	3.4	3.6	0.1	1.2	3.8	47.2
TG 15:0/16:1/20:5	13.4	13.0	0.6	0.3	4.7	68.1
TG 15:0/16:1/22:6	12.6	13.2	2.0	0.2	4.8	228.4
TG 15:0/18:1/18:2	5.9	6.2	13.6	0.6	2.6	30.6
TG 15:0/18:1/22:6	18.2	19.3	0.2	0.5	0.7	4.5
TG 15:0/20:5/22:6	11.0	10.5	0.1	0.1	0.0	2.3
TG 15:1/18:1/18:2	5.2	5.5	5.7	0.2	2.1	37.0
TG 15:1/18:2/18:2	15.1	15.7	1.2	0.1	1.1	19.4
TG 15:1/20:5/22:6	1.6	0.8	0.0	0.0	0.1	0.5
TG 16:0/16:0/16:1	46.8	3.2	15.6	2.4	0.4	5.4
TG 16:0/16:0/17:0	0.2	0.2	0.2	0.2	0.3	3.7
TG 16:0/16:0/17:1	10.9	11.0	1.7	2.2	2.2	27.2
TG 16:0/16:0/18:0	0.4	0.3	4.1	3.7	27.0	381.3
TG 16:0/16:0/18:1	52.8	56.7	115.7	122.1	418.8	6321.9
TG 16:0/16:0/18:2	0.0	0.0	0.0	0.0	0.5	6.4
TG 16:0/16:0/20:5	141.9	79.3	129.1	149.7	984.1	14764.6
TG 16:0/16:1/16:2	20.2	21.3	13.8	16.4	1.3	19.0
TG 16:0/16:1/18:1	96.2	102.8	179.5	200.8	757.3	12308.6
TG 16:0/16:1/18:2	36.0	38.7	106.8	124.6	13.0	192.4
TG 16:0/16:4/16:4	7.4	7.1	0.0	0.1	0.1	2.1
TG 16:0/16:4/20:5	77.2	75.3	0.2	0.4	0.1	2.7
TG 16:0/17:0/18:0	0.0	0.0	0.0	0.0	0.0	0.2
TG 16:0/17:0/18:1	7.5	7.5	9.4	10.0	7.4	110.1
TG 16:0/17:0/18:2	0.5	0.5	19.1	1.6	1.5	22.0
TG 16:0/17:0/20:5	9.8	10.5	1.1	8.9	33.7	456.0
TG 16:0/17:1/18:1	15.1	15.4	19.1	21.2	15.5	259.6
TG 16:0/17:1/20:5	27.3	29.1	1.7	2.1	17.0	119.6
TG 16:0/17:1/24:1	3.0	2.9	0.6	0.7	36.8	575.1
TG 16:0/18:0/18:0	0.3	0.3	0.0	3.0	19.3	365.1
TG 16:0/18:0/18:1	30.2	30.7	270.9	301.2	555.3	8578.9
TG 16:0/18:0/20:0	0.0	0.0	0.0	0.0	0.0	0.1
TG 16:0/18:0/21:5	4.0	4.2	0.4	0.4	0.5	120.9
TG 16:0/18:0/22:4	0.0	0.0	0.0	0.0	0.0	0.7
TG 16:0/18:1/18:1	120.7	130.9	963.7	1057.7	2674.4	41028.7
TG 16:0/18:1/18:2	82.3	87.9	848.4	959.1	3729.5	58614.3
TG 16:0/18:1/19:1	8.1	8.3	26.4	30.4	23.1	329.4
TG 16:0/18:1/19:2	1.0	1.3	0.2	0.9	2.0	8.9
TG 16:0/18:1/20:1	51.0	52.1	324.7	384.4	1501.4	22465.4



TG 16:0/18:1/20:5	175.3	189.4	0.2	422.1	9199.2	147260.5
TG 16:0/18:1/21:5	19.8	21.0	0.1	1.2	0.2	9.7
TG 16:0/18:1/22:1	27.6	28.4	25.0	29.3	467.8	7500.5
TG 16:0/18:1/23:1	3.0	2.9	0.6	0.7	36.8	575.1
TG 16:0/18:2/18:2	0.0	0.0	0.0	0.0	0.0	0.4
TG 16:0/20:0/18:1	11.7	11.8	57.6	65.2	251.0	4089.3
TG 16:0/20:1/22:1	15.5	15.1	3.4	4.2	358.5	5749.7
TG 16:0/20:5/21:5	11.5	11.3	0.1	0.1	0.0	1.4
TG 16:0/20:5/22:5	67.9	69.7	0.7	1.1	0.1	1.1
TG 16:0/20:5/22:6	124.5	126.5	0.6	1.4	0.2	3.1
TG 16:0/21:0/18:1	1.6	1.6	0.0	0.5	4.2	66.7
TG 16:0/21:0/18:2	4.9	4.9	3.0	3.5	15.7	235.9
TG 16:0/21:0/20:5	1.5	1.6	0.0	0.1	1.6	23.0
TG 16:0/21:5/22:6	8.7	8.9	0.0	0.1	0.1	0.7
TG 16:0/22:0/18:1	3.9	3.7	0.1	2.9	119.8	1914.2
TG 16:0/22:1/20:5	27.2	30.8	5.1	5.5	2.2	29.9
TG 16:0/22:1/21:5	4.9	3.8	0.0	0.1	0.2	5.5
TG 16:0/22:1/22:1	5.6	5.3	0.0	0.7	121.9	2078.7
TG 16:0/22:1/22:6	27.0	28.3	0.0	0.1	0.0	3.9
TG 16:0/22:5/22:6	32.4	25.4	0.1	0.3	0.0	3.3
TG 16:0/22:6/32:6	0.2	0.1	0.0	0.0	0.0	0.0
TG 16:0/23:0/18:1	0.5	0.5	0.0	0.1	5.1	116.7
TG 16:0/23:0/18:2	3.0	2.9	0.0	0.7	36.8	575.1
TG 16:0/23:0/20:5	0.8	0.8	0.0	0.2	7.3	89.8
TG 16:0/23:0/22:6	2.1	2.1	0.0	0.0	0.1	0.9
TG 16:0/24:0/18:1	1.1	1.0	0.0	0.5	71.5	1255.2
TG 16:0/24:1/20:5	14.9	15.2	0.0	0.4	1.5	19.7
TG 16:0/24:1/22:6	18.2	18.5	0.0	0.1	0.1	2.4
TG 16:0/24:3/22:6	3.5	3.6	0.0	0.0	0.1	4.2
TG 16:0/28:5/22:6	1.1	1.2	0.0	0.0	0.0	0.3
TG 16:1/16:1/16:3	55.6	53.4	0.0	0.8	1.5	21.6
TG 16:1/16:1/16:4	14.3	14.4	0.2	0.3	0.6	9.3
TG 16:1/16:1/17:2	3.3	3.3	0.1	0.4	0.6	12.3
TG 16:1/16:1/20:5	86.9	85.5	0.8	1.3	0.2	5.6
TG 16:1/16:1/22:6	53.8	67.6	0.0	14.5	819.7	14164.3
TG 16:1/16:2/20:5	57.1	56.7	0.2	0.3	0.6	2.0
TG 16:1/16:3/18:4	28.1	24.7	0.1	0.2	0.4	2.3
TG 16:1/16:4/16:4	2.7	2.7	0.0	0.0	0.2	1.1
TG 16:1/16:4/18:4	28.9	27.4	0.1	0.2	0.0	1.6
TG 16:1/16:4/20:5	35.1	32.6	0.1	0.2	0.2	4.9
TG 16:1/17:1/16:4	2.2	2.1	0.0	0.0	0.1	4.4
TG 16:1/18:1/16:4	89.9	87.6	0.7	1.3	2.4	35.7
TG 16:1/18:1/18:2	90.5	96.1	530.4	17.1	4972.9	75334.3
TG 16:1/18:1/20:5	120.1	130.8	0.1	136.6	72.8	1092.2
TG 16:1/18:1/22:6	52.4	56.3	0.0	7.2	0.1	30.8
TG 16:1/18:2/18:3	185.2	0.2	11.3	14.8	0.8	9.1
TG 16:1/20:1/22:1	9.3	9.5	5.8	6.9	39.6	642.2
TG 16:1/20:5/22:6	49.9	49.9	0.3	0.6	0.1	5.1
TG 16:2/16:4/20:5	6.2	5.8	0.0	0.0	0.0	2.8
TG 16:2/20:5/21:5	1.6	0.8	0.0	0.0	0.1	0.5
TG 16:2/20:5/22:6	14.1	13.4	0.0	0.3	0.5	14.7
TG 16:3/20:5/21:5	1.0	0.8	0.0	0.0	0.1	3.7
TG 16:4/20:5/21:5	1.3	1.2	0.0	0.0	0.3	5.2
TG 16:4/20:5/22:6	5.7	5.6	0.0	0.0	0.1	28.7
TG 16:4/22:6/22:6	0.8	0.7	0.0	0.0	0.0	0.2
TG 17:0/17:1/19:1	8.1	8.3	26.4	30.4	23.1	329.4
TG 17:0/18:0/18:1	3.8	3.7	6.0	6.6	5.2	83.9
TG 17:0/18:0/18:2	0.0	0.0	0.0	0.0	0.0	0.2
TG 17:0/18:0/22:6	9.0	9.5	0.1	0.4	0.0	1.2
TG 17:0/18:1/18:1	0.7	0.8	26.4	4.6	4.6	64.1
TG 17:0/18:1/18:2	5.2	5.5	1.3	35.8	30.7	519.0
TG 17:0/18:1/22:6	10.0	10.8	0.0	0.2	0.1	0.6
TG 17:0/18:2/18:2	4.9	5.1	0.7	26.5	38.7	569.7
TG 17:0/20:1/22:1	1.0	0.9	0.2	0.2	27.9	445.1

TG 17:0/20:1/22:6	4.6	4.7	0.0	0.0	0.1	3.2
TG 17:0/20:1/24:1	0.2	0.1	0.0	0.0	0.8	86.5
TG 17:0/22:1/22:6	3.0	3.1	0.0	0.0	0.1	0.6
TG 17:0/24:1/22:6	1.6	1.7	0.0	0.0	0.1	0.3
TG 17:1/18:1/18:2	4.9	5.1	22.0	1.1	3.4	48.1
TG 17:1/18:1/20:1	2.2	2.2	4.2	4.8	9.5	122.3
TG 17:1/18:1/22:1	1.6	1.5	0.6	0.7	21.1	366.7
TG 17:1/18:1/22:6	5.3	5.6	0.0	0.2	0.1	0.3
TG 17:1/18:1/24:1	0.9	0.9	0.3	0.4	34.2	528.1
TG 17:1/18:2/18:2	4.4	0.2	8.2	0.3	2.3	36.1
TG 17:1/18:2/18:3	0.1	29.1	1.6	0.0	1.0	18.5
TG 17:1/18:2/20:5	6.4	6.7	0.1	0.1	0.7	2.8
TG 17:1/18:2/22:6	2.7	3.0	0.1	0.1	0.5	1.5
TG 17:1/20:1/24:1	0.3	0.3	0.0	0.0	4.8	157.3
TG 17:1/20:5/22:6	5.9	5.4	0.0	0.1	0.0	1.7
TG 17:1/22:1/22:6	1.3	1.3	0.0	0.0	0.3	3.7
TG 17:1/22:6/22:6	1.4	1.4	0.0	0.0	0.1	0.4
TG 17:1/24:1/22:6	1.0	1.0	0.0	0.0	0.1	0.6
TG 18:0/18:0/18:1	11.7	11.8	57.6	65.2	185.1	2577.1
TG 18:0/18:1/18:1	51.0	52.1	324.7	384.4	1501.4	22465.4
TG 18:0/18:1/18:2	56.4	60.1	451.8	507.9	3811.9	55643.4
TG 18:0/18:1/19:1	4.9	4.9	3.0	1.9	10.5	144.2
TG 18:0/18:1/20:1	27.6	28.4	25.0	7.0	58.6	939.0
TG 18:0/18:1/20:2	0.6	0.7	37.3	3.7	25.1	318.2
TG 18:0/18:1/20:5	58.2	60.2	38.4	45.9	12.3	185.6
TG 18:0/18:1/22:4	11.6	14.4	4.2	4.0	26.1	375.9
TG 18:0/20:0/18:1	3.9	3.7	2.5	2.9	67.0	928.4
TG 18:0/21:5/22:6	2.5	2.6	0.0	0.0	0.2	1.2
TG 18:0/23:0/22:6	0.5	0.3	0.0	0.0	0.0	0.6
TG 18:0/24:0/18:1	0.1	0.1	0.0	0.0	0.2	1.7
TG 18:0/24:1/22:6	7.5	7.6	0.0	0.0	0.1	1.7
TG 18:1/17:2/18:2	4.4	4.4	1.1	8.9	33.7	456.0
TG 18:1/18:1/18:2	76.8	81.3	514.5	559.7	5135.4	81977.3
TG 18:1/18:1/20:5	114.5	123.5	1.8	24.7	2.8	1.8
TG 18:1/18:1/22:4	27.2	30.8	5.1	1.0	1.5	26.7
TG 18:1/18:1/22:6	33.5	36.8	0.0	1.1	0.2	3.0
TG 18:1/18:2/18:2	10.6	10.5	501.0	72.3	1123.7	16102.0
TG 18:1/18:2/18:3	92.7	96.8	360.6	422.1	9199.2	147260.5
TG 18:1/18:2/22:4	0.4	0.4	5.5	0.6	0.6	7.1
TG 18:1/18:2/22:5	0.3	0.3	4.5	0.2	0.2	4.4
TG 18:1/18:2/22:6	25.8	26.6	0.0	0.9	0.1	2.4
TG 18:1/18:3/20:3	0.5	0.4	19.6	24.7	2.8	45.5
TG 18:1/19:1/18:2	0.3	0.2	3.7	1.6	4.1	44.0
TG 18:1/19:1/22:6	1.8	2.0	0.0	0.0	0.1	0.4
TG 18:1/20:1/18:2	10.4	10.8	21.2	37.8	20.6	96.5
TG 18:1/20:1/20:2	6.3	6.2	4.1	4.9	254.5	4006.0
TG 18:1/20:1/20:5	52.6	56.0	0.5	0.7	0.1	3.3
TG 18:1/20:1/22:1	4.1	4.0	1.1	1.3	24.6	370.1
TG 18:1/20:1/22:6	11.9	12.8	0.4	0.2	0.1	1.5
TG 18:1/20:1/24:1	1.3	1.2	0.1	0.0	1.2	6.5
TG 18:1/20:2/22:6	5.4	5.9	0.2	0.2	0.0	1.0
TG 18:1/20:5/22:6	36.7	35.5	0.0	0.4	0.1	1.9
TG 18:1/21:5/22:6	1.3	1.5	0.0	0.0	0.0	6.0
TG 18:1/22:1/22:6	8.1	8.4	0.0	0.0	0.1	1.8
TG 18:1/22:1/24:1	0.5	0.4	0.0	0.0	0.0	1.0
TG 18:1/22:6/24:6	2.3	2.4	0.0	0.0	0.0	1.7
TG 18:1/24:1/22:6	5.8	5.8	0.0	0.0	0.0	1.9
TG 18:1/25:1/22:6	0.3	0.3	0.0	0.0	0.0	0.5
TG 18:1/28:2/22:6	0.2	0.2	0.0	0.0	0.0	0.2
TG 18:2/18:2/18:2	3.9	3.6	360.6	18.8	577.1	8001.6
TG 18:2/18:2/18:3	36.0	34.9	102.6	2.1	110.9	1564.6
TG 18:2/18:2/19:2	19.8	21.0	0.3	1.2	4.4	61.7
TG 18:2/18:3/18:3	14.0	0.3	11.6	0.1	5.0	93.3
TG 18:2/18:3/20:3	52.4	56.3	5.7	7.2	0.2	30.8

TG 18:2/20:2/18:3	114.5	123.5	1.8	24.7	2.8	45.5
TG 18:2/20:5/22:6	18.8	18.6	0.1	0.2	0.0	0.8
TG 18:4/20:5/21:5	1.3	1.1	0.0	0.0	0.1	2.8
TG 19:0/18:1/18:2	0.2	0.3	4.2	1.5	4.0	38.0
TG 19:0/22:6/22:6	0.3	0.4	0.0	0.0	0.0	0.3
TG 19:0/24:1/22:6	0.3	0.3	0.0	0.0	0.0	0.2
TG 19:1/18:2/18:2	3.4	3.5	0.4	2.3	7.1	120.9
TG 19:5/22:6/22:6	0.1	0.1	0.0	0.0	0.0	0.7
TG 20:0/18:1/18:1	27.6	28.4	0.0	29.3	467.8	7500.5
TG 20:0/18:1/18:2	13.9	14.0	37.3	43.7	419.4	6617.5
TG 20:0/24:1/22:6	0.7	0.7	0.0	0.0	0.0	1.0
TG 20:1/18:2/18:2	33.5	34.8	44.6	48.8	65.7	1104.9
TG 20:1/22:1/24:1	0.2	0.2	0.0	0.0	0.0	0.2
TG 20:1/24:1/18:2	0.6	0.6	0.1	0.1	0.6	6.8
TG 20:1/24:5/22:6	1.8	2.0	0.0	0.0	0.1	1.5
TG 20:2/20:5/22:6	17.4	17.4	0.0	0.2	0.1	0.8
TG 20:3/20:5/22:6	6.0	5.8	0.0	0.1	0.0	0.4
TG 20:4/20:5/22:6	13.4	12.8	0.0	0.1	0.1	0.5
TG 20:5/20:5/21:5	2.1	2.1	0.0	0.0	0.0	0.4
TG 20:5/20:5/22:6	26.4	27.0	0.1	0.2	0.0	0.2
TG 20:5/22:5/22:6	4.2	4.1	0.0	0.0	0.1	0.3
TG 20:5/22:6/22:6	9.9	9.9	0.0	0.1	0.0	0.3
TG 22:0/18:1/18:1	15.5	15.1	3.4	4.2	54.5	741.6
TG 22:0/18:1/18:2	9.3	9.5	5.8	0.4	39.6	642.2
TG 22:0/18:2/18:2	6.3	6.2	4.1	4.9	254.5	4006.0
TG 22:1/20:5/22:6	3.5	3.8	0.0	0.0	0.0	1.0
TG 22:1/22:1/22:6	2.7	2.8	0.0	0.0	0.0	0.3
TG 22:1/22:6/22:6	1.2	0.9	0.0	0.0	0.0	1.6
TG 22:1/24:1/22:6	0.6	0.6	0.0	0.0	0.0	0.0
TG 22:1/26:4/22:6	0.1	0.2	0.0	0.0	0.0	0.5
TG 22:1/28:5/22:6	0.1	0.1	0.0	0.0	0.0	0.4
TG 22:6/22:6/22:6	2.4	2.4	0.0	0.0	0.2	2.7
TG 23:0/18:1/18:1	1.0	0.9	0.0	0.2	27.9	445.1
TG 23:0/18:2/18:2	0.7	0.8	0.4	0.4	36.6	555.3
TG 24:0/18:1/18:1	5.6	5.3	0.5	0.0	25.8	352.5
TG 24:0/18:1/18:2	4.1	4.0	1.1	0.3	24.6	370.1
TG 24:0/18:2/18:2	2.7	2.6	1.3	0.1	13.0	42.8
TG 24:1/18:2/18:2	4.0	4.0	0.5	0.6	20.3	330.8
TG 24:1/18:2/22:6	1.3	1.4	0.0	0.0	0.0	0.5
TG 24:1/20:2/22:6	0.5	0.6	0.0	0.0	0.0	1.4
TG 24:1/22:6/22:6	0.6	0.8	0.0	0.0	0.1	0.2
TG 24:1/24:1/22:6	0.1	0.1	0.0	0.0	0.0	0.0
TG 24:2/22:6/22:6	0.4	0.4	0.0	0.0	0.0	0.0
TG 25:0/18:2/18:2	0.2	0.2	0.0	0.1	12.5	185.2
TG 26:0/18:1/18:1	0.0	0.0	0.0	0.0	10.2	87.9
TG 8:0/18:1/18:2	0.2	0.2	2.0	2.4	2.1	30.4
TG 8:0/18:2/18:2	0.0	0.0	0.4	0.5	1.9	27.0
TG O-18:0/16:0/20:5	0.1	0.2	0.3	0.1	0.6	2.5
TG O-19:3/18:2/18:3	0.4	0.3	3.9	1.9	13.1	239.3

Supplementary table 2: Composition of rations in duplicates by class:

Component	FishOil 1	FishOil 2	Lard 1	Lard 2	Control 1	Control 2
13-Docosamide	0.14%	0.39%	0.47%	0.39%	0.24%	0.61%
ASG	0.01%	0.01%	0.00%	0.00%	0.63%	0.62%
CE	0.02%	0.02%	0.00%	0.00%	0.00%	0.00%
Cer	0.00%	0.00%	0.00%	0.00%	0.13%	0.00%
DG	0.71%	0.72%	0.30%	0.36%	21.80%	24.53%
DGDG	0.00%	0.00%	0.00%	0.00%	0.27%	0.24%
HexCer	0.00%	0.00%	0.00%	0.00%	2.27%	0.05%
LPC	0.01%	0.01%	0.01%	0.01%	0.01%	0.00%

<b>MGDG</b>	0.00%	0.00%	0.00%	0.00%	0.04%	0.04%
<b>PC</b>	0.00%	0.00%	0.00%	0.00%	0.02%	0.00%
<b>PE</b>	0.01%	0.01%	0.00%	0.00%	0.00%	0.00%
<b>PG</b>	0.00%	0.00%	0.00%	0.00%	0.00%	0.00%
<b>SE</b>	0.00%	0.00%	0.00%	0.00%	0.50%	0.49%
<b>TG</b>	99.11%	98.84%	99.22%	99.23%	74.08%	73.43%

Supplementary table 3: Composition of rations in duplicates by fatty acid:

<b>Fatty Acids</b>	<b>FishOil 1</b>	<b>FishOil 2</b>	<b>Lard 1</b>	<b>Lard 2</b>	<b>Control 1</b>	<b>Control 2</b>
<b>FA 10:0</b>	0.16%	0.08%	0.18%	0.08%	0.01%	0.01%
<b>FA 12:0</b>	0.63%	0.65%	0.04%	0.01%	0.00%	0.00%
<b>FA 13:1</b>	0.00%	0.00%	0.00%	0.00%	0.00%	0.00%
<b>FA 14:0</b>	3.04%	3.29%	0.51%	0.84%	0.04%	0.04%
<b>FA 15:0</b>	1.03%	1.10%	0.13%	0.06%	0.03%	0.03%
<b>FA 15:1</b>	0.01%	0.01%	0.00%	0.00%	0.02%	0.02%
<b>FA 15:1</b>	0.18%	0.19%	0.04%	0.00%	0.00%	0.00%
<b>FA 16:0</b>	17.61%	17.06%	18.96%	22.72%	17.60%	17.59%
<b>FA 16:1</b>	12.32%	11.20%	4.96%	3.20%	4.73%	4.73%
<b>FA 17:0</b>	0.58%	0.63%	0.49%	0.65%	0.11%	0.11%
<b>FA 17:1</b>	0.92%	1.20%	0.47%	0.34%	0.12%	0.12%
<b>FA 18:0</b>	2.52%	2.73%	6.98%	7.33%	4.20%	3.96%
<b>FA 18:1</b>	21.06%	23.14%	42.36%	42.68%	44.17%	44.66%
<b>FA 18:2</b>	6.01%	4.76%	16.84%	10.32%	12.27%	11.84%
<b>FA 18:3</b>	5.12%	3.76%	2.94%	2.67%	5.90%	5.98%
<b>FA 18:4</b>	0.48%	0.46%	0.00%	0.00%	0.00%	0.00%
<b>FA 19:0</b>	0.01%	0.01%	0.02%	0.01%	0.00%	0.00%
<b>FA 19:1</b>	0.22%	0.24%	0.33%	0.35%	0.04%	0.04%
<b>FA 19:2</b>	0.17%	0.19%	0.00%	0.01%	0.00%	0.00%
<b>FA 20:0</b>	0.48%	0.51%	0.53%	0.74%	0.76%	0.76%
<b>FA 20:1</b>	0.00%	0.00%	0.00%	0.00%	0.03%	0.04%
<b>FA 20:1</b>	1.95%	2.09%	2.36%	2.61%	1.49%	1.44%
<b>FA 20:2</b>	1.21%	1.34%	0.24%	0.18%	0.18%	0.18%
<b>FA 20:3</b>	0.49%	0.54%	0.14%	0.17%	0.00%	0.00%
<b>FA 20:4 (ARA)</b>	0.51%	0.54%	0.00%	0.25%	0.02%	0.02%
<b>FA 20:5 (EPA)</b>	13.50%	13.89%	1.00%	4.21%	6.51%	6.57%
<b>FA 21:0</b>	0.07%	0.07%	0.02%	0.02%	0.01%	0.01%
<b>FA 21:1</b>	0.00%	0.00%	0.00%	0.00%	0.00%	0.00%
<b>FA 22:0</b>	0.29%	0.30%	0.07%	0.06%	0.30%	0.30%
<b>FA 22:1</b>	1.20%	1.29%	0.22%	0.26%	0.67%	0.69%
<b>FA 22:4</b>	0.33%	0.39%	0.08%	0.03%	0.02%	0.02%
<b>FA 22:5</b>	0.87%	0.86%	0.03%	0.01%	0.00%	0.00%
<b>FA 22:6 (DHA)</b>	6.20%	6.64%	0.03%	0.16%	0.52%	0.58%
<b>FA 23:0</b>	0.07%	0.07%	0.00%	0.01%	0.07%	0.07%
<b>FA 23:1</b>	0.02%	0.03%	0.00%	0.00%	0.02%	0.02%
<b>FA 24:0</b>	0.11%	0.11%	0.02%	0.00%	0.09%	0.09%
<b>FA 24:1</b>	0.53%	0.56%	0.01%	0.01%	0.06%	0.07%
<b>FA 24:2</b>	0.00%	0.00%	0.00%	0.00%	0.00%	0.00%
<b>FA 24:3</b>	0.03%	0.03%	0.00%	0.00%	0.00%	0.00%
<b>FA 24:5</b>	0.01%	0.02%	0.00%	0.00%	0.00%	0.00%
<b>FA 25:1</b>	0.00%	0.00%	0.00%	0.00%	0.00%	0.00%
<b>FA 26:0</b>	0.00%	0.00%	0.00%	0.00%	0.01%	0.00%
<b>FA 26:4</b>	0.00%	0.00%	0.00%	0.00%	0.00%	0.00%

<b>FA 28:2</b>	0.00%	0.00%	0.00%	0.00%	0.00%	0.00%
<b>FA 28:5</b>	0.01%	0.01%	0.00%	0.00%	0.00%	0.00%

## Final remarks

Plasmalogens are phospholipids characterized by the vinyl ether group at the sn1 position of glycerol. This electron-rich group makes plasmalogen much more reactive with reactive oxygen species (ROS). This work was focused on understanding the reaction mechanisms of plasmalogens when oxidized by ROS, with photo in singlet oxygen. For this, it was necessary to develop methods for purifying plasmalogen from beef and pig brains (chapter 1).

Purified plasmalogens were used extensively to develop methods and pilot experiments before commercial standards were used. With this, it was possible to develop low temperature photooxidation methods (chapter 2) for analysis of fatty aldehydes. In addition to being very important for membrane leakage studies that require 15 mg of lipid for the preparation of liposomes (chapter 3), it is impracticable for the use of commercial standards. The purification method proved to be very reproducible for both brains used and during the process other value-added lipids (cerebrosides and sulfatides) were simultaneously obtained. In addition, in the purified fractions, a type of phosphatidylserine methyl ester plasmalogen was observed, but little is known about this type of phospholipids, but this may be an opportunity to better understand this lipid and understand why it exists in brains.

It is known that plasmalogens are very reactive with singlet oxygen, but there is still a lack of studies focused on the characterization of the products. To fill this gap, we tried to analyze the different products formed by photooxidation using different techniques that show the different reactivity of each product (chapter 2). We show evidence of the production of dioxetanes by chemiluminescence, which already has deleterious effects for cells. Furthermore, we show that the production of plasmalogen dioxetanes produces a new singlet oxygen that is able to propagate the oxidation. In this same work, we characterized the hydroperoxide produced and performed some unpublished

studies of this species and showed that this hydroperoxide produces a new singlet oxygen in a different mechanism than dioxetane. Furthermore, we showed that plasmalogen hydroperoxide can be easily reduced and produces alpha beta unsaturated fatty aldehydes and plasmalogen hydroperoxide when oxidized by metals produces diacyl phospholipids with alpha beta unsaturated carbonyls. We confirmed alpha beta unsaturated groups of fatty aldehydes and diacyl phospholipids by reacting with a fluorescent probe which reacts by Michael addition due to a thiol group. In this way, we developed a simple method to detect alpha beta unsaturated groups and showed that the formed species react easily with thiol group. Which has a great biological relevance because these plasmalogen hydroperoxide products can modify proteins and other biomolecules by thiol group reaction.

During chapter 3, we showed that phosphoethanolamine plasmalogens (pPE) are very present in HaCat keratinocyte cells and pPE are the most reactive lipids by photosensitivity reaction. Knowing the reactivity of pPE (chapter 2), we investigated how pPE oxidation could facilitate membrane leakage. We have shown that membranes made of plasmalogen rupture with only singlet oxygen, but only in the presence of reductants. In this way, an antioxidant mechanism such as the reduction of hydroperoxides can be harmful to the integrity of the membrane. Therefore, this work shows another deleterious action of plasmalogens.

Throughout the analysis of fatty aldehydes produced by plasmalogen oxidation, we used different probes and chromatographic methods. We then used this acquired expertise and applied it to free fatty acid analysis (FFA, Chapter 4). The analysis method was quickly optimized and applied to plasma samples from SOD1 G93A transgenic mice supplemented with different diets. In this work, we showed that diet interferes much more in the FFA profile than the ALS disease. Thus, this is a method that can be applied in other contexts and be very important for future analyzes of our group.

## **CURRICULUM VITAE**

### **PERSONAL DATA**

Name: Rodrigo Lucas de Faria

Place and date of birth: January 27, 1991, São Paulo, Brazil

### **OCUPATION**

Scholarship Doutorado Direto, FAPESP, 10/10/2017 to 01/31/2023.

### **EDUCATION**

2013 - 2016 Bachelor's degree at Chemistry, Universidade de São Paulo, São Paulo, SP, Brazil.

2010-2012 Unfinished graduation in materials science FATEC-SP.

### **Participation in events and mini-courses:**

2022- 39th SGMS Meeting will take place in Beatenberg at 27-28 October 2022. Poster presentation.

2022- The 24th Annual Meeting of the **Redox** Medicine Society, **Paris**, France Poster presentation.

2022- 49th Annual Meeting of the Brazilian Society for Biochemistry and molecular Biology. Aguas de Lindóia, SP, Brazil, 2022. Poster presentation.

202- CEPID Redoxoma Annual Meeting 2022. Oral presentation.

2021-20th IUPAB Congress, 45th Annual SBBf Meeting, and 50th Annual SBBq Meeting. Poster presentation

2019- 48th Annual Meeting of the Brazilian Society for Biochemistry and molecular



Biology. Aguas de Lindóia, SP, Brazil, 2019. Poster presentation

2018- 47th Annual Meeting of the Brazilian Society for Biochemistry and molecular Biology. Joinville, SC, Brazil, 2019. Poster presentation

2017-Minicurso Omics Sciences in Infectious Diseases (OSID) 2017-ICB USP- Responsável Prof. Dr.

Giuseppe Palmisano

2017- CEPID Redoxoma Annual Meeting 2017

2016- CEPID Redoxoma Annual Meeting 2016

2016- XXXIV Encontro Nacional dos Estudantes de Química

2015- Monitor no Instituto de Química durante a Virada Científica 2015

2014-Minicurso Chemical Neuroscience –IQUSP-Responsável Prof. Dr. Luiz Fernando da Silva Junior.

Proficiency in:

English: TOEFL ITP level B1

German: onDaF level B1

## **RESEARCH EXPERIENCE**

2017 – 2023 PhD student in Sayuri Miyamoto's laboratory. University of Sao Paulo, São Paulo, Brazil.

2015 – 2016 Undergrad student in Sayuri Miyamoto's laboratory. University of Sao Paulo, São Paulo, Brazil.

2014- Undergrad student in Luiz Fernando da Silva Junior's laboratory. University of

São Paulo, Brazil.

## LIST OF PUBLICATIONS

Chaves-Filho, A. B., Pinto, I. F. D., Dantas, L. S., Xavier, A. M., Inague, A., **Faria, R. L.**, ... & Miyamoto, S. (2019). Alterations in lipid metabolism of spinal cord linked to amyotrophic lateral sclerosis. *Scientific reports*, 9(1), 11642.

Khan, Z. U., Khan, L. U., Uchiyama, M. K., Prado, F. M., **Faria, R. L.**, Costa, I. F., ... & Di Mascio, P. (2023). Singlet Molecular Oxygen Generation via Unexpected Emission Color-Tunable CdSe/ZnS Nanocrystals for Applications in Photodynamic Therapy. *ACS Applied Nano Materials*.

**Faria, R.L.**, Miyamoto, S. (2023). A rapid and simple method to purify PE plasmalogens, cerebroside and sulfatides from bovine or porcine brains (In preparation)

**Faria, R.L.**, Prado, F. M., Junqueira, H. C., Fabiano, K. C., Baptista, M. S, Mascio, P. Miyamoto, S. (2023). Plasmalogens pro-oxidant action by generation of singlet molecular  $O_2(^1\Delta g)$  and others deleterious products with characterization of oxidation products by tandem mass spectrometry (In preparation)

**Faria, R.L.**, Diniz, L. R., Pinto, I. F., Britto, A. C., Dantas, L., Miyamoto, S. Determination of changes in plasma free fatty acids in a high-fat diet in amyotrophic lateral sclerosis by UHPLC-Florescence (In preparation)